PD
539.7
A 693
v.5, No 4

REACTOR FUEL PROCESSING

A Quarterly Technical Progress Review

Prepared for DIVISION OF TECHNICAL INFORMATION, USAEC, by
STEPHEN LAWROSKI and ASSOCIATES, ARGONNE NATIONAL LABORATORY

ILLINOIS STATE LIBRARY
JAN 23 1963

October 1962

● VOLUME 5

● NUMBER 4

TECHNICAL PROGRESS REVIEWS

To meet the needs of industry for concise summaries of current atomic developments, the Atomic Energy Commission is publishing this series, Technical Progress Reviews. Issued quarterly, each of the reviews digests and evaluates the latest findings in a specific area of nuclear technology and science.

The four journals published in this series are:

Nuclear Safety, Wm. B. Cottrell, W. H. Jordan, and associates, Oak Ridge National Laboratory

Power Reactor Technology, W. H. Zinn and J. R. Dietrich, General Nuclear Engineering Corporation

Reactor Materials, R. W. Dayton, E. M. Simons, and associates, Battelle Memorial Institute

Reactor Fuel Processing, Stephen Lawroski and associates, Chemical Engineering Division, Argonne National Laboratory

Each journal may be purchased ($2.00 per year for subscription and individual issues $0.55) from the Superintendent of Documents, U. S. Government Printing Office, Washington 25, D. C. See back cover for remittance instructions and foreign postage requirements.

The views expressed in this publication do not necessarily represent those of the United States Atomic Energy Commission, its divisions or offices, or of any Commission advisory committee or contractor.

Availability of Reports Cited in This Review

Unclassified AEC reports are available for inspection at AEC depository libraries and are sold by the Office of Technical Services, Department of Commerce, Washington 25, D. C. Some of the reports cited are not available owing to their preliminary nature; however, the information contained in them will eventually be made available in formal progress or topical reports.

Unclassified reports issued by other Government agencies or private organizations should be requested from the originator.

Unclassified British and Canadian reports may be inspected at AEC depository libraries. British reports are sold by the British Information Service, 45 Rockefeller Plaza, New York, N. Y.; Canadian reports (AECL series) are sold by the Scientific Document Distribution Office, Atomic Energy of Canada, Ltd., Chalk River, Ontario, Canada.

Classified U. S. and foreign reports identified in this journal as Classified may be purchased by properly cleared Access Permit Holders from the Division of Technical Information Extension, U. S. Atomic Energy Commission, P. O. Box 1001, Oak Ridge, Tenn. Such reports may be inspected at classified AEC depository libraries.

REACTOR FUEL PROCESSING

A REVIEW OF RECENT DEVELOPMENTS

Prepared for DIVISION OF TECHNICAL INFORMATION, USAEC,
by STEPHEN LAWROSKI and ASSOCIATES,
ARGONNE NATIONAL LABORATORY

● OCT. 1962
● VOLUME 5
● NUMBER 4

Foreword

This quarterly review of reactor fuel processing has been prepared at the request of the U. S. Atomic Energy Commission, Division of Technical Information. It is intended to assist those interested in keeping abreast of important developments in this field. In each Review it is planned to cover those particular subjects in which significant new results have been obtained. The Review does not purport to abstract all the literature published on this field during the quarter. Instead it is intended to bring each subject up to date from time to time as circumstances warrant.

Interpretation of results, where given, represents the opinion of the editors of the Review, who are personnel of the Argonne National Laboratory, Chemical Engineering and Idaho Divisions. Those taking part in the preparation of this issue are J. Barghusen, L. Burris, Jr., I. G. Dillon, P. Fineman, A. A. Jonke, S. Lawroski, W. J. Mecham, D. Paige, J. Royal, W. B. Seefeldt, J. Simmons, R. K. Steunenberg, C. E. Stevenson, and R. C. Vogel. The reader is urged to consult the original references for more complete information on the subject reported and for the interpretation of results by the original authors.

PD
539.7
A693
V.5, No4

Contents

Foreword

I COMMERCIAL ASPECTS OF FUEL PROCESSING 1

Industrial Participation in Fuel Processing 1
Fuel-Processing Economics 2
Fuel-Cycle Economics 4
Shipping and Storing Fuels 6
References 6

II RESEARCH AND DEVELOPMENT ON AQUEOUS PROCESSING 7

Preparation for Fuel Processing 7
Separations Processes 12
Process Instrumentation 17
Plant Design and Operation 19
Corrosion and Construction Materials . . . 20
Corrosion in Waste Processing 25
References 28

III RESEARCH AND DEVELOPMENT ON NONAQUEOUS PROCESSING 30

Volatility Processes 30
Pyrometallurgical Processes 36
Other Nonaqueous Processes 46
References 50

IV WASTE DISPOSAL 52

Tank-Storage Management of High-Level-Activity Liquid Wastes . . . 52
Treatment of Liquid Wastes by Adsorption and Ion-Exchange Materials 56
Reduction to Solids of High-Level-Activity Liquid Wastes . . . 58
Final Disposal Methods 64
Recovery of Fission Products 67
References 69

V PRODUCTION OF URANIUM, THORIUM, PLUTONIUM, AND THEIR COMPOUNDS 72

Recovery of Uranium from Ores 72
Production of Uranium Dioxide 73
Production of Uranium Tetrafluoride . . . 76
Preparation of Uranium Carbides 78
Production of Uranium Metal 82
Thorium 83
Electrorefining of Plutonium Metal 84
References 86

INDEX, VOLUME 5 89

Issued quarterly by the U. S. Atomic Energy Commission. Use of funds for printing this publication approved by the Director of the Bureau of the Budget on November 1, 1960.

Section

I

Reactor Fuel Processing

Commercial Aspects of Fuel Processing

Industrial Participation in Fuel Processing

The status of plans for the first privately owned fuel-processing plant was reported to the 1962 Nuclear Congress by Runion of the Davison Chemical Division, W. R. Grace & Company.[1] The firm has been engaged in negotiations with the Atomic Energy Commission (AEC) and industry which are expected to lead to construction of a $22 million plant having a nominal capacity of 1 ton of uranium per day. The plant would be built and operated through a new subsidiary of W. R. Grace & Company, known as Nuclear Fuel Services, Inc. (NFS).

The NFS plant is being planned to offer a service capable of filling all present fuel-processing requirements. The plant is optimized around the processing of unalloyed or unmixed fuels of low U^{235} enrichment which are amenable to direct dissolution in nitric acid. Such uranium dioxide fuels require the minimum of process plant capital and result in the minimum waste-storage requirements. Tubular fuel assemblies (either stainless steel or Zircaloy encased) will be chopped into short pieces, and the uranium content will be leached from the cladding. The solid cladding will then be inspected and buried. Waste solutions generated from the solvent-extraction processing of the uranium and plutonium will be stored in an alkaline condition in mild-steel tanks.

The "chop-leach" concept is the basic process for the plant. More complex fuels will use other head-end processes and will require additional processing equipment. For zirconium-based fuels a modified Zirflex process will be used, in which the entire fuel element is dissolved by controlled additions of hydrofluoric acid and nitric acid in stainless-steel dissolvers. Maximum capacity would be 600 kg of zirconium per day. At 5% uranium content, this would represent 30 kg of uranium per day.

For stainless-steel cermet fuels, a Darex dissolution scheme will be employed, although consideration is also being given to the use of recently developed electrolytic dissolvers. For aluminum or molybdenum alloy fuels, direct dissolution in nitric acid will be employed. In each case the concentration of alloying constituents limits the throughput rate for fuels of low enrichment. For highly enriched fuels the throughput may be limited by either the concentration of alloying constituents or by criticality considerations. For concentration control of criticality, the feed concentration will be limited to 5 g of U^{235} per liter. On this basis the plant throughput and basic processing charges are estimated as follows:

Enrichment, %	Feed concentration (total U), g/liter	Throughput, kg/day	Cost per ton
1	150	1000	$ 22,500
4	150	1000	22,500
10	50	250	100,000
100	5	30	750,000

The basic solvent-extraction process for the NFS plant is a conventional three-cycle Purex process using pulse columns. The reference flow sheet provides for storage of 400 gal of waste per ton, including 180 gal of self-heating wastes with a total solids limitation of 30% and undissolved solids limitation of 5%. Radioac-

tivity limitation is tentatively set at 8000 curies/gal for 160 Btu/(hr)(gal). Cost of this storage is estimated at $2.40 per gallon and is included in the $22,500 per ton charge. An additional charge for perpetual storage of waste will be added if imposed by the AEC and is estimated to be about $0.70 per gallon for wastes stored in mild-steel tanks. Such figures will not be known definitely until AEC policy is established relating to the costs and requirements for perpetual storage.

The plant will be built in a low-population area with a large protective perimeter (minimum 1-mile radius). Off-gases from fuel dissolution operations will be treated for iodine removal and filtered to remove entrained solids. Discharge of krypton and xenon fission-product gases is considered acceptable at the processing rates involved.

If the NFS plant becomes operational in 1965 as planned, its basic processing charge is estimated to be $22,500 per ton for enrichments up to 4%. Detailed engineering and costing are being done by Bechtel Corporation to arrive at guaranteed maximum costs for a plant located in New York State. Final site selection and exact daily processing charges will be based on these guaranteed costs.[1]

Fuel-Processing Economics

A recent Du Pont study of the costs associated with the construction and operation of a large processing plant was discussed in a previous issue of *Reactor Fuel Processing*.[2] Some additional comments based on the Du Pont study were made in a paper presented at the 1962 Nuclear Congress by Thayer and Colven.[3] It was pointed out that the scale of operation is perhaps the overriding factor in the economics of spent-fuel processing. Whereas in conventional chemical plants the capital cost of a manufacturing unit varies approximately as the 0.7 power of the capacity, the Du Pont cost study indicates that, in the range of 1 to 10 tons of fuel processed, the capital cost of a processing plant varies as the 0.145 power of the capacity. Similarly the annual operating costs for a 10 ton/day plant were estimated to be only about 1.7 times as high as for a 1 ton/day plant.

The above cost factors are based on a plant processing a simple type of natural-uranium fuel. For a multipurpose plant handling a variety of power-reactor fuels, the complexity of the plant and its operation is greatly increased. For such a plant the instantaneous processing rate must be considerably higher than the expected average operating rate. If this situation is foreseen, however, the capital cost penalty for the extra capacity will not be unacceptable, since the change in capital costs with design capacity is relatively small. Thus, as Thayer and Colven point out, the present trend in power-reactor design, whereby each reactor uses a different type of fuel, is not in itself an important handicap to the achievement of an economic fuel cycle provided that the total quantity of fuel available is sufficient to justify the initial investment in a processing plant. However, once a processing plant is in operation handling a variety of fuels, the throughput of that particular plant could be increased in the future by standardizing the fuels.

Although the Du Pont study was based on aluminum-clad fuels, the authors believe that the capital costs would not be significantly different, except for higher maintenance costs due to greater dissolver corrosion, for either stainless-steel cladding or zirconium cladding. If, however, the plant is designed to handle all three types of fuels, then the capital costs will be higher, perhaps 10% higher, than for a plant designed to handle any one fuel. If the fuel core requires much cutting apart before it can be charged to the dissolver, then this also will be a significant cost item.

The authors also discussed the following variations in process and equipment, now under development, which may prove advantageous for use in a commercial processing plant:

1. An electrolytic dissolution procedure, under development at the Savannah River Plant (SRP) and other sites, offers the possibility of dissolving aluminum-clad, stainless-steel-clad, and zirconium-clad fuels in a single dissolver vessel, thus avoiding the installation of two or more dissolvers fabricated from different alloys.

2. Savannah River is developing centrifugal mixer-settlers with the object of reducing the residence time required for settling so that radiolytic damage to the organic solvent will be reduced. The low holdup and consequent ease of flushing of these contactors might achieve a significant reduction in the "turn-around time" between processing campaigns and might also offer the possibility of controlling criticality by

equipment geometry rather than by solution concentration.

3. Control of nuclear criticality by adding neutron poisons (such as boron and cadmium) to the dissolving reagents offers a definite advantage in simplicity of dissolver design for enriched fuels, provided it can be made to offer the same assurance of safety as that provided by presently used methods of geometry and concentration control.

Possible Expansion of the ICPP

An expansion of the zirconium fuel-processing capacity of the Idaho Chemical Processing Plant (ICPP) has recently been given consideration. Several processes have been or are being developed for zirconium fuels, and selection of the particular process to be used in any new installation is of primary importance. According to a recent report prepared by Burn at the ICPP,[4] six processes were selected for preliminary evaluation. These are the present Submarine Thermal Reactor (STR) process, the barium fluozirconate process, the sodium formate process, the Zirflex process, the Alloy Reguline Chloride Oxidation (ARCO) process, and the fused-salt fluoride-volatility process. The first four processes are aqueous, and the last two are nonaqueous.

The two nonaqueous processes were eliminated from further consideration because both processes, according to Burn, have inherent process weaknesses that have not been overcome in the development work thus far completed. The future potential of these processes was not evaluated in detail, but both of them appear promising.

The feasibility of the aqueous processes has been fairly well established, although additional development work is necessary to complete the process data and to provide solutions to some of the still unresolved operating problems. The amount of such development work required varies among the four processes but is least for the present STR process (with certain proposed modifications).

Economic evaluations of the four aqueous processes were made for processing capacities of 5 and 10 kg of uranium per day from 40% burned-up pressurized-water-reactor (PWR) seed fuel elements. The results of these evaluations are summarized in Table I-1.

The STR process requires the least investment of the four processes but has the highest operating cost. It is apparent that a selection of the optimum process on an economic basis will require complete knowledge of the schedule of fuel to be processed.

Table I-1 ECONOMIC EVALUATIONS OF FOUR AQUEOUS PROCESSES

Process	Investment required	Processing cost per gram of uranium*	Investment recovery, kg of uranium†
For Installations Having a Capacity of 5 kg of Uranium per Day			
STR	$ 355,000	$2.79	185
Barium fluozirconate	1,270,000	2.33	535
Sodium formate‡	1,270,000	2.33	535
Modified Zirflex	1,510,000	2.04	570
For Installations Having a Capacity of 10 kg of Uranium per Day			
STR	$ 450,000	$1.97	165
Barium fluozirconate	1,430,000	1.40	435
Sodium formate‡	1,430,000	1.40	435
Modified Zirflex	2,220,000	1.23	640

*Direct cost plus depreciation for dissolution and first-cycle extraction. This does not include final purification of uranium or indirect cost allocations. The comparable cost for the presently installed zirconium fuels process is $4.70 per gram of uranium.

†Kilograms of uranium that must be processed to recover the investment by savings resulting from the reduction in the comparable cost of $4.70 per gram of uranium processed through the present system.

‡Sodium formate process investments and processing costs have been tentatively estimated to be comparable to those for the barium fluozirconate process.

The STR process is definitely preferable on the basis of minimum development time required. The development work done to support the design of the original ICPP installation, and the knowledge gained during operation of this system, put this process at least a year ahead of the other aqueous processes. It is estimated that an expanded STR process could be installed in about 18 months after project approval.

Fuel-Cycle Economics

Effective July 1, 1962, the AEC reduced its base charges for enriched uranium for the second time within a year.[5] The latest revision consists of a reduction in the component of charge for the work of separating uranium isotopes and is made possible by improvements in the economics of operation of the gaseous-diffusion plants. The component of charge for the natural uranium used in this process was reduced on July 1, 1961, owing to a reduction in the cost of natural uranium oxide which has now dropped domestically to a uniform $8 per pound in the form of concentrates.

The base charges are a schedule of values the AEC places on enriched and depleted uranium, varying with the percentage of U^{235} present. The schedule of base charges is used in financial transactions involving the lease, sale, or consumption of uranium. Examples of the new base charges for enriched and depleted uranium are given in Table I-2. The complete schedule of charges was published in the *Federal Register* on May 29, 1962, in amendments to the notice that appeared in the *Federal Register* (Vol. 26, No. 4765) on May 30, 1961.

In a speech before the 1962 Nuclear Congress in New York, AEC Chairman Seaborg said the net effect of the reduction corresponds to a decrease of 0.15 to 0.20 mill/kw-hr in fuel costs. In the past two years, the adjustments in the base charges for enriched uranium have reduced depletion and use charges[5] by fully 30% or, roughly, 0.5 mill/kw-hr.

Table I-2 EXAMPLES OF BASE CHARGES FOR ENRICHED AND DEPLETED URANIUM AS URANIUM HEXAFLUORIDE[5]

U^{235} assay, wt.%	New charges: $/kg of contained uranium*	New charges: $/g of contained U^{235}	Previous charges, $/g of contained U^{235}	
Enriched uranium				Reduction, %
90	10,808.00	12.01	13.65	12
20	2,252.00	11.26	12.74	12
10	1,062.00	10.62	11.95	11
5	479.40	9.59	10.71	10
3	254.30	8.48	9.37	10
2	146.50	7.33	8.00	8
1.5	95.30	6.35	6.84	7
1.0	47.70	4.77	4.99	4
Depleted uranium				Increase, %
0.7	22.60	3.23	3.23	0
0.6	15.35	2.56	2.47	4
0.5	8.90	1.78	1.61	10
0.4	3.70	0.93	0.75	24
0.38	3.00	0.79	0.79	0

If a user specifies a U^{235} assay between 0.38 and 0.22 wt.%, the charge will be $3 per kilogram of contained uranium. However, if the U^{235} assay is not specified by the user, the AEC will supply uranium having a U^{235} assay to be determined by the AEC in the range below 0.38% and will charge $2.50 per kilogram of uranium.

*Official base charges.

Estimates of Fuel-Cycle Costs

Kuhn and Walton, speaking at the Nuclear Congress,[6] have presented additional estimated fuel-cycle costs, based on a report, "Costs of Nuclear Power," which was discussed in a previous issue of this Review.[7] A tabulation of estimated fuel-cycle costs was presented,[6] as shown in Table I-3, for eight power reactors which are presently in operation or which are being built.

Each of these reactors is of a demonstrational nature, and the fuel-cycle costs for the subsequent generations of nuclear-power reactors required to meet long-term energy needs are expected to be quite different. The cost estimates are calculated on the basis of consistent definitions and assumptions and are believed to be representative of the present stage in the overall development of competitive nuclear power. It is noteworthy that for this generation of reactors the chemical processing costs represent a rather small percentage of the total fuel-cycle costs, whereas fuel-fabrication costs represent a large fraction of the totals.

The costs shown in Table I-3 are based on the schedule of charges for enriched uranium in effect prior to July 1, 1962. To show the ef-

Table I-3 ESTIMATED FUEL-CYCLE COSTS[6]

Plant	Power, Mw(e) net	Irradiation level, Mwd/metric ton of U	Estimated cost, mills/kw-hr						
			Fabrication	Transportation	Processing	Burnup	Pu* credit	Charge	Total
Peach Bottom	40	48,000†	1.10	0.03	0.27	1.22‡		0.41	3.0
BONUS (Puerto Rico)	16.3	11,020	1.59	0.15	0.56	1.32	0.47	0.42	3.6
Hallam	76	8,800	1.02	0.15§	0.52	1.58	0.42	1.12	4.0
Dresden	180	9,000	3.03	0.21	0.53	1.05	0.68	0.21	4.4
Yankee	136¶	7,830	2.91	0.19§	0.76	1.85	0.82	0.43	5.3
Indian Point	255**	21,000†	3.12	0.07§	0.26	2.22‡		0.83	6.5
Carolinas-Virginia	17.0††	11,150	6.94	0.23	0.82	1.99	0.57	0.22	9.6
Piqua	11.4	3,380	5.99	0.49§	2.19	2.66	1.10	0.78	11.0

*Pu credit is the value of plutonium as metal in spent fuel and is subtracted from the sum of the other costs when determining the total cost.

†Approximate values in Mwd/metric ton (U + Th).

‡Burnup less credit for U^{233}.

§Unirradiated fuel transportation is included in fuel-fabrication cost.

¶Yankee is now operating at a higher power level.

**255 Mw(e) net including oil-fired superheater; 151 Mw(e) net is assigned to the nuclear portion of the plant.

††17.0 Mw(e) net including oil-fired superheater; we assigned 13.5 Mw(e) net to the nuclear portion of the plant.

fect of the new price reduction for U^{235}, the same authors have calculated the new costs shown in Table I-4. The decrease in fuel-cycle costs ranges from 0.12 to 0.34 mill/kw-hr for these reactors.

In another paper presented at the Nuclear Congress, some of the factors that will affect fuel-cycle costs in the future were discussed.[8] In contrast to the fuel-cycle costs calculated by Kuhn and Walton for reactors whose construction was started several years ago, it was reported by Staebler of the AEC that equilibrium fuel costs for large reactors whose construction could be started today are estimated to be in the range of 1.8 to 2.2 mills/kw-hr based on the new price schedule for enriched uranium.

Table I-4 EFFECT OF 1962 PRICE REDUCTION[6] FOR U^{235}

(Estimated Fuel-Cycle Cost Is in Mills per Kilowatt-Hour)

Plant*	Burnup		Use charge		Change†
	Old	New	Old	New	
BONUS (Puerto Rico)	1.32	1.19	0.42	0.39	−0.16
Hallam	1.58	1.48	1.12	1.02	−0.20
Dresden	1.05	0.94	0.21	0.20	−0.12
Yankee	1.85	1.65	0.43	0.40	−0.23
Carolinas-Virginia	1.99	1.79	0.22	0.20	−0.22
Piqua	2.66	2.38	0.78	0.72	−0.34

*New values for Peach Bottom and Indian Point were not calculated because a new price has not been established for mixtures of U^{233} and U^{235}.

†This is the sum of the changes in burnup and use charge resulting from the 1962 reduction and the effect on total fuel-cycle cost.

In the next 10 to 15 years, fuel-cycle costs are likely to be affected both by changes in economic policies and by technical developments. In this period a change to private ownership of nuclear fuel is likely, and a change to privately owned fuel-processing services seems fairly certain. Fuel-cycle costs will also be affected by changes in the value of reactor-produced fissionable materials such as plutonium and U^{233} as their values become dependent on the supply and demand forces of a free market. Considering all these factors in total, Staebler states that it does not appear that there will be large net economic shifts as nuclear power proceeds through a transition toward a normal American industrial framework.

Future fuel-cycle costs will depend on technical accomplishments, including improvements in manufacturing processes and cost reductions permitted by greater volumes. There appears to be rather broad optimism that fuel-cycle costs of something like 1.0 to 1.5 mills/kw-hr can be achieved during approximately the next decade. Staebler gives an approximate range within which the components of cost are expected to fall to achieve this overall fuel-cycle cost. Fuel fabrication should contribute only about 0.25 to 0.50 mill/kw-hr. For a system with 40% thermal efficiency and 25,000 Mwd/ton average exposure, this is equivalent to fabrica-

tion costs of $60 to $120 per kilogram. Inventory charges should be in the range of 0.3 to 0.5 mill/kw-hr. At 10% per year for inventory charge, this allows only $20 to $35 for fuel value per kilowatt of capacity. Processing costs should not be more than about 0.2 mill/kw-hr, which permits costs of up to about $48 per kilogram of fuel for the assumed conditions. Shipping costs should be in the range of 0.05 to 0.10 mill/kw-hr, which corresponds to $12 to $24 per kilogram of fuel. The net cost of depletion or burnup should be in the range of 0.2 to 0.5 mill/kw-hr. This permits a net effective cost of only about $1.60 to $4 per gram of material destroyed.

Shipping and Storing Fuels

The problem of shipping large amounts of fuel, with high degrees of irradiation and possible short decay times, from power reactors to fuel-processing plants has been discussed by Smiley et al. of Savannah River.[9] Since this subject has been discussed in a previous issue of *Reactor Fuel Processing*,[2] it will not be repeated here. In the same paper, however, the authors describe the receiving facility at Savannah River for various power-reactor fuels. The construction of this facility, designated as Receiving Basin for Off-Site Fuels (RBOF) was about one-third completed in February 1962. Some aspects of the design as described in the paper may not be immediately incorporated in the facility.

The RBOF is a building about 139 ft wide by 148 ft long containing six water-filled basins and associated facilities. Direct access to existing underground storage tanks and a large seepage basin is provided for disposal of radioactive liquid wastes. The basin area contains a decontamination pit, two cask unloading basins, three basins for disassembling and repackaging fuel elements, a storage basin, and interconnecting canals for movement of elements between basins. About 130 tons of fuel at an average U^{235} content of 3% can be stored in the basin.

Fuel assemblies will be removed from shipping casks in RBOF and stored until processing is required at either the SRP or a commercial plant. Since spent fuel will be stored in RBOF for an undefined period prior to processing, a preliminary financial settlement will be made by the AEC with the reactor operator according to the terms in the contract. This preliminary settlement will be made on the basis of quantities of plutonium and uranium calculated from reactor operating conditions.[9]

If they are to be processed at SRP, most fuels stored in RBOF will first be sent to the working basins for alterations prior to dissolution. For example, massive end fittings may be removed from fuel assemblies along with housings and other materials that are either incompatible with the dissolving schemes or could possibly hinder economical dissolving. In addition, fuel assemblies will be packaged into shapes that can be readily charged to the dissolvers. (The equipment for performing these operations has not yet been designed because of the possibility that the processing will be done by a commercial plant.)

Fuel-assembly packages, and in some cases individual assemblies, will be moved from the working basin area to the unloading basins as needed for loading into a cask for shipment to the processing area. It is planned to use existing 70-ton casks for shipment of these fuels from RBOF to the processing area via plant railroad if processing is done at SRP.

References

1. T. C. Runion, NFS Chemical Processing Plant Capability and Cost Bases, Nuclear Fuel Services, Inc., May 2, 1962.
2. *Reactor Fuel Process.*, 5(1): 1–5 (January 1962).
3. V. R. Thayer and T. J. Colven, Some Comments on the Economics of Fuel Processing, Preprint Paper No. 83, 1962 Nuclear Congress, New York, June 4–7, 1962.
4. P. Burn, An Evaluation of Four Processes for Recovering Uranium from Zirconium Fuels at the Idaho Chemical Processing Plant, USAEC Report IDO-14564, Phillips Petroleum Co., Apr. 27, 1962.
5. AEC To Revise Charges for Enriched and Depleted Uranium, AEC Press Release E-176, May 29, 1962.
6. D. W. Kuhn and R. D. Walton, Jr., Fuel-Cycle Costs for Power Reactors, Preprint Paper No. 19, 1962 Nuclear Congress, New York, June 4–7, 1962.
7. *Reactor Fuel Process.*, 4(4): 1–3 (October 1961).
8. U. M. Staebler, Fuel-Cycle Economics, paper presented at 1962 Nuclear Congress, New York, June 4–7, 1962.
9. S. D. Smiley, J. W. Langhaar, and R. Maher, Shipping and Storing Power Fuels Prior to Reprocessing, Preprint Paper No. 82, 1962 Nuclear Congress, New York, June 4–7, 1962.

Section

II

Reactor Fuel Processing

Research and Development on Aqueous Processing

The recovery of plutonium and unused uranium from major quantities of irradiated uranium and its alloys has been accomplished for over a decade by dissolving the nuclear fuels in strong acids or other aqueous solvents and effecting separations of the desired materials from the products of fission by precipitations, organic solvent extraction, adsorption, or ion exchange. Serious consideration is now being given to constructing a commercial plant using a solvent-extraction process. Vast improvements in the technology of the processes used have been and are being accomplished by vigorous research and development efforts, and the novel features of fuels devised for nuclear-power reactors are leading to new processes and still further improvements and adaptations to permit treating such fuels.

Preparation for Fuel Processing

Prior to separating the valuable heavy metals from the products of their fission, it may be necessary to remove structural materials from the reactor fuel assemblies by mechanical or chemical operations, to penetrate cladding materials, and to dissolve the fuel. Special treatment of the fuel solutions may also be desirable to simplify subsequent operations.

Mechanical Processing Methods

Oak Ridge National Laboratory (ORNL) reports[1–3] on a size distribution test on material produced by cutting four Mark I ORNL prototype fuel assemblies (porcelain-filled stainless-steel tube bundles) on the 250-ton shear.[4] Particle-size measurements showed that the less than 9520-μ (~$^3/_8$ in.) fractions from $^1/_4$-, $^5/_8$-, and 1.5-in. sheared lengths constituted 69, 21, and 6.6%, respectively, of the total particles, and fractions less than 44 μ were 5.2, 3.0, and 0.9%, respectively, of the total particles produced. Stainless-steel and braze-metal particles in the less than 9520-μ fractions were 33.3 and 2.6% of the total metal from $^1/_4$- and $^5/_8$-in. sheared lengths, respectively, with stainless steel comprising 33.1 and 2.57%, respectively, of the total metal. The amount of porcelain in the less than 9520-μ fractions were 93, 46, and 12% of the original amount from the $^1/_4$-, $^5/_8$-, and 1.5-in. cuts, respectively; porcelain constituted more than 99% of the material in the less than 590-μ fractions from all sizes sheared. Visual comparison of the sheared pieces larger than 9520 μ indicated that a sheared length of about $^9/_{16}$ in. would probably be optimum.

Fairly small amounts of fines (material smaller than 44 μ) were produced and were 1.5, 2.4, 4.3, and 5.2% for 1-, $^3/_4$-, $^1/_2$-, and $^1/_4$-in.-long cuts, respectively. Of this material approximately 50% was less than 3 μ.

Chemical Removal of Fuel Cladding Materials

In a report to the 1962 Nuclear Congress, Martens, Poe, and Wible[5] described the process used at Savannah River and Hanford for removing aluminum jackets by caustic dissolution from uranium fuels. The dissolver, which may contain a heel of declad slugs from previous operation, is charged with a fresh batch of slugs. Sufficient 23% sodium nitrate (which suppresses the evolution of hydrogen during the caustic-aluminum reaction) is added to cover the charge; this aids removal of decay heat until decladding is started. The solution is then brought to a boil using steam coils, and 50% sodium hydroxide is added at a rate that is controlled to limit the rate of hydrogen

evolution. Boiling is continued until the aluminum is dissolved, at which time the solution is jetted to waste. At least 1.25 moles of caustic are used per mole of aluminum; this yields a solution that is stable to precipitation for at least a day. Solution stability may be extended to a month with a caustic-to-aluminum molar ratio of 1.65. The ratio of sodium nitrate to aluminum varies from 1.0 to 1.4 at different plants. The presence of bare uranium, aluminum-silicon bonding agent, and magnesium appreciably increases the amount of hydrogen evolved, as compared to the reaction with 2S aluminum alone.

Dissolution Problems of Beryllium

Beryllium is a potentially useful cladding metal for nuclear fuels; it is indicated that beryllium resists dissolution in dilute nitric acid. Straumanis[6] states that beryllium dissolves with reasonable speed in $2N$ or $3N$ hydrofluoric, hydrochloric, or sulfuric acids. Lumps weighing on the order of 30 mg dissolved completely in these acids in less than 30 min at 36°C. In $0.5N$ hydrochloric acid, a black deposit that forms on the metal surface is dispersed later throughout the solution.

Electrolytic Dissolution

Clark and others[7] have recently summarized bench-scale work at the Savannah River Laboratory (SRL) on the electrolytic dissolution (or disintegration) of stainless steel, zirconium, aluminum, and graphite in nitric acid. In their work electrical contact was made with the fuel by containing it in a basket of tantalum or niobium. Maintenance of the high overvoltage of these metals under radiation was verified in a field of 10^7 rep/hr up to a total exposure of 10^9 rep. Sustaining uniformity of electrical contact is aided by vibrating or periodically tapping the basket. Arcing may occur unless

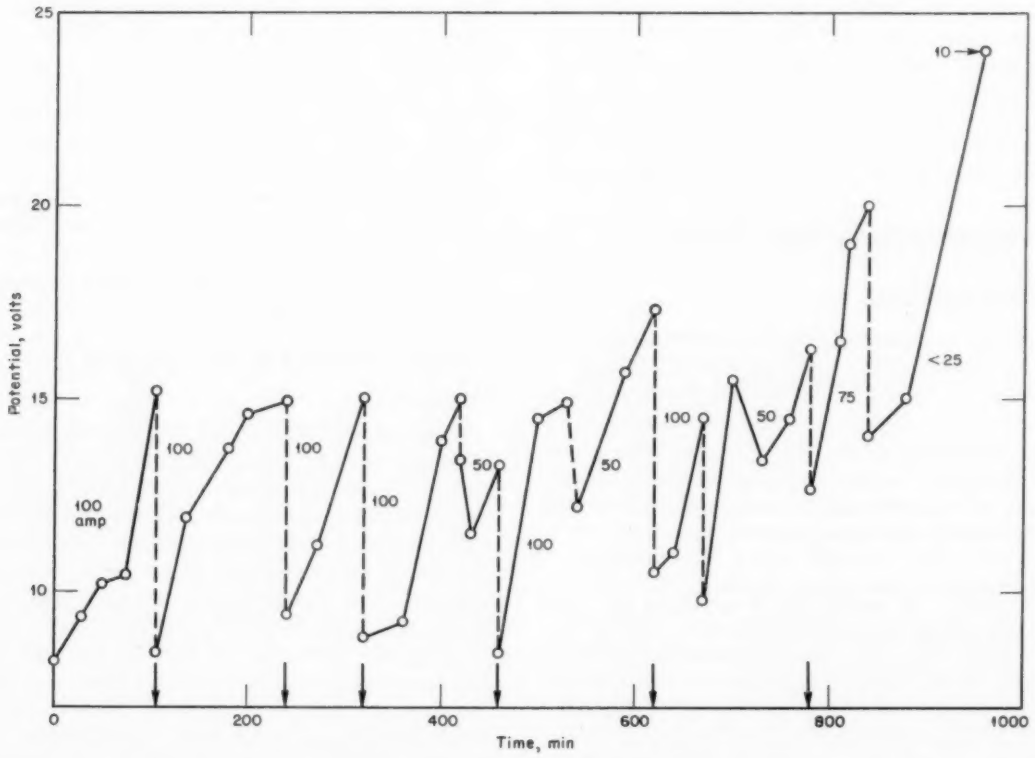

Fig. II-1 Electrolytic dissolution of stainless steel.[7] The electrolyte is 2 liters of $4M$ HNO_3, and the anode is 840 g of ½-in. stainless-steel tubing in a tantalum basket. Arrows indicate times at which acid was changed (new electrolyte).

this is done. The variations in contact effectiveness result in corresponding potential variations as illustrated in Fig. II-1.

Stainless steel is penetrated at a rate of 30 mils/hr (0.6 g/amp-hr) at a current density of 1 amp/cm^2, although side reactions may reduce the rate if the nitric acid strength is less than 2 M. Aluminum dissolves at a rate of 0.37 g/amp-hr in 1.5 M to 6M nitric acid, and the rate is not affected by the presence of mercuric nitrate, which is normally required as a catalyst for aluminum dissolution. Zirconium and Zircaloy-2 anodes disintegrate in nitric acid (1M to 10M) at an average rate of 1 g/amp-hr, although about 85% of the zirconium forms an insoluble zirconium dioxide precipitate, which spalls off the base metal and settles rapidly. In tests of electrolytic dissolution of Zircaloy-2-clad uranium dioxide cores in boiling 10M nitric acid, the uranium dioxide was rapidly dissolved and the zirconia sludge contained only 0.15% of the total uranium. Zirconium-clad uranium-molybdenum alloy is also electrolytically dissolved with little loss of uranium.

In recent large-scale studies at Savannah River, difficulties in maintaining good contact between the stainless-steel charge and the niobium basket in the 5000-amp dissolver led to an investigation of the series or liquid contact dissolver.[8,9] A sloped-bottom basket as shown in Fig. II-2 was developed for use in the 5000-amp dissolver previously described.[10] A mock fuel assembly of $\frac{1}{4}$-in. stainless-steel pipe, 10 ft in length, was progressively dissolved in this unit in several days at 2500 to 3500 amp with no evidence of arcing. The bottom of the dissolving charge assumes the shape of the basket, and the charge drops down as dissolution is continued.

Studies of the electrolytic dissolution technique have continued at the ICPP. Aylward[11] has recently described an electrochemical study of the potential-current relations for type 304 stainless steel in solutions with total nitrate concentrations up to 6 M. The Tafel relation ($E = a + b \log I$) was obeyed at current densities above 1 ma/cm^2. Secondary passivation occurred in the medium current density range at low hydrogen-ion and nitrate concentrations and at low temperatures. A limiting current density (about 1 amp/cm^2) was found above 6M nitric acid. Efficient anode operation was noted over a wide range of solution compositions at temperatures above 60°C.

Recent work at the ICPP has involved initial tests of a 500-amp electrolytic dissolver equipped with a niobium basket.[12] In dissolving a Nichrome rod, erratic operation was observed, even when cyclic hammering was used to improve electrical contact. In the beginning of the test, vibration was moderately effective in restoring and maintaining operation; however, the current could not be maintained long by this method alone. A platinum disk in the bottom of the basket increased the period of satisfactory operation by improving the electrical contact with the dissolving rod. The use of titanium, which forms a conducting oxide, was found to afford steadier operation, but the titanium was pitted by arcing at contact points. Corrosion of stainless-steel tubing downstream from the dissolver was severe. Tests of insulation materials for use in electrolytic dissolvers have been conducted at the boiling point up to an irradiation level of 10^{10} r. A polyethylene sample decreased markedly in its dimensions, but an alumina ceramic and a silicone glass fabric resin laminate were little changed.

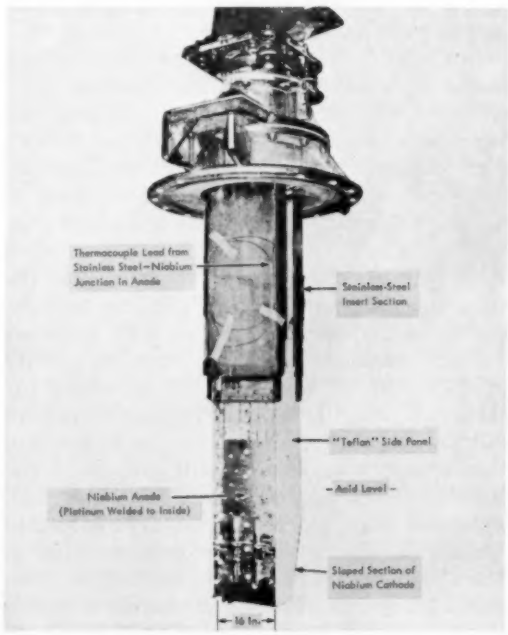
Thermocouple Lead from Stainless Steel–Niobium Junction in Anode
Stainless-Steel Insert Section
"Teflon" Side Panel
Acid Level
Niobium Anode (Platinum Welded to Inside)
Sloped Section of Niobium Cathode
16 In.

Fig. II-2 Liquid contact electrode and insert superstructure.[9]

Ammonium Fluoride Process

At Oak Ridge, demonstration has been completed of the ammonium fluoride decladding process on irradiated Zircaloy-clad uranium dioxide pellets.[13] In 22 runs with pellets irradiated up to 17,000 Mwd/ton of uranium, the cladding was removed in 2 to 3 hr by 6*M* ammonium fluoride containing 1*M* ammonium nitrate. Zirconium end plugs remained. Losses of soluble uranium and plutonium to the decladding solution averaged about 0.05%. One or 2% of the uranium dioxide was suspended as fines from fracture of low-density (93 to 95% of theoretical) pellets in the decladding solution; this could presumably be removed by centrifuging.

About 5 hr was required to dissolve the declad uranium dioxide core material in 4*M* nitric acid to produce a solvent-extraction feed containing 100 g of uranium per liter and 3*M* nitric acid. This was extracted under Purex-process conditions to yield one-cycle gamma decontamination factors of 1300 and 2100, respectively, for uranium and plutonium.

Dissolution of Fuel Cores

Martens[5] has recently described the production plant technology for batch dissolution of declad natural-uranium slugs, 14-ft-long enriched uranium–aluminum alloy tubes, and the declad NRX and NRU uranium rods and plate bundles which are 10½ ft long. Sufficient 50% nitric acid is added to the declad fuel to dissolve approximately one-half of the uranium charged (the first cut). The acid is added in two parts to minimize the vigor of the reaction, and the dissolver is heated rapidly to 70 to 80°C to start the reaction. At the SRP, the remaining acid is not added until the specific gravity of the solution reaches 1.55. Dissolution is continued until the specific gravity reaches 1.67 to 1.69, but, if the rate of increase in specific gravity is less than 0.012 unit/hr for 2 hr, dissolving is stopped to ensure that free acid is still present. If the dissolving reaction consumes too much acid, plutonium may hydrolyze and form insoluble compounds. At the end of the reaction, dilution water is added to prevent uranyl nitrate from crystallizing out, and the dissolver is rinsed with water after transfer of the solution.

With the existing equipment at Savannah River, it has been found that dissolving time is reduced by increasing the nitric acid concentration from 37 to 50% but cannot be further reduced with 57% acid because of inability to handle higher off-gas rates. Dissolving rates for uranium also appear to increase somewhat with increased irradiation of the uranium. Dingot uranium metal, which is low in impurities and is prepared by omitting the usual vacuum remelt in graphite crucibles, dissolves more slowly than the standard ingot material.

Enriched uranium–aluminum alloy tubes are dissolved in a standard batch dissolver fitted with special inserts and columns to hold the tubes above the floor of the dissolver and to provide a downdraft condenser. Dissolution may be carried out in 15 to 40% nitric acid containing up to 0.017*M* mercuric nitrate, but it is not carried out to completion for each batch of fuel charged. A heel remains to be dissolved with the next batch.

Sintered Unirradiated UO_2

Taylor and others[14] in work at Harwell have studied the dissolution of sintered unirradiated uranium dioxide pellets in nitric acid. They report that up to a concentration of at least 8*M* nitric acid the dissolution rate is about proportional to the third power of the acid concentration, whereas at high concentrations the dissolution rate is directly proportional to the acid concentration. To a first approximation, the speed of dissolving depends much more on the total nitrate concentration than on the nitric acid concentration itself. Thus replacing up to 90% of the free acid present in the system by its nitrate equivalent of metal salt has relatively little effect, although with no free acid the dissolution rate falls to a negligible value.

Dissolution of uranium dioxide is accelerated by oxidants such as ferric ion, by polyvalent nitrates, and by the products of dissolution. Agitation, as by mechanical stirring or boiling, can reduce the dissolution rate quite markedly, as shown in Fig. II-3.* This effect is attributed mainly to the dispersion of nitrite ions away from the reaction face.

The rate of dissolution of uranium dioxide increases with temperature at a level corresponding to an activation energy of about 15 kcal/mole up to a region [corresponding to a rate of about 4 mg/(cm²)(min)] at which the rate appears to become diffusion controlled. In 6*N* nitric acid at 80°C, the rate of dissolu-

*Figure II-3 is reprinted here by permission from the United Kingdom Atomic Energy Authority.[14]

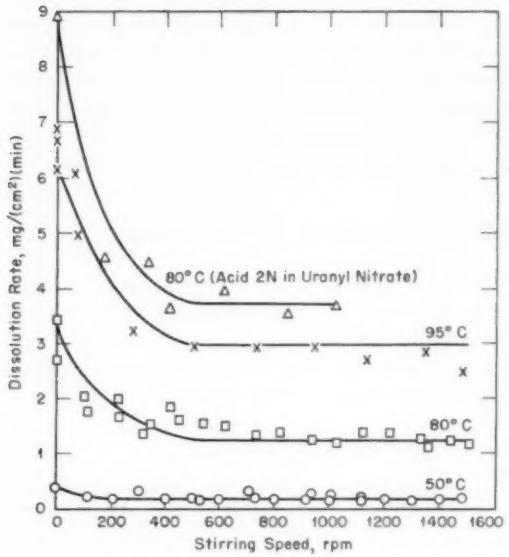

Fig. II-3 Effect of agitation on the dissolution rate of sintered uranium dioxide in 6*N* nitric acid (with and without uranyl nitrate).[14]

tion was decreased as much as severalfold as pellet bulk density was increased in the range 10.4 to 10.7 g/cm^3.

Aluminum-Clad Plutonium-Aluminum Alloys

Alloys of plutonium and aluminum are used as reactor fuels in programs both for the production of higher plutonium and transplutonic isotopes and for the development of plutonium as a power-reactor fuel. Perkins[15] at SRL has studied the dissolving of an irradiated aluminum-clad alloy of 7% plutonium in aluminum which is used for producing higher plutonium isotopes. In a typical dissolution the clad fuel was immersed in boiling 6*M* nitric acid containing 0.003*M* mercuric nitrate, which dissolved the 0.1-in.-thick aluminum cladding in about 30 min. Core material was then attacked very slowly. The mercuric nitrate concentration was then increased to 0.05*M*, and hydrofluoric acid was added to a concentration of 0.02*M*, to dissolve the core. A rapid attack followed, and the core (about 0.8 in. in diameter) was dissolved in about 4 hr to yield a 1.5*M* aluminum nitrate solution containing 0.9 g of plutonium per liter and 1.3*M* nitric acid. Although the addition of fluoride to the dissolver solution was not essential for rapid reaction in every case, its use provided consistent attack. The presence of free acid is essential to avoid the precipitation of a polymeric plutonium compound.

At Hanford, aluminum alloyed with 1.8% plutonium and 2% nickel, and clad with Zircaloy-4, is one of the fuels used in the Plutonium Recycle Test Reactor (PRTR). Irradiated fuel of this type has shown markedly different behavior toward dissolution in nitric acid–mercuric nitrate than the unirradiated material.[16,17] Removal of Zircaloy cladding was readily accomplished with ammonium fluoride–ammonium nitrate. In two instances the irradiated declad fuel was not activated in boiling 6*M* nitric acid containing 0.005*M* to 0.05*M* mercuric nitrate and 0.03*M* ammonium fluoride. Activation was effected by partial immersion in 1*M* nitric acid, with less mercury and fluoride, and it was then possible to achieve rapid dissolution by adding nitric acid to reach a concentration of 6*M*.

Total Dissolution of Metallic Fuels

At the ICPP interest continues in adapting the hydrofluoric acid dissolution process to the continuous dissolution of fuels composed of small percentages of highly enriched uranium alloyed and clad with Zircaloy. A limitation of this process is imposed by the solubility of uranium tetrafluoride in acid zirconium fluoride solutions. The complete dissolution of alloys containing more than 1 to 2% uranium requires oxidation of uranium to the hexavalent state. Oxidants in conjunction with hydrofluoric acid impose a severe corrosion problem. In operation of a continuous dissolver, it is thought that complete dissolution is not essential provided that solids do not accumulate too rapidly and can be removed.

Small-scale continuous dissolving has been made using 4.8*M* hydrofluoric acid containing 0.03*M* nitric acid as the dissolving reagent. In a 300-hr run with a simulated fuel containing a nominal 2.3% uranium,[12] dissolver deposits were no heavier at 300 than at 100 hr and were not such as to affect operability. At the conclusion of the test, a simulated heel cleanout was attempted by continuing the reaction for 10 hr with Zircaloy containing no uranium, followed by water flushing. Deposits were markedly reduced but were not completely removed.

Kitts and Clark[18] have recently summarized Oak Ridge work on dissolving stainless steel

uranium dioxide fuel compositions using dilute aqua regia (nitric-hydrochloric acid solutions), from which the chloride is removed by distillation after dissolving. Illustrations and data are given of batch and continuous processes applied to the SM-1, Yankee, and N.S. *Savannah* reactor fuels. A considerable portion of the report is devoted to problems of and techniques for chloride removal.

Dissolution of Aluminum-Clad Oxide Elements in HCl

In the Oak Ridge program for the production of higher transuranic elements, it is proposed to dissolve aluminum-clad oxide target elements in hydrochloric acid. In the High-Flux Isotope Reactor (HFIR), it is calculated that about 2% of the aluminum will be transmuted to silicon per year,[19] and tests on alloys containing 0.1, 0.3, and 3% silicon indicate that silicon will inhibit the dissolution of aluminum. In the range of 1*M* to 6*M* hydrochloric acid, the dissolution rate of all three alloys was proportional to the third power of the acid concentration. For a given acidity the dissolution rate was inversely proportional to the silicon content of the alloy.

Treatment of Fuel Solutions Before Extraction

Martens, Poe, and Wible[5] have also described the operations carried out at AEC'S large-scale fuel-processing facilities to prepare fuel solutions for solvent extraction. At Hanford, until 1959, uranium fuel solutions were first clarified by centrifuging to separate suspended solids, but no significant adverse effects on the performance of solvent-extraction columns or on decontamination have been noted since this operation was suspended. At the SRP, precipitations may be carried out on the feed solutions, which may be centrifuged and the clarified solution evaporated.

A process employed at Savannah River on natural-uranium solutions utilizes freshly formed manganese dioxide to remove the bulk of the zirconium and niobium fission products. Manganous nitrate is added to a batch of metal solution heated to 70°C. Sufficient 3% potassium permanganate is added to react with 85% of the manganous ion. The slurry is digested 1 hr, cooled, and centrifuged in a 40-in. bowl at 1740 rpm. This generally removes 80 to 90% of the zirconium-niobium, although less is removed if acidity is increased. This head-end treatment may also remove up to 30% of the ruthenium, which is given off largely as the volatile tetroxide. This is absorbed in a steam-heated tank packed with stainless-steel wool. A gelatin scavenging process that was used first at Savannah River to remove silica from enriched-uranium solutions is also described.

Separations Processes

Organic solvent extraction is largely used for the separation and decontamination of uranium, plutonium, and thorium, but ion exchange and precipitation may also be used to effect separation of one element from another.

Solvent-Extraction Processes

Extraction-Process Developments. Harmon, in a review of current solvent-extraction technology presented at the 1962 Nuclear Congress,[20] has described a number of improvements in the methyl isobutyl ketone (Redox) and tributyl phosphate (Purex) solvent-extraction processes for uranium and plutonium as carried out at the Hanford, Savannah River, and Idaho chemical processing plants. Perhaps the most significant of these are waste backcycle and acid destruction to reduce waste volumes and process adaptations to recover neptunium.

In the past 10 years of Redox-process development at Hanford, the volume of high-level radioactive waste stored per unit of uranium processed has been reduced by a factor of 8, largely by the use of raffinates from the second and third extraction cycles as scrub and salting agents for the first and second cycles. Figure II-4 illustrates schematically one way in which three cycles of solvent extraction can be operated on the equivalent of the salt requirement for a single cycle (heavy lines denote the aluminum nitrate flow pattern). Owing to the marked change in flow sheet resulting from waste backcycle, interest in recovery and decontamination of aluminum nitrate is apparent, and development work is in progress which could mean a Redox process competitive with the Purex system and possessed of the advantages of methyl isobutyl ketone solvent with respect to simple cleanup for reuse.

A similar waste backcycle application has been made to the Hanford Purex process as shown in Fig. II-5. The aqueous wastes from

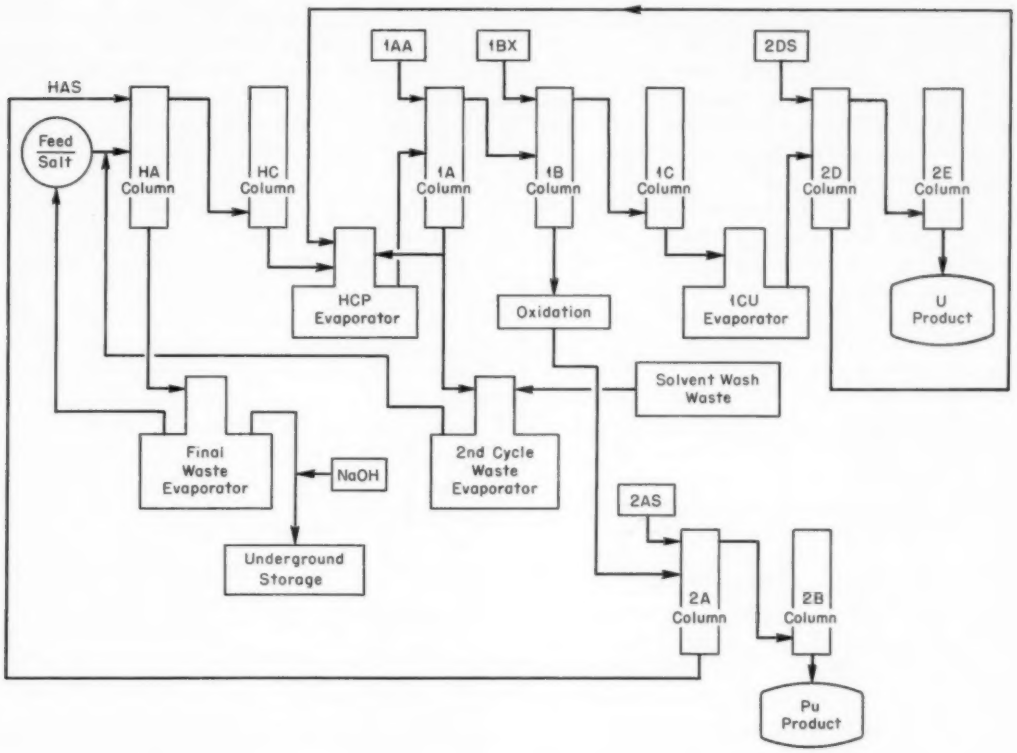

Fig. II-4 Waste backcycle flow pattern — Redox three-cycle process.[20]

the final uranium and plutonium cycles are combined, concentrated, and recycled to the first extraction column. This permits the use of conditions that result in incomplete extraction of uranium or plutonium in the later cycles, since such waste losses are simply returned to the first cycle for recovery. Acid fed to the 2A column may also contain uranium (as derived from uranyl nitrate decomposition) since the final partition occurs subsequently.

This flow sheet permitted the reduction of the high-level waste volume by a factor of 3 and the losses of uranium and plutonium by factors of 2 as compared to earlier operations. Separation of uranium and plutonium is more than adequate for this flow sheet. Gamma decontamination of both products requires supplemental treatment, however. The uranium product solution is passed over a silica-gel bed, whereas the plutonium product is purified in a continuous anion exchanger. A 20% further economy in waste volume is effected by formaldehyde destruction of nitric acid and concentration of the waste.

In the acid-deficient Redox process, neptunium and transplutonic isotopes are quantitatively routed to the first-cycle raffinate. A flow sheet has been developed to allow recovery of this element along with plutonium and uranium. The heavy dashed line in Fig. II-6 shows the normal path of neptunium, and the heavy solid line shows how this element can be continuously accumulated by internal recycle for subsequent removal on a batch basis. This flow sheet works on the principle that hexavalent neptunium is extracted by methyl isobutyl ketone in an acidic system and is not extracted in an acid-deficient system. To compensate for the loss of ruthenium decontamination (by factors of 10 to 100) in the acidic system, ozone sparging of both products was necessary.

A similar accumulation and batch removal system can be used to recover neptunium en-

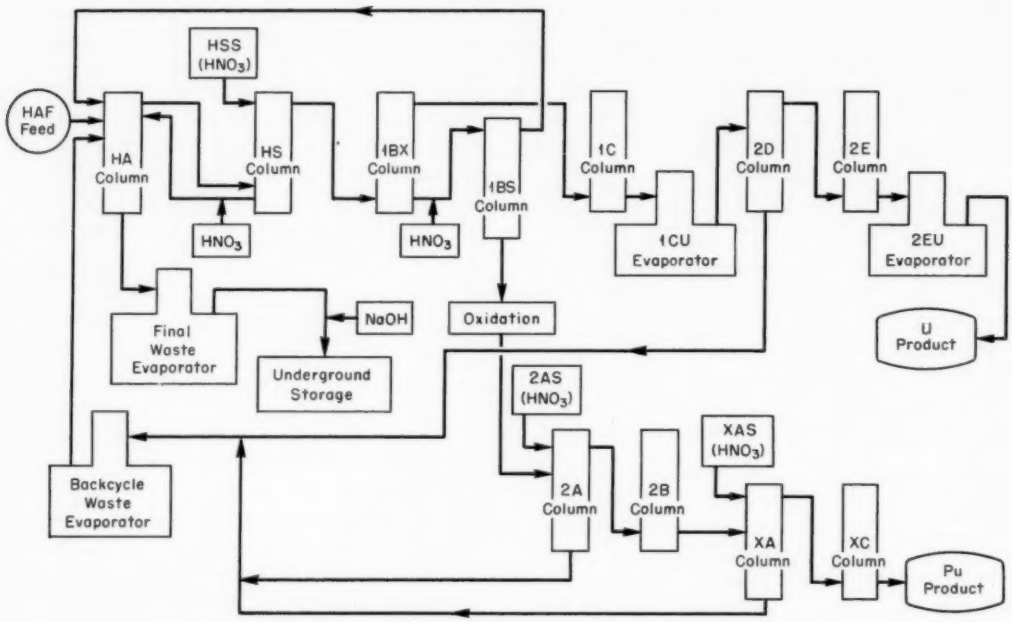

Fig. II-5 Waste backcycle flow pattern — Purex two-cycle process.[20]

tering with the fuel in the Hanford Purex process. At Savannah River, neptunium is recovered along with minor quantities of plutonium contained in first-cycle raffinate by further processing of the raffinate.

New Uranium-Thorium Recovery Processes

Rainey and Moore[21] have recently published the laboratory studies leading to an acid Thorex (using TBP) process for uranium-thorium recovery from fuel of a Consolidated Edison reactor type (95% thorium dioxide–5% uranium dioxide). An acid-deficient thorium nitrate feed is extracted with 30% TBP in a diluent. Concentrated nitric acid is added partway down the column to decrease thorium losses. The rising organic phase is first scrubbed with 1 *M* nitric acid containing phosphate ion and ferrous sulfamate, and then with the phosphate and sulfamate alone. This gives high decontamination from both ruthenium and zirconium and good recovery.

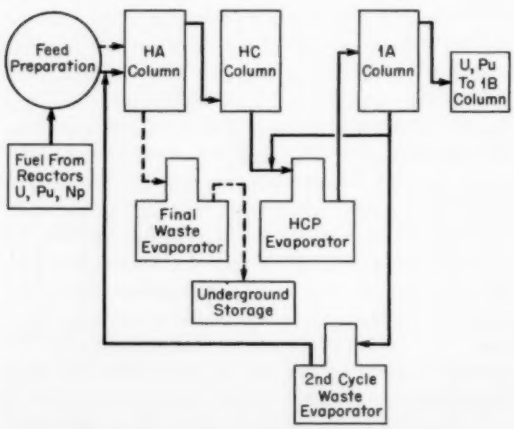

Fig. II-6 Neptunium accumulation, Redox process.[20]

At Oak Ridge, studies are being made of uranium-thorium separation by solvents other than TBP. In a countercurrent batch extraction of an acid-deficient, aluminum nitrate-salted solution containing 5 g of uranium and 10 g of thorium per liter with 2.5% di-*sec*-butylphenyl phosphonate, the uranium was freed from thorium with a decontamination factor of over 20,000 and a 0.03% uranium loss. In a similar test with a TBP solvent, the thorium decontamination factor was only 2500 but the uranium loss[2] was less than 0.01%.

Russian Solvent-Extraction Data

Three Russian articles, providing basic data of interest in TBP solvent-extraction process

calculations, have recently appeared in the form of English translations. The first, by Shevchenko and others,[22] gives data on the effect of the nature of the TBP diluent and on the effect of the concentration of TBP on the distribution coefficients for nitric acid between water and solvent solutions. At low TBP concentration, variations in distribution coefficients within a factor of about 2 were found using kerosene, benzene, toluene, carbon tetrachloride, and difluorotetrachloroethane as diluents. A second article, by Fomin and others,[23] reports that an apparent deviation from linearity in the relation between the Pu(IV) distribution coefficient from a 2.0*M* nitric acid solution and the TBP concentration in TBP-diluent systems, for data obtained by alpha-counting techniques, is due to inextractable americium. In a third article, by Maiorova and Fomin,[24] distribution data are given for thorium between nitric-sulfuric and nitric-perchloric acid systems and 1.0*M* TBP in benzene. The existence of complex ions with two ligands was indicated in the sulfate-nitrate systems.

Solvent Stability. In a review of solvent-extraction processing, Harmon[20] notes that one of the severest limitations on attainable product purity is the quality of the solvent and that much work has been expended in searching for better diluents and in developing better methods of treating used solvents for recycle. Plant tests of potentially better diluents have been made. Hanford for a long time used Shell E2342 diluent and Savannah River used Ultrasene, both of which are nonaromatic petroleum fractions ranging from 20 to 70% in naphthenes. Hanford has recently tried Soltrol-170, a synthetic alkylate produced by polymerization and hydrogenation of short-chain olefins. Improvement in overall process performance was indicated but not definitely proved. A marked shift was observed in the spectrum of activity in the used solvent after washing, when, without appreciable change in the ruthenium content, the zirconium-niobium content dropped by about a factor of 3 from the level normally observed with Shell E2342.

At Savannah River, detailed laboratory studies have been made of the stability of a variety of proposed TBP diluents. Dennis and West[25] have recently described tests of 25 such materials. Harmon[20] reports that these investigations revealed that saturated straight-chain hydrocarbons showed the greatest stability and that Savannah River had recently adopted Adakane-12 for first-cycle use in the natural-uranium process flow sheet. This diluent, a synthetic dodecane, proved superior to Ultrasene to an extent that justified its greater cost.

Harmon[20] also reports an interesting study made by Orth at Savannah River of solvent-extraction decontamination performance in relation to other process variables. Average weekly values of first-cycle decontamination factors for uranium and plutonium were plotted against washed solvent activity content. On log-log scales, data were correlated as shown in Fig. II-7, in which the ordinate and abscissa units are strictly arbitrary, but in which the data bandwidths include a factor of about 2. It was concluded that solvent quality, as indicated by activity level, is the principal variable affecting process performance and that, with good solvent quality, decontamination approaches a limiting factor that can represent the ultimate efficiency attainable with the given process and equipment. With a given solvent treatment system, the quality of the treated solvent is simply the result of an equilibrium established between the rate of damage done to the input solvent and the rate of removal of degradation products in the solvent treatment operation.

It is well known that one of the undesirable products at TBP solvent degradation is dibutyl phosphoric acid, whose compounds with uranium and zirconium more strongly favor the aqueous phase than do those of TBP. At the

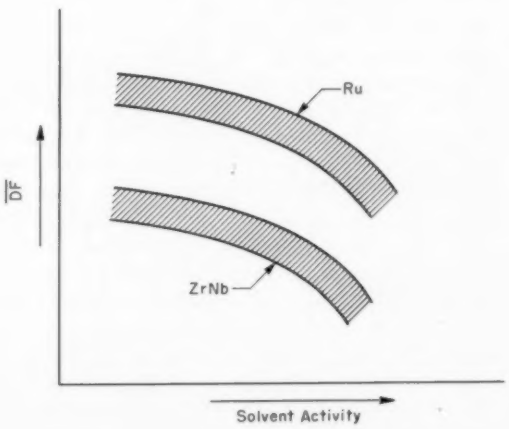

Fig. II-7 First-cycle decontamination as a function of solvent activity at SRP.[20]

ICPP the removal of dibutyl phosphoric acid from an aqueous phase by the zirconium oxide ion-exchange material Bio-Rad HZO-1 is being investigated.[12] In contact with a 0.03*M* nitric acid solution containing 0.05*M* dibutyl phosphoric acid, the ion-exchange material had a capacity of 0.4 meq of dibutyl phosphoric acid per gram of ion exchanger, which dropped to 0.05 meq if the solution also contained 0.03*M* uranium.

Separation of Transuranic Elements. Gram quantities of transuranium elements for research uses are to be produced in the HFIR and transuranium processing facility (TRU) being built at Oak Ridge. Isotopes that will be separated in the TRU facility include those of curium, berkelium, californium, einsteinium, and fermium. These will result from irradiation of higher plutonium, americium, and curium isotopes that will be produced by long irradiation of Pu^{239} at Savannah River.

A tertiary amine extraction process that was developed by Baybarz at Oak Ridge for separation of the transuranium elements from the lanthanides was previously described.[4] In another extraction process, which was developed for separation of berkelium, californium, and einsteinium from americium and curium, the solvent used is 2-ethylhexylphenyl phosphoric acid in diethylbenzene.[19] A preliminary flow sheet for this process is given in Fig. II-8. In a seven-stage laboratory test under similar conditions, 99.9% of the californium was recovered with an americium removal of greater than 99.9%.

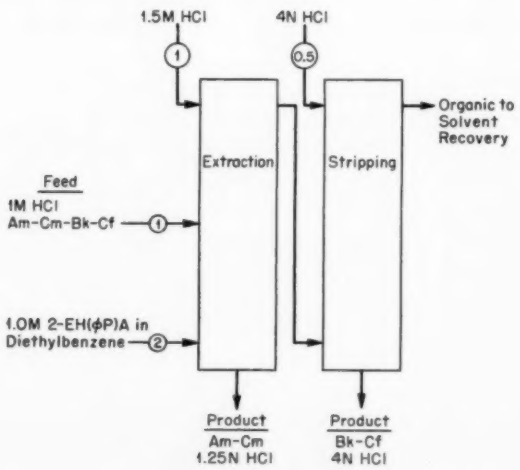

Fig. II-8 Transuranium-element separation flow sheet.[19]

Ion-Exchange Processes

In connection with Hanford studies of the efficiency of an ion-exchange contactor for plutonium recovery, Carroll[26] has determined the transfer kinetics and equilibrium distribution coefficients for thorium on Permutit SK anion-exchange resin in a nitrate system. Thorium is absorbed as a hexanitrate complex from concentrated nitrate solutions in complete analogy to the plutonium system. Effects of acid and thorium concentrations and the effect of temperature were determined. Equilibrium resin loadings were found to decrease markedly with decreasing acid or thorium concentration and to some extent with increased temperature. Diffusivity of thorium within the resin was found to increase by a factor of 6 as the nitric acid concentration was decreased from 8*M* to 0.5*M* and was found to be independent of thorium concentration.

In the Oak Ridge studies of inorganic ion-exchange materials, equilibration of a dilute nitric acid solution containing uranium, sodium nitrite, and a small amount of plutonium with a zirconium-silicon-phosphate exchanger removed 99% of the plutonium.[1] Less plutonium was removed from a more acid solution.

Precipitation Processes

In a previous Review, studies carried out at the ICPP on the precipitation of zirconium and fluoride as barium fluozirconate from hydrofluoric acid solutions of low-uranium-content zirconium alloy fuels were described.[27] This process would permit a marked increase in extraction-column feed concentration and, consequently, of system capacity; a significant decrease in the volume of difficult-to-store waste; and the production of a major fraction of the long-lived fission-product waste in solid form. Studies have continued on an alternate process to accomplish similar ends. This involves the precipitation of sodium fluozirconate following addition of sodium formate.[28]

A proposed flow sheet for sodium fluozirconate precipitation is shown in Fig. II-9. To a solution resulting from dissolving the zirconium alloy in hydrofluoric acid (hydrogen peroxide may be used to dissolve uranium to achieve the

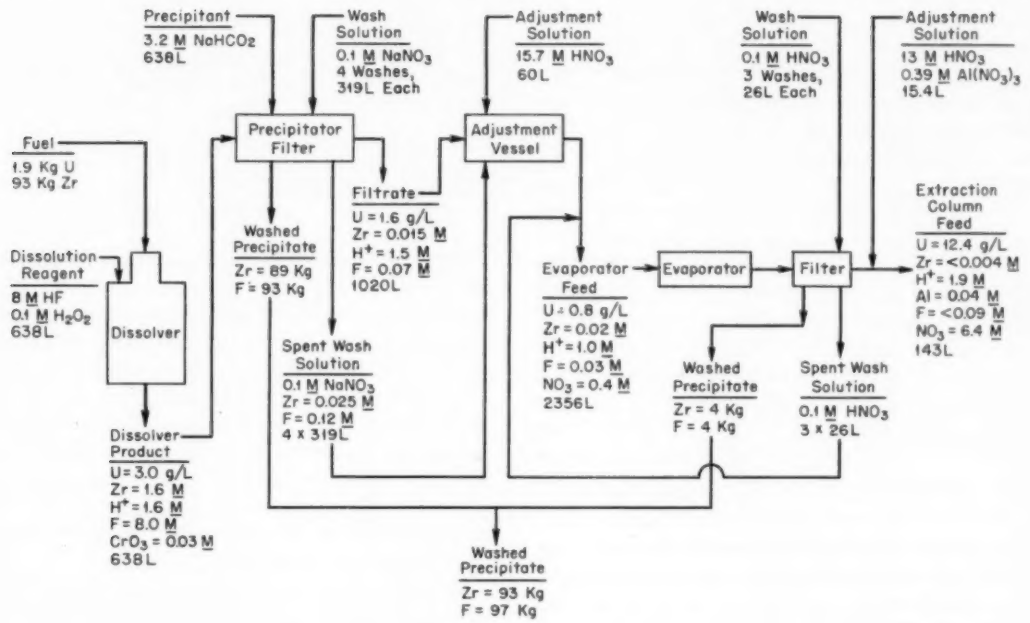

Fig. II-9 Sodium formate precipitation of zirconium and fluoride from hydrofluoric acid solutions.[28]

solubility attainable in the uranyl state), an equal volume of 3.2*M* sodium formate is added to about 60°C. The ratio of fluoride to zirconium is preferably about 5. Within a few minutes a precipitate is formed which corresponds approximately to the composition $Na_3Zr_2(OH)F_{10}$ and which settles readily. The precipitate, which contains 95% of the zirconium, is filtered from the solution and washed with two volumes (four washes) of dilute sodium nitrate. The combined filtrate and washings are adjusted to 0.4*M* nitric acid with concentrated acid and boiled down to about one-twentieth of the evaporator feed volume (one-fifth of the dissolver volume), and the solution is then filtered. This filtrate is adjusted to make a suitable extraction-column feed by adding a volume of 13*M* nitric acid–0.39*M* aluminum nitrate solution equal to one-eighth of the filtrate volume. A few percent of additional zirconium fluoride is precipitated in the evaporation step and must be washed with dilute nitric acid unless the acidity is increased to about 1.0*M* and the boildown is reduced somewhat. Precipitate washings from the last step may be recycled to the evaporation step. Boiling with sufficient nitric acid to destroy the sodium formate is necessary since the formate inhibits subsequent uranium extraction.

Process Instrumentation

In any pulse-column system, it is desirable to obtain an indication of the pulse amplitude and of possible means of controlling the amplitude. This was especially desirable with the recent installation of air pulsers at the ICPP.[4,29]

Toward this end, experiments that are reported by Erickson[30] are being run using instrumentation to integrate flow with respect to time. Figure II-10 shows a block diagram of this setup. A Ramapo flow transducer installed in the pulser leg provides a millivolt-level signal that is proportional to the square of the volumetric flow rate of the fluid in the pulser leg. A Sanborn strain gauge preamplifier is part of the data recording system and includes the necessary excitation voltage, bridge balance, and calibration controls for the flow transducer. It also provides an output voltage that is a voltage analog of the transducer output as recorded and therefore is influenced by the attenuator setting on the preamplifier. This output voltage is the input to a three-stage computer using standard d-c operational am-

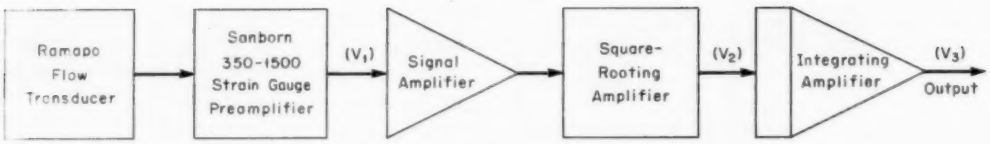

Fig. II-10 Block diagram of flow and position computer.[30]

plifiers. The first stage is a voltage amplifier, the second stage extracts the square root of the amplifier voltage to provide a signal proportional to the velocity, and the third stage integrates the velocity signal to represent the position of the fluid in the pulse leg. It was reported that calibration of the instrument by comparison with visual observation at either low frequency or low amplitude was within 5%.

Thermal Flowmeter

Kessie at Argonne National Laboratory reports[31] on some refinements to the conventional thermal flowmeter. Figure II-11 shows the essential arrangement of the classical thermal flowmeter. However, this form of the thermal flowmeter has two important disadvantages: (1) the calibration curve is such that any particular reading can be given by either one of two flow rates, and (2) the time of response to flow changes is slow at lower flow rates.

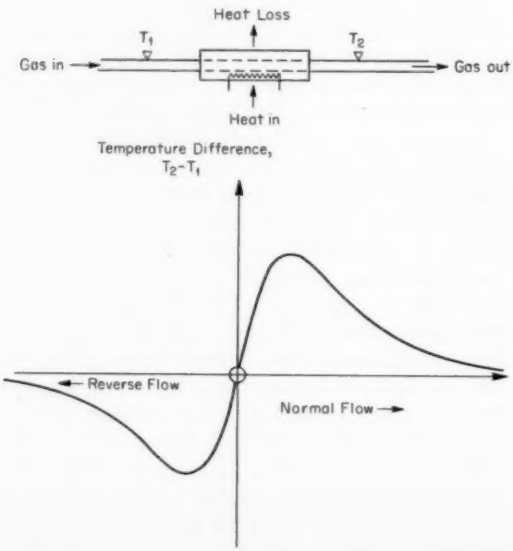

Fig. II-11 Classical thermal flowmeter.[31]

The two-valued calibration curve is a consequence of the following. For a given heat input rate, the temperature difference decreases from a higher value as the flow rate is increased. However, for a symmetrical construction the temperature difference is zero at zero flow. Thus the pattern of the classical flowmeter is such that the temperature difference rises from zero to a maximum after which it falls asymptotically to zero again. The maximum value is determined by heat losses and conduction in the pipe.

A modified thermal flowmeter design has been developed which does not have the above disadvantages. In principle it consists of a short length of pipe with different constant temperatures maintained at the ends. With no flow, the temperature along the pipe is determined by heat conduction along the pipe wall due to the temperature difference. Midway between the fixed temperatures, the pipe temperature will be the average of the two temperatures. As the flow increases, the midpoint temperature will approach the inlet temperature.

A design using two pipe sections in a symmetrical U configuration is shown in Fig. II-12. The top block is held at a fixed temperature above the lower block, which is not necessarily at a controlled temperature. This reduces the amount of control equipment and allows the bottom block to approach the inlet gas temperature. Use of two gas passes in opposite directions between the fixed temperatures, and measurement of the output across the two midpoints, reduces the effect of external temperature changes and temperature cycling of the top block. This version of the thermal flowmeter has a very wide useful range. It is capable of measuring gas flow rates of 10 ml/min to 100 liters/min. Among the gases used have been hydrogen fluoride, uranium hexafluoride, bromine pentafluoride, and fluorine.

The report gives details on the construction of the particular model used. An extensive dis-

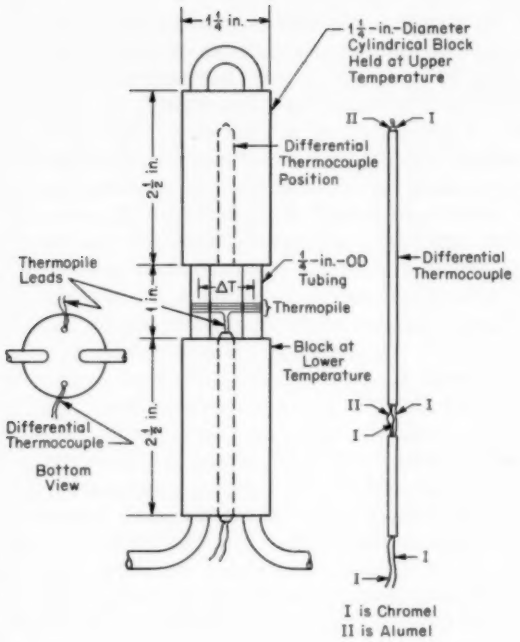

Fig. II-12 Mark II thermal flowmeter and differential thermocouple.[31]

cussion of temperature measurement and a mathematical analysis of the design are also included.

Plant Design and Operation

Two papers of general interest to the aqueous processing plant designer were presented at the 1962 Nuclear Congress. In one of these papers, Christl and Daking[32] discussed the latest thinking on remote maintenance, and, in the other paper, Bresee and Long[33] discussed direct maintenance.

Christl suggested that one of the new concepts that would enhance a remotely maintained plant is the use of television monitors for crane work to eliminate the shielded cab, optical system, and cab runway. Better ventilation design would result in less likelihood of contaminating areas outside the cells. Costs of original installation of equipment can be reduced by relaxing installation tolerances on remote connections from $\pm 1/16$ in. in all directions to about $\pm 1/4$ to $\pm 1/2$ in. and then fixing locations of these connections by optical measurements (although some flexibility would be lost in the interchangeability of jumpers). It was further pointed out that, for equipment beyond the second cycle of decontamination, direct maintenance would probably prove more economical. Compartmentalization was considered for all phases of the equipment, especially for normally cold equipment (such as steam traps) that service highly radioactive equipment.

The general field of waste disposal was discussed, and included in the discussion was the relatively new problem of tritium from fission [600 curies/day from the processing of fuels from reactors totaling 50,000 Mw(t)]. The tritium appears as the oxide HTO and follows the aqueous stream. Dilution by large amounts of water or by disposal to the atmosphere appears feasible but must be evaluated.

Bresee's paper on direct maintenance indicated that, in most cases, the design would be tempered by some remote maintenance techniques and good design would fall at a very definite location on the so-called maintenance spectrum (see Fig. II-13). One of the necessary requirements for direct maintenance is that there be a reasonable means of decontaminating the equipment. The paper mentions the ORNL fluoride-volatility process and the chop-leached head-end process as two cases where direct maintenance would be impractical.

The effect of expected equipment failure during plant life, which might reasonably be short during a period of rapidly changing technology, was discussed relative to installing duplicate equipment; Table II-1 illustrates this.

Costs of duplicating equipment can be high, especially if separate lines are installed in different cells, and this constitutes one of the disadvantages of a directly maintained plant. Advantages mentioned for a directly maintained plant were the following: no in-cell crane, more

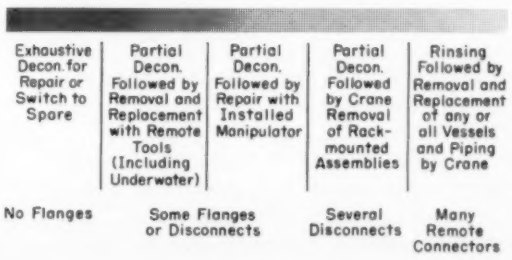
Exhaustive Decon. for Repair or Switch to Spare
Partial Decon. Followed by Removal and Replacement with Remote Tools (Including Underwater)
Partial Decon. Followed by Repair with Installed Manipulator
Partial Decon. Followed by Crane Removal of Rack-mounted Assemblies
Rinsing Followed by Removal and Replacement of any or all Vessels and Piping by Crane
No Flanges
Some Flanges or Disconnects
Several Disconnects
Many Remote Connectors

Fig. II-13 The maintenance spectrum.[33]

Table II-1 EFFECT OF NUMBER OF EQUIPMENT FAILURES ON CHOICE OF MAINTENANCE COURSE[33]

No. of major* failures during expected life of plant	Maintenance course
0	Decontamination only
1	Equipment duplication
2	Limited replacement, or equipment duplication with facilities for decontamination and repair of standby line
3 or more	Provision for replacement, increasing with the probable number of major failures

*A major failure is any failure which, in the absence of equipment duplication or provision for replacement, would necessitate plant decontamination and cell entry for repair.

efficient use of space, and generally more compact plants.

From these two papers it would seem that the large-capacity plants would lend themselves to remote maintenance and smaller plants to direct maintenance, with each design making use of both concepts, depending upon economics and safety.

Corrosion and Construction Materials

A topical report on the application of the Darex process to the dissolution of stainless-steel-containing reactor fuels has been published by ORNL.[18] The report concerns itself principally with the total dissolution of fuels containing uranium dioxide, such as those from the SM-1 (formerly called the Army Package Power Reactor) and Yankee reactors. This report consolidates much of the corrosion work that has been reported previously in *Reactor Fuel Processing*. Some of the more generalized conclusions regarding the selection of construction materials for the various components of a Darex plant, together with more detailed information that has not been published previously, are given below.

The process consists of decladding and dissolving stainless-steel-matrix fuels in a mixture of 5*M* nitric acid–2*M* hydrochloric acid. In order to reduce the corrosiveness of the dissolver product in subsequent processing steps, it is stripped in a distillation column with 15*M* nitric acid vapors. This reduces the chloride content to an acceptable level for handling in austenitic stainless-steel extraction equipment. Following feed adjustment, the solution is processed by solvent extraction. The corrosion data presented in the report confirm that titanium, of all the materials tested, is best able to withstand normal dissolver, condenser, stripper, and feed-adjustment conditions. Under none of the conditions encountered does the corrosion rate exceed 1 mil/month. Tantalum also showed negligible corrosion rates under all conditions tested, but it became slowly embrittled due to hydrogen pickup when held for long times at the potential that tantalum assumes when in contact with dissolving uranium metal. Titanium at no time was observed to suffer from hydrogen embrittling phenomena. Corrosion results for other alloys are included in the report.

Corrosion that occurs under heat-transfer conditions is usually more serious than that obtained when no heat is transferred. In order to evaluate titanium corrosion under these conditions, steam at about 135°C was passed through tubes immersed in boiling dissolver solutions that were characteristic of the beginning and final dissolution conditions. Rates of corrosion ranged up to a maximum of 2 mils/month, which is considered acceptable.

It was established that type 304L stainless steel should not be used for lines for the transfer of Darex dissolver solutions. The chloride content, solution velocity, and temperature were considered to be adverse factors. However, in long-term tests extending up to two years, little corrosion of type 347 stainless steel was observed when it was exposed to conditions simulating the Purex extraction of uranium from Darex dissolver solutions which had been stripped of chloride and in which the feed had been adjusted. Two types of aqueous solutions were used for these tests, both containing 2*M* nitric acid: one had a high concentration of dissolved stainless steel and a low concentration of uranium, whereas the second solution had a high concentration of uranium and a low concentration of stainless steel. The chloride content varied from 2 ppm to 1 wt.%. These aqueous solutions were mixed with an organic phase in a ratio of 2 to 3. The organic phase consisted of 1 volume of TBP and 2 volumes of Amsco 125. Stressed and welded specimens were included in the test. After two years no

sign of attack was observed on any specimen except a slight brightening of the surfaces. Weight changes were considered to be insignificant. No cracking or other localized attack could be found by metallographic study of the specimens.

Neither stainless-steel type 304L nor 347 can be recommended for equipment used to extract fission products from the Darex-Purex raffinate. The surfaces of specimens of these two steels were heavily corroded in 1000 hr when exposed to boiling solutions of the composition expected for such processing, namely, 3*M* nitric acid containing the equivalent of 60 g of dissolved type 304 stainless steel per liter and 0, 400, and 800 ppm chloride. There was no stress-corrosion cracking, but a knife-line attack in one of the stressed type 347 specimens was so severe that the weldment was completely separated from the parent metal. Intergranular attack was considerable in both alloys.

The suitability of austenitic stainless-steel tanks for the storage of unneutralized Darex-Purex raffinate waste was determined at temperatures of 50 to 80°C. Welded, unwelded, and stressed specimens were exposed to simulated waste solutions having a composition of 5*M* nitric acid, 1.82*M* dissolved stainless steel, and 0 to 100 ppm chloride. The stainless steels included in the test were types 304L and 308L. Stressed specimens showed no indications of localized attack, but all specimens showed grain-boundary attack after 500 to 1500 hr of exposure. The attack was independent of the concentration of chloride contaminant and was found to increase with time.[18]

Although titanium is a very suitable construction material for the Darex process, it does not meet the desirable quality of being compatible with any process capable of handling zirconium-matrix fuels. A Darex plant having such a dual capability would possess obvious advantages in terms of initial investment. In recognizing this advantage Oak Ridge has been making efforts to identify construction materials that would be compatible with both the Darex process for stainless-steel-matrix fuels and one of the processes designed for zirconium-matrix fuels (chloride-volatility process).[34] Two cobalt-base alloys, Haynes 25 and 21, are being tested in Darex dissolvent (5*M* nitric acid–2*M* hydrochloric acid) after being welded, heat-treated, and quenched in various ways. In general, the performance of Haynes 21 in the solution was considerably improved by heat-treatment followed by air-quenching, whereas the resistance of Haynes 25 was seriously impaired by post-weld heat-treatments. In nearly all tests the corrosion rates appeared to increase somewhat with exposure time. This was probably due to intergranular attack that was observed after several hundred hours of exposure. It is thought that this attack could be alleviated somewhat by specifying a special low-carbon vacuum-melted heat.[34] Corrosion observed in the vapor phase and at the interface was less severe than that observed in the liquid phase. Typical results are shown in Table II-2.

Corrosion in HNO_3 Solutions

The electrolytic dissolution of reactor fuels is receiving considerable attention at Idaho[35] and Savannah River.[8] This method of dissolution is attractive because it affords the possibility of processing a variety of fuels in a common plant. The results of corrosion evaluations at both of these sites have been reported periodically in this Review. The dissolution medium usually considered in this process is nitric acid. Normally the austenitic stainless steels are considered to be good construction materials for exposure to nitric acid solutions that are reasonably free of impurities. The presence of chromium in nitric acid solutions is known to increase corrosion rates markedly, and the observed attack is

Table II-2 CORROSION OF HAYNES 21 AND 25 IN REFLUXING INITIAL DAREX DISSOLVENT[34]

(Dissolvent: 5*M* HNO_3–2*M* HCl)

Alloy and heat-treatment	Corrosion rate, mils/month	
	48-hr exposure	192-hr exposure
Haynes 21:		
As welded	3.7	8.7
Welded, heat-treated,* water quenched	1.4	2.1
Welded, heat-treated, air cooled	1.3	1.9
Haynes 25:		
As welded	0.3	0.4†
Welded, heat-treated,* water quenched	6.6	13.8
Welded, heat-treated, air cooled	6.3	14.5

*2100°F for 1 hr followed by water quench or air cooling.
†408-hr exposure.

usually intergranular in character. Quantitative information presented in the past has usually related this increased corrosion to total dissolved chromium present. In a progress report from Savannah River,[8] the corrosion rates of austenitic stainless steels have been related quantitatively to the presence of hexavalent chromium. It has been found that the rate of attack is independent of dissolved chromium present in some other form. The rate is also independent of acid concentration within the range of acid contents tested. The relation of corrosion rate to hexavalent chromium-ion concentration is shown in Fig. II-14. The points shown in the figure represent equilibrium conditions that were approached from both high- and low-concentration ranges of hexavalent chromium.

Savannah River has been actively engaged also in the study of the control of the oxidation state of chromium in nitric acid solutions.[8] Chromium(III) is slowly oxidized to Cr(VI) by boiling nitric acid. Studies were made to determine oxidation rate as a function of acid concentration. Results obtained with solutions containing dissolved chromic nitrate are shown in Fig. II-15. The tendency toward oxidation to hexavalent chromium is counteracted by the presence of oxides of nitrogen. In qualitative tests in which individual gases were sparged through boiling solutions of nitric acid, it was found that the oxide that inhibited corrosion, presumably by reduction of hexavalent chromium to trivalent chromium, was nitric oxide (NO). Nitrous oxide (N_2O) and nitrogen dioxide (NO_2) did not influence the concentration of hexavalent chromium or the corrosion rate of austenitic stainless steels. This phenomenon explains the low corrosion of stainless steels during electrolytic dissolution of reactor fuels. Relatively large quantities of nitrogen oxides (including nitric oxide) are generated at the cathode; these oxides maintain the dissolved chromium in the trivalent form. When it has been possible to retain these dissolved gases in solution, the corrosion rates have remained relatively low. One such laboratory method is the use of a cold-finger type of condenser as opposed to a reflux condenser. The use of cold-finger condensers has led to a reduction in corrosion rates by a factor of 3 to 5. It is evident that the equilibrium hexavalent chromium concentration is a function of nitric acid concentration, the rate at which nitrogen oxide gases are being

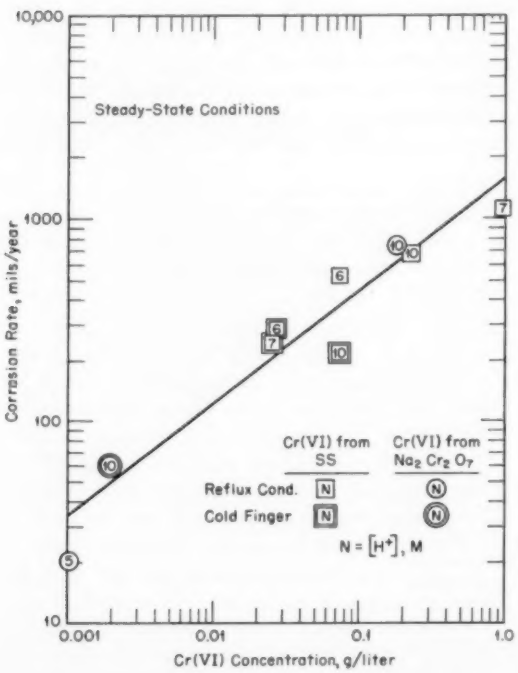

Fig. II-14 Rate of corrosion of type 304L stainless steel by boiling nitric acid—Cr(VI) solutions.[8]

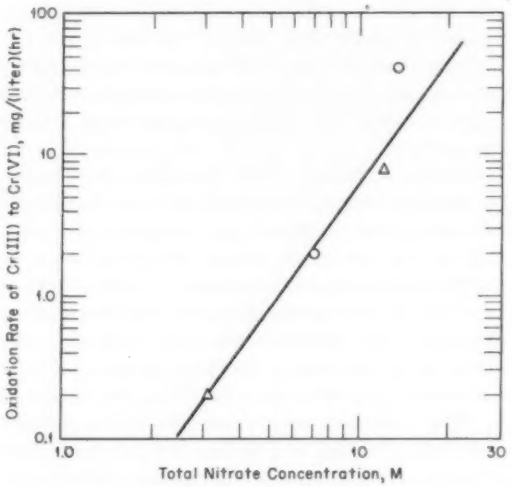

Fig. II-15 Rate of oxidation of Cr(III) to Cr(VI) by boiling nitric acid.[8] All rate measurements were made before 5% of the Cr(III) had been oxidized. All nitrate was from HNO_3 and $Cr(NO_3)_3$. ○, 20 g of Cr(III) per liter. △, 1 g of Cr(III) per liter.

generated, and the provisions that have been made for the retention of such gases in solution.[8]

A topical report on the electrolytic solution of power-reactor fuels in nitric acid has been published by Savannah River.[7] This report is a summary of the corrosion information in this area and, therefore, of most of the corrosion data that have been presented in previous issues of *Reactor Fuel Processing*.

Idaho is also doing considerable experimental work on the application of electroyltic dissolvers to fuel-element processing.[30,36] Insulating materials will be needed which will be capable of withstanding both the chemical and radiation environments that will be encountered in electrolytic processing. In the preceding Review,[4] it was reported that Marlex polyethylene was the only one of several materials tested which did not suffer excessive cracking, spalling, or disintegration in a combined chemical and irradiation environment. Additional materials were irradiated to 10^8 r in boiling simulated dissolver-product solution (1*M* nitric acid containing 1.5*M* dissolved stainless steel as nitrates). Obvious damages and color changes were slight at this radiation level to the following four materials: G-7 laminate,* polypropylene, polystyrene, and annealed Kynar.† G-7, annealed Kynar, and 96% alumina were subsequently given additional exposure to 10^9 r; no additional damage or color changes were observed.[30]

Zirflex Process

A hot-cell demonstration of the Zirflex process was conducted during November and December 1961. The purpose was to test the equipment and operations and to monitor the uranium and plutonium losses of the process. A total of 12 Zircaloy-clad uranium dioxide specimens, which had been irradiated in the NRX (Chalk River Naval Reactor) to about 15,500 Mwd/ton and cooled about nine months, were declad, and core dissolutions were completed. Nionel corrosion coupons were exposed during the decladding step, which used refluxing 6*M* ammonium fluoride–1*M* ammonium nitrate.[37] The total exposure of the Nionel specimen was about 19 hr, and corrosion evaluations were made at both the end and the midpoint of the exposure. During the first 10 hr the measured corrosion rate was 1.3 mils/month, whereas in the latter 9 hr the rate was 8.0 mils/month for an overall average of 4.5 mils/month. The sixfold increase in corrosion rate during the second period over that of the first was not explained in the report, nor was there any indication that the higher rate was expected to continue.

Idaho Process for Zirconium-Matrix Fuels

The process presently in use at the ICPP for zirconium-matrix fuels dissolves the fuel and cladding together, and, following a feed-adjustment step, this material is introduced into the solvent-extraction processing equipment. The high zirconium concentration in this feed stream restricts the uranium concentration and thereby reduces throughput. Idaho is performing experimental work to find ways of removing the bulk of the zirconium by precipitation in order to increase process capacity. In the preceding issue of *Reactor Fuel Processing*,[4] corrosion information was presented on several aspects of a sodium formate precipitation process. More recently additional corrosion work has been done on that part of the process in which the filtrate resulting from precipitation is concentrated, prior to introduction into the solvent-extraction system.[36] All three alloys tested (stainless-steel type 316L, Hastelloy F, and Carpenter-20) showed, at worst, mild corrosion in the vapor and rates that varied from 2.8 to 4.2 mils/month in the liquid. These rates are considered satisfactory for the process, and no additional work is contemplated.

A method under consideration at the ICPP for the dissolution of zirconium-matrix fuels having uranium contents of greater than 2 wt.% involves the addition of hydrogen peroxide to the hydrofluoric acid dissolution medium, which makes it possible to dissolve such fuels homogeneously. Corrosion experiments have been performed to determine the compatibility of this modified process with existing Monel dissolution equipment.[36] The welded and unwelded Monel coupons were exposed to liquid and vapor during 50 batch dissolutions conducted in the laboratory. The corrosion rates of both as-received and as-welded Monel were comparable in both liquid and vapor phases and showed a modest decrease in corrosion rate with time. Typical corrosion values were 6.5 to 8.0 mils/month in the vapor phase and 20 to

*A glass fabric–silicone resin, a product of Taylor Fiber Co.

†A product of Pennsalt Co.

25 mils/month in the liquid phase. Microscopic examination indicated that the Monel suffered both grain-boundary and weld attack. The former was more severe on the samples exposed to the vapors, and knife-line attack occurred at the weld-wrought interfaces. No evidence of stress-corrosion cracking was observed. Monel 60X weld wire was also exposed during the 50 dissolutions. The degree of embrittlement of these samples was determined by tensile testing. The greatest loss of strength occurred at the point where the Monel coupons were supported ($2\frac{1}{2}$ in. above the liquid level). It was felt that this loss of strength was due largely to inadequate nitrogen purging and the elevated temperature at that location.[36]

These observations indicate that the use of the hydrogen peroxide batch flow sheet in the existing Monel dissolver in the ICPP would result in a predictably high corrosion rate. This might be tolerable for a limited amount of production (short processing period) but would be questionable for extended processing periods.

Other corrosion tests were made at the ICPP by operating miniature continuous dissolvers made from $\frac{1}{2}$-in. standard pipe and using six different flow sheets designed for the handling of zirconium-matrix fuels. The two materials tested for these various flow sheets were Monel and Carpenter-20Cb. Typical exposure times were 180 and 190 hr, and all solutions were refluxed.[30] The six dissolvents used contained hydrofluoric acid with various oxidants. The experiments indicated that Monel and Carpenter-20Cb were suitable for service in aerated 10M hydrofluoric acid and in 10M acid containing 0.03M hydrogen peroxide. Neither material would be suitable for long-term use with solutions containing a greater concentration of oxidant. Monel may be preferred over Carpenter-20Cb because of the possibility that the latter can not be field welded because it requires special annealing procedures and may fail at sensitized areas at or adjacent to welds; Monel can be satisfactorily field welded without requiring special annealing procedures.

Alloys Resistant to Nitric Acid

Several graphite- and carbide-containing fuels have been proposed or are being used at the present time. One possible method of processing these fuels involves a disintegration in fuming nitric acid followed by leaching with dilute nitric acid with or without the addition of a hydrofluoric acid. Titanium and Corronel 230 (nominal composition: 65% nickel, 35% chromium; obtained from International Nickel Company; produced by Henry Wiggins, Ltd., Birmingham, England) are being evaluated for this type of service. The results indicate that the overall corrosion rate for titanium in 20M nitric acid is far lower than that for Corronel (0.07 as compared with 7.0 mils/month for 168 hr of exposure). The vapor-phase Corronel corrosion coupon apparently suffered considerable intergranular attack. To simulate the second portion of the process (the leaching of the uranium with dilute nitric acid), titanium-45A and Corronel 230 were tested in boiling 10M nitric acid–0.5M sodium fluoride–0.75M aluminum nitrate. The data indicate that the initial maximum corrosion rates of both materials were nearly equal (1.5 mils/month for 24-hr exposure) but that the decrease in rate with time was considerably greater for titanium. The surfaces of the Corronel 230 specimen had a uniform acid etch, and no localized attack was apparent.[34]

The alloy Corronel 230, which is said to have been developed to resist corrosion by hot nitric acid, was tested in a number of typical Hanford environments.[38] Hanford concluded that the alloy appears to have good resistance to nitric acid–hydrofluoric acid solutions and that it may prove useful for certain Hanford applications. Huey tests[4] and tests in boiling synthetic 1WW solution (first-cycle aqueous waste) indicate that the alloy is inferior to stainless-steel type 304L for use in Purex waste concentrators.

Corrosion Tests of Stainless Steels

At Idaho a corrosion evaluation was conducted on a heat-exchanger tube bundle and on a deentraining head of a continuous thermosiphon evaporator that had been replaced after 14,000 hr of service as an intercycle uranium-product evaporator. This vessel was constructed of type 348 stainless steel.[36] Visual examination showed that all the tubes within the steam chest were free of perforations, pits, or areas of localized attack. However, severe end-grain corrosion occurred at the feed end of the tubes at the lower tube sheet. A metallographic examination indicated that the cross-sectional thickness of weld deposits was less than the tube thickness and that interdendritic

attack had occurred in the weld deposit. No evidence of corrosion was found in the vapor head pipe section, the inlet, or the outlet.

The corrosion of sensitized type 304L stainless steel in a solution simulating that occurring in uranyl nitrate hexahydrate evaporators is being conducted at Hanford.[39] The solutions tested under reflux include 3.5*M* uranyl nitrate hexahydrate–2.3*M* aluminum nitrate with nitric acid concentrations of +0.1*M*, −0.2*M*, and −0.6*M* (negative molarities indicate acid deficiency). Coupons were exposed in the liquid, vapor, and interface regions; exposure periods ranged from 240 to 400 hr. The maximum corrosion rate observed was 4.7 mils/month and occurred in the liquid phase of the solution that was 0.6*M* acid deficient. The corrosive attack was of a very selective intergranular nature.

A literature survey on the stress-corrosion cracking of stainless steel has been compiled by a researcher at SRL.[40] The bulk of the references included covered the period from 1955 to the present, with some additional selected references prior to that date.

Corrosion in Waste Processing

Considerable research and development effort is being expended on methods of reducing the volume of radioactive solutions and of storing them safely. One of the principal techniques is the calcination of liquid wastes to produce low-volume solids. Development work associated with this technique is being done with synthetic Purex, Darex, and TBP-25 wastes containing millicurie amounts of ruthenium.[34,41] Corrosion evaluations are being made simultaneously with development work.

The pot-calcination flow sheet at ORNL involves the distillation of gross amounts of solution at about 110°C followed by increasing temperature levels of up to 900 or 950°C for calcination to final solid. Glass-making additives such as borates and phosphates are sometimes added to initial waste solutions to produce an ultimate product that is more resistant to leaching. Corrosion tests have been made with a variety of waste solutions. Welded specimens of austenitic stainless-steel types 304L and 347 were placed in a Vycor tube containing the synthetic waste solutions. The volume of solution was such that a 3-in. length of each specimen was above the solution-vapor interface. The Vycor tube was inserted into a type 304L stainless-steel vessel; a condenser system was attached, and the entire assembly was placed into a vertical tube furnace. The vessel was slowly heated to 110°C, at which temperature distillation of the volatile components started. When the distillation rate began to decrease, the vessel temperature was raised to 250°C and was held there until the distillation rate again began to decrease. This procedure was repeated until the vessel reached the desired temperature (900 to 950°C), where it was maintained for the remainder of the test. To determine the relative corrosiveness of the conditions in various portions of the contemplated process, exposure test times were varied from short increments of 1 hr up to 345 hr. The chemical composition of the simulated waste solutions used is shown in Table II-3, and a summary of corrosion results is shown in Table II-4.

For all three waste solutions tested, the corrosion rate during the first 24 hr was substantially greater than the rate averaged over longer periods of time. This would suggest that the distillation and volatilization portion of the test contributed most to the corrosion and that holding the calcined product at the ultimate temperature contributed less to the corrosion observed. In a single test an effort was made to define further the portion of the test which contributed the most to corrosion. In this test type 304 stainless steel was exposed to Purex solution containing glass-making additives. The system was held at 110°C until distillation ceased. When the system was cooled and the specimen was examined and weighed, no measurable corrosion had occurred. The specimen was placed in the system again, the temperature was raised to 850°C for 1 hr, and the system was again cooled and the specimen evaluated. Again, no corrosion was observed. When the specimen was returned to the system and heated to 950°C for 2 hr, the specimen showed considerable intergranular corrosion over the entire surface, and a general corrosion rate of 1330 mils/month was calculated. The specimen was again placed in the system and held at 950°C for an additional 75 hr. The corrosion rate during this 75 hr period was 19 mils/month. This experiment indicates that essen-

Table II-3 CHEMICAL COMPOSITIONS OF SIMULATED WASTE SOLUTIONS INVESTIGATED IN EVAPORATION-FIXATION CORROSION STUDIES[41]

Component	Simulated waste-solution composition, *M*					
	Formaldehyde-treated Purex*	Purex*	Purex and additive No. 1	No. 2	No. 3	TBP-25
H^+	0.3	5.6				1.3
NO_3^-	1.2	6.1				6.6
SO_4^{2-}	2.0	1.0				
Na^+	1.2	0.6				
Al^{3+}	0.2	0.1				1.72
Fe^{3+}	1.0	0.5				~0.003
Cr^{3+}	0.02	0.01				
Ni^{2+}	0.02	0.01				
Hg^{2+}						0.02
Ru	0.004	0.002				0.0003
$Na_2B_4O_7$			0.13	0.344	0.086	
NaH_2PO_4			0.76			
NaH_2PO_2						2.0
H_3PO_2			0.76	1.52	1.52	
MgO				0.80	0.80	
$Ca(OH)_2$			1.1			
NaOH			0.22	1.32	1.49	
PbO						0.25

*Data have not been obtained for Purex waste without addition of either formaldehyde or fluxing agents. Corrosion should correspond closely to that in the formaldehyde-treated waste.

Table II-4 SUMMARY OF CORROSION OF STAINLESS STEELS IN EVAPORATION-FIXATION TESTS OF SIMULATED HIGH-LEVEL-WASTE SOLUTIONS[34,41]

Material	Environment	Exposure time, hr	Temp.,* °C	Overall corrosion rate, mils/month
S.S. 304L	Purex waste, formaldehyde treated	24	110–900	7
	1000°C calcination residue from formaldehyde-treated Purex waste	123	900	3.6
S.S. 304L	Purex waste plus additive	24	110–900	130
	Purex waste plus additive	78	110–950	60†
S.S. 304L	TBP-25 waste	24	110–900	5.1
	TBP-25 waste	168	110–900	1.6
S.S. 304L	TBP-25 waste plus additive	19	110–920	42
	TBP-25 waste plus additive	345	110–910	5
S.S. 347	TBP-25 waste	24	110–900	10.5
	TBP-25 waste	168	110–900	1.9

*Temperature was held at 110°C until distillation ceased and was then increased in steps to temperature indicated.

†The following incremental corrosion rates were observed: during distillation period at 110°C: 0 mil/month; during first hour of calcination, 850°C: 0 mil/month; during next 2 hr of calcination, 950°C: 1330 mils/month; during following 75 hr of calcination, 950°C: 19 mils/month.

tially all the observed corrosion occurred during the first 2 to 4 hr at the temperature required to remove the last of the acid and water from the system.[34,41]

The formaldehyde-treated Purex waste and the TBP-25 waste, both with and without glass-making additives, had corrosion rates that can be considered acceptable for this process. Purex waste plus glass-making additives resulted in rates of attack ranging up to 130 mils/month. This might be considered acceptable since the calcination pot is used only once for processing, after which it becomes the storage vessel for the contained calcined product.

The condenser and off-gas system does not have the advantage of one-time usage, and hence, in a sense, the selection of a construction material is more critical for this system than for the calcination pot. Corrosion tests were made during the evaporation and calcination (without additives) of high-sulfate-containing Purex-waste solutions (both initial and final concentrations), as well as with an estimated average condensate from such a process. Typical corrosion results and the composition of environments are shown in Table II-5. Of the four alloys, titanium-45A had the greatest resistance to all environments tested. The maximum rate for titanium-45A was 2 mils/month for an 1145-hr exposure in the solution phase of refluxing 15*M* nitric acid–1*M* sulfuric acid. Low-carbon Nionel and Hastelloy F showed grain-boundary attack in the condensates expected from all solutions studied. Not shown in the table is the somewhat increasing corrosion rate with time which was evident for Hastelloy F and low-carbon Nionel in 6*M* nitric acid; this increased corrosion rate indicates increasing progressive localized attack would

Table II-5 TYPICAL CORROSION RESULTS AND COMPOSITION OF ENVIRONMENTS USED FOR CORROSION STUDIES OF THE CONDENSER SYSTEM OF THE HIGH-LEVEL-WASTE CALCINATION PROCESS[41]

Component	High-sulfate Purex-waste solution		Average condensate from high-acid Purex waste	
	Initial concentration, *M*	Final concentration, *M*	Initial concentration, *M*	Final concentration, *M*
H^+	5.6	0.3		
NO_3^-	6.1	1.3 to 1.8		
SO_4^{2-}	1.0	2.0 to 3.0		
Na^+	0.6	1.2 to 1.8		
Al^{3+}	0.1	0.2 to 0.3		
Fe^{3+}	0.5	1.0 to 1.5		
Cr^{3+}	0.01	0.02 to 0.03		
$RuCl_3$	0.002	0.004 to 0.006		
Na^{2+}	0.01	0.02 to 0.03		
HNO_3			6	15
H_2SO_4			0.05	1

Alloy tested	Specimen position	Corrosion, mils/month: High-sulfate Purex-waste solution, At initial concentration	High-sulfate Purex-waste solution, At final concentration	Average condensate from high-acid Purex waste, At initial concentration	Average condensate from high-acid Purex waste, At final concentration
Titanium-45A	Vapor	0.03	0.1	0.04	0.33
	Solution	0.04	0.2	1.5	2.0
Hastelloy F	Vapor	0.3		2.8	11.2
	Solution	3.2		0.4	6.0
LCNA*	Vapor	0.1	0.1	2.7	9.9
	Solution	0.8	0.1	1.3	1.0
S.S. 347	Vapor	0.8			
	Solution	3.6			

*LCNA = low-carbon Nionel.

be encountered in a continuous process. Two additional parameters tested (but not indicated in the table) were the presence of peroxide and the presence of ruthenium. The former had little, if any, effect on the corrosion of either low-carbon Nionel or Hastelloy F. It is not clear whether or not the presence of ruthenium exerted a real effect on the corrosion of Hastelloy F (Nionel not tested).

Stainless-steel type 347 showed severe grain-boundary attack with overall rates as high as 3.6 mils/month when exposed to refluxing initial Purex-waste solution.

References

1. F. L. Culler, Jr., Chemical Technology Division Monthly Report for March 1962, USAEC Report ORNL-TM-180, Oak Ridge National Laboratory, Apr. 2, 1962.
2. F. L. Culler, Jr., Chemical Technology Division Monthly Report for May 1962, USAEC Report ORNL-TM-245, Oak Ridge National Laboratory, June 1, 1962.
3. M. E. Whatley, Chemical Technology Division, Unit Operations Section Monthly Progress Report, January 1962, USAEC Report ORNL-TM-150, Oak Ridge National Laboratory, June 6, 1962.
4. *Reactor Fuel Process.*, 5(3): (July 1962).
5. R. I. Martens, W. L. Poe, Jr., and A. E. Wible, Preparation of Aluminum-Clad Uranium Fuels for Solvent Extraction, presented at 1962 Nuclear Congress, June 4–7, New York, Preprint Paper No. 50.
6. M. E. Straumanis and D. L. Mathis, The Dissolution Reaction and Attack of Beryllium by HF, HCl, and H_2SO_4, *J. Electrochem. Soc.*, 109: 434–436 (May 1962).
7. A. T. Clark, Jr., L. H. Meyer, J. H. Owen, and F. G. Rust, Electrolytic Dissolution of Power Reactor Fuels in Nitric Acid, USAEC Report DP-647, Savannah River Laboratory, October 1961.
8. F. G. Rust (Comp.), Processing of Power Reactor Fuels, Sixteenth Quarterly Progress Report, July 1–October 1, 1961, USAEC Report DP-706, Savannah River Laboratory, February 1962.
9. V. P. Caracciolo (Comp.), Processing of Power Reactor Fuels, Seventeenth Quarterly Progress Report, October 1, 1961–January 1, 1962, USAEC Report DP-720, Savannah River Laboratory, April 1962.
10. *Reactor Fuel Process.*, 4(4): 20 (October 1960).
11. J. R. Aylward and E. M. Whitener, Electrolytic Dissolution of Nuclear Fuels. Part III. Stainless Steel (304) in Nitrate Solutions, USAEC Report IDO-14584, Phillips Petroleum Co., June 1, 1962.
12. J. A. McBride, Idaho Chemical Processing Plant, May 1962. (Unpublished)
13. F. L. Culler, Jr., Chemical Technology Division Monthly Report for April 1962, USAEC Report ORNL-TM-213, Oak Ridge National Laboratory, May 1, 1962.
14. R. F. Taylor, E. W. Sharratt, L. E. M. de Chazal, and D. H. Logsdail, Processing in Limited Geometry. Part III. The Dissolution of Uranium Dioxide Sintered Pellets in Nitric Acid, British Report AERE-R-3678, January 1962 [to be published in *Journal of Applied Chemistry (London)* under the title: Dissolution Rates of Uranium Dioxide in Nitric Acid Systems].
15. W. C. Perkins, Dissolution of Pu-Al Alloy, USAEC Report DP-702, Savannah River Laboratory, March 1962.
16. S. Goldsmith, Hanford Atomic Products Operation, May 31, 1962. (Unpublished)
17. S. Goldsmith, Hanford Atomic Products Operation, Apr. 20, 1962. (Unpublished)
18. F. G. Kitts and W. E. Clark, Darex Process: Processing of Stainless-Steel-Containing Reactor Fuels with Dilute Aqua Regia, USAEC Report ORNL-2712, Oak Ridge National Laboratory, June 7, 1962.
19. D. E. Ferguson (Comp.), Transuranium Quarterly Progress Report for Period Ending February 28, 1962, USAEC Report ORNL-3290, Oak Ridge National Laboratory, June 13, 1962.
20. M. K. Harmon, Current Status of Solvent Extraction Processing of Irradiated Uranium Fuels, presented at 1962 Nuclear Congress, June 4–7, New York, Preprint Paper No. 51.
21. R. H. Rainey and J. G. Moore, Laboratory Development of the Acid Thorex Process for Recovery of Consolidated Edison Thorium Reactor Fuel, USAEC Report ORNL-3155, Oak Ridge National Laboratory, May 11, 1962.
22. V. B. Shevchenko, N. S. Povtiskii, A. S. Solovkin, I. V. Shilin, K. P. Lunichkina, and Z. N. Tsvetkova, Extraction of Nitric Acid with Tributyl Phosphate, *J. Inorg. Chem., Acad. Sci. U.S.S.R.*, III(9): 155–159 (1958) (English translation).
23. V. V. Fomin, E. P. Maiorova, M. I. Krapivin, and V. G. Yudina, Extraction of Plutonium(IV) with Tributyl Phosphate, USAEC Translation AEC-tr-4457, pp. 161–166, 1958.
24. E. P. Maiorova and V. V. Fomin, Extraction of Thorium with Tributyl Phosphate, USAEC Translation AEC-tr-4456, pp. 295–316, 1958.
25. B. P. Dennis and D. L. West, Evaluation of Hydrocarbon Diluents for the Purex Process, USAEC Report DP-671, Savannah River Laboratory, November 1961.
26. J. L. Carroll, Absorption of Thorium on an Ion Exchange Resin, USAEC Report HW-70536, Hanford Atomic Products Operation, Sept. 8, 1961.
27. *Reactor Fuel Process.*, 4(2): 19–20 (April 1961).

28. B. J. Newby, Sodium Fluozirconate Precipitation Process for Zirconium Fuels. Part I. Laboratory Development, USAEC Report IDO-14582, Phillips Petroleum Co., May 25, 1962.
29. *Reactor Fuel Process.*, 5(2): 13 (April 1962).
30. J. R. Bower (Ed.), Chemical Processing Technology Quarterly Progress Report, October–December 1961, USAEC Report IDO-14583, Phillips Petroleum Co., Mar. 28, 1962.
31. R. W. Kessie, The Design and Construction of Thermal Flowmeters, USAEC Report ANL-6531, Argonne National Laboratory, March 1962.
32. R. J. Christl and A. E. Daking, Design Philosophy for a Remote-Maintenance Radiochemical Processing Plant, presented at 1962 Nuclear Congress, June 4–7, New York, Preprint Paper No. 79.
33. J. C. Bresee and J. T. Long, Design Philosophy for Direct-Maintenance Radiochemical Processing Plants, presented at 1962 Nuclear Congress, June 4–7, New York, Preprint Paper No. 80.
34. R. E. Blanco, Chemical Technology Division, Chemical Development Section B, Quarterly Progress Report, October–December 1961, USAEC Report ORNL-TM-177, Oak Ridge National Laboratory, May 18, 1962.
35. *Reactor Fuel Process.*, 4(4): (October 1961).
36. J. R. Bower (Ed.), Chemical Processing Technology Quarterly Progress Report, July–September, 1961, USAEC Report IDO-14574, Phillips Petroleum Co., Dec. 18, 1961.
37. J. H. Goode and M. G. Baillie, Hot Cell Demonstration of Zirflex and Sulfex Processes: Report No. 2, USAEC Report ORNL-TM-130, Oak Ridge National Laboratory, Jan. 26, 1962.
38. W. H. Reas, Chemical Research and Development Operation Monthly Report, May 1962, USAEC Report HW-73905C, Hanford Atomic Products Operation, June 15, 1962. (Classified)
39. W. H. Reas, Chemical Research and Development Operation Monthly Report, March 1962, USAEC Report HW-73202C, Hanford Atomic Products Operation, Apr. 15, 1962. (Classified)
40. M. S. Feldman, Stress-Corrosion Cracking of Stainless Steel, A Literature Search, USAEC Report DP-683, Savannah River Laboratory, February 1962.
41. R. E. Blanco and E. G. Struxness, Waste Treatment and Disposal Progress Report for December 1961 and January 1962, USAEC Report ORNL-TM-169, Oak Ridge National Laboratory.

Section

III

Reactor Fuel Processing

Research and Development on Nonaqueous Processing

Volatility Processes

Various types of processes based on the volatilities of uranium and plutonium hexafluoride have been proposed for the processing of various types of irradiated nuclear-reactor fuels. Liquid-phase processes under consideration include fused-salt processes that are being considered for application to the recovery of uranium from molten-salt-reactor fuel and from zirconium-uranium alloy fuel. Also included is the Nitrofluor process (nitrogen dioxide–hydrogen fluoride system) for processing reactor fuel elements. Solid phase–gas phase halogenation processes have also been proposed for application to zirconium-uranium alloy fuel and to uranium dioxide fuels. Fluidization techniques are employed in some of these dry halogenation processes to enhance reactor control.

Liquid-Phase Processes

Nitrofluor Process. The initial step in the Nitrofluor process, under development at Brookhaven National Laboratory (BNL), involves the dissolution of the reactor fuel assembly in an anhydrous N_2O_4-HF solution. Solutions containing 25 mole % as nitrogen dioxide are capable of dissolving a wide variety of fuel-element or cladding materials at satisfactory rates over a temperature range of 100 to 200°C. The high reactivity of the solvent has limited the choice of container materials to Monel and nickel. These materials, however, are severely attacked during the solvent evaporation and condensation steps, although corrosion is relatively mild during dissolution of fuel materials. Oxidizing agents such as molecular nitric acid or the nitryl ion (NO_2^+) are believed to be responsible for the attack on Monel and nickel. Two alternative solvents, NOF·3HF and N_2O_3-HF, are presently being evaluated[1] since they do not possess these oxidizing characteristics.

Studies with N_2O_4-HF Solvent. When uranium metal or oxide dissolves in N_2O_4-HF solutions, the compound nitrosylium hexafluorouranate ($NOUF_6$) is produced. After evaporation of the excess solvent, this material is converted to uranium hexafluoride by reaction with bromine trifluoride. A major problem associated with the Nitrofluor process continues to be demonstration of complete uranium recovery during fluorination. Recent work[1] has shown that very high uranium recoveries may be achieved by carrying out the fluorination at 150°C rather than at 100 to 115°C as was done previously. Approximately 95% of the uranium was recovered with a single contact of bromine trifluoride at 150°C from a salt containing an excess of zirconium fluoride.

In processing of high-zirconium alloy fuel containing enriched uranium, the bulk of the zirconium precipitates as a complex salt that must be washed free of soluble uranium with fresh solvent. Several washes are required to assure recovery of uranium. An alternative procedure is to evaporate the solvent and treat the entire salt mass with bromine trifluoride. This approach has been studied,[1] and, in a single test, 94% of the uranium was recovered by one contact with bromine trifluoride at 200°C. Additional contacts with fluorine or bromine trifluoride would be expected to improve uranium recovery.

Studies with NOF·3HF Solvent. The dissolution rates of various reactor fuel materials have been measured in the NOF·3HF solvent and, in general, it was observed that the dissolution rates were higher than in N_2O_4-HF solutions. An attractive feature of the NOF·3HF solvent

is that, at the temperatures employed during dissolution, the vapor pressure of the solvent is significantly less than that of the N_2O_4-HF system. The NOF · 3HF solvent has a boiling point of 95°C. The solvent is prepared by bubbling nitrosyl chloride gas into anhydrous hydrogen fluoride, continuously venting the hydrogen chloride formed, and thermally decomposing the intermediate compound NOF · 6HF by distillation.

The complex uranium salt produced by dissolution of uranium dioxide in NOF · 3HF has been identified as $NOUF_6$. Treatment of the uranium product with bromine trifluoride at 177°C resulted in the recovery of 99% of the uranium as uranium hexafluoride.

Development of New Alloys for the Fused-Salt Volatility Process. In the fused-salt fluoride-volatility process being developed at ORNL, zirconium-uranium alloy fuel is dissolved in molten fluoride by sparging with hydrogen fluoride, and uranium hexafluoride is produced by fluorine sparging in a separate vessel. Extensive corrosion studies have been performed for these processing conditions, and these have been reviewed previously for both the hydrofluorination[2] and the fluorination[3] steps. Promising results obtained in preliminary studies on a new alloy (79 wt.% nickel, 4 wt.% molybdenum, balance iron) has led to the further tests reviewed here. The new alloy has been called both Hymu 80 and Alloy 79-4. Its composition and those of other alloys mentioned have been given in detail in an earlier Review.[3]

These corrosion studies, made at Battelle Memorial Institute (BMI) under subcontract to ORNL, indicated that Alloy 79-4 is more resistant to fluorination conditions than either INOR-8 or L-nickel, which preveiously had been selected as the most favorable metals. Two series of tests were made: in one, molten NaF-LiF-ZrF_4 was used, and in the other, molten NaF-LiF-BeF_2-ZrF_4 was used. The metal specimens were exposed at 500°C in both series. Fluorine was passed through the melt for 150 and 162 hr, respectively, and uranium tetrafluoride was added to both salts periodically. In contrast to L-nickel, there was no significant intergranular attack of the INOR-8 or of Alloy 79-4. The presence of beryllium in the fuel salt increased its corrosiveness. Results are shown[4,5] in Table III-1.

Table III-1 CORROSION OF ALLOY SPECIMENS UNDER FLUORINATION IN MOLTEN SALT[4,5] AT 500°C

(Molten-Salt Compositions: No. 1, 27.5-27.5-45 Mole % NaF-LiF-ZrF_4; No. 2, 27.8-20.4-6.8-45 Mole % NaF-LiF-BeF_2-ZrF_4)

	Maximum penetration rate, mils/month						
	No. 1 molten salt				No. 2 molten salt		
Location	INOR-8 (by weight loss)	Alloy 79-4 (by weight loss)	L-nickel (by weight loss)	L-nickel (metallographic)	INOR-8 (metallographic)	Alloy 79-4 (metallographic)	L-nickel (metallographic)
Vapor	3	1	0.2	8	9	7	11
Liquid	11	4	3.8	25	38	13	31
Interface	11	2	1.3	28	6	5	22

The oxidation resistance of Alloy 79-4 in a 2000-hr exposure to air at 700°C was equivalent to that of INOR-8 and L-nickel. The advantage of an adherent scale on L-nickel was offset by the extensive intergranular attack that occurred. The results showed that complete protection from oxidation could be provided by Chromallizing, a proprietary chromium-coating process.[4,5]

Alloy 79-4 also appeared favorable in tests in the hydrogen fluoride environment. Conditions of melt composition and temperature were chosen for high corrosivity to provide accelerated attack. At 650°C, in a 50.5-37.0-12.5 mole % NaF-LiF-BeF_2 melt, the test was continued for 93 hr with hydrogen fluoride sparge. Alloy 79-4 was more corrosion resistant than INOR-8, previously selected as a superior alloy, and also superior to several other experimental alloys of nickel[6] (see Table III-2).

Sodium Fluoride Absorber Studies. The ORNL fused-salt process has utilized a decontamination procedure provided by the sorption and desorption of uranium hexafluoride on a

Table III-2 CORROSION OF ALLOY SPECIMENS UNDER HYDROFLUORINATION[6]

(Molten-Salt Temperature, 650°C; Molten-Salt Composition, 50.5-37.0-12.5 Mole % NaF-LiF-BeF_2; Test Duration, 93 hr with HF Sparge)

Alloy	Maximum penetration rate, mils/month	
	Weight loss data	Micrometer measurements
Alloy 79-4	4.08, 8.02*	23, 23*
INOR-8	23.23, 12.85*	81, 107*
90% Ni–10% Mo	23.68, 2.19*	75, 15*
85% Ni–10% Mo–5% Fe	17.16, 11.45*	70, 38*
86% Ni–5% Mo–4% Fe–5% V	16.28, 17.90	171, 111
82% Ni–8% Fe–10% V	17.18, 22.62	46, 61
86% Ni–14% Al	Specimen completely severed	
84% Ni–13% Al–3% Si	Section nearly dissolved	

*First number is from test with fresh salt, and second number is from repeat test with same salt; others were duplicate tests.

packed bed of sodium fluoride pellets. (Both basic laboratory and pilot-plant decontamination studies have been described in previous Reviews.[7,8]) Recently a mathematical model was developed for this sorption process.

In the mathematical model, partial differential equations were derived for the concentration of unreacted uranium hexafluoride as a function of time and position in a sphere of sodium fluoride during sorption of the uranium hexafluoride. The model includes the effects of (1) stagnant-gas-film resistance, (2) rate of diffusion of uranium hexafluoride in pores of the sphere, (3) reaction rate at the pore walls, and (4) effect of local uranium hexafluoride loading on the rate of transport and rate of reaction. The equations were converted to finite-difference form in preparation for numerical solution. This analysis appears to explain the different effects of temperature on absorber load obtained for the pellets as compared to powder, while retaining the same basic kinetic characteristics of the system.[9]

Experiments are under way to check the mathematical model. Preliminary data on the loading of uranium hexafluoride $\frac{1}{8}$-in. right-circular cylinders were obtained. A strong dependence of loading on gas concentration in the range 0.58–8.0 mole % uranium hexafluoride and a weaker dependence on temperature in the range 25 to 100°C was obtained.[10]

Dry Halogenation Processes

Several processes that involve separation methods based on the relative volatility of the chlorides are being developed for processing of reactor fuel elements. Engineering-scale studies are continuing at Argonne on a process for the recovery of highly enriched uranium from zirconium alloy fuels. The process is based on the use of hydrogen chloride, at a temperature of 350 to 450°C, to convert the zirconium-uranium alloy to volatile zirconium tetrachloride and nonvolatile uranium trichloride. Recovery of uranium values is achieved by the reaction between uranium trichloride and fluorine at 350 to 400°C to produce volatile uranium hexafluoride. Both reactions are conducted in a fluidized bed of inert alundum particles. Fluidized beds offer the advantage of permitting the highly exothermic hydrochlorination reaction to be carried out under nearly isothermal conditions.

Process studies are being conducted in a $1\frac{1}{2}$-in.-diameter fluid-bed reactor. Recent tests[11] have shown that holdup of uranium in the inert alumina solids after fluorination becomes constant upon reuse of the bed. Five separate hydrochlorination-fluorination cycles were made, and the residual uranium values decreased from a value of 4.4% of the uranium charged for one run to about 1% for the fifth trial. Individual charges contained about 17 g of uranium as 5 wt.% alloy in the form of $\frac{1}{4}$-in. chips.

The major problem associated with this process is how to achieve 99% recovery of the uranium as uranium hexafluoride. In general, it appears that the uranium which is not recovered during fluorination remains associated with the inert bed of solids. Studies have shown that the quantity of zirconium remaining in the bed after hydrochlorination may affect the degree of uranium removal during fluorination. Tests are being made to study the effect of hydrogen chloride excess on both zirconium and uranium behavior. The use of phosgene or other chlorinating agents in an intermediate step is also being considered.

Processes Involving Chlorine Compounds

J. Schmets and associates at Centre d'Étude de l'Énergie Nucléaire (CEN) are developing a

method for processing irradiated uranium and uranium compounds based on the fractional sublimation of chlorides. Recent work[12,13] has concerned the study of the reaction between uranium dioxide and various chlorinating agents. It was observed[12] that chlorination with carbon tetrachloride in the presence of chlorine produces a rapid reaction with the formation of uranium chlorides of a valence greater than 4. These higher chlorides are volatile; and in order to assure only the production of uranium tetrachloride, other reactants must be employed. Reaction with a gaseous mixture of carbon tetrachloride and methane at 350°C appears to be the most efficient method for obtaining relatively pure uranium tetrachloride. An alternative chlorinating agent that appears promising is a gaseous mixture of carbon tetrachloride and benzene.[13] This mixture, however, has the disadvantage of producing a fairly heavy carbon deposit.

Several preliminary tests[13] have been made to ascertain the degree of separation achieved between uranium and certain fission products during chlorination. Of particular concern are the elements niobium and zirconium. Niobium oxide is readily chlorinated in carbon tetrachloride–methane mixtures at 300°C. Chlorinations of zirconium dioxide in carbon tetrachloride–methane mixtures have shown that the environment is too reducing, the reaction being arrested after only a fraction of the zirconium has reacted. It appears that, because of the reducing environment, the products of the chlorination of zirconium dioxide by carbon tetrachloride are lower chlorides of zirconium. These nonvolatile products appear as solid deposits on the surface of the oxide. The separation of a UO_2-Nb_2O_5 mixture is complete at 340°C with the formation of volatile niobium pentachloride, whereas the separation of zirconium from a UO_2-ZrO_2 mixture by sublimation of zirconium tetrachloride is not achieved using a methane–carbon tetrachloride gas mixture.

In the processing of certain reactor fuels, it may be advisable to convert initially the uranium to volatile chlorides (UCl_5 and UCl_6) in order to achieve preliminary decontamination.[14] Final decontamination would be effected by the conversion of the volatile chlorides to uranium hexafluoride.[13] Processing of uranium carbide fuels might be carried out using this scheme, since the reaction between uranium monocarbide and chlorine proceeds rapidly at 340°C with the production of volatile uranium chlorides. Since there appears to be considerable uncertainty concerning the nature of the products of the reaction between uranium hexachloride and hydrogen fluoride, a comprehensive study[13] is being made to determine under what conditions, if any, uranium hexafluoride may be prepared by this reaction.

Direct Fluorination Processes

A direct fluorination volatility process is being developed at Argonne National Laboratory to recover uranium and plutonium from spent uranium oxide fuel elements that are clad with Zircaloy or stainless steel. The proposed process for recovery of uranium and plutonium from spent fuel involves decladding by an appropriate reaction in a fluidized bed. Plutonium and uranium hexafluorides, which result from the reaction of the declad oxide fuel with fluorine, may be separated from volatile fission products by distillation and separated from one another by thermal decomposition of plutonium hexafluoride.

Engineering-scale studies[11] of the direct fluorination of uranium dioxide pellet fuel are being made in a 3-in.-diameter air-cooled reactor. The technique of fluidization of alumina particles in the voids of the pellet bed is used as an aid in heat removal. Current studies have involved fluorination of 18-in.-deep pellet beds (13.2 kg of uranium dioxide) using fluorine-gas recycle to maximize fluorine economy. In one test a uranium dioxide charge was 96% fluorinated in 22 hr with an overall fluorine utilization efficiency of 77%. Although this result was considered satisfactory with regard to fluorination time and efficiency, the test was unsatisfactory in that caking or agglomeration of the fluid bed occurred. It appears that high oxygen concentration in the gas recycle stream produces fine particles within the bed which cause caking of the bed. An 18-in. pellet bed was completely fluorinated at 500°C in a test without gas recycle. In this case caking did not occur. However, both the fluorination time (31 hr) and overall fluorination efficiency (30%) were considered unsatisfactory.

Laboratory development work at ANL[11] has centered around experiments designed to elucidate the factors involved in the removal of plutonium by fluorination from mixtures of

alumina, uranium dioxide, plutonium oxide, and fission-product element oxides. The results of these experiments have shown that (1) plutonium is retained on alumina residues to about 0.03 wt.%, and this corresponds to a plutonium loss of 2.25%; (2) with the addition of fission-product element oxides, the retention is raised to between 0.05 and 0.06 wt.%; when fission-product elements are present initially as the fluorides, they do not increase plutonium retention; (3) plutonium retained on alumina residues can be effectively removed, leaving less than 0.02 wt.% plutonium in the residue, by either pyrohydrolysis followed by fluorination at 450°C or by refluorination alone at 500°C; (4) a fluorination scheme that offers the greatest promise of resulting in low plutonium retention in fluorination residue involves a two-step procedure using 10 vol.% fluorine (65% N_2, 25% O_2) at 450°C initially, followed by a second fluorination using 75 vol.% fluorine (25% O_2) at 550°C.

Selective thermal decomposition of plutonium hexafluoride is being considered as a means of separating the mixture of uranium and plutonium hexafluoride produced in the fluorination of uranium dioxide. It has been demonstrated[11] that the circulation of gaseous mixtures of uranium hexafluoride and plutonium hexafluoride through nickel vessels containing nickel wool and plutonium tetrafluoride at 200 to 300°C reduces the ratio of plutonium to uranium by factors between 10^2 and 10^3. The residence time of the gas in the heated vessel necessary to accomplish this separation is about 1 min. The concentration of uranium in the plutonium deposited as plutonium tetrafluoride varied from 0.4 to 1.3%. Berard,[15] in France, has also studied the influence of temperature and container materials on the decomposition of plutonium hexafluoride.

Sintered Uranium Oxide

Schmets and associates at CEN[12,13] have developed a fluorination process for the recovery of uranium from sintered uranium oxide fuel. To conserve fluorine requirements, the oxide fuel is initially converted to uranium tetrafluoride. The sintered oxide is activated by an oxidation-reduction procedure prior to conversion to uranium tetrafluoride with fluorine. All of these reactions have been studied in fluid-bed reactors. To facilitate the fluidization of fine powders, the reactors have been equipped with a series of vibrators. Preliminary tests have shown that suitable oxidation rates were achieved at 450°C using air as the fluidizing gas. Optimum conditions for reduction have been established in fluid-bed equipment:[13] a 50% hydrogen concentration in the fluidizing gas, a gas velocity in the fluid-bed reactor of approximately 0.65 ft/sec; a reaction temperature of 575°C; and a reaction time of 4 hr. Hydrofluorination of uranium dioxide powder is carried out at 575°C. In the conversion of uranium tetrafluoride to uranium hexafluoride by reaction with fluorine, an inert bed of aluminum oxide particles is provided to maintain a continuous inventory of fluidized solids throughout the reaction.

Schmets and Heremans[16] have initiated studies of the decontamination obtained during fluorination of irradiated uranium dioxide. Although

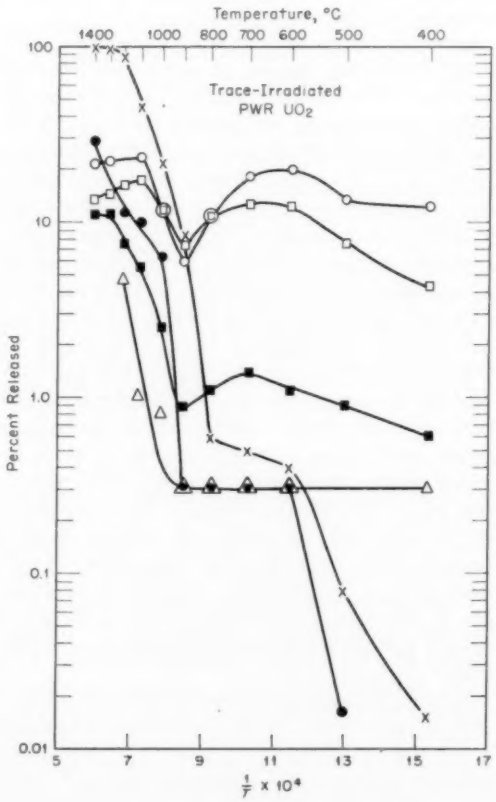

Fig. III-1 Fission-product release by the oxidation of PWR type uranium dioxide to U_3O_8 in air (tracer-level irradiation.[17] ×, ruthenium, ●, tellurium. ■, gross gamma. △, cesium. □, xenon-krypton. ○, iodine.

the results of the reported tests are rather preliminary, it appears that the most troublesome fission product to remove was iodine.

Workers at ORNL[17] have reported results of studies on the release of fission products on the oxidation of uranium dioxide to U_3O_8. The percentage of fission-product activities released from PWR type uranium dioxide (93% of theoretical density), irradiated at tracer level, is shown in Fig. III-1. Figure III-2 shows release data that were obtained when uranium dioxide irradiated to 1000 Mwd/ton was treated in air to a maximum of 1100°C and when uranium dioxide irradiated to 4000 Mwd/ton was treated in air to a maximum of 900°C. Comparison of these data indicates that the rate of release of fission products increases with increasing irradiation level. It is probable that fission-product impurity defects in the uranium dioxide and the greater surface area of irradiated samples led to a higher oxidation rate and thus to higher release values. In Fig. III-1 there is a distinct discontinuity at 800 to 900°C, which is also the temperature range in which the minimum oxidation rate for uranium chloride in air occurs. This behavior is believed to be associated with the occurrence of the maximum degree of plastic deformation of the U_3O_8 oxidation product at this temperature, thereby affording a maximum degree of surface-layer protection against further oxidation. This discontinuity appears in Fig. III-2 for iodine only.

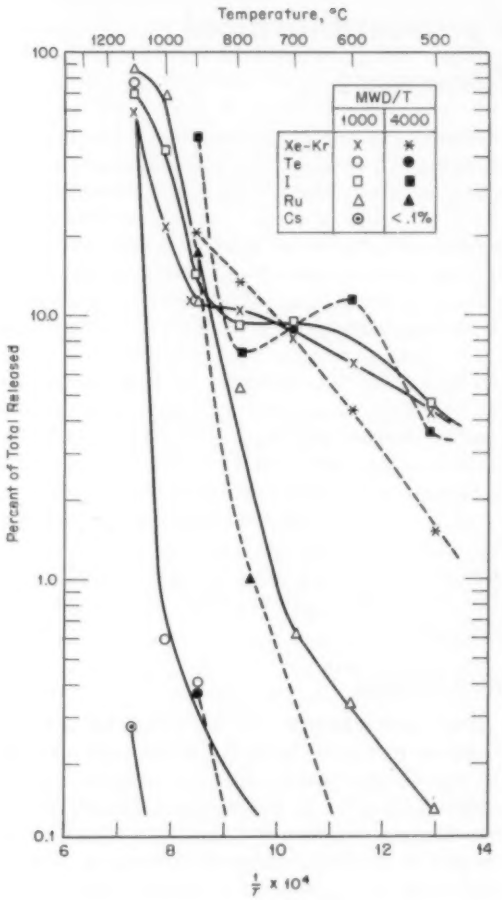

Fig. III-2 Fission-product release by oxidation of highly irradiated uranium dioxide (1000 and 4000 Mwd/ton).[17]

Properties of Fluoride Compounds

Stein[18] at ANL has measured the heats of reaction of fluorine and bromine with an adiabatic calorimeter at 25 and 105°C. When excess fluorine was used, BrF_3 and BrF_5 were formed at 25°C, and BrF_5 alone was formed at 105°C. The standard heats of formation (ΔH_f° of BrF_5, BrF_3, and BrF calculated from the measurements and data in the literature were −106.2, −64.8, and −17.7 kcal/mole, respectively (reactants and products in the gaseous state at 25°C). The standard free energies of formation (ΔF_f°) are −84.1, −55.2, and −18.0 kcal/mole, respectively.

Using the fundamental frequencies of IF_5, Nagarajan[19] has calculated the heat content, free energy, entropy, and heat capacity for this molecule at several temperature levels between 100 and 1300°K. A rigid rotator, harmonic oscillator model was assumed, and the values were calculated for the ideal gaseous state at 1 atm pressure.

Alenchikova and associates have recently reported[20] the preparation of several alkali metal plutonyl fluorides. They have identified an isostructural series of $M_2PuO_2F_4$, where M is Na, K, NH_4, or Rb. A second isostructural series of salts with cubic lattices was also reported, $MPuO_2F_3 \cdot H_2O$, where M is Na, K, NH_4, Rb, or Cs. The results of a comprehensive study on the PuO_2F_2-HF-H_2O system has also been reported.[21] It was established that there are three phases in the system: plutonyl fluoride (PuO_2F_2), plutonyl fluoride dihydrate ($PuO_2F_2 \cdot 2H_2O$) and a complex acid ($H_2PuO_4 \cdot 4H_2O$).

Pyrometallurgical Processes

Pyrometallurgical processes for recovery of discharged reactor fuel material include processes in which metal fuel materials are processed directly as metals and those processes in which both metal and ceramic fuel materials are processed in liquid metal–salt solvent systems. The incentive for development of pyrometallurgical processes stems principally from economies that are expected to be derived from the capability of such processes for handling short-cooled fuels with an attendant reduction of fuel inventories and from avoidance or simplification of chemical conversions. Pyrometallurgical processes are, in general, not high-decontamination processes, and their development must therefore be accompanied by a parallel development of methods for remote refabrication of reactor fuel elements.

Melt Refining

The melt-refining process will be used to recover uranium from the first core loading of the Experimental Breeder Reactor No. 2 (EBR-II) located at the National Reactor Testing Station in Idaho. This first large-scale testing of a pyrometallurgical process will be conducted in a fuel-cycle facility whose construction adjacent to the reactor is essentially complete. Progress in readying the facility for occupancy, in equipment design and installation, and in other miscellaneous areas associated with plant construction is discussed in a recent progress report of the Argonne Chemical Engineering Division.[11]

The melt-refining process is a simple melting process in which fission products are removed by volatilization and selective oxidation reactions. In recent studies of the melt-refining process, the behavior of condensable fission products volatilized during melt refining of highly irradiated EBR-II prototype fuel at 1400°C for 1 hr has been investigated.[11] (Other studies of fission-product behavior during melt refining of highly irradiated EBR-II fuel have been reported in previous Reviews.[22,23]) The iodine activity that volatilized during melt refining largely deposited on surfaces having temperatures of between 450 and 700°C, either as cesium iodide or as the iodide of an inactive element. Cesium, also volatilized during melt refining, was largely condensed in the same temperature region. These results are somewhat clouded by low material balances, about 50%, which presently are attributed to losses incurred during remote handling of the highly radioactive apparatus. Volatilization of tellurium, zirconium, ruthenium, and uranium was negligible. Barium and strontium were found mainly in the zirconia crucible, whereas cesium was deposited in a reaction layer on the inner wetted surface of the crucible.

Since the argon atmosphere in the processing cell of the EBR-II fuel-cycle facility may contain up to 5% nitrogen, the extent of nitridation of declad EBR-II fuel pins that are exposed to the atmosphere is of some concern. Excessive nitride formation on fuel pins might have an adverse effect in the melt-refining process. Some information on this point has been previously reported in these Reviews.[22,24,25] Recent studies[11] with fuel irradiated to 1.2 at.% burnup and cooled 80 days have indicated that irradiation has no large effect on the nitridation rate at temperatures below about 500°C. No significant effect on melt-refining yield was found after storage of unirradiated fuel pins for 2 hr at 350°C (Ref. 26) and at 650°C (Ref. 27) in 5% nitrogen–argon atmospheres. These exposure conditions bracket those anticipated for EBR-II fuel pins in process. Although these results appear to indicate that fuel-pin nitridation under anticipated process conditions will be of little consequence, it has nevertheless been recommended[11] that exposure of the fuel pins to the cell atmosphere be limited, that fuel-pin temperatures not be allowed to exceed about 300°C, and that the nitrogen content of the cell atmosphere be lowered significantly.

The mechanism of cerium extraction from molten uranium at temperatures between 1170 and 1450°C has been reported.[28] The study indicated that cerium removal (believed to be representative of the removal of other rare earths) is controlled by different mechanisms in three successive time periods as follows: (1) chemical reaction at the molten uranium–uranium dioxide interface, (2) diffusion of cerium in molten uranium, and (3) diffusion of oxygen through a solid reaction product layer.

Information on the swelling of irradiated (0.6 at.% burnup) EBR-II fuel pins and the release of noble fission gases, xenon and krypton,

from these pins during melt-refining operations has been previously reported in these Reviews.[22,29,30] Fission-gas release began at 750°C. It continued smoothly and rapidly as the temperature was increased at a rate of about 5°C/min and was complete by the time the fuel pins had melted completely (1090°C). Swelling also began at 750°C and continued to a maximum diametral increase of about 50% at 1000°C. Because of the softness of the metal and the large void volume in a melt-refining crucible, no trouble has been experienced with crucible breakage or swelling of the mass of pins out of the crucible.

In work with irradiated uranium, as contrasted with EBR-II fuel material which is uranium alloyed with 5 wt.% noble metals (principally ruthenium and molybdenum), somewhat different results were obtained[31] with regard to both swelling and fission-gas release. In this work uranium cubes and cylinders with principal dimensions (diameter or edge) ranging between 0.3 and 1.1 cm were used. At heating rates of between 50 and 100°C/min, rapid release of fission gases began about 10°C below the melting point. It was suggested that, at the point of fission-gas release, the strength of the uranium is so low that, under the internal pressure of the fission gases, bubbles and cracks are extended to the surface, permitting fission-gas escape. More than 99.5% of the Kr^{85} was lost on melting, and the final configuration was a pool of almost full-density uranium covered by a low-density froth. Over the range of uranium burnups employed, 0.14 to 0.4 at.%, uranium burnup and irradiation temperature had little effect on the pattern of fission-gas release. At lower heating rates of 10 and 5°C/min, 23 and 32%, respectively, of the fission gases were released prior to the rapid release beginning just before melting.

Because of the gross swelling caused by the gas bubbles, density values as low as 2 to 4 g/cm^3 were observed shortly after melting. During the expansion, bubbles of up to 3 mm in diameter were formed. A series of photographs* shown in Figs. III-3*a* to III-3*g* illustrates the growth sequence and shows that bubbles were formed in the following manner:

1. Macrocracks appear in the specimen and rapidly increase in both length and width.
2. These cracks, in general, do not appear to extend to the edge of the specimen but grow by increasing in width. At this stage the metal is apparently still solid because the edges of the cracks are jagged, but their extension in width instead of length suggests that the metal is very soft.
3. As the metal begins to melt, the jagged edges of the cracks smooth themselves out, forming irregular bubbles (at this stage the specimen has swollen to a roughly spherical form).
4. These bubbles round themselves, presumably by surface tension forces.
5. Favored bubbles increase in size by absorption of their neighbors, leading to a specimen containing a small number (in some cases only one) of very large bubbles.

The release of krypton from irradiated uranium on thermal-cycling the uranium through its solid phase changes has also been reported.[32] It was shown that significant releases occur, especially at the alpha-to-beta phase transformation. The magnitude of the release depends on the previous history of the uranium. The release of krypton on temperature-cycling a 3-mm uranium cube irradiated to 0.23 at.% burnup at 500°C is shown in Fig. III-4. The first peak occurring between room temperature and 550°C is not a genuine peak but is due to

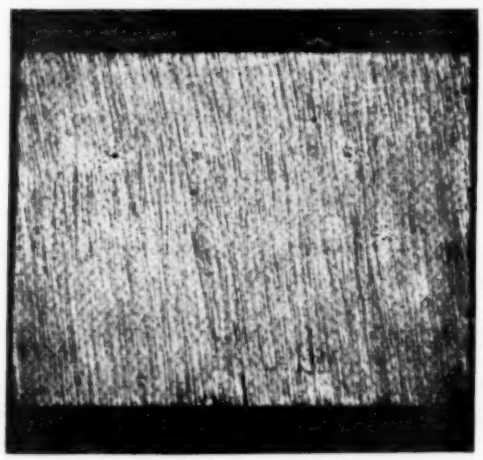

Fig. III-3*a* A typical unheated specimen.[31] Magnification 26×.

*Figures III-3*a* to III-3*g* and Fig. III-4 are reprinted here by permission from the *Journal of Nuclear Materials*.[31,32]

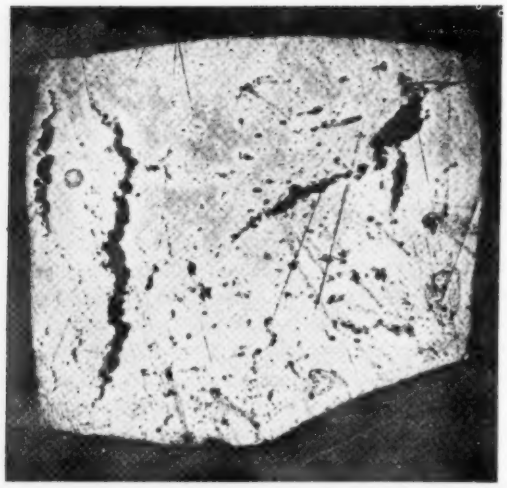

Fig. III-3*b* A specimen quenched 5 sec after the start of rapid gas evolution, showing the appearance of macrocracks. The metal retains its cubic outline indicating it to be still solid.[31] Magnification 22×.

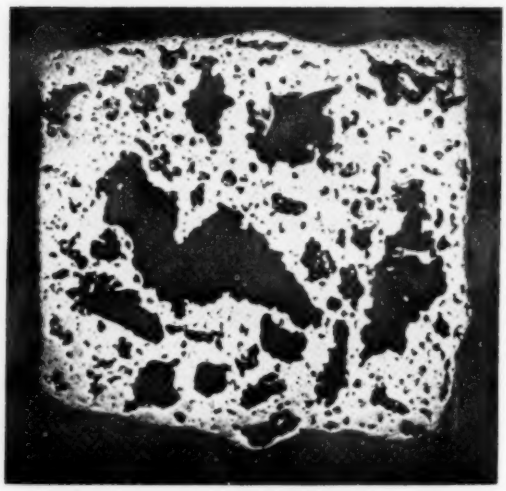

Fig. III-3*c* A specimen quenched 10 sec after the start of rapid gas evolution. The metal is now close to its melting point, and the cracks are forming irregular bubbles.[31] Magnification 18×.

the rapid heating in this region which shortened and magnified a continuous release region. A sharp reproducible peak at 695°C on heating is attributed to the alpha-to-beta phase transformation. It was concluded that uranium fuel elements cycled through the alpha-to-beta phase change could release appreciable amounts of their contents of fission-product gases.

General Information. A bibliography containing 761 annotated references to unclassified

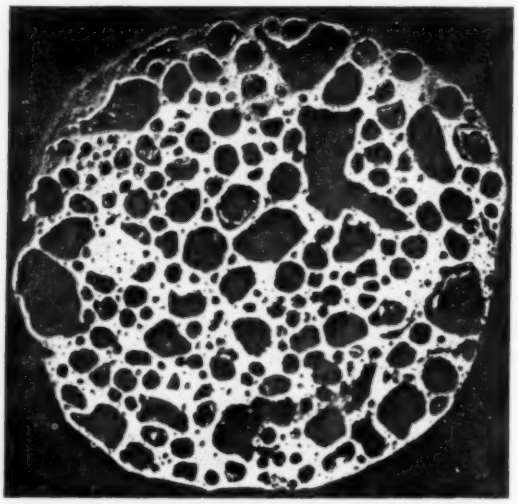

Fig. III-3*d* A specimen quenched 15 sec after the start of rapid gas evolution. The uranium, which is now molten, has become almost spherical in shape, and the bubbles are rounding themselves.[31] Magnification 15×.

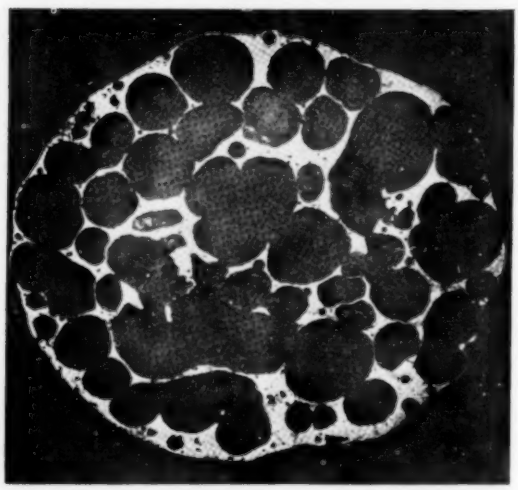

Fig. III-3*e* A specimen quenched 20 sec after the start of the rapid gas release, showing the increase in size of favored bubbles by absorption of their neighbors.[31] Magnification 15×.

reports and the published literature is available on the subject of plutonium technology.[33] The radioactivity distribution patterns produced in the metallurgical processing, particularly by consumable-arc melting, have been studied. Separation of radium from thorium and the release of thoria gas are the two important effects that were observed.[34]

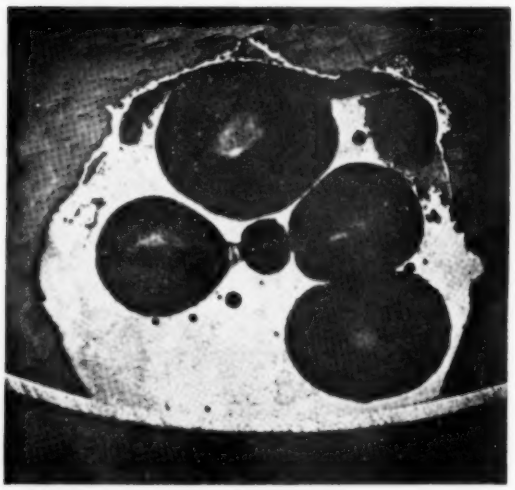

Fig. III-3*f* A vertical section through a specimen that has been molten for 2 min, showing only a small number of very large bubbles remaining. The arc of metal at the bottom is the tantalum cup that has adhered to the uranium.[31] Magnification 15×.

Fig. III-3*g* Part of a specimen that had been molten for 12 min, displaying the almost solid uranium on the tantalum cup with a thin friable shell of uranium above.[31] Magnification 11×.

Fundamental Studies of Liquid-Metal and Salt Systems

Solubilities in Liquid-Metal Systems. Basic to the design of processes utilizing liquid-metal systems is knowledge of the solubilities of fission-product, fissionable, and structural elements in metal solvents. The solubility of uranium in liquid gallium between 343 and 649°C has been measured[11] and may be represented by the equation U_{sol} (log of atomic percent) = $6.70 - 8840T^{-1} + 1.99 \times 10^{6}T^{-2}$. A second report[35] relating to the Liquid-Metal Fuel Reactor Experiment (LMFRE) provides extensive data on the solubility of uranium in bismuth and in bismuth containing other additives. This information was previously published in the February 1961 issue of the *Transactions of the Metallurgical Society of AIME* and was referred to in the October 1961 issue of this Review.

Nature and Thermodynamic Properties of Metals and Intermetallic Compounds. The utility of solubility measurements is increased considerably when the solid phase in equilibrium with the saturated melt is identified and characterized. An article on the thermodynamics of the uranium-cadmium system has recently been published.[36] The thermodynamic properties of uranium in dilute concentrations in liquid cadmium and the free energy, enthalpy, and entropy of formation of the intermetallic compound UCd_{11} were determined. Unusually large negative values of the partial molal relative enthalpy and excess entropy of uranium in cadmium solutions suggest partial ordering of cadmium around uranium in these solutions. The recently determined diffusivities of uranium in molten cadmium[26] of 1.3×10^{-5} cm^2/sec at 450°C to 2.3×10^{-5} cm^2/sec at 650°C also suggest ordering, since these values are below diffusivities calculated by the Einstein-Stokes equation on the assumption of noncoordinated atoms of the diffusing element. Measurements of the diffusivity of uranium in molten zinc have also been made.[11]

The annual summary research report on metallurgy[37] at Ames Laboratory provides con-

siderable information on phase diagrams and the thermodynamic properties of various alloy systems (thorium-zinc, yttrium-zinc, uranium-rhenium, thorium-tantalum, and many others). The cerium-cadmium system has been studied by means of a recording effusion balance.[11] The following sequence of intermetallic phases was found: $CeCd_{11}$, $CeCd_{6.4-5.6}$, Ce_2Cd_7, $CeCd_{4.1-3.4}$ $CeCd_2$, and CeCd. Except for differences in the homogeneity ranges, the cerium-cadmium system is the same as the praseodymium-cadmium system.[26]

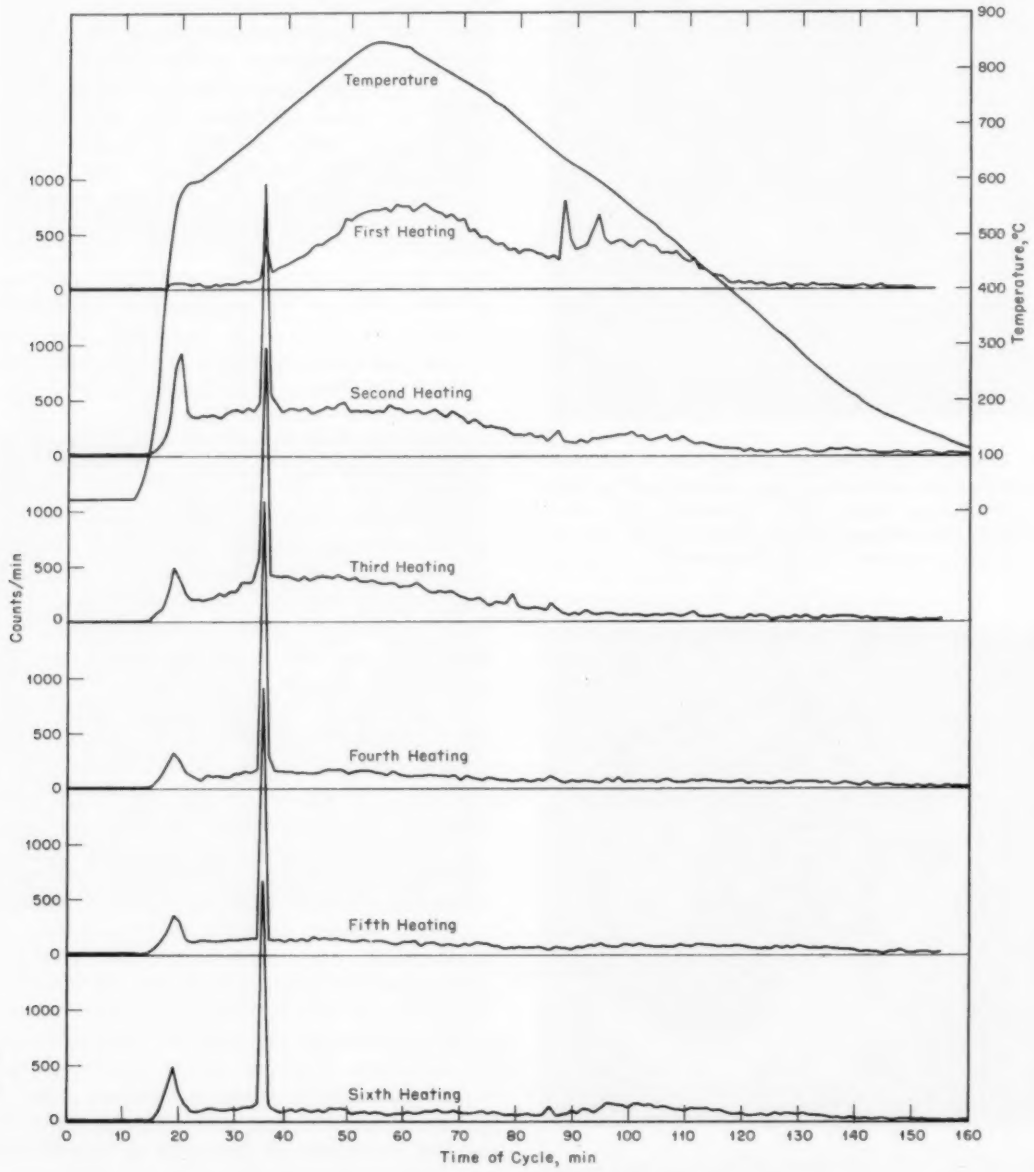

Fig. III-4 Release of Kr^{85} during successive thermal cycles of irradiated uranium through the solid-state phase changes.[32]

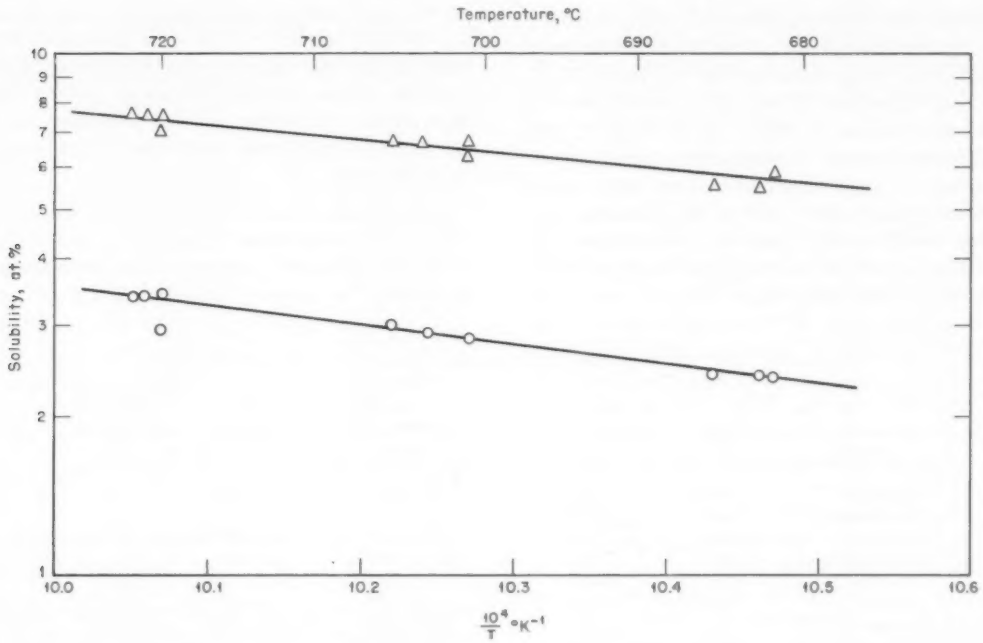

Fig. III-5 Mutual solubilities of aluminum and cadmium.[43] ○, cadmium in aluminum. △, aluminum in cadmium.

The following publications of general interest have been issued:

1. *The Temperature Range of Liquid Metals and an Estimate of Their Critical Constants*[38]

2. *Structure of Liquid Metals*,[39] Progress Report for June 1961 to February 1962

3. *The Density of Liquid Bismuth and of Dilute Solutions of Copper in Bismuth*[40]

4. *The Metallurgical Properties of Bismuth Solutions and Slurries*[41]

5. *Liquid Metals Technology Abstracts Bulletin*,[42] a quarterly bibliography of references, many with abstracts, on liquid-metal technology.

Distribution of Elements Between Immiscible Phases. Studies of the partition of various solutes between immiscible phases provide useful information for separation processes as well as for determination of thermodynamic functions. The mutual solubilities of molten aluminum and cadmium have been measured[43] (see Fig. III-5), and the partition of palladium, lanthanum, cerium, praseodymium, and uranium between these solvents has been determined[43] (Table III-3).* Various associated thermodynamic functions were derived.

The distribution of various elements between salt and metal phases is being studied at Ames Laboratory. The distribution coefficients of various solutes between a potassium chloride–lithium chloride eutectic salt containing 15 wt.% magnesium chloride and a zinc–3 wt.% magnesium alloy are summarized in Table III-4. Distribution data between the same salt phase and a magnesium–40 wt.% thorium solution are summarized[44] in Table III-5. Such data may provide the basis of processes for processing uranium-thorium fuels.

An investigation of the distribution of plutonium and various fission products between molten alloy phases has been completed at Ames Laboratory.[45] In this program an irradiated uranium–5 wt.% chromium eutectic was treated with magnesium-silver alloys of varying composition to determine the distribution of elements between the two phases. The

*Figure III-5 and Table III-3 are reprinted here by permission from the *Journal of Physical Chemistry*.[43]

equilibrations were conducted for 1 hr at 1000°C using approximately equal volumes of the two phases. The data summarized in Table III-6 show a pronounced effect of composition on solute distribution.[45] With alloys of low and intermediate silver content, the extraction of plutonium is small and becomes large only with essentially pure silver. Rare-earth extraction coefficients, however, are larger for alloys high in magnesium content than for those low in magnesium content.

Table III-3 PARTITION COEFFICIENTS IN THE ALUMINUM-CADMIUM SYSTEM[43]

Solute	Temp., °C	Concentration in upper layer, wt.%	Concentration in lower layer, wt.%	Partition coefficient, K	Estimated reliability, %
Palladium	680	6.35	$1.0_7 \times 10^{-3}$	$5.9_4 \times 10^{3}$	1.5
Lanthanum	686	8.31	$1.8_9 \times 10^{-1}$	$4.6_2 \times 10^{1}$	3
Cerium	680	4.63	$2.4_8 \times 10^{-2}$	$1.8_7 \times 10^{2}$	3
Praseodymium	686	7.82	$4.7_8 \times 10^{-2}$	$1.6_4 \times 10^{2}$	3
Uranium	686	4.80	3.3×10^{-5}	1.5×10^{5}	12
Uranium	689	3.63	2.3×10^{-5}	1.6×10^{5}	12
Uranium	686	2.33	1.7×10^{-5}	1.4×10^{5}	12
Uranium	710	4.98	3.2×10^{-5}	1.6×10^{5}	12

A part of this study was concerned with the interphase solubilities at 1000°C of the four metals, uranium, chromium, silver, and magnesium, which constitute the two phases. The solubility of uranium in silver is about 4 wt.% and decreases to 0.03% in pure magnesium. The amount of silver transferring to the uranium-chromium phase decreased from 0.03 wt.% for a pure silver phase to 4×10^{-4} wt.% for a magnesium–5 wt.% silver phase. The transfer of magnesium to the uranium-chromium phase and of chroumium to the magnesium-silver phase was qualitatively determined to be very small.

Both uranium and thorium carbides have been considered as reactor fuels. Reaction of these carbides in a potassium chloride–lithium chloride–zinc system is considered of potential interest to the processing of carbide fuels. Data have been obtained[37] which indicate that uranium monocarbide reacts with liquid zinc in the temperature range of 600 to 800°C, giving a uranium-zinc intermetallic compound of an as yet undetermined composition and U_2C_3. In the presence of a salt containing zinc chloride, it is presumed that uranium is transferred to the salt phase according to the equilibrium reaction

$$U_2C_3 + 3ZnCl_2 \rightleftharpoons 2UCl_3 + C + Zn$$

Study of this reaction as well as that of thorium carbide should yield information on the thermodynamic properties of the carbides and on the feasibility of such reactions for processing carbide fuels.

Reduction of Compounds in Liquid-Metal Systems. The reduction of compounds, particularly those of uranium, thorium, and plutonium, is necessary in several pyrometallurgical processes and is, of course, essential in the production of metals. The reduction at 500°C of uranium trichloride from a 30 wt.% concentration in a lithium chloride–potassium chloride eutectic by 0.5 wt.% magnesium–cadmium solutions has recently been reported.[46] Reductions were essentially complete in 5 min, final uranium concentrations in the salt phase being only 0.015%. On reduction, uranium dissolved in the cadmium to a final concentration of 2.25 wt.%, which is essentially the saturation concentration.

The preparation of aluminum-uranium ingots by the aluminum reduction of uranium dioxide for use as NRX (Canadian reactor) fuel elements has been described.[47] Thermet reductions of uranium dioxide by aluminum and beryllium have been conducted[48] which show reactions below 2000°F. These reactions are being investigated with a view toward forming refractory mixtures. A method for preparing magnesium-thorium alloys by reduction of thorium tetrafluoride with magnesium has been outlined.[49] The method consists of forming a salt mixture of thorium tetrafluoride with lithium fluoride and either magnesium fluoride or calcium fluoride and contacting the mixture with molten magnesium at 700 to 1000°C.

Table III-4 DISTRIBUTION COEFFICIENTS FOR VARIOUS COMPONENTS BETWEEN A POTASSIUM CHLORIDE–LITHIUM CHLORIDE EUTECTIC SALT CONTAINING 15 WT.% MAGNESIUM CHLORIDE AND A ZINC–3 WT.% MAGNESIUM ALLOY[44]

Component	Temp., °C	Wt.% in salt/ wt.% in metal solution
Yttrium	700	3.0×10^{-1}
	600	1.9×10^{-1}
Cerium	700	5.3×10^{-2}
	600	3.5×10^{-2}
Neodymium	700	2.1×10^{-2}
	600	3.8×10^{-2}
Samarium	700	23.5
	600	16.0
Thorium	700	$\sim 5.0 \times 10^{-4}$
	600	$\sim 5.0 \times 10^{-4}$

Development of Liquid-Metal and Salt Processes

Molten-metal and molten halide-salt systems are being utilized as processing media in several fuel-recovery processes now under development. At ANL the skull reclamation process utilizing molten halide-salt and zinc-based-metal systems is under development for recovery of skull material that remains in a crucible after melt refining. The process, shown schematically[26] in Fig. III-6, presently involves removal of a melt-refining skull from a crucible by oxidation of the skull to convert it to a powder, selective extraction of noble metals into zinc from the skull oxides by magnesium in a zinc solution, two uranium precipitations to enable removal of various fission products in supernatant solutions, and a retorting step to isolate a uranium metal product. A demonstration run of the skull reclamation process has been made in a recently completed inert-atmosphere glove box, using a charge of 190 g of oxidized skull.[11] An encouraging overall uranium recovery of about 90% was realized, with much of the remaining 10% residing in recoverable heels. The major components have been ordered for processing $2\frac{1}{2}$-kg uranium batches of skull oxide in integrated equipment.[11]

A study of the fates of stainless-steel constituents in the skull reclamation process showed that iron and nickel were readily separated from uranium in the noble extraction step but that substantial chromium accompanied uranium in this step. Before stainless steel can be accommodated in the process, as a result of either deliberate or inadvertent introduction, provision must be made for the separation of chromium from uranium.

Work was continued at ANL on the EBR-II blanket process in which plutonium and uranium are separated by utilizing the high solubility of plutonium in magnesium-rich solutions and the contrasting low solubility of uranium in such solutions. In the blanket process[26] (see Fig. III-7), blanket material is first dissolved in a zinc-rich alloy, and then magnesium is added to effect precipitation of the uranium away from the plutonium. Direct dissolution of stainless-steel-clad blanket elements would be allowable if the stainless-steel elements did not affect plutonium recovery and if they could be separated from the plutonium. Results of a demonstration run indicate that stainless steel and fission elements, which were added in the appropriate amounts, would have no effect on plutonium behavior. A plutonium recovery of 96% was obtained by separation of the supernatant phase, and a total recovery of 99% was obtained with the use of a single magnesium wash. However, in another run in which plutonium was not present, it was determined that chromium and iron would be precipitated with the uranium and thus be separated from the plutonium but that nickel would quantitatively follow the plutonium unless the process were modified.

Table III-5 DISTRIBUTION COEFFICIENTS FOR VARIOUS COMPONENTS BETWEEN A POTASSIUM CHLORIDE–LITHIUM CHLORIDE EUTECTIC SALT CONTAINING 15 WT.% MAGNESIUM CHLORIDE AND A MAGNESIUM–40 WT.% THORIUM ALLOY[44]

Component	Temp., °C	Wt.% in salt/ wt.% in metal
Yttrium	700	
	600	7.5 ± 0.8
Cerium	700	2.5 ± 0.1
Neodymium	700	10.5
	600	2.4
Samarium	700	>500
	600	>500
Thorium	700	$(2.0 \pm 0.3) \times 10^{-3}$
		$(1.8 \pm 0.5) \times 10^{-3}$
Palladium	700	2.3×10^{-3}
	650	0.8×10^{-3}

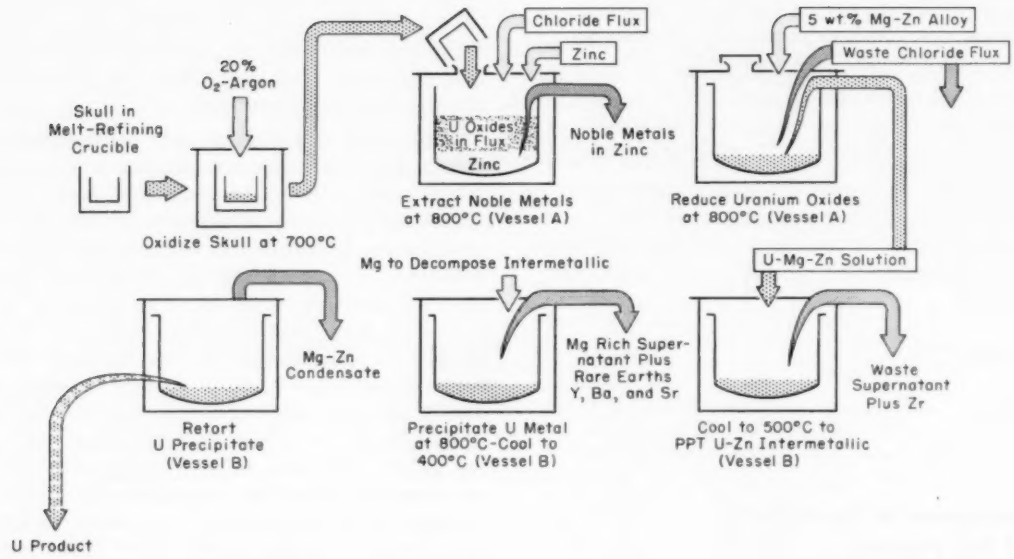
Skull in Melt-Refining Crucible
20% O_2-Argon
Oxidize Skull at 700°C
Chloride Flux
Zinc
U Oxides in Flux
Zinc
Noble Metals in Zinc
Extract Noble Metals at 800°C (Vessel A)
5 wt% Mg-Zn Alloy
Waste Chloride Flux
Reduce Uranium Oxides at 800°C (Vessel A)
U-Mg-Zn Solution
Mg to Decompose Intermetallic
Mg Rich Supernatant Plus Rare Earths Y, Ba, and Sr
Precipitate U Metal at 800°C-Cool to 400°C (Vessel B)
Waste Supernatant Plus Zr
Cool to 500°C to PPT U-Zn Intermetallic (Vessel B)
Mg-Zn Condensate
Retort U Precipitate (Vessel B)
U Product

Fig. III-6 EBR-II liquid-metal process for reclamation of melt-refining skulls.[26]

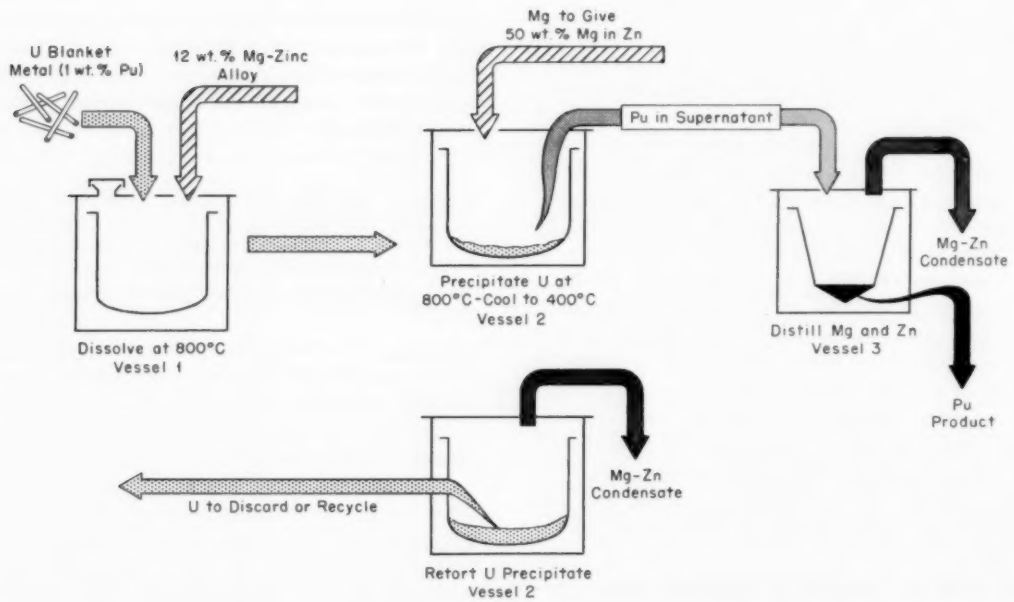
U Blanket Metal (1 wt.% Pu)
12 wt.% Mg-Zinc Alloy
Dissolve at 800°C Vessel 1
Mg to Give 50 wt.% Mg in Zn
Precipitate U at 800°C-Cool to 400°C Vessel 2
Pu in Supernatant
Distill Mg and Zn Vessel 3
Mg-Zn Condensate
Pu Product
U to Discard or Recycle
Mg-Zn Condensate
Retort U Precipitate Vessel 2

Fig. III-7 EBR-II liquid-metal process for uranium blanket metal.[26]

The pyrometallurgical purification of uranium by fractional crystallization of uranium from zinc-based solvent systems has been investigated by the Japanese.[50] After dissolution of uranium in zinc at about 750°C in the presence of a flux, the uranium was crystallized as U_2Zn_{17} from solution by cooling to 550°C. After removing the supernatant liquid, the zinc in the uranium concentrate, which contained between 6 and 16% uranium, was removed by vacuum distillation at 1000°C. Decontamination from zirconium by factors of between 2.2 and 9.5 were demonstrated.

Procedures that were developed for the removal of the noble-metal fission products from the dilute uranium-bismuth fuel solution of the Liquid-Metal Fuel Reactor concept (LMFR) have recently been described.[51] The noble-metal fission products would comprise about 28% of the fission products that are less reactive chemically than uranium. Most of these (about 90%) have low solubilities in the bismuth fuel and would be precipitated continuously from the fuel solution. A portion of the remainder would be occasionally removed from the liquid fuel by reaction with zinc to form low-density intermetallic compounds, and the rest would be removed by selective oxidation reactions. Processing frequency, as dictated by fission-product yields, rates of fission-product buildup, and resultant reactor poisoning effects, were calculated and discussed.

A method has been patented[52] for selectively reducing plutonium and rare-earth oxides, but not uranium oxides, using uranium dissolved in zinc or cadmium as the reducing agent.

Construction Materials

The success of pyrometallurgical processes under development and the feasibility of molten reactor fuels are dependent on the availability of suitable container materials. Tungsten is one of the most promising materials for contain-

Table III-6 EXTRACTION OF IRRADIATED URANIUM-CHROMIUM ALLOY WITH MAGNESIUM-SILVER ALLOYS[45]

	Extractant alloy composition					
Element	33.5 wt.% Mg	26.4 wt.% Mg	5.4 wt.% Mg	2.5 wt.% Mg	0.114 wt.% Mg	0 wt.% Mg
Plutonium:						
K_d*	1.10	1.12	19.9	48.9	123	109
% removed	27.8	18.5	91.9	96.7	98.7	98.6
% extracted	19.9	19.0	79.7	91.1	97.4	96.5
Strontium:						
K_d	110	26.7	30.5	37.2	22.2	8.6
% removed	98.0	93.0	96.7	98.1	96.3	87.9
% extracted	56.2	38.7	50.1	59.1	48.8	68
Barium:						
K_d		61.7	22.6	22.4	15.0	
% removed		97.2	96.5	97.1	95.7	
% extracted		35.9	38.6	36.7	38.9	
Yttrium:						
K_d	1024	181	26.8	93.9	11.4	16.5
% removed	99.7	98.0	99.6	99.6	96.0	96.5
% extracted	69.9	78.2	4.6	20.6	27.8	37.2
Cerium:						
K_d	1028	308	82.7	654	73.3	46.6
% removed	99.7	98.9	99.5	99.9	99.1	98.5
% extracted	81.8	63.8	20.3	42.1	49.5	47.2
Zirconium:						
K_d	0.079	0.087	0.15	0.25	0.44	0.39
% removed	25.8	38.7	23.1	33.5	58.7	30.7
% extracted	1.5	1.1	5.8	9.2	10.9	17.7

*K_d is defined as the activity of the component per gram of extractant phase divided by its activity per gram of uranium phase.

ment of flux and metal systems of the Argonne skull reclamation process described in the preceding section. Tests in tungsten crucibles have shown good stability of uranium-zinc-magnesium solutions of process interest.[11]

Beryllia has shown considerable promise as a material in which to conduct the last three steps of the skull reclamation process (two uranium-precipitation steps and the retorting step). Beryllia possesses the advantages of high thermal conductivity (consequently, low susceptibility to thermal shock), (2) high chemical stability, and (3) nonwetting by zinc-magnesium-uranium systems. Various methods of manufacture of large-sized beryllia crucibles are being explored and tested.

A study of the phenomena involved in liquid-metal corrosion is under way at Ames Laboratory using the lead-bismuth eutectic in a low-alloy stainless steel (2.25 wt.% chromium–1 wt.% molybdenum–iron alloy). A trace of zirconium in the eutectic alloy has been found to be highly effective in inhibiting corrosion. A thermal convection loop involving the eutectic with 100 ppm zirconium has now been operating[44] for 5850 hr at cold-leg temperatures of between 300 and 530°C and hot-leg temperatures of between 400 and 700°C.

Chemical analysis of the circulating eutectic after 4700 hr of operation indicated that iron and chromium concentrations were still below spectrographic detection limits. Earlier spinner type tests at 600°C with alloy of the same composition showed significant concentrations of corrosion products after 50 to 100 hr. The superior performance in the loop is as yet unexplained. The loop will be operated at a hot-leg temperature of 700°C until failure. Subsequent examination should reveal reasons for the superior loop performance.

Other Nonaqueous Processes

Pyrochemical processes, which are applicable principally to oxide and carbide reactor fuels, generally utilize gases, molten salts, and liquid metals as reagents and reaction media. They resemble pyrometallurgical processes in the use of high-temperature reactions, in a capability for handling short-cooled fuels, in simplicity, and in compactness. Only moderate fission-product removals are obtained in both types of processes, and they are usually combined with remote fuel refabrication procedures to form a complete fuel cycle.

Oxide Fuel Processing

Development work has continued at Hanford[53–55] on a close-coupled pyrochemical process in connection with the Plutonium Recycle Program.[56] This process is being developed for ceramic fuels consisting of uranium dioxide–plutonium dioxide mixtures. The mixed oxides are first dissolved in a molten-chloride salt by sparging the mixture with chlorine or hydrogen chloride. A portion of the dissolved uranium present as uranyl ion is reduced cathodically to uranium dioxide, which is essentially free of plutonium and is a by-product of the process. Further reduction results in the codeposition of uranium and plutonium dioxides, forming a product sufficiently enriched in plutonium for recycle to the reactor. Various alternative procedures for processing uranium, plutonium, and thorium oxide fuels are also being examined.

Additional studies of the electrochemical reactions of uranium in molten-chloride media have been reported.[54,55] Measurements of the electromotive-force values for the cell reaction

$$UO_2(s) + Cl_2(g) = UO_2Cl_2(\text{solution})$$

have been made at various temperatures and uranyl chloride concentrations. The resulting thermodynamic values at 993°K indicate a decreasing tendency for complex formation by uranyl(VI) ion as its concentration is increased, e.g.,

Uranyl(VI) molal concentration	ΔF, cal/mole	ΔS, entropy units	ΔH, cal/mole
0.074	−31,900	6.7	−25,200
1.37	−24,600	16.5	−8,200

Although the actual values are not certain, because of an unmeasured junction potential, the uncertainty from this source is believed to be small. Impedance measurements[54] have confirmed the two sequential reactions for elec-

trolytic reduction of uranyl chloride at low uranium concentrations:

$$UO_2^{2+} + e^- = UO_2^+ \quad (1)$$

$$UO_2^+ + e^- = UO_2 \quad (2)$$

At uranium concentrations of about 0.01 molal, however, the potentials of the two reactions become approximately equal, and, at concentrations above this level, only a single-step reaction is observed. Rate data from the impedance measurements give rate constants and exchange densities for reaction 1 that are about the same as those for the reduction of Cd^{2+}, Zn^{2+}, and Ag^+, which are considered to be rapid electrode reactions. The existence of uranyl(V) has been strongly indicated by an experiment in which solid uranium dioxide was added to a $3 \times 10^{-3} M$ solution of uranyl(VI) in molten KCl-NaCl (1 : 1 mole ratio) at 715°C. The reaction was accompanied by a color change from yellow-orange to brown (by reflected light), and a chronopotentiometric measurement on the resulting solution showed only the wave characteristic of uranyl(V) reduction to uranium dioxide.[55]

The tendency of certain ions to form complexes with cerium, thereby affecting the relative stabilities of Ce(III) and Ce(IV) in NaCl-KCl solution, was examined briefly.[53] Using chlorine gas as an oxidant and a solution containing 1.2 wt.% Ce(III) initially, the effects of fluoride and sulfate ions were determined. A fluoride-to-cerium ratio of 4 or more was required before Ce(IV) could be detected in the salt, and the effect was nullified when uranium was present in the salt. Sulfate ion at concentrations up to 10 times the cerium concentration did not show any effect. In these experiments cerium was used as a stand-in in order to assess the probable behavior of plutonium.

Since fuels for the Plutonium Recycle Program may involve mixed oxides of uranium, plutonium, and thorium,[56] codeposition studies were conducted on the electrolytic reduction process.[53,54] Solutions of uranyl chloride and thorium chloride in molten LiCl-KCl were used in the preparation, by cathodic reduction, of mixed oxides containing 1.85 to 48 wt.% thorium dioxide in uranium dioxide. The higher thorium dioxide concentrations (> 14 wt.%) required the use of chlorine or hydrogen chloride sparging during the electrolysis, chlorine being somewhat more effective. The product from the gas-sparged melts consisted of fine, needlelike whiskers with no visible voids in the cross sections. The addition of 2 wt.% thallium as thallous chloride to a 2.6 LiCl–NaCl-KCl melt at 600°C was investigated as a possible improvement in electrolytic codeposition of plutonium dioxide–uranium dioxide.[54] The melt contained 1.5 wt.% plutonium and 5 wt.% uranium initially, and it was sparged with chlorine during the electrolysis. It was hoped that the thallic ion formed in the presence of chlorine would tend to increase the ratio of Pu(IV) to Pu(III) ratio in the melt, thereby producing a corresponding increase in the ratio of plutonium dioxide to uranium dioxide in the product. The latter ratio was in fact increased by a factor of about 3 from a value of 0.007 to 0.02. Neither the melt temperature nor the use of chlorine vs. hydrogen chloride as a sparge gas had an appreciable effect on the plutonium-to-uranium ratio of the mixed oxide product produced by electrolysis of a 1.7 LiCl–KCl melt initially containing 4 wt.% uranium and 4 wt.% plutonium.

Work has continued on the crystal-growth characteristics of uranium dioxide resulting from electrolysis of uranyl chloride. A KCl-LiCl bath containing 33 wt.% uranium, a hydrogen chloride sparge, and a 0.5-volt cell potential at 5 amp of current were used to produce uranium dioxide cylinders about 1 in. in diameter on a cathode 2 in. long in 16 hr. Systematic studies have been conducted on the variables affecting the bulk density, oxygen-to-uranium ratio, impurity content, and other pertinent properties of the uranium dioxide deposits. Bulk densities of 10.8 to 10.9 g/cm^3 with corresponding lithium impurity contents below 10 ppm are achieved at melt temperatures of 500°C or higher. At 450°C both the bulk density and the purity decrease markedly. X-ray diffraction studies[55] of the crystal-face growth patterns in various melts show variations with different melts. In general, the initial growth was on the 1 1 1 faces, followed by 1 0 0 and 1 1 0 growth to form cubes (in $PbCl_2$–2.5 KCl and NaCl-KCl) or 3 1 1 and 5 1 1 growth to form polygons (in LiCl-KCl). When melts are not dry, dendrites with rapidly growing 2 1 0 faces are formed throughout the process.

In connection with the X-ray diffraction studies, lattice constants for the face-centered

cubic structures of thorium, uranium, and plutonium dioxides were determined:[53]

ThO_2	5.598
UO_2	5.469
PuO_2	5.395

As a possible alternative to the electrolytic method, chemical techniques for precipitating single and mixed oxides from molten chloride systems are being examined:[53,55]

Plutonium Dioxide. Two different methods were employed to precipitate plutonium dioxide from a 2.6 LiCl–KCl melt containing 1 wt.% plutonium trichloride at 575°C: (a) The melt was sparged with a mixture of 55% oxygen and 45% chlorine, producing a black, crystalline material. (b) A water-saturated helium sparge produced an olive-green compound. Both products were identified as plutonium dioxide, the black material consisting of larger crystals. The precipitation of plutonium dioxide by oxygen-chlorine sparging from melts containing 1 and 0.1 wt.% plutonium initially left about the same concentrations of soluble plutonium in the melt (i.e., 0.012 to 0.03 wt.%), suggesting that the completeness of the precipitation may be solubility limited.[55]

Mixed Plutonium-Uranium Oxides. On sparging a 2.6 LiCl–KCl melt initially containing 4.3 wt.% Pu(III) and 1.4 wt.% U(IV) with water-saturated helium at 575°C, a black, finely divided product was formed. This material was identified by X-ray methods as a solid solution of plutonium and uranium dioxides with a plutonium-to-uranium ratio of about 5 : 3.

Mixed Plutonium-Thorium Oxides. A green-colored product was produced by sparging a 2.6 LiCl–KCl solution containing 1 wt.% plutonium and 5 wt.% thorium with an oxygen-chlorine mixture. The oxide product had a plutonium-to-thorium ratio of 0.4. Initial concentrations of 2 wt.% each of plutonium and thorium in the melt were used to obtain a mixture of two plutonium oxide–thorium oxide compounds with plutonium-to-thorium ratios of 4 and 1.

Mixed Uranium-Thorium Oxides. A solid solution consisting of about 9 wt.% uranium dioxide in thorium dioxide was produced by sparging a LiCl-KCl melt containing thorium and U(IV) chlorides with moist helium. The product was a gray, finely divided solid.

Further pilot-plant investigations have been conducted on the salt-cycle process at Hanford.[54,55] A 24-hr dissolution test was made to determine the minimum time required to dissolve U_3O_8 in the melt (60 wt.% KCl–40 wt.% LiCl) with chlorine sparging. The U_3O_8 was added in two 30-lb increments at zero and 8 hr, followed by a 20-lb increment at 16 hr. The melt was circulated through a gas lift by means of 4.4 liters of chlorine per minute, and another 3 liters of chlorine per minute was added through a sparge tube. A total of 81 lb (fourfold excess) of chlorine was added. A maximum dissolution rate occurred after each U_3O_8 addition, and it was concluded that with properly timed additions the dissolution could be completed in about 12 hr, followed by 2 hr of drying with hydrogen chloride gas.

Electrolytic reductions have been conducted in a 60 wt.% potassium chloride–40 wt.% lithium chloride melt in an 80-liter quartz vessel. The U_3O_8 feed to the process was dissolved by chlorine sparging at 600°C, and the resulting solution was dried by chlorine and hydrogen chloride sparging at 535°C. Several batches of uranium dioxide varying from about 45 to 85 lb each were produced. In general, the reference potentials were about 0.45 to 0.8 volt, and the current densities were 0.5 to 1.0 amp/sq in. The oxygen-to-uranium ratios of the products fell between 2.002 and 2.007, and the bulk densities were higher than 95% of theoretical. The product was generally of excellent quality and, after a preliminary water rinse, contained lithium and potassium impurities of less than 100 ppm.

A mechanical crushing device developed for the electrolytic uranium dioxide product has proved to operate satisfactorily, although some further crushing in the −200 mesh range is needed. All the material passed a 6-mesh screen, and about 60% was larger than 30 mesh.

Some development has been reported[54] on a technique for impregnating graphite crucibles by immersion in molten barium chloride (melting point 960°C) to limit their permeation by molten salts. Although the technique did not eliminate the problem completely, it shows promise for use in combination with other frozen-wall ap-

proaches. The possibility of induction-heated graphite vessels is also receiving consideration. For use as electrodes, nonporous pyrolytic graphite appears promising.[55] Uranium dioxide deposits are easily removed from the electrode, leaving a smooth, shiny surface.

Alternating-current resistance heating of melts has been studied, using carbon electrodes of various configurations.[54] In a 60 wt.% potassium chloride–40 wt.% lithium chloride melt containing 20 to 30 wt.% uranium, electrolysis using a separate pair of d-c electrodes was conducted satisfactorily in the presence of a-c resistance heating. The a-c supply (60 cycle) was capable of 320 amp at 12 volts.

Two recent developments in instrumentation applicable to the salt-cycle process have been reported.[53,55] The first is a probe type filter photometer. Absorption in the regions of 1100 and 500 mμ will be used to determine U(IV) and U(III) plus U(VI), respectively, in the salt solution. The instrument is also believed to be adaptable for continuous analysis of constituents other than uranium. The other development consists of a submerged quartz plummet connected to a strain gauge and recorder so as to provide density data on salt solutions. With an expected accuracy of 1%, this method permits a measurement of variations in uranium concentration in the salt.

Oxidation-Reduction Process for UO_2

At Atomics International[57–59] the development of the low-decontamination oxidation-reduction process for uranium dioxide fuels has continued. The irradiated uranium dioxide fuel is alternately oxidized by air or oxygen at 200 to 600°C and reduced by hydrogen at 600°C until the particle size is reduced to a degree that the material is suitable for refabrication by remote cold pressing and sintering. The oxidation-reduction cycle is used both to remove the oxide fuel from stainless-steel cladding and to produce the particle sizes required for refabrication. Although some fission-product removal is achieved in this procedure (mainly cesium, ruthenium, tellurium, iodine, and the noble gases), the primary goal of the process is to facilitate reenrichment and refabrication of fuel elements for recycle to the reactor.

The processing of 100-g quantities of uranium dioxide irradiated to 15,000 Mwd/metric ton by gas phase oxidation-reduction has been reported previously.[59] A final check-out on the remotely operated pressing and sintering equipment has been completed, and experiments with the irradiated oxide have been started. When a carbowax binder was used in the pressing step, pellets prepared with water as the solvent had consistently higher densities than those prepared with ethanol as the solvent in preliminary tests with inactive material. Pellets pressed from the reprocessed, irradiated uranium dioxide appeared sound on the basis of visual examination through the cave window.[58]

Carbide Fuel Processing

Three low-decontamination pyrochemical processes for uranium carbide reactor fuels are under investigation at Atomics International.[57–59] The major effort is being applied to a carbide-oxide-carbide cycle. The carbide is first oxidized by oxygen or carbon dioxide at about 400°C to form uranium oxide, which is then converted to the carbide by carbothermic reduction at or above 1300°C. The carbide product is arc melted to form a solid product suitable for use as a fuel. A second process for carbide fuels involves a somewhat similar cycle in which the carbide is converted to uranium nitride by reaction with nitrogen; then the reaction is reversed by heating the uranium nitride and carbon under vacuum. The third procedure consists of electrolytic dissolution of the carbide in a lithium chloride–potassium chloride salt bath, which deposits the uranium as metal on a molybdenum cathode. The metallic uranium deposit is dissolved in mercury and is then converted to carbide with propane as the mercury is removed by distillation. Only the electrolytic procedure produces significant fission-product removal. The other two processes are essentially reenrichment and refabrication operations.

Experimental work has been continued on removing uranium carbide fuel from cladding by means of steam.[57] On treating samples of the uranium carbide with steam at pressures from 10 to 30 psig for 1 hr, the percentage of –400 mesh product decreased with increasing steam pressure from 78.5 to 64.0%. In two additional runs at lower steam pressures (5, and 0 to 1 psig), about 80% of the product was –400 mesh, but the reaction rate was somewhat slower.

Further investigations have been made on the activation of uranium monocarbide by exposing the unreactive 200-mesh powder to water vapor

at temperatures from 20 to 213°C in a thermobalance. An empirical correlation of weight gain with time was developed by assuming an initial second-order autocatalytic reaction followed by a first-order reaction. For the initial reaction, which is believed to be the conversion of unreactive uranium carbide to the reactive state, an activation energy of 8.8 kcal/mole was obtained.

The carbothermic reduction of uranium dioxide is being investigated on a kilogram scale.[57–59] The first phase of the program involves the reaction of uranium dioxide and carbon in a vacuum-induction furnace. Preliminary experiments with ½-kg quantities of material utilized furnaces with graphite susceptors and lampblack or alumina insulation. The reactants were agglomerated with a binder and water, oven dried at 80°C, and then heated under vacuum at 900°C to remove the binder and residual moisture. The charge was then heated to the reaction temperature (1600 and 1750°C). The product, however, proved to be somewhat inhomogeneous, with carbon contents ranging from 5.0 to 5.2 wt.% carbon in one experiment and 4.7 to 5.6 in the other (theoretical value for UC: 4.8 wt.% carbon).

Further information has been reported[57–59] on the reaction of nitrogen with uranium monocarbide. The particle size of the product is shown to decrease steadily as the reaction proceeds, and the particle size at a given stage of the reaction increases with temperature, probably as a result of sintering. The reactions involved in the nitridation of uranium carbide are assumed to be

$$UC + \tfrac{3}{4}N_2 \rightarrow \tfrac{1}{2}U_2N_3 + C \qquad (3)$$

$$\tfrac{1}{2}U_2N_3 \rightarrow UN + \tfrac{1}{4}N_2 \qquad (4)$$

for which the following overall rate equation has been derived:

$$K_{obs} = A_3 \exp(-16{,}350/T) - A_4 \exp(-18{,}800/T) \qquad (5)$$

References

1. J. H. Reynolds (Ed.), Nuclear Engineering Department Progress Report, September 1–December 31, 1961, USAEC Report BNL-705, Brookhaven National Laboratory, March 1962.
2. *Reactor Fuel Process.*, 5(2): 23–25 (April 1962).
3. *Reactor Fuel Process.*, 4(4): 30–32 (October 1961).
4. Oak Ridge National Laboratory, April 1962. (Unpublished)
5. F. L. Culler, Jr., Chemical Technology Division Monthly Report for March 1962, USAEC Report ORNL-TM-180, pp. 4–5, Oak Ridge National Laboratory, Apr. 2, 1962.
6. F. L. Culler, Jr., Chemical Technology Division Monthly Report for May 1962, USAEC Report ORNL-TM-245, pp. 4–5, Oak Ridge National Laboratory, June 1, 1962.
7. *Reactor Fuel Process.*, 5(1): 31 (January 1962).
8. *Reactor Fuel Process.*, 3(4): 24 (October 1960).
9. M. E. Whatley et al., Unit Operation Section Monthly Progress Report, September 1961, USAEC Report ORNL-TM-112, pp. 42–53, Oak Ridge National Laboratory, Apr. 5. 1962.
10. M. E. Whatley et al., Unit Operations Section Monthly Progress Report, December 1961, USAEC Report ORNL-TM-136, pp. 18–22, Oak Ridge National Laboratory, Apr. 10, 1962.
11. Argonne National Laboratory, Chemical Engineering Division Summary Report, January, February, March 1962, USAEC Report ANL-6543, July 1962; also Chemical Engineering Division Summary Report, April, May, June 1962, USAEC Report ANL-6569, October 1962.
12. Centre d'Étude de l'Énergie Nucléaire, Brussels, Reprocessing of Spent Fuels, Quarterly Report No. 3 (4th Quarter, 1960), USAEC Report EURAEC-81, 1960.
13. Centre d'Étude de l'Énergie Nucléaire, Brussels, Reprocessing of Irradiated Uranium, Quarterly Report No. 2 (3rd Quarter, 1961), USAEC Report EURAEC-207, November 1961.
14. *Reactor Fuel Process.*, 4(4): 35 (October 1961).
15. P. Berard, The Handling of Plutonium Hexafluoride, French Report CEA-2123, 1962.
16. J. Schmets and R. Heremans, Decontamination Factor in Processing of Irradiated Uranium Oxide by Volatilization, USAEC Translation AEC-tr-4880, Sept. 1, 1961.
17. Oak Ridge National Laboratory, Reactor Chemistry Division Annual Progress Report for Period Ending January 31, 1962, USAEC Report ORNL-3262, May 11, 1962.
18. L. Stein, Heats of Formation of Bromine Fluorides, *J. Phys. Chem.*, 66(2): 288–291 (February 1962).
19. G. Nagarajan, Potential Constants and Thermodynamic Properties of IF_5 and IF_7, *Current Sci.*, 30(11): 413–414 (November 1961).
20. I. F. Alenchikova et al., The Properties of Complex Plutonium Fluorides, *Russ. J. Inorg. Chem.*, 6(7): 777–781 (July 1961); translated by the Chemical Society from *Zh. Neorgan. Khim.*, 6(7): 1513 (July 1961).
21. I. F. Alenchikova et al., Investigation of the PuO_2F_2-HF-H_2O System (20 C Isotherm), *Soviet*

J. At. Energy, 10(6): 587–591 (March 1962); translated by Consultants Bureau from *At. Energ.*, 10(6): 592–596 (June 1961).
22. *Reactor Fuel Process.*, 4(1): 31 (January 1961).
23. *Reactor Fuel Process.*, 5(3): (July 1962).
24. *Reactor Fuel Process.*, 4(2): 41 (April 1961).
25. *Reactor Fuel Process.*, 4(3): 31 (July 1961).
26. Argonne National Laboratory, Chemical Engineering Division Summary Report, October, November, December 1961, USAEC Report ANL-6477, March 1962.
27. G. A. Bennett, Argonne National Laboratory, private communication.
28. T. Smith, *Trans. Met. Soc. AIME*, 224: 206–214 (April 1962).
29. *Reactor Fuel Process.*, 4(4): 38 (October 1961).
30. *Reactor Fuel Process.*, 5(2): 29 (April 1962).
31. J. D. Buddery and K. T. Scott, *J. Nucl. Mater.*, 5: 81–93 (January 1962).
32. K. T. Scott and J. D. Buddery, *J. Nucl. Mater.*, 5: 94–100 (January 1962).
33. R. J. Smith (Comp.), Plutonium, USAEC Report TID-3096, July 1961.
34. R. E. Colfield, *Health Phys.*, 7: 191–204 (February 1962).
35. A. F. Weinberg and R. J. Van Thyne, Solubility of Uranium in Liquid Bismuth, USAEC Report TID-14878, Armour Research Foundation, Illinois Institute of Technology, Jan. 26, 1959.
36. I. Johnson and H. M. Feder, *Trans. Met. Soc. AIME*, 224(3): 468–473 (June 1962).
37. Ames Laboratory, Annual Summary Research Report in Metallurgy, July 1960–June 1961, USAEC Report IS-351, December 1961.
38. A. V. Grosse, *J. Inorg. Nucl. Chem.*, 22: 23–31 (December 1961).
39. R. B. Gordon, Structure of Liquid Metals, Progress Report, June 1961–February 1962, USAEC Report TID-15135, Yale University, February 1962.
40. S. W. Strauss and L. E. Richards, *J. Nucl. Mater.*, 5: 12–16 (January 1962).
41. G. W. Greenwood, The Metallurgical Properties of Bismuth Solutions and Slurries, *Progr. Nucl. Energy, Ser. IV*, 3: 135–139 (1960).
42. MSA Research Corp., Liquid Metals Technology Abstract Bulletin for September 1961 to January 1962, Report LM/TAB-19.
43. F. A. Cafasso, H. M. Feder, and I. Johnson, *J. Phys. Chem.*, 66(6): 1028–1030 (June 1962).
44. A. F. Voigt, Ames Laboratory, April 1962. (Unpublished)
45. A. F. Voigt, Ames Laboratory, May 1962. (Unpublished)
46. B. A. Partridge and R. J. Moulton, The Reduction of UCl_3 in LiCl-KCl Eutectic by Magnesium in Cadmium, British Report AERE-R-3607, November 1961.
47. J. Baird and O. J. C. Runnalls, The Preparation of Aluminum-Uranium Alloys by the Aluminum Reduction of Uranium Dioxide, Canadian Report CRRM-1065, December 1961.
48. J. D. Fleming and J. W. Johnson, Materials for High Temperature Nuclear Energy Applications, Progress Report No. 2, Part 2, August 15, 1959 to August 15, 1960, USAEC Report ORO-325(Pt. 2), Georgia Institute of Technology.
49. J. N. Reding, Jr., U. S. Patent 3,026,196, Mar. 20, 1962.
50. Masayoshi Kanno and Sanya Kokubo, *J. At. Energy Soc. Japan*, 4: 30–36 (January 1962) (in Japanese).
51. O. E. Dwyer, H. E. Howe, and E. R. Avrutik, *Nucl. Sci. Eng.*, 12: 15–22 (January 1962).
52. L. Burris, Jr., and A. Schneider, U. S. Patent 3,023,097, Feb. 27, 1962.
53. W. H. Reas, Chemical Research and Development Operation Monthly Report, March 1962, USAEC Report HW-73202C, Hanford Atomic Products Operation, Apr. 15, 1962. (Classified)
54. W. H. Reas, Chemical Research and Development Operation Monthly Report, April 1962, USAEC Report HW-73514C, Hanford Atomic Products Operation, May 15, 1962. (Classified)
55. W. H. Reas, Chemical Research and Development Operation Monthly Report, May 1962, USAEC Report HW-73905C, Hanford Atomic Products Operation, June 15, 1962. (Classified)
56. S. Goldsmith (Ed.), Plutonium Recycle Program Annual Report, Fiscal Year 1961, USAEC Report HW-70000, Hanford Atomic Products Operation, Aug. 11, 1961.
57. C. E. Weber, Atomics International, March 1962. (Unpublished)
58. C. E. Weber, Atomics International, April 1962. (Unpublished)
59. C. E. Weber, Atomics International, May 1962. (Unpublished)

Section

IV

Reactor Fuel Processing

Waste Disposal

Tank-Storage Management of High-Level-Activity Liquid Wastes

At the 1962 Nuclear Congress (New York), Campbell, Doud, and Tomlinson[1] of Hanford presented a review of the design and operation of current U. S. waste-storage facilities for the more than 50 million gallons of high-level-activity radioactive solutions and sludges being stored in nearly 200 underground tanks throughout the AEC complex.

A wide variety of tank designs has been used to contain radioactive wastes. This variety results from variations in volumes and compositions of wastes to be stored, in environmental conditions surrounding the storage sites, and in engineering judgment factors. Of the many factors that influence the design and operation of facilities for high-level-waste containment, the radiochemical and chemical compositions of wastes are of primary importance.

For storage purposes, high-level wastes can be segregated into self-heating wastes and nonheating wastes, depending on relative fission-product content. The self-heating wastes are the most active wastes. Enough heat is generated in them by fission-product decay to heat the liquid to boiling, and special provisions must be made to dissipate this heat safely. Nonheating wastes are the less active wastes, which nevertheless contain enough radioactive materials to require storage. The point of demarcation between self-heating and nonheating wastes in Hanford type tanks is about 0.1 to 0.5 Btu/hr per gallon of waste.

Most of the tanks used for the storage of radioactive process wastes range in size from 300,000 to 1,330,000 gal capacity; they are 50 to 85 ft in diameter and have a usable depth ranging from 18 to 32.5 ft. The tanks are generally covered with 7 to 10 ft of earth, which serves as a radiation shield. The types of tanks used for the storage of self-heating wastes at Hanford, Savannah River, and ICPP (Idaho) are shown in Figs. IV-1 to IV-3, respectively. A typical tank for the storage of nonheating wastes at Hanford is shown in Fig. IV-4. Tanks of a similar design are also used at Savannah River for the storage of concentrated nonheating wastes. At ICPP, nonheating wastes are stored in stainless-steel tanks which are similar to the tanks shown in Fig. IV-3 but which do not have cooling coils. Unit cost data for storage facilities using these two types of tanks are summarized in Table IV-1.

No valid basis has been established for predicting the service life of waste-storage tanks. Corrosion data on tank service life are not yet sufficient to be meaningful. Examination of the actual service life of the existing storage tanks in use is also inconclusive. Table IV-2 summarizes the available information on the performance of these tanks.

The failure of the two Hanford tanks through flexure of the tank liner should not be considered typical. Before the tank containing bismuth phosphate failed, the vessel was filled and emptied repeatedly. The design of the liner is such that the weight of the side liner tends to be transmitted around the knuckle at the junction of the side and base plate in such a way that the bottom tends to buckle upward. The first indication of a nonstandard condition was the inability to install a jet dip-leg of the proper length; investigation revealed that the bottom liner was elevated a few feet from its original position. Later the tank started leaking. The Redox tank was withdrawn from service when erratic liquid-level measurements indicated an

abnormal condition. Subsequent investigation revealed that the steel bottom liner had buckled upward when self-heating Redox wastes were added to the tank. The liner slowly receded to its original position after the boiling wastes were pumped out. It is postulated that the heat vaporized some water from the concrete grout below the liner, building up sufficient steam pressure to lift the liner and the small amount of waste in the tank at the time. Although all evidence indicates the tank did not leak, the tank has remained empty since that time.

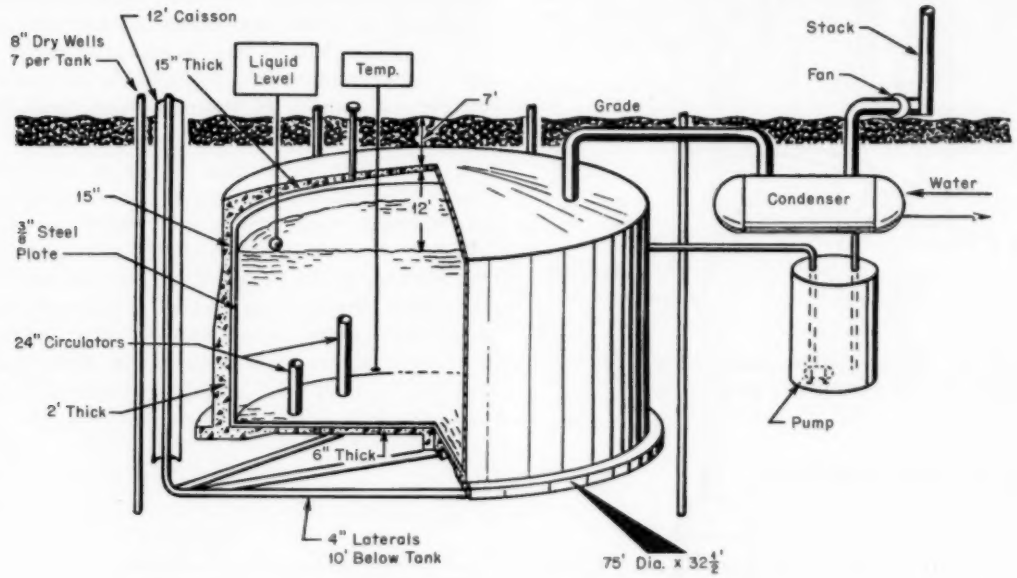

Fig. IV-1 The 1,000,000-gal storage tank for Hanford self-heating type liquid wastes.[1]

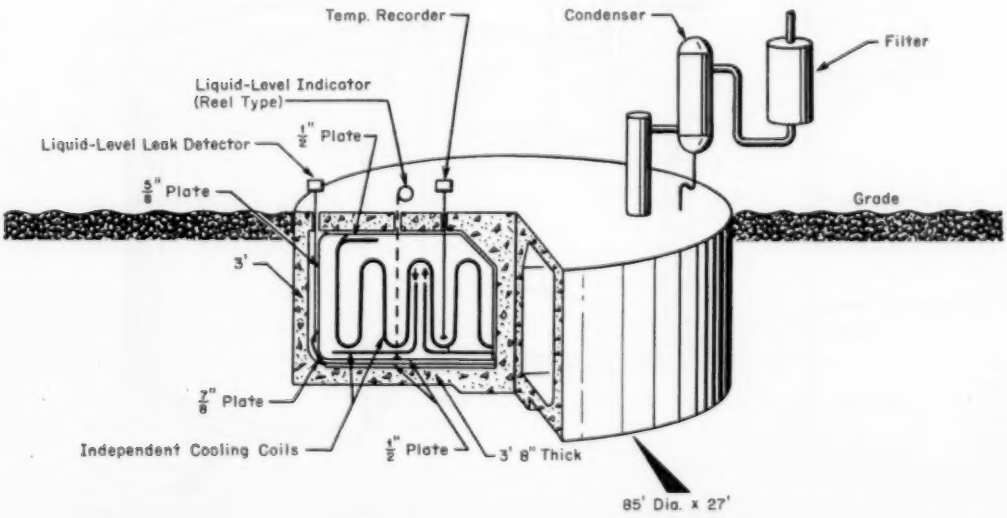

Fig. IV-2 The 1,070,000-gal tank for storing Savannah River self-heating type liquid wastes.[1]

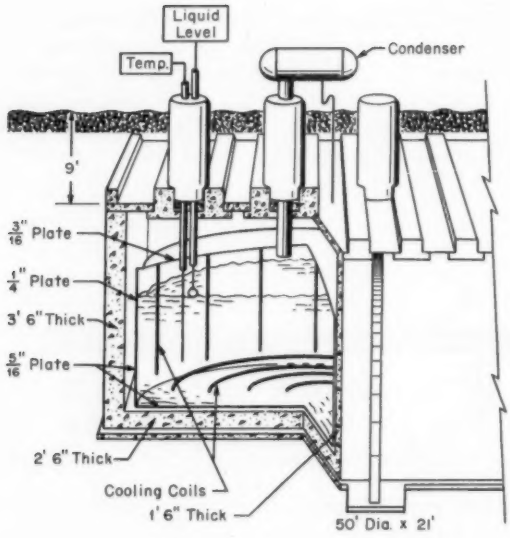

Fig. IV-3 The 300,000-gal waste-storage tank for Idaho (ICPP) self-heating type process waste.[1]

The other three Hanford tanks that are suspected of failing through pit corrosion were used to store a concentrated waste from the formerly used bismuth phosphate process. These wastes contain appreciably more sulfate and phosphate ions than current wastes, and laboratory studies indicate that these wastes are much more corrosive than current Redox and Purex wastes. It is clear that more failures of tanks storing these wastes can be expected, but it is not clear how these data apply to the estimation of life expectancy of waste-storage tanks for current process wastes.

In the four tanks that failed at Savannah River after several months of use, seeping began through areas of the side walls that were affected by welding. Investigation indicated that the seepage is the result of stress corrosion of the carbon steel by the alkaline nitrate system. A careful review of the records revealed that the materials and workmanship in these tanks are of the same high quality that went into the

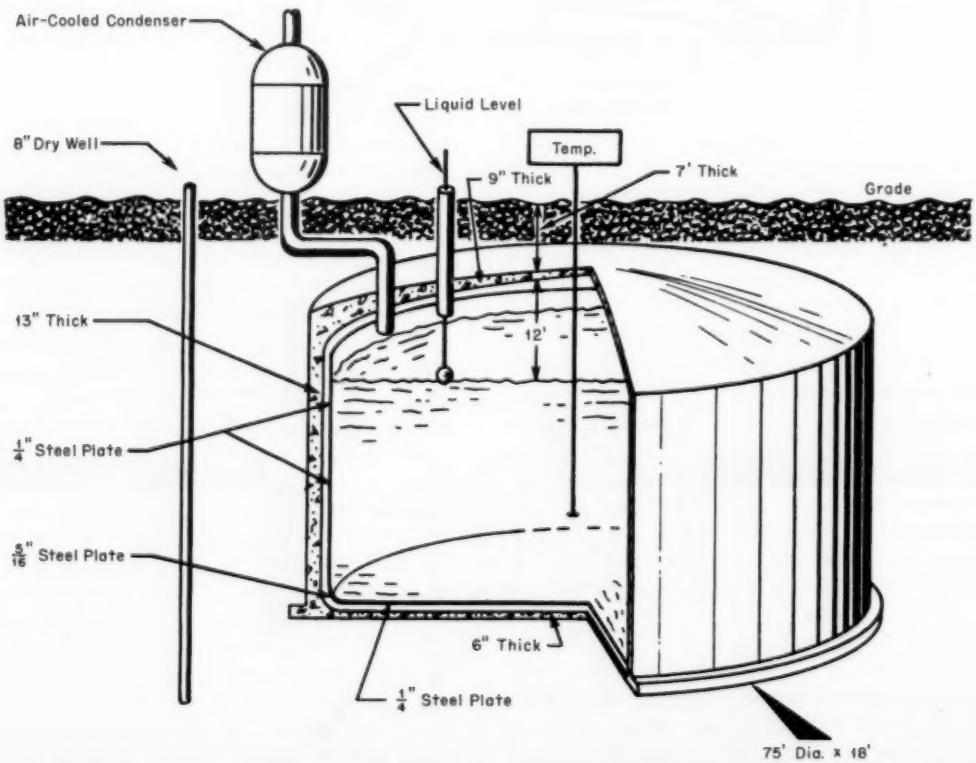

Fig. IV-4 The 533,000-gal waste-storage tank for Hanford nonheating type liquid wastes.[1]

construction of the other storage tanks in use at Hanford and Savannah River. At present it is not clear why these tanks leak while so many other tanks are giving longer service life under very similar chemical and thermal conditions. It is possible that the true difference lies in the ability to detect very small leaks in tanks of this design. In any event the tests indicate that the stress corrosion can be avoided in future construction by heat-treating the tank in place before use.

Throughout the years of operating experience, considerable attention has been given to procedures that are designed to assure that the high-level wastes are contained so that the radioactive materials do not enter the potable waters in the environment. At Hanford, measurements are made monthly of the liquid level in inactive

Table IV-1 APPROXIMATE UNIT COST OF STORAGE FACILITIES FOR RADIOACTIVE WASTES[1]

Type of waste	Capital cost per gallon*	Reference	
		Site	Volume, thousands of gallons
Alkaline (nonheating):			
As solution or salt cake	$0.47	Savannah River	1330
As solution or salt cake	0.89	Hanford	533
Alkaline (self-heating):			
Self-concentrating	0.99†	Hanford	1000
Cooled	1.69‡	Savannah River	1070
Acid (nonheating)	2.00	Idaho (ICPP)	300
Acid (self-heating)	2.66	Idaho (ICPP)	300

*Cost data adjusted to 1962 prices.
†Based on a stored volume of 775,000 gal.
‡Savannah River quotes $1.40 as a more appropriate figure.

Table IV-2 SUMMARY OF PERFORMANCE OF TANKS STORING RADIOACTIVE WASTES[1]

Location	Type waste	No. of tanks		Tank use, years	Probable failure mechanism
		Failed	In use		
Hanford	Nonheating (bismuth phosphate)	4	76	9–17	Liner flexure (1); pit corrosion (3)
Hanford	Nonheating (Redox and Purex)	0	44*	10–17	
Hanford	Self-heating (Redox)	(1)†	14	2–8	Liner flexure; no leakage indicated
Hanford	Self-heating (Purex)	0	6	0–6	
Savannah River	Nonheating (Purex)	0	7	0–6	
Savannah River	Self-heating (Purex)‡	4§	14§	0–6	Stress corrosion
Idaho (ICPP)	Nonheating (acid)	0	3	0–11	
Idaho (ICPP)	Self-heating (acid)	0	10	0–11	

*Some of these tanks were previously used to store bismuth phosphate ($BiPO_4$) wastes.
†See text.
‡Some of these tanks are used to store wastes from the processing of enriched uranium–aluminum fuels. One of these tanks leaked.
§Savannah River notes that these numbers are misleading. At present, 16 tanks have been put into use for self-heating wastes; of these, four showed one or more leaks at one time or another, but none is now leaking at a perceptible rate, and all four are still in use. One of the four is only half full and will not be filled further because of the leak. The other three are full or nearly so; the leaks have plugged. The "leakage" was contained by the outer vessel of the double-tank construction and was not lost from the tank system.

storage tanks, and more frequently if transfers are made into or out of the vessel or if a leak is suspected. The second line of defense at Hanford is the more than 200 ft of dry soil between the tank and the ground water. A grid of dry wells is used regularly to monitor the soil for radioactivity and thus to detect any leakage that might have escaped detection through liquid-level measurement. In the four Hanford tanks that failed, the leak was first detected in each case, by liquid-level measurement, with leak rates of 100 to 700 gal per day being observed. Subsequently, radioactive was detected in the dry wells in the vicinity, but in no case was radioactivity from a leaking tank found in the ground water. The contents of the leaking tanks were transferred to other vessels.

For all tanks at Idaho, and the tanks for self-heating waste at Savannah River, the second line of defense is the concrete vault that contains the storage tank. The absence of radioactive solution in the vault attests the integrity of the storage vessels. The additional leak protection afforded by the vaults compensates for the less favorable geological situation existing at Idaho and Savannah River. No leakage has been detected from any radioactive waste-storage tank at ICPP; however, four tanks are seeping at Savannah River. The small volume is being caught within the vault and returned to the vessels.

The risk of leakage from tanks containing nonheating wastes at Savannah River is minimal, since the wastes are being concentrated to the point of incipient crystallization at the boiling temperature just before discharge to the tank. Upon cooling in the tank, the wastes will largely crystallize to a massive salt cake, with a small volume of residual aqueous phase. Hanford is also planning to concentrate its nonheating wastes to salt cakes during the next several years.

Radiolytic hydrogen that is produced by the fission-product irradiation decomposition of water and other chemicals must be removed from these tanks. An estimated 40 cu ft of hydrogen (STP) is produced per million British thermal units of heat. At Hanford this hydrogen is swept from the tank with the steam from self-boiling. At Savannah River the concentration of hydrogen is kept well below the lower explosive limit by periodically blowing air into the tank above the liquid and exhausting the gases to the atmosphere through the fibrous glass filter. At Idaho hydrogen has never been detected in a waste-storage tank. It appears that the air changes from natural causes (convection, changes of atmospheric temperature, and pressure) are sufficient to remove the hydrogen as rapidly as it is formed in systems containing relatively little radioactivity.

Treatment of Liquid Wastes by Adsorption and Ion-Exchange Materials

Hanford is continuing its sorption studies to determine the role of sorption processes in their overall waste treatment and fixation program.[2–4]

A column of sulfonated polystyrene resin (Amberlite IR-120) in the sodium form was used in a Micro Pilot Plant run to evaluate the removal of radioisotopes from a steam-stripped and acidified Purex tank-farm condensate feed.[3] Previous experiments indicated that the addition of acid is necessary to convert strontium and cerium to the cationic forms.[4] Since hydrogen ions compete with cesium for ion-exchange sites, the *p*H must be maintained high enough so that cesium capacity is not significantly decreased. The steam-stripped condensate waste was acidified to *p*H 4.3 by the addition of nitric acid, passed through a bed of activated carbon to remove residual organic not removed by the stripper, and finally through the ion-exchange resin at a flow rate[3] of 16 ml/(min)(cm^2).

The resin was effective in removing cesium, strontium, zirconium, cerium, and ruthenium from the waste. Cesium-137 was the only radioisotope to exceed its MPC_w (maximum permissible concentration in water) in the resin-column effluent during the run; this occurred after 11,000 resin-column volumes of waste had been treated. The resin was regenerated with 4*N* sodium hydroxide. Cesium and strontium isotopes were eluted nearly completely from the resin, but very little of the other isotopes was removed. Regeneration of a similar exhausted resin column was accomplished more effectively with 4*N* nitric acid.

Aluminum shavings and naturally occurring minerals have been studied for their effectiveness in decontaminating Hanford reactor coolant (water) effluents, a category of low-level-

activity waste.[5-7] The ability of a reactive metal such as aluminum to remove isotopes from reactor effluent water has been demonstrated[5] and is attributed to a reaction between the ions from solution and the surface oxide film formed on the aluminum as a water corrosion product.

The aluminum shavings were tested in an 800 gal/min pilot plant at Hanford.[5,6] The shavings, which are grade 1100 F aluminum, are cylindrically shaped and are $^{7}/_{16}$ in. long by 0.45 in. in diameter with a thickness of about 0.020 in. The free-pack density is 18 lb/cu ft.

The removal efficiency for several isotopes was determined by feeding actual reactor effluent through the bed of shavings at various linear velocities, initially 3.8 ft/min, then 6 ft/min, and finally 2.7 ft/min. The highest reductions were at 2.7 ft/min: 90% for Mn^{56}, 80% for Cu^{64}, 70% for Zn^{65}, 65% for As^{76}, 55% for P^{32}, and 12% for Cr^{51}.

Some 21 minerals were studied in a series of Hanford experiments for their effectiveness to remove P^{32} from simulated reactor coolant (tap water in this study).[7] Eleven of the minerals adsorbed 30% or more of the influent P^{32}. Mixed mineral columns were better adsorbents than single mineral columns. The best mineral mixtures (pyrite–Florida pebble phosphate–calcite and pyrite–Idaho rock phosphate–calcite) adsorbed 65 to 70% of the influent P^{32}, whereas the best adsorption by single minerals (sodalite, epidote, goethite, fluorite, pyrite, and pyrrhotite) ranged from 37 to 60%. A limited number of experiments indicated that the adsorption of P^{32} from actual reactor coolant may be lower than the adsorptions reported for the tap-water experiments. This difference is believed to be caused by the presence of an oily solid crud in the actual reactor coolant which, by coating the mineral surfaces, limited free access of the reactants and thus reduced the adsorption of P^{32}.

Effects of Sodium Nitrate on Removal of Strontium by Certain Minerals

ORNL is carrying on fundamental studies on the reactions of Sr^{90} with minerals.[8,9] As a part of these studies, the role of sodium nitrate in the removal of strontium by calcite and rock phosphate columns was examined.[9] The presence of sodium nitrate in waste solutions increases the removal of strontium by a calcite column but decreases strontium removal by a rock phosphate column. In either system the material beneficial for strontium removal is calcium phosphate.

The experimental results indicated that the amount of calcium dissolved from calcite by 1*M* sodium nitrate was 1.1*M*, almost four times the solubility of calcite in water. The dissolution of calcite was the same in three successive leaches, but the amount of calcium in solution contacted with rock phosphate decreased in each of three successive leaches. Equilibrium was reached within 15 min for calcite particles up to 0.5 mm in diameter; rock phosphate samples showed increasing calcium in the solution contacted with increasing contact time up to 5 hr.

Preliminary results from tests with rock phosphate indicate differences in the response of calcite and rock phosphate. As with calcite, more calcium was dissolved in the presence of sodium nitrate, but unlike calcite, less calcium was dissolved with successive leachings, suggesting that the high initial calcium concentration is caused by the presence of some very fine particles in each size range. An increase in calcium concentration was shown with a decrease in the particle size. There was some indication that that the sodium nitrate concentration affected the rock phosphate solubility.

Centrifuge Process

Dorr-Oliver Incorporated (Stamford, Conn.) has investigated the use of the continuous centrifuge[10] for dewatering and removing suspended solids from the plant effluent of the ORNL Process Waste-Treatment Plant, which is a single-stage treatment plant employing a lime-soda softening process.[11] The effects of continuous sludge removal and recirculation of sludge on clarification efficiency were also studied.

These tests[10] have given the following results: (1) the sludge can be dewatered to a concentration of 40 to 50 wt.% total solids, and the sludge volume can be reduced by 88%; (2) continuous centrifugation was capable of removing 37 to 91% of the suspended solids present in plant effluent; and (3) flocculation reactions were improved and the suspended solids concentration of the plant effluent was reduced by 28% by recirculating sludge from the settling tank to the flocculating basins (increasing the solids concentration in them to 0.1%).

In another study[12] by Dorr-Oliver Incorporated, the particle size was determined for the

suspended solids in the ORNL waste-treatment plant raw process waste and effluent. The particle size of the separated solids was also related to the activity level, which was found to vary with particle size. Data were presented to show activity-level–particle-size relations for gross gamma activity and for Cs^{137}, Sr^{90}, Ce^{144}, Co^{60}, Ru^{106}, and Zr^{95}-Nb^{95}. The level of activity of the solids was approximately 10^4 times greater than the level of activity of both the raw (untreated) process waste and the plant effluent from which the solids were removed.

Reduction to Solids of High-Level-Activity Liquid Wastes

Calcination in Molten Sulfur

Savannah River is developing a method of converting radioactive wastes to a relatively insoluble form that could then be stored in a suitable container.[13] In this process the aqueous acidic wastes are heated in molten sulfur so that the water and volatile acids are driven off, and the chemical compounds, such as the aluminum nitrate that may be a major component, are decomposed and/or chemically reduced. The product, a mixture of calcined waste in sulfur, has a smaller volume than the original waste solution, is relatively insoluble, and can be transferred to storage as a liquid. A suitable storage vessel would be shaped to facilitate cooling and thus prevent the melting of the sulfur by fission-product heat. Melting is considered undesirable because it would permit the solids to settle. High concentrations of solids in sulfur lead to severe cracking of the sulfur mass when mixtures that contain aluminum-bearing wastes are exposed to water.

Promising results have been obtained by the use of a two-step process in which the waste is dehydrated and denitrated in a molten-sulfur bath at 150°C and is then heated for a prolonged period (1 to 5 hr) at 400 to 440°C. Sulfur reaches its minimum viscosity (about six times that of water at 20°C) at about 150°C. The disengagement from the reaction mass of large quantities of water vapor and off-gas is therefore more readily accomplished at this temperature, thus permitting a higher rate of feed to the reaction vessel.

Wastes containing both stainless-steel nitrates and aluminum nitrate have been treated in this manner. Appreciable quantities of water-soluble sulfates are formed by the denitration of both stainless-steel nitrates and aluminum nitrate in sulfur at 150°C. The subsequent high-temperature step converts most of the stainless-steel sulfates to sulfides or oxides, but the aluminum sulfate is reduced to the oxide more slowly, and appreciable quantities of aluminum sulfate remain after the high-temperature step. Residual sulfuric acid and water are appreciably reduced by heating the aluminum wastes at high temperatures.

Results of extensive leaching tests at room temperature (25°C) indicate that products resulting from the calcination of both aluminum nitrate and stainless-steel nitrate can be formed under conditions that make them very resistant to water leaching. Leaching rates are low for both mixed fission products and plutonium. The best products from feeds that contain stainless-steel nitrates are formed by heating the calcined slurry at 444°C for periods of 3 and 5 hr with agitation. The most stable product from the calcination of aqueous feed containing aluminum nitrate was formed by heating at 400°C for 5 hr with agitation.

Pot Calcination

ORNL is continuing its laboratory and engineering-scale studies of the pot-calcination process for converting high-activity-level wastes to solids (Refs. 2, 9, 14, and 15). Equipment is also being designed and fabricated for a small-scale demonstration (4-in.-diameter by 24-in.-high pot) of pot calcination at ORNL. Synthetic wastes containing added fission products will be used for pot-calciner feed solutions.

Chemical flow sheets are being prepared for Purex, TBP-25, and Darex types of wastes to be processed in this calciner pilot plant, the major effort being on the TBP-25 flow sheet since this is the proposed first feed for the pilot plant.[14] Heat-transfer calcinations for Purex type wastes indicate that an 8-in.-diameter pot must be used for wastes decayed less than 180 days in order to prevent a temperature greater than 900°C at the center of a pot containing the calcined cake.[9] A flow sheet was also prepared for wastes aged greater than 180 days which would be processed in 12-in.-diameter pots.

The results of 11 engineering-scale, nonradioactive tests, utilizing an 8-in.-diameter by 90-in.-high pot, which were summarized in a previous Review[2] are presented in Table IV-3. Synthetic wastes (Darex, TBP-25, and TBP-25 containing organic residues) were demonstrated in batch and continuous flow sheets. Average system feed rates are based on the filling period only, since calcination and change-out time will depend on the activity level of the waste and the mechanical design of the pot-changing facility.[9,15]

With TBP-25 waste, the average feed rate varied with the fraction of pot filled (bulk density) at the end of the tests, from 19.4 liters/hr at a density of 0.6 g/cm^3 to 11.6 liters/hr at a density of 0.8 g/cm^3. Increasing the operating liquid level about 6 in. gave a rate of 17.6 liters/hr with a density of 0.83 g/cm^3. The addition of 0.01*M* tributyl phosphate to the feed decreased the average rates and density about 50%. Darex type feeds gave lower average feed rates but higher bulk densities. The average feed rates varied from 8.6 to 16.5 liters/hr with bulk densities of 0.63 to 1.42 g/cm^3. The inverse effect of bulk density and average feed rate cannot be seen here since the feed concentration was allowed to vary from run to run and during a run.

The calciner-pot feed rate is controlled by calciner liquid-level control. The use of the differential pressure bubbler type was discontinued because of the plugging of the probes in favor of a thermocouple type liquid-level probe.[15] Many different types of thermocouple liquid-level probes have been tested to determine a type with proportional response suitable for controlling. The most suitable type is a $\frac{3}{8}$-in.-diameter type 347 stainless-steel tube closed on the end. The closed end of the tube is filled with a 15-in.-long piece of solid copper with a 6-in.-long hole drilled in it for a $\frac{1}{8}$-in.-diameter stainless-steel covered chromel-alumel thermocouple. This arrangement of 9 in. of rod below the couple acts as a heat sink and allows the couple temperature to change as a function of liquid height on the rod.

Fluid-Bed Calcination

Laboratory and pilot-plant fluidized-bed calcination process studies are continuing at ICPP.[2,16-18] Currently a 12-in.-diameter electrically heated unit and a 24-in.-square NaK-heated unit are used for pilot-plant studies with nonradioactive material. A 48-in.-diameter 60 gal/hr Demonstrational Waste Calcining Facility (DWCF) has been built for demonstration

Table IV-3 SUMMARY OF ENGINEERING-SCALE POT-CALCINATION RUNS[9]

Run No.	Feed type	Av. feed rate, liters/hr	Evaporator concentration factor*	Water-to-feed volume ratio	Off-gas† to feed ratio, cu ft/liter	NO_3 in solids, wt.%	Solids‡ bulk density, g/cm^3	Total feed volume, liters
49	TBP-25	17.6	1.08–0.70	2.6	1.9	6.6–0.36	0.83	478
50	TBP-25§	11.5	1.30–0.71	2.4	2.4	4.1–0.08	0.52	346
51¶	TBP-25§	7.0	1.35–1.15	2.5	3.2	6.0–0.08	0.59	308
52¶	TBP-25§	9.8	1.02–0.93	2.3	2.4	0.2–0.06	0.44	440
54	TBP-25	17.2	1.37–0.95	2.7	1.8	0.8–0.1	0.65	428
55	TBP-25	19.4	2.00–0.90	3.5	1.4	0.6–0.1	0.63	468
62	TBP-25	16.8	1.43–0.74	4.5	1.0	2.0–0.10	0.63	446
63	TBP-25	16.3	1.22–0.87	2.3	0.9	2.0–0.20	0.61	421
64	TBP-25	11.6	1.1–0.63	2.1	1.2	0.2–0.002	0.80	560
59¶	TBP-25§	12.4	1.0	0	1.3	1.0–0.07	0.61	397
56	Darex	13.6	1.24–0.71	4.1	1.4	0.1–0.02	0.86	383
57	Darex	8.9	1.47–0.79	3.2	2.2	0.5–0.01	1.40	641
58	Darex	16.5	1.69–1.38	3.0	0.8	1.0–0.2	1.42	576
60¶	Darex	8.6	1.09–0.65	5.5	1.8	2.0–0.10	1.29	336
61¶	Darex	10.6	1.0–0.82	3.8		1.0–0.02	1.13	307

*Ratio of concentrations during feeding.
†Off-gas volume includes 10 to 20 cu ft/hr system inleakage.
‡Total weight of solids averaged over a 60-liter pot volume.
§Organic added to feed, 0.01*M* tributyl phosphate.
¶Batch tests.

of this process with full-level wastes. Startup testing with nonradioactive feeds testing of the DWCF is under way.

Although exploratory studies have been made to demonstrate the feasibility of the fluidized-bed calcination process for stainless-steel and zirconium fuel wastes, the work has been primarily concerned with wastes from the processing of uranium-aluminum alloy fuels. Studies have shown that calcination between 350 and 550°C, with a superficial fluidizing-gas velocity of about 1 ft/sec, produces a suitable product at high throughput rates. Volume-reduction factors from aqueous waste to bulk stored solids of from 8 to 24 have been demonstrated. A desirable product has been defined as one having a mass median diameter between 0.3 and 0.6 mm, a low intraparticle porosity, and a low attrition rate. Particle size has been found to be controllable by variation in the nozzle air-to-liquid ratio, and particle porosity has been found to vary directly with calcination temperature and feed aluminum concentration.

The principal remaining problem is determination of the factors affecting the rate of conversion of the originally formed, attrition-resistant amorphous form of alumina to the more friable alpha form that undergoes severe attrition in the calciner and thereby results in excessive loading of the off-gas cleaning equipment. Four variables affecting the formation of alpha alumina are temperature, composition gaseous environment, method of alumina formation, and sodium content of the feed solution. Two investigations were initiated to study the rate of transformation of amorphous to crystalline alumina.[16-18] One study[17] at the ICPP followed the chemistry of alumina calcination in close relation to the performance of the several calcination units at the ICPP. The second study,[18] subcontracted to Stanford Research Institute, investigated the formation of various forms of alumina, with particular emphasis on the effect of temperature, irradiation, minor components, addition agents, etc., on the rate of phase transformations and on the phase diagram. The results of this study are summarized as follows:

New phases of alumina were found in the course of the research. The A phase, which formed at 150 psi and 400°C, had also been found to be formed at 1200 psi from aluminum metal and water. The C phase that was found may be a dibasic aluminum nitrate (Diban); this was different from the crystalline Diban compounds found at the ICPP. The B phase that was found was not of sufficient purity to characterize. These new phases may be important in the transformation of aluminum nitrate to alpha alumina. Structural considerations suggest that amorphous alumina produced in the pilot plant might be structurally related to alpha alumina. Various factors that contribute to formation of alpha alumina are (1) sodium acting as a mineralizer or included in the structure, (2) nitrate and water vapor in intermediate compounds or aiding the mobility of the aluminum and oxygen atoms, and (3) conditions unique to fluidization (e.g., cycling of temperature and cycling of composition in various zones and rate of decomposition).

The phase-transformation studies have shown that synthetic aluminas produced in the laboratory have not transformed to alpha alumina at 400 to 700°C in the presence of nitric acid and water vapor. Amorphous alumina produced in the pilot plant is transformed to alpha alumina.

Alumina samples prepared synthetically were heated in a microreactor at pressures of 150 to 1300 psi. Most of the synthetic alumina samples containing sodium formed alpha alumina, whereas those without sodium did not, which agrees with the pilot-plant results. Additives that allowed alpha alumina to form were calcium, iron, and lithium. Potassium, silicate, sulfate, and zinc allowed alpha alumina to form when sodium was also present. Phosphate, boric acid, and magnesium seemed to prevent the formation of alpha alumina. Fission products, at 10 times the expected amount, also appeared to prevent formation of alpha alumina. Phosphate and boric acid deserve additional research to determine concentration limits.

Theoretical considerations were applied to the effect of additives on the type of crystal (i.e., alpha or gamma alumina), on the size of crystallites, and on amorphous alumina. Formation of alpha alumina might be aided by elements (i.e., sodium, calcium) which form structures in which there is hexagonal close packing of the oxygen atoms. Other additives (e.g., zinc), which form spinels with a cubic close-packed arrangement of oxygen atoms, might favor a gamma type of alumina. The prevention of growth of crystallites by strong adsorption of foreign atoms is a possibility. Some additives (e.g., boron, phosphorus, and silicon) form strong bonds with aluminum and oxygen atoms

but have sizes, coordination numbers, and atomic charges which hinder the growth of continuous regular structure. These are used in glasses and would be likely to favor amorphous alumina.

Electron diffraction examination was made on particles from selected pilot-plant samples. Wedge-shaped sections were examined along a diameter to determine where alpha alumina was initially formed. The random distribution of the most intense patterns indicated that alpha alumina formed over fairly large sections of the particles (not necessarily at the center or edge) and not randomly in small spots distributed throughout the particle. The electron diffraction also showed that amorphous alumina had sufficiently small crystallites to appear amorphous to electron diffraction as well as to X-ray diffraction.

In the ICPP studies the formation of alpha-phase alumina from the amorphous phase continued to be investigated.[16,17] The effect of environmental gas composition on the formation of alpha alumina was examined in a series of experiments. It was demonstrated that very little alpha alumina was formed by heating amorphous pilot-plant product in air, moderate amounts were formed by heating in an air–water vapor atmosphere, and larger amounts were formed when the atmosphere also contained nitric acid vapors.[16] Temperature and method of alumina formation (i.e., conditions of pilot-plant calciner operation) also affected the conversion but appeared to be interrelated so that no clear-cut conclusion on individual effects could be drawn. Water vapor in combination with the oxides of nitrogen, nitric oxide (NO), or nitrogen dioxide (NO_2) accelerated the growth of the alpha phase as compared to the growth in the dry gases when calcined alumina was heated for 24 hr at 400°C in these atmospheres.[17] The wet nitrogen dioxide appeared to be more effective than wet nitric oxide; however, the relatively wide differences between the alpha content at the end of the runs of the two identical control samples suggest that the difference in the effect of the two gases may not be great.

When an air–water vapor atmosphere was used with calcined alumina from various pilot-plant runs, alpha alumina formed in samples that had been shown previously to be alpha formers in a nitric acid atmosphere.[16] However, the alpha alumina formed in the air–water vapor atmosphere was only one-third to one-half of that formed previously in the air–water vapor–nitric acid vapor atmosphere.

Samples of the overhead fines from the laboratory fluidized-bed calciner were collected when the calcination conditions approached spray drying (very low fluidized-bed level). These samples produced an X-ray-diffraction pattern that was the same as a pattern previously obtained from a solid material that had been dried from a solution of 8*M* dibasic aluminum nitrate. These results suggest that the dibasic aluminum nitrate compound may be an intermediate form produced during the calcination process.

Five runs that were made in the 24-in.-square pilot-plant calciner showed that a direct effect existed between feed sodium content and alpha-alumina formation rate,[16] that mercury normally present in the waste solutions did not have a detectable effect on the process or product,[16] that alpha-alumina formation was effectively suppressed by addition of boric acid to the waste aluminum nitrate feed[17] (also confirmed in the DWCF), and that a possible relation was indicated between nozzle design and alpha-alumina formation.[17] A boron carbide feed-nozzle cap,[8,16,17] removed after about 740 operating hours, showed no visible evidence of erosion.[16] Although boron carbide is the most attrition resistant of any material tested, its inherent brittleness makes its use undesirable unless a change in the cap design can eliminate installation stresses.

The relative effect of nozzle air rate, feed rate, and fluidizing air velocity on off-gas particulate loading was studied.[17] The boric acid concentration in the feed was increased from 0.05*M* to 0.10*M*. A reduction of about one-fifth in the fines elutriation rate was obtained by lowering the fluidizing velocity from 1.0 to 0.5 ft/sec. A two-thirds reduction in rates of fines production was shown when the feed rate was lowered from 80 to 40 liters/hr, indicating that spray characteristics affect the rate of fines production. An extreme reduction in fines production was obtained by cutting off the liquid feed making it apparent that the bulk of the fines is being produced from the fresh feed, either through spray drying or breakoff of the fresh coating from the particle surface. Nearly identical rates were observed when using either water or synthetic waste feed. This indicates

that abrasion of the particle coating, rather than spray drying, is the major source of fines.

In the DWCF, two runs were completed in which the starting operating conditions were a feed rate of 60 gal/hr; a bed temperature of 400°C; an average recycle rate of 20 gal of scrub solution per hour to the feed; a nozzle air-to-liquid volume ratio of 300; and a feed composition simulating the contents of a waste hold tank (1.74*M* aluminum nitrate, 0.59*M* nitric acid, and 0.039*M* sodium nitrate).

The effects of equipment changes and of a sand starting bed on calciner operability and on product properties were determined in a single run. In this run the alpha alumina reached 45% by the end of the 13-day operating period. The properties of the final product were those typical of a high-alpha-content material; the final bulk density of the product was 1.62 g/cm^3, and the final mass median particle diameter was 0.23 mm. During the run, helium leaks developed unexpectedly after 8 and 13 days of operation in a blanket tube in the calciner heat-exchanger bundle. Both leaks occurred in heat-affected zones adjacent to the tube weld. Each time the leak was repaired, and the run was continued.

In another run, amorphous alumina was used as the starting bed, and boric acid was added to the feed after 50 hr of operation to suppress alpha-alumina formation. In this run the originally amorphous starting bed converted to 71% alpha alumina during the first 50 hr of operation. At that time, 0.2*M* boric acid was added to the feed, and the alpha-alumina concentration began to decrease immediately. By the end of the run, 19 days later, the alpha-alumina concentration was 8%, the bulk density was 0.94 g/cm^3, and the mass median particle diameter was 0.5 mm and was still increasing.

An experimental program (for ICPP) at Battelle Memorial Institute (BMI) studied a feed system for introducing slurries and solutions into a fluidized-bed calciner.[19] In this system the feed solution is sprayed on the surface of the bed through tubing installed axially through the top of the calciner.

Process operation and product characteristics were adequately maintained by adjusting the air rate to the feed gun. Volumetric air-to-feed ratios above 240 gave a product with a mean diameter of less than 0.3 mm and an alpha-alumina content above 30 wt.%. Air-to-feed ratios of approximately 100 gave a product with a mean size greater than 0.6 mm and an alpha-alumina content below 20 wt.% throughout the tests. The absolute density varied from 3.6 g/cm^3 for 60% alpha to 3.0 g/cm^3 for 10% alpha. Mechanically the feed gun operated without difficulty throughout a total operating time of 25 days, and no serious caking occurred in the bed.

Product containing a high content of alpha-phase alumina, i.e., greater than 50 wt.%, was successfully contained within the calciner system. The weight of solids returned from a knockout cyclone to the bed during such a period averaged five times the theoretical product rate. Nevertheless the solids leaving the system in the off-gas downstream of the cyclone were less than 4% of theoretical product rate. The weight of solids returned from the cyclone to the bed during periods of low alpha generation, i.e., less than 25%, was less than the theoretical product rate. However, solids in the off-gas downstream of the cyclone were as high as 30% of the theoretical product rate. The results of this work indicated that a product with high alpha-alumina content could be contained in a calciner system at least to the same extent as a product with low alpha content.

A comparison of the BMI and ICPP feed-introduction systems does not show conclusively a superiority of one over the other. The properties of the product from the limited Battelle tests compare favorably with the product properties from similar tests in the ICPP 2-ft-square calciner. Mechanically the ICPP nozzles should be better for remote operation, since cleanout plungers for clearing the tips, should plugging occur, are easily installed. However, the velocity of the air through the ICPP nozzles is approximately tenfold greater than that through the BMI feed gun, and erosion of the nozzle tips has caused considerable concern. If erosion cannot be eliminated by changes either in design or in construction materials, the BMI system may prove the more desirable.

Conversion to Glasses

Brookhaven National Laboratory (BNL) is continuing its study of ultimate disposal of high-level-activity wastes based on the formation of phosphate glasses as a means of incorporating the fission products in stable media.[8,20,21] A fully continuous process in which the glass would be formed in a central crucible

and fed to separate storage containers is being currently developed.

The recently completed pilot plant for producing phosphate glass from various types of simulated high-level-activity waste was operated briefly with Purex feed using a 5-in.-ID by 6-ft-long high-density alumina crucible.[20] The run was terminated after 14 hr when a crack developed in the crucible.

BNL has also been corrosion-testing platinum and platinum alloys of rhodium, gold, and iridium as an alternate crucible construction material.[8,21] They have shown good resistance to corrosion when exposed at 1100°C to molten Purex-phosphate glass and Redox-phosphate glass. Designs have been completed for a platinum-clad Inconel alloy 702 crucible (8 in. in inside diameter and 24 in. long).[20] In addition, testing of Inconel 600 and Hastelloy has indicated that these materials may be expected to serve satisfactorily as a crucible to support the 40-mil platinum liner. To prevent migration of the nickel from the Inconel alloy into the platinum, a thin aluminum oxide layer several mils in thickness will be deposited between the two metals.

The advantages of the all-liquid system for processing phosphate glasses from Purex waste are now being considered with respect to high-salt-content aluminum nitrate waste (Redox).[21] In a series of scouting experiments, a number of glasses with good appearance have been made from simulated aluminum nitrate wastes at 1100°C. The volume reduction for this glass is 6.5 compared to 10 for aluminum oxide calcined directly from aluminum nitrate. The small disadvantage in volume reduction might well be compensated for by the increased thermal conductivity of the glass as compared with bulk aluminum oxide.

The thermal conductivity of a phosphate-lead glass incorporating TBP-25 waste oxides was determined at ORNL, and it varied[2,9,22] from about 1.05 Btu/(hr)(ft)(°F) at 300°F to about 1.60 Btu/(hr)(ft)(°F) at 1050°F. The glass had a positive temperature coefficient of thermal conductivity, a characteristic of amorphous solids and powders, but the variation of the thermal conductivity was nonlinear, a characteristic of amorphous solids but not of powders. Calculations have shown that a thermal conductivity of 0.1 Btu/(hr)(ft)(°F) is probably high enough for storage of calcined wastes. The glass, which had a density of 2.9 g/cm^3, was prepared by semicontinuous evaporation, calcination, and melting of a TBP-25 waste made 2*M* in sodium hypophosphite and 0.25*M* in lead oxide. The sodium hypophosphite is added to control the ruthenium, and the lead oxide is added to lower the softening point of the glass product.

Fixation in Porous Ceramic Sponges

The Coors Porcelain Company and the Los Alamos Scientific Laboratory (LASL) are jointly studying the fixation of liquid radioactive wastes in ceramic sponges.[23–26] A highly porous fired clay is prepared, soaked repeatedly in the liquid waste, and then fired at a temperature of 1300°C to fix the wastes. About 10 gal of waste can be absorbed per cubic foot of packed spheres. The heat generation of these spheres on storage does not appear to present a problem since air could be circulated through the volume of stored spheres.[25,26] When ceramic materials are used for fixation of high-level-activity wastes, the containment vessel need not be constructed of equally high heat-resisting materials. The temperature gradients are high within the ceramic mass; however, the ceramic material is capable of withstanding high temperatures. As a result, more waste can be concentrated into a smaller volume with less concern. The cost of treatment of wastes (10,000 gal/day) was calculated to be about $0.60 per gallon, the major portion of the cost being in the ceramic sponges ($0.50 per gallon of waste).[25] It is expected that this cost will be decreased by improvement in sponge characteristics to permit larger amounts of waste to be sorbed.

At LASL early in 1962, a 25 gal/day demonstration pilot plant was placed in operation. In the pilot plant the spherical ceramic sponges are placed in a wire cage that is lowered into a soaking and drying tank into which the radioactive waste is pumped. After the soaking cycle the tank is drained. Electrically heated air is then blown through the tank to a condenser where the evaporated liquid is condensed and collected. The air is then recycled through an electric heater and the tank until the ceramic spheres are essentially dry. Noncondensable gases are passed through an absolute filter before discharge to the atmosphere. This cycle is repeated several times until the optimum capacity of the spheres has been reached. The

spheres are then transferred to a tunnel kiln for the heating cycle.

The electrically fired tunnel kiln is 45 ft long with a useful firing cross section of 9 by 7 in. The ceramic spheres move through the kiln at the rate of about 45 ft/day. To minify the amount of off-gases to be cleaned, it was decided to use electric heating in the tunnel kiln despite difficulties expected with heating elements operating at these elevated temperatures. The air that passes through the furnace (less than 10 cfm) goes through a silica-gel filter (for ruthenium removal) before entering the condenser. Any liquid remaining in the spheres will be driven off in the kiln preheat section and condensed in the condenser. It is anticipated that some moisture will be added to the air entering the furnace to make certain that there is enough water to be condensed to carry the volatilized fission products with the condensate. The noncondensable gases will pass from the condenser through two glass-fiber absolute filters.

Results of laboratory investigations[25] of this process are summarized below. Most of this work was done with 1-in.-diameter spheres composed of 20% silica, 45% feldspar, 20% diatomaceous earth, and 15% No. 4 ball clay.

1. The time required to dry a ceramic sponge to constant weight varied with the sorbed material, e.g., a shape soaked in water can be dried in 30 min at 180°C, but a similar shape soaked in aluminum nitrate waste required $3\frac{1}{2}$ hr at the same temperature. Some factor or factors other than simple surface evaporation are believed to affect the evaporation rate from the spherical sponges.

2. Increasing the relatively humidity of the incoming air from 22 to 55% decreases the drying time from $3\frac{1}{2}$ to $2\frac{1}{2}$ hr. The results would indicate the possible use of high-pressure dry steam or a gas with a heat capacity greater than that of air.

3. The porosity of the spheres was shown to decrease with the number of soaking cycles. Within practical limits, only about one-fourth of the pore space of the sphere is utilized. The utilization of more pore space is negated with a high aluminum waste since the ball tends to deteriorate and spall after five or six cycles of soaking and drying. The deterioration does not occur in the absence of aluminum nitrate.

4. In tests of the volatility of mixed fission products (two to four years old), the only fission product volatilized to any degree was Ru^{106}. Reducing agents, sucrose or sodium hypophosphite, did suppress the volatilization of ruthenium up to about 300°C; but, after the reducing agents had been oxidized, the ruthenium soon volatilized. Preliminary results with spheres soaked in a solution of sugar and subsequently fired in an atmosphere of helium indicated that the ruthenium remained in the sphere up to a temperature of 1300°C (similarly for Cs^{137}).

5. Leaching in distilled water was determined for 1-in.-diameter ceramic spheres soaked in a simulated aluminum nitrate solution containing either added Sr^{90}, Cs^{137}, or mixed fission products. The data indicated that nearly all the leachable radionuclides appeared during the first 30 days of the testing period (about 0.10% leached for Sr^{90}; about 0.06% leached for Cs^{137} and mixed fission products).

Final Disposal Methods

Seepage Pits

ORNL has announced that it is planning to discontinue its soil disposal operation for intermediate-level-activity liquid wastes.[2,27] It will be replaced by an evaporation procedure wherein these wastes will be reduced in volume and the concentrates eventually converted to solids and disposed of in permanent containers.[27] The evaporator is now being designed and is expected to be in operation late in 1963.

These wastes are produced at a rate of about 7000 gal/day and contain the bulk of the activity in wastes generated by ORNL. They are disposed of by pumping them to two limestone-filled trenches from which they seep through the soil to the nearby stream and river system. The trenches, which are filled and covered, replace a number of open pits that were taken out of service (June 1960) when excessive amounts of Ru^{106} created a radiation hazard. Continuous monitoring has indicated that Sr^{90} is effectively removed by these disposal procedures, but relatively large quantities of Ru^{106} reach the river. However, the ruthenium seepage problem is now reduced because the trenches are no longer used for disposal of highly concentrated Ru^{106} wastes. These are separated and permanently stored in tanks. The two covered trenches are also located in an area where seepage to the

surface is expected to take a much longer time so that the Ru^{106} will be considerably reduced by decay before it is released.

Ground Disposal

The proceedings of the Second Conference on Ground Disposal of Radioactive Wastes have become available.[28] This conference, a followup of a meeting at Berkeley, California,[8] in 1959, was held at Chalk River, Canada, on September 26 to 29, 1961, and was jointly sponsored by Atomic Energy of Canada, Limited, and the Division of Reactor Development of the USAEC. At this meeting, detailed panel discussions were held on hydrogeology, geochemistry, waste injection, and solid waste disposal. Operating data from ground-disposal operations at Hanford, Oak Ridge, National Reactor Testing Station, Brookhaven, and Chalk River were also presented.

The U. S. Geological Survey has issued summary reports on the geology and hydrology of the National Reactor Testing Station (Idaho), the Appalachian basin, and the Atlantic and Gulf coastal plain.[23,29–31] The data in these reports define the geophysical characteristics of these areas and provide a basis for evaluating sites for the management and disposal of radioactive wastes to ground.

Favorable geological conditions at Hanford make it possible to use ground disposal under controlled conditions for certain of their large-volume process wastes containing small amounts of radioactive materials.[8] Wastes are disposed to underground cribs or caverns. Cribs are buried, open-bottom boxes filled with timber cribbing. Caverns are long trenches filled with graded gravel and covered with an impermeable membrane. These structures allow for a surge of waste material and also provide for spreading the solutions over a larger infiltration area.

It is the practice at Hanford to stop disposal to a crib or cavern when isotopes with a half life greater than three years appear in the ground water below the facility in concentrations greater than one-tenth of maximum permissible concentrations as defined by the National Committee on Radiation Protection and Measurement. Because of this practice, it is necessary to have a reasonably accurate knowledge of the capacity of the soil to sorb radionuclides and of the movement of waste solutions through the soil above the water table.

Knoll and Nelson, reporting on a Hanford field experiment,[32] have shown that laboratory soil columns can be used to forecast the life of a waste-disposal crib. Two model cribs, one 6 in. square and the other 24 in. square, were used. Depth to ground water was about 10 ft. The influent solution to the cribs was traced with nitrate ion and Sr^{85}. They have also shown that the amount of lateral spread is independent of the size of the crib and becomes a smaller fraction of the total crib size as the dimensions of the crib increase. Results of probing beneath the small crib with a neutron moisture probe gave the distribution of moisture in the soil. Results from a representative probing are given in the form of maps. These also show that the wetted soil assumes a napiform (turnip-shaped) shape.

Disposal into Permeable Formations

The use of wells to dispose of brine to deep permeable formations is a current practice in the petroleum industry.[8,9] Of the additional factors to be considered for the disposal of radioactive liquids, the most significant are those which concern the safety of the method and the additional costs because of the safety requirements. The safety aspect can be resolved into two problems: (1) radiation exposure to personnel and surface contamination due to handling of radioactive liquids at the disposal site and (2) environmental contamination due to movement of the radionuclides in the disposal formation. The first problem is encountered in every scheme for handling radioactive liquids, and the techniques for evaluating and controlling these hazards have a firm basis. However, in order to assess the hazards associated with environmental contamination, one must be able to predict the movement of the radionuclides in the environment.

In the environment, radionuclides move along the same stream lines as the transporting solution but are retarded in movement by sorptive processes in the disposal formation. Movement of the radionuclides can be predicted by describing the movement of water in the formation and correcting for sorptive processes.

In an ORNL study[9] of sodium-calcium-strontium exchange, columns of Richfield sand were presaturated with 0.005M calcium nitrate solution containing various concentrations of sodium nitrate. The columns were subsequently satu-

rated with chloride solutions of the same cationic composition to which was added Sr^{85} (about $2 \times 10^{-8}M$ strontium chloride). The results of these experiments, corrected for pore volume, show that strontium is selectively sorbed over calcium by a factor of about 50 g/cm^3. From these experiments an exchange capacity of 4.27 meq/100 g was obtained for the Richfield sand.

The selective sorption of strontium over calcium on Richfield sand agrees with observations of strontium-calcium exchange on various clay minerals studied. Divalent-exchange studies, made with Conasauga shale, indicated that the preference of the cation-exchange surface for strontium over other alkaline-earth cations decreases with decreasing size of the hydrated ion. The selectivity of calcium over sodium is also of the same order of magnitude for Richfield sand as for the strontium to sodium selectivity of clay minerals.

Because anions are not actively sorbed by cation exchangers, they can be used to measure the dispersion of solution passing through a cation-exchange column. Experimental data showed that the normalized strontium breakthrough curves corresponded to the anion breakthrough curves, indicating that strontium breakthrough can be predicted from the solution dispersion in the column. This implies that radionuclide breakthrough at a particular point in the environment can be predicted by observing the breakthrough of a water tracer and correcting for the sorptive properties of the formation for the radionuclide in question.

Calcined Solids Storage in Salt Mines

ORNL is continuing its comprehensive study to evaluate the economics and hazards associated with alternative methods for ultimate disposal of highly radioactive liquid and solid wastes. The feasibility of using salt mines for the storage of packaged calcined wastes is a part of this study.[2,9,22]

Space requirements to dissipate the fission-product heat in the waste from a 56,000-Mw(t) nuclear-power economy were calculated for cylinders of calcined waste buried in a vertical position in the floors of rooms in salt media.[9] Acres per year of mined space required was calculated for Purex and Thorex wastes in acidic and reacidified forms in 6-, 12-, and 24-in.-diameter vessels buried at ages of 0.33 to 30 years. Calculations were made also for an acidic Thorex glass in 6-in.-diameter vessels. The maximum allowable temperatures in the salt and in the calcined wastes were chosen to be 400 and 1650°F, the same as they were in the calculation of space requirements for the storage of calcined wastes above the floor in salt rooms. The cylindrical vessels, 10 ft long, were assumed to be arranged in vertical holes 33% larger in diameter than the vessel diameter (e.g., 8-in.-diameter holes for 6-in.-diameter vessels) and 15 ft deep, with the top 5 ft occupied by salt or concrete plugs for shielding purposes.

The minimum spacing for acidic Purex in 6- and 12-in.-diameter cylinders ranged from 20 and 36 ft at minimum burial age to 10.5 and 23 ft at 30 years, respectively. Acidic Purex cannot be stored in 24-in.-diameter cylinders in this manner at ages below 30 years. The minimum spacing for reacidified Thorex in 6- and 24-in.-diameter cylinders ranged from 6 and 20 ft at minimum burial age to 10 ft at 30 years.

The net area requirements for Purex waste calculated from cylinder production rate and cylinder spacing range from 20 acres/year at 0.65 year to about 2 acres/year at 30 years burial age. Corresponding results for Thorex wastes were 10 and 0.7 acres/year. The primary effects of the form of the waste (acidified, reacidified, glass) and vessel diameter are to limit the minimum burial age, although area requirements may be affected by factors of 2 to 3 by waste form and vessel size near the minimum burial ages.

Heat-transfer calculations[22] of shipping containers for pot-calcined wastes of various ages showed that as many as 36 6-in.-diameter pots of calcined acidic Purex waste can be shipped in a single finned carrier after 2.4 years of decay without mechanical cooling en route. Four 24-in.-diameter pots of acidic Purex waste can be shipped per carrier after 11 years of decay.

High-Level-Waste Heating Problems

At the Los Alamos Scientific Laboratory, generalized methods have been developed for solving high-level-waste heating problems.[25,26] Three computer codes were evolved which include solutions for packed-bed, multiregion, variable-geometry, and variable-property problems.

Numerical and analytical methods for estimating temperature rises are presented in this report.[26] The basic heat equation is solved, and

a variety of variables are considered. A selected range of values for these variables is used to demonstrate the relation between temperature rises and geometry of the physical models, effective thermal conductivities, specific heats, densities, age of wastes, waste concentrations, and reactor operations. One-dimensional solutions of the heat equations are presented for the spherical configuration, as well as the infinitely long cylindrical and slab systems. Temperature- and time-dependence examples are analyzed. Also, the physical models are presented in a manner such that temperatures may be calculated on a multiregion basis, i.e., the effective thermal conductivities and other parameters may be varied. For example, a region may be inserted whereby radiant, conductive, and convective transfers are considered.

Finally, a solution to the heat problem is presented that corrects itself for effective thermal conductivities, depending on the temperature rise. In this solution the effective thermal conductivity is adjusted in accordance with the level of temperature attained and the concurrent influence of radiant transfer. In this latter case the solution is particularly applicable to packed beds with motionless air.

Problems with containment vessels that are filled with fluids other than air are solved in the same manner. Complete mixing is assumed, i.e., the gradient from the center of the vessel to the boundary is considered to be very small. Partially filled containment systems are not considered in this report, nor are fluids that might undergo changes of state, changes of pressure, and latent heat.

Recovery of Fission Products

ORNL has been studying on a laboratory scale the recovery of Sr^{90} from Purex 1WW waste.[2,33] A proposed flow diagram is shown in Fig. IV-5, and it is based on utilizing a head-end double precipitation step prior to ion exchange.[33] The procedure involves eliminating sulfate ion from the waste solution at 55 to 60% nitric acid and recovering strontium from an almost pure nitrate system at greater than 85% nitric acid. The results of a single run with this flow sheet indicated that 75 to 80% of the original strontium was recovered together with less than 1% each of iron, aluminum, sodium, and sulfate. The strontium yield probably could be increased 5 to 10% by minimizing the volume of liquid used to precipitate strontium at 85% nitric acid. Extrapolated solubility data of the

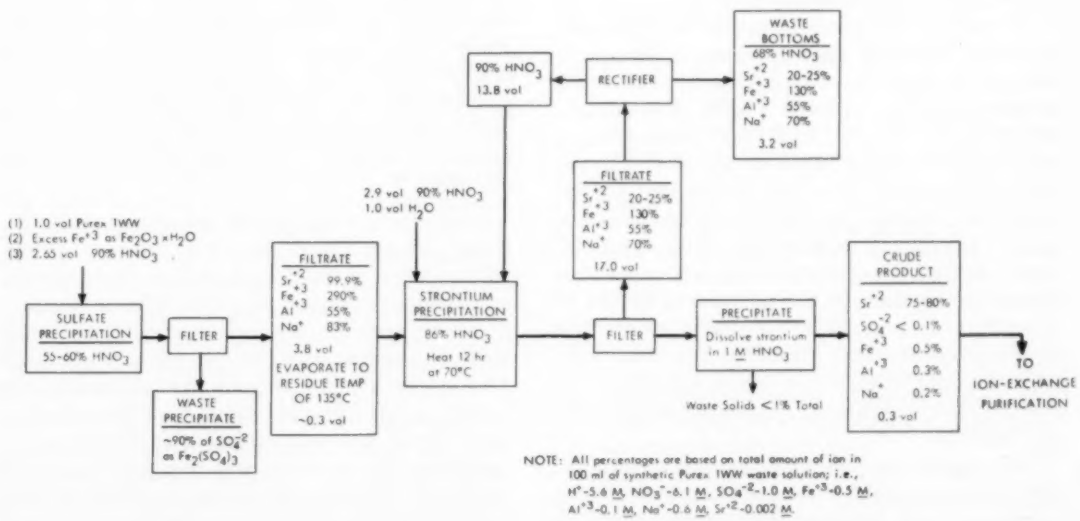

Fig. IV-5 Proposed ORNL flow diagram for strontium recovery from synthetic Purex 1WW by precipitation.[33]

system $Sr(NO_3)_2$-HNO_3-H_2O indicated that greater than 15% of the 20 to 25% strontium not recovered had dissolved in the large volume (1.7 liters) of greater than 85% nitric acid solution.

Hanford Purex Wastes

Hanford is continuing to examine Purex-plant process waste streams as a source of fission products. Ion-exchange and solvent-extraction studies are under way to recover Cs^{137} from a high-level-activity neutralized waste supernatant solution and from a formaldehyde-treated first-cycle acid waste.[2,3,23]

Acid-washed 20- to 50-mesh clinoptilolite was used to recover Cs^{137} from a 1-to-1 dilution of centrifuged supernatant from actual Purex-plant high-level-activity neutralized waste.[3] Cesium-137 breakthrough of 1% was detected at 14 column volumes, and Cs^{137} breakthrough of 50% occurred at 18 column volumes of undiluted waste. The 50% breakthrough point can be compared with that for Duolite C-3 resin at 13 column volumes in a previous experiment with untreated waste and 24 column volumes when the waste was adjusted to 2*M* sodium hydroxide. Ninety-nine percent of the cesium was eluted with 5*N* ammonium nitrate in a 3-column-volume fraction. The cesium concentration of the eluate dropped to 1% of the feed concentration by 6 column volumes.

Cesium loadings on columns of clinoptilolite and Decalso were increased by a factor of 10 to 20 times (as compared to untreated high-salt waste) by reducing the mole ratio of sodium to cesium in high-salt wastes with ammonium phosphomolybdate (APM).[3,23] APM is extremely selective for cesium. APM and ammonium nitrate were added to simulate Purex high-level neutralized waste supernatant solution, diluted 1 to 1 with water, to final concentrations of 8 and 11.4 g/liter, respectively. The dissolved APM was then precipitated along with more than 95% of the cesium by the addition of 200 ml of 70% nitric acid per liter of diluted waste. The APM was filtered and dissolved in a small volume of dilute sodium hydroxide solution. This solution was then fed to columns of clinoptilolite and Decalso.

The solvent extraction of cesium from Hanford process waste solutions complements the extensive work that has been in progress for some time on carrier precipitation and ion-exchange processes for cesium removal.[3] Possible advantages of solvent extraction, if an efficient and economical extractant can be found, would include (1) easier integration with solvent-extraction recovery of strontium and rare earths; (2) higher recoveries, or greater degree of cesium removal, than is readily achieved by precipitation; and (3) a choice of either continuous or batch operation. Solvent extraction should be equally applicable for either fission-product recovery or for cesium removal in behalf of waste management (to isolate this long-lived heat-generating isotope from the bulk of the salt waste).

Preliminary scouting experiments included a large number of compounds. Most effective were tetraphenyl boron, triiodide, and dipicrylamine (DPA) all of which have a very high degree of selectivity for cesium. Triiodide was rejected for Hanford application because of the halide corrosion hazard to stainless-steel process equipment and to mild-steel waste-storage tanks. Tetraphenyl boron was rejected because extraction with it was considered irreversible in the sense that, although the cesium could be stripped with dilute acid, the extractant could not be reused, apparently because of decomposition of the reagent. DPA was found to be a satisfactory and effective extractant for cesium. It has long been employed as an analytical reagent for precipitating the heavy alkali metals.

The extraction of cesium by DPA is enhanced by dilution with a high-dielectric-constant solvent, such as nitrobenzene. Nitrobenzene has yielded the highest extraction coefficients of the diluents tested, although other nitrohydrocarbons are in the same range. Very little extraction is observed with low-dielectric-constant aliphatic or aromatic hydrocarbon diluents.

Over a wide range of concentrations, aqueous-waste compositions, and *p*H's, the equilibrium constant for extraction of cesium from neutral or alkaline solutions into DPA-nitrobenzene is little affected by the composition (other than sodium concentration) of the aqueous solution. The extraction coefficients can be varied over a wide range by controlling the dipicrylamine and sodium concentrations, being directly proportional to dipicrylamine concentration and inversely proportional to aqueous sodium content. Cesium extraction is also favored by decrease in temperature. The extracted cesium is readily stripped with 0.5*M* acid. Solubility of

both dipicrylamine and nitrobenzene in the aqueous solution is quite low, and the organic solvent can be reused repeatedly. Extraction tendency of the other alkali metals is much lower than that of cesium, the separation factors (ratio of extraction coefficients) of cesium from rubidium, potassium, and sodium being about 6, 28, and 2500, respectively.

In high-level cell experiments performed with actual Purex 1WW and Purex neutralized waste supernatant, the extraction coefficient of cesium from neutralized, tartrate-complexed (to prevent iron precipitation) 1WW into 0.01*M* DPA-nitrobenzene was 2.7, the same as from synthetic solution. Three successive equal-volume ambient-temperature batch extractions removed over 98% of the initial cesium, and the extracted cesium was readily back-extracted with 0.5*M* to 1.0*M* nitric acid. Purification from other fission products and sodium was excellent, with the decontamination factors from Ce^{144}, Ru^{106}, Zr^{95}, and Nb^{95} ranging from several hundred to several thousand. Extended contact (190 hr) of the aqueous and organic solutions had no deleterious effect, implying negligible radiation damage. Similar results were obtained with neutralized waste supernatant, where the cesium extraction coefficient was about 4.

Shipment of Hanford Fission Products

Fission-product Cs^{137} and Sr^{90} are being shipped via rail from Hanford to ORNL in shielded transfer casks.[8,34–41] The ORNL cesium casks have a $3\frac{1}{2}$-in.-thick liner of lead, weigh 15 tons when empty, and can contain some 30,000 curies adsorbed on 400 gal of Decalso.[35] Specially modified gondola railroad cars, which are capable of handling two of these casks at one time, are reinforced with crash shields and roll-over supports to protect the casks. The Sr^{90} is shipped in a Hanford-designed shielded cask of high structural integrity which is within a buffer shield.[8] The buffer shield provides protection against impact and penetration and is attached to a standard railroad flatcar or depressed-center flatcar.

Several Hanford papers have become available which discuss the design criteria and the inactive testing aspects of the Sr^{90} shielded transfer casks.[34–38] The design characteristics for Hanford's HAPO-I and HAPO-II fission-product casks have been summarized.[39] These two casks have been designed for shipping fission products as stable, dried solids, HAPO-I for Ce^{144} and HAPO-II for Sr^{90}. The design of HAPO-I has been modified to permit shipping Sr^{90} adsorbed on an inorganic ion-exchange material.

Cerium-144 is to be shipped as a sodium cerous sulfate salt [$Na_2SO_4 \cdot Ce_2(SO_4)_3 \cdot 2H_2O$] in the HAPO-I cask.[40,41] In experiments supporting a hazards evaluation of these shipments, the maximum measured release of cerium was 0.11% at an air flow rate of 230 cm^3/min (STP) and with a programmed temperature increase of 10°C/min up to 1450°C. A maximum release of 3% ruthenium and 5.5% zirconium was obtained with helium flowing at 850 cm^3/min (STP) and under similar temperature programming. Releases under isothermal conditions at 1350°C for 2 hr in either helium or air atmospheres were 0.005, 0.6, and 0.1% for cerium, ruthenium, and zirconium, respectively.

Cesium Glass

BNL is interested in incorporating Cs^{137} into various glasses to obtain sources of varying shapes with low cesium solubility.[42] Glasses formed of cesium salts and phosphoric acid alone were found to be highly soluble. To reduce this effect, a number of additive elements were investigated, iron being the most effective. The best glass, at the time of the report, contained cesium, iron, and phosphorus in the mole ratio of 2 to 1 to 3, respectively.

References

1. B. F. Campbell, E. Doud, and R. E. Tomlinson, Management of High-Level Wastes—Current Practice, USAEC Report HW-SA-2478, Hanford Atomic Products Operation, Feb. 5, 1962. Presented at the Nuclear Congress, New York, June 1962.
2. *Reactor Fuel Process.*, 5(3): (July 1962).
3. E. R. Irish (Ed.), Fixation of Radioactive Residues, Research and Development Activities, Quarterly Progress Report, January–March 1962, USAEC Report HW-73412, Hanford Atomic Products Operation, April 1962.
4. E. R. Irish (Ed.), Fixation of Radioactive Residues, Research and Development Activities, Quarterly Progress Report, July–September 1961, USAEC Report HW-71374, Hanford Atomic Products Operation, Oct. 13, 1961.
5. *Reactor Fuel Process.*, 4(2): (April 1961).
6. H. G. Rieck, Pilot Scale Aluminum Bed Decontamination of Reactor Effluent. II. Final Report, USAEC Report HW-72215, Hanford Atomic Products Operation, March 1962.
7. D. W. Bensen, Mineral Adsorption of Phosphorus-32 from Reactor Coolant, USAEC Report HW-

71583, Hanford Atomic Products Operation, March 1962.

8. *Reactor Fuel Process.*, 5(2): (April 1962).
9. R. E. Blanco and E. G. Struxness, Waste Treatment and Disposal Progress Report for December 1961 and January 1962, USAEC Report ORNL-TM-169, Oak Ridge National Laboratory.
10. Dorr-Oliver, Inc., Report on Investigation as to the Achievable Results of Radioactive Sludge Dewatering by Continuous Centrifugation, USAEC Report ORO-452, May 1, 1961.
11. *Reactor Fuel Process.*, 2(1): (January 1959).
12. Dorr-Oliver, Inc., Final Report of an Investigation on the Degree of Activity Associated with Particulate Solids of Different Particle Size Removed from Large-Volume, Low-Level Radioactive Process Waste at ORNL, USAEC Report ORO-453, May 1, 1961.
13. M. W. Davis, Jr., E. S. Occhipinti, and C. B. Goodlett, Savannah River Laboratory, March 1962. (Unpublished)
14. M. E. Whatley, P. A. Haas, R. W. Horton, A. D. Ryon, J. C. Suddath, and C. D. Watson, Unit Operations Section Monthly Progress Report, October 1961, USAEC Report ORNL-TM-121, Oak Ridge National Laboratory, Apr. 5, 1962.
15. M. E. Whatley, P. A. Haas, R. W. Horton, A. D. Ryon, J. C. Suddath, and C. D. Watson, Unit Operations Section Monthly Progress Report, December 1961, USAEC Report ORNL-TM-136, Oak Ridge National Laboratory, Apr. 10, 1962.
16. J. R. Bower (Ed.), Chemical Processing Technology Quarterly Progress Report, July–September 1961, USAEC Report IDO-14574, Phillips Petroleum Co., Dec. 18, 1961.
17. J. R. Bower (Ed.), Chemical Processing Technology Quarterly Progress Report, October–December 1961, USAEC Report IDO-14583, Phillips Petroleum Co., Mar. 28, 1962.
18. H. J. Eding, M. L. Huggins, and A. G. Brown, Phase Transformations in Alumina, USAEC Report IDO-14580, Phillips Petroleum Co., Dec. 5, 1961.
19. G. E. Lohse (Ed.), Tests of a Vapor-Space Feed Nozzle for Calcining Aluminum Nitrate Solutions in a Fluidized Bed, USAEC Report IDO-14568, Phillips Petroleum Co., Mar. 15, 1962.
20. L. P. Hatch, E. J. Tuthill, R. F. Domish, G. G. Weth, and L. Emma, Brookhaven National Laboratory, May 10, 1962. (Unpublished)
21. J. H. Reynolds (Ed.), Nuclear Engineering Department Progress Report, September 1–December 31, 1961, USAEC Report BNL-705, Brookhaven National Laboratory, March 1962.
22. Oak Ridge National Laboratory, May 10, 1962. (Unpublished)
23. *Reactor Fuel Process.*, 4(4): (October 1961).
24. Atomic Energy Research for 1961 in Life and Physical Sciences, Reactor Development, and Waste Management, A Special Report of the United States Atomic Energy Commission, December 1961.
25. C. W. Christenson, R. G. Thomas, W. H. Adams, E. B. Fowler, and G. D. Kelly, The Use of Ceramic Sponges for High Level Waste Disposal, USAEC Report TID-14784, Los Alamos Scientific Laboratory and Coors Porcelain Co. For Presentation at the International Conference on Water Pollution Research, England, September 1962.
26. H. J. Longley, E. F. Gloyna, and C. W. Christenson, Heat Generation in the Disposal of High Level Radioactive Wastes, USAEC Report LA-2664, Los Alamos Scientific Laboratory, January 1962.
27. E. J. Witkowski and J. F. Manneschmidt, Ground Disposal of Liquid Waste at Oak Ridge National Laboratory, USAEC Report ORNL-TM-142, Oak Ridge National Laboratory, Feb. 13, 1962.
28. J. M. Morgan, Jr., D. K. Jamison, and J. D. Stevenson (Comps. and Eds.), Ground Disposal of Radioactive Wastes, Second Conference Proceedings, Chalk River, Canada, September 26–29, 1961, USAEC Report TID-7628, Johns Hopkins University, March 1962.
29. P. H. Jones, Hydrology of Waste Disposal, National Reactor Testing Station, Idaho, An Interim Report, USAEC Report IDO-22042, U. S. Department of the Interior, Geological Survey, December 1961.
30. G. W. Colton, Geologic Summary of the Appalachian Basin, with Reference to the Subsurface Disposal of Radioactive Waste Solutions, USAEC Report TEI-791, U. S. Department of the Interior, Geological Survey, June 1961.
31. H. E. LeGrand, Geology and Ground-Water Hydrology of the Atlantic and Gulf Coastal Plain As Related to Disposal of Radioactive Wastes, USAEC Report TEI-805, U. S. Department of the Interior, Geological Survey, January 1962.
32. K. C. Knoll and J. L. Nelson, Radioisotope and Moisture Distribution Beneath a Model Crib, USAEC Report HW-71573, Hanford Atomic Products Operation, January 1962.
33. R. E. Blanco, Chemical Technology Division, Chemical Development Section B, Quarterly Progress Report, October–December 1961, USAEC Report ORNL-TM-177, Oak Ridge National Laboratory, May 18, 1962.
34. *Major Activities in the Atomic Energy Programs*, January–December 1961, U. S. Government Printing Office, Washington, January 1962.
35. C. W. Smith, Hanford Atomic Products Operation, May 20, 1960. (Unpublished)
36. C. W. Smith, Strontium-90 Shipping Cask Design Criteria and Hazards Evaluation, USAEC Report HW-68081, Hanford Atomics Products Operation, Jan. 13, 1961.

37. W. V. DeMier, Nonradioactive Testing of the HAPO II Strontium Carbonate Filter Cask Insert, USAEC Report HW-69781, Hanford Atomic Products Operation, May 29, 1961.
38. W. V. DeMier, Demonstration of Unloading Technique for the HAPO II-2 Strontium Filter Cask, USAEC Report HW-72295, Hanford Atomic Products Operation, Jan. 17, 1962.
39. C. W. Smith, Development and Design of Off-Site Fission Product Shipping Casks at Hanford, USAEC Report HW-SA-2295, Hanford Atomic Products Operation, Jan. 26, 1962. Presented at the Nuclear Congress, New York, June 1962.
40. W. H. Reas, Chemical Research and Development Operation Monthly Report, November 1961, USAEC Report HW-71921C, Hanford Atomic Products Operation, Dec. 15, 1961. (Classified)
41. W. H. Reas, Chemical Research and Development Operation Monthly Report, October 1961, USAEC Report HW-71535C, Hanford Atomic Products Operation, Nov. 15, 1961. (Classified)
42. J. H. Reynolds (Ed.), Nuclear Engineering Department Progress Report, May 1–August 31, 1961, USAEC Report BNL-696, Brookhaven National Laboratory, January 1962.

Section

V

Reactor Fuel Processing

Production of Uranium, Thorium, Plutonium, and Their Compounds

Recovery of Uranium from Ores

Leaching of Uranium from Ores

Dilute aqueous leaching with sulfuric acid is the most widely used process for producing uranium concentrates from ore. Usually an oxidant such as manganese dioxide, sodium chlorate, or nitric acid is required to enhance the leaching process. The losses of uranium in the hydrometallurgical treatment of ores are mainly determined by the degree of extraction during leaching. A study[1] has been made to evaluate substances that would catalyze the transfer of uranium into solution, thereby effecting a higher uranium recovery and reducing overall leaching time.

The addition of divalent iron and copper ions to a sulfuric acid leaching solution containing manganese dioxide oxidant increased greatly the degree of oxidation of uranium. In the absence of iron and copper ions, the uranium was oxidized 50% by manganese dioxide in a solution containing 10 g of sulfuric acid per liter. With copper and iron ions in the solution, uranium was completely oxidized. Similar effects were observed by the addition of Co^{3+} and V^{5+} to the sulfuric acid leach. Minerals of copper and iron in uranium ores accelerate the oxidation of uranium, but their effect depends on the solubility of these minerals in the acid leach.

The effect that divalent iron ions have on the oxidation of uranium by manganese dioxide in sulfuric acid solutions has been studied in connection with an investigation on the reaction between uranium dioxide and manganese dioxide.[2] In a sulfuric acid solution, the reaction between uranium dioxide and manganese dioxide apparently occurs at the points of contact of the hydrated surface layers of the two oxides, and the extent of the process is limited to these points of contact. The role of iron ions during sulfuric acid leaching of uranium ores appears to involve an oxidation-reduction reaction between the solid uranium dioxide and manganese dioxide.

Chlorination of Uranium Ores and Amalgam Reduction to Metal

Workers at Columbia University have made a preliminary study[3] of the direct chlorination of shale ores as a means for recovering the contained uranium. The uranium content of the shale ore generally analyzed 0.006 wt.%. At the prevailing prices for uranium, there exists no process that could be used for the economic recovery of uranium. To render practical the use of shale as a source of uranium, it is necessary to consider the shale as a source of other metal values and to regard uranium as the by-product of an otherwise economical process. In this regard a process was studied which involved high-temperature chlorination for the separation of metals from shale by volatilization of the chlorides.

Since shale contains too much hydrogenous material to allow direct chlorination, a prior roasting in steam at 800°C was required to prepare the shale for chlorination. Preliminary tests indicated that nearly all the uranium and iron and 50% of the aluminum were volatilized during chlorination with chlorine at 900 to 1000°C. Results of both batch fixed-bed and continuous fluidized-bed tests indicated that very short residence times in the high-temperature zone would give high metal chloride yields. In several tests, fused potassium chloride was employed as a sorbent to remove uranium chloride from the gas stream. Al-

though it was demonstrated that uranium could be removed from the shale matrix by a direct chlorination process, the considerable difficulty experienced in recovery of uranium from the off-gases precluded further development of this process.

Amalgam Reduction to Metal

Jangg[4] has described a process for obtaining uranium metal from ore concentrates based on the reduction of uranium chloride with sodium amalgam. Uranium dioxide, prepared from ore concentrates by conventional solvent extraction and hydrogen reduction procedures, is converted to volatile uranium chloride by reaction with a gaseous mixture of carbon tetrachloride and chlorine at approximately 700°C. Details of the chlorination process have been described in a previous Review.[5] The uranium chloride product (primarily uranium pentachloride) is volatilized from the chlorinator and collected separately in a pure form. The uranium chloride is reduced directly to metal with 0.5% sodium amalgam. Efficient contact between uranium chloride particles and the amalgam was provided by conducting the reduction step in a vibrating vessel. Over 90% conversion to metal was achieved in 4 hr at a reaction temperature of 300°C. The rate of reaction does not appear to be influenced by either the quantity of excess sodium present or the concentration of sodium in the amalgam. This allows the use of amalgam containing 0.3 to 0.4% sodium which is produced in mercury cathode cells employed in the production of electrolytic chlorine.

The reaction between uranium pentachloride and sodium appears to proceed through the formation of an intermediate uranium trichloride with the reduction of uranium trichloride to metal proceeding more slowly than the concomitant reduction of uranium pentachloride to uranium trichloride. The products of the reduction are a mixture of uranium amalgam, sodium amalgam, sodium chloride, and unreacted uranium chloride. A preliminary wash of the reduction residue with a dilute nonoxidizing acid (sulfuric acid) removes the sodium metal, uranium chloride, and sodium chloride from the insoluble amalgam. Less than 1% of the uranium is lost to the acid wash solution. The bulk of the excess mercury is removed from the uranium amalgam by filtration of the amalgam solution through porous filters. The uranium content in the partially purified amalgam is increased to approximately 5%. Since the uranium content in the filtered mercury is less than 10^{-4}%, the mercury may be recycled directly for the preparation of sodium amalgam in an electrolytic chlorine cell.

Purification of the uranium is conducted in a combined retort and furnace where the mercury is removed by distillation. To achieve a uranium metal product free from mercury, it was important to heat the amalgam slowly to 550°C. Heating to this temperature at a rapid rate would cause the porous uranium product to sinter, trapping residual mercury. The uranium sponge is melted and consolidated to massive metal by heating to 1280°C. Products consistently analyzing less than 6 ppm mercury have been obtained by this technique.

According to Jangg[4] this process possesses many advantages over the conventional process for producing uranium metal by the magnesium reduction of uranium tetrafluoride. Primarily the advantages lie in the reduction of the costs of chemicals. Also, the amalgam process allows the direct alloying of uranium with other metals in the amalgam phase and offers the choice of obtaining a uranium metal product either in the form of massive metal or as a sinterable powder. Stoll[6] has evaluated the industrial and economic advantages of the amalgam process as compared with existing methods and has concluded that from 10 to 20% of uranium production costs can be saved by using the amalgam process in combination with a chloride-alkali electrolysis process.

Production of Uranium Dioxide

Catalytic Reduction of Uranyl Carbonate Slurries

A hydrometallurgical method for producing uranium dioxide from aqueous slurries of uranyl carbonate has been developed by Warren and Forward.[7] The process involves a reduction with compressed hydrogen of aqueous suspensions of uranyl carbonate, acidified with carbon dioxide, in the presence of metal catalysts and organic promoters. The sequence of reactions for the reduction of uranium trioxide may be represented as

$$UO_3(\text{slurry}) + CO_2(\text{aqueous}) \rightarrow UO_2CO_3(\text{slurry})$$

$$UO_2CO_3(\text{slurry}) \xrightarrow{H_2CO_3} UO_2(HCO_3)_2(\text{aqueous}) \longrightarrow UO_2^{2+} + 2HCO_3^-$$

$$UO_2^{2+} + 2HCO_3^- + H_2 \xrightarrow{\text{catalyst}} UO_2(\text{slurry}) + 2H_2CO_3$$

Demonstration tests were performed using a high-pressure autoclave equipped with a stirrer. The catalyst (nickel gauze, 10 mesh/in., 0.025-in.-diameter wire) was attached as a cylinder to baffles located on the wall of the autoclave. Uranium trioxide and ammonium diuranate were carbonated by treating the aqueous suspensions with carbon dioxide at 100 psi. Approximately 95% conversion was achieved in 1 hr at 130°C. The reduction procedure involved placing sufficient water into the autoclave to cover the nickel-gauze catalyst, heating to operating temperature (210°C) under 100 psi carbon dioxide pressure, introducing hydrogen gas at 1000 psi, and, finally, injecting the concentrated slurry of uranyl carbonate. Examination of X-ray patterns of intermediate products showed that reduction occurred in three stages: uranyl carbonate is reduced to U_3O_8 which, in turn, reacts to form beta UO_2 and, finally, alpha UO_2.

The addition of anthraquinone to the slurry feed in a concentration of 0.2 g/liter significantly increased the rate of reduction to uranium dioxide. Demonstration tests showed that a slurry feed containing the equivalent of 60 g of uranium dioxide was completely reduced in 2 hr using the anthraquinone promoter. The function of anthraquinone appears to be that of a vehicle for bringing the reducing hydrogen to the surface of the U_3O_8 particles.

The surface area of the uranium dioxide product may be controlled by varying the carbon dioxide pressure during reduction. Increasing the carbon dioxide pressure reduces both the particle surface area and the rate of reduction. Recycling uranium dioxide product in the slurry feed yields a product with coarser particle size. It is reported that the process has the advantages of producing a uranium dioxide product of uniform surface area. Several tests have shown that high-density sintered compacts can be prepared by sintering at temperatures 200 to 300°C lower than required with conventional material.

Flame Denitration of Uranyl Nitrate Liquors

Pilot-plant facilities have been installed at the Mallinckrodt Chemical Works to study the one-step conversion of uranyl nitrate liquors to uranium dioxide.[8] The concept involves atomizing aqueous uranyl nitrate directly into a reducing flame of propane gas. The pilot-scale equipment, installed for continuous operation, was designed to process 100 lb of uranium per hour. The equipment was illustrated in Fig. IV-2 of a previous Review.[5] Propane, air, and uranyl nitrate are introduced to the reactor through a burner-nozzle assembly. The uranium dioxide powder and reaction off-gases exit from the bottom of the reactor and pass to a cyclone. The off-gases and unseparated powder then enter a filter chamber which discharges to a common hopper in which a powder level is maintained. The powder drains from the hopper through a cooling screw to a product reservoir.

Since the residence time of the liquid feed in the high-temperature zone is very short, good atomization of the liquid is required to provide a large surface area for heat transfer. Several nozzle and burner configurations were investigated; and, in the final design, the burner surrounded the nozzle, and the liquid feed was introduced along the burner axis through an assembly of three atomizing nozzles. Evaluation tests performed with this nozzle indicated that the highest feed rate consistent with good operation appeared to be 15 gal/hr per nozzle; above this rate, coarse droplets began to develop in the spray pattern of the nozzle and resulted in poor product quality.

The major problems encountered in pilot-plant tests were the continuous formation of heavy deposits of dry powder on the walls of the reactor and the difficulty of producing high-assay (> 97%) uranium dioxide product. By inserting conical liners within the reactor, caking of powder on the reactor walls was minimized. However, owing to the concomitant decrease in residence time in the reactor, product of low uranium dioxide assay was produced. In isolated tests, products containing 94 to 96% uranium dioxide were obtained, but it was not possible to reproduce these results consistently. Increasing the residence time by lengthening the reactor appears to be the most promising method for improving the product assay.

The uranium dioxide product from the flame reactor was in the form of a fine powder with an average particle size of 0.8 to 1.2 μ. In general, the product was more reactive to hydrogen fluoride than oxides produced by other processes. Flame-produced uranium di-

oxide has been successfully hydrofluorinated in a series of plant-scale agitated-bed reactors.

Development of Other Processes

In the preparation of uranium dioxide by hydrogen reduction of higher uranium oxides, the physical properties of the uranium dioxide product are greatly affected by the properties of the parent oxides. In an effort to produce a uranium dioxide powder that would sinter to high density, Ainscough[9] has studied a preparation method based on the homogeneous precipitation with urea of uranyl nitrate solutions, followed by calcination of the precipitate and reduction in hydrogen, as an alternate to the ammonium diuranate process. The homogeneous precipitation method produced uranium dioxide particles with small specific surface area, and the densities attained after sintering were slightly less than those of sintered compacts of oxide prepared from ammonium diuranate under similar calcination and reduction conditions.

Workers at Comitato Nazionale per l'Energia Nucleare[10] in Rome have studied a process for the wet preparation of uranium dioxide powders of high surface area and capable of sintering to high-density compacts. The process involves the reduction of a solution of uranyl chloride with zinc to produce uranous chloride. Precipitation of uranous hydroxide is effected by addition of ammonium hydroxide to the uranous chloride solution. It appears that precipitation from an acid medium (pH < 5) is most satisfactory for control of zinc contamination. Uranium dioxide powder is prepared by drying the precipitate in a hydrogen atmosphere at 600°C. Preliminary tests have indicated that the uranium dioxide product sinters to densities less than those of sintered compacts of oxide prepared by hydrogen reduction of U_3O_8.

Mechanism and Kinetics of Reduction of Uranium Oxides

Gas-solid reactions, particularly the reduction of uranium trioxide with hydrogen and the hydrofluorination of uranium dioxide to produce uranium tetrafluoride, are important steps in the production of both uranium metal and uranium hexafluoride. The rate of these reactions has been shown to be determined by the structure of the solid surface which, in turn, is modified by the progress of the reactions. Notz, Huntington, and Burkhardt have studied the successive phase changes that occur during the hydrogen reduction of uranium trioxide at temperatures of 480 and 750°C. The reaction sequence for the reduction of gamma UO_3 (prepared by the denitration of uranyl nitrate hexahydrate at 230°C) is

$$\gamma\,UO_3(\text{orthorhombic}) \xrightarrow{1} U_3O_8(\text{hexagonal}) \xrightarrow{2} U_3O_8^-(\text{orthorhombic}) \xrightarrow{3} UO_2^+(\text{cubic}) \xrightarrow{4} UO_2(\text{cubic})$$

Each time a structural change occurs, as at steps 1, 2, and 3, there is also a change in the reaction rate.

It is suggested[11] that the reduction of high-surface-area uranium trioxide (hexagonal alpha UO_3) would be expected to proceed by the above reaction and not by the sequence

$$UO_3 \rightarrow UO_{2.56} \rightarrow UO_2$$

described in a previous Review.[12] A rate change was not observed at the U_3O_8 composition corresponding to the intermediate formation of hexagonal U_3O_8. Since the uranium trioxide was the hexagonal polymorph, the actual reduction reaction would probably follow

$$\alpha\,UO_3(\text{hexagonal}) \xrightarrow{1} U_3O_8(\text{hexagonal}) \xrightarrow{2} U_3O_8^-(\text{orthorhombic}) \xrightarrow{3} UO_2(\text{cubic phases})$$

A rate change would not be expected at the end of reaction 1 since both structures are hexagonal.

The kinetics of the reduction of uranium trioxide with carbon monoxide have been studied[13] in the temperature range of 260 to 400°C. The results showed that the initial stage of the reaction proceeds by reduction of uranium trioxide to $UO_{2.9}$ at a rate independent of the degree of oxygen removal. The reduction process then proceeds autocatalytically to form orthorhombic U_3O_8. Further reduction at a new constant rate produces U_4O_9 as an intermediate phase. From U_4O_9 to uranium dioxide, the rate diminishes with increasing degree of reduction and is controlled by diffusion of oxygen in the solid phase.

Oxidation-Reduction Equilibria in the UO_2-U_3O_8 System

Considerable research is being carried out to measure the oxidation and reduction equilibria in the UO_2-U_3O_8 system. This system is complicated by the existence of several intermediate stoichiometric and metastable oxides. Sudo and Kigoshi[14] have measured the oxidation and reduction equilibria among UO_2, U_4O_9, and U_3O_8 at temperatures up to 1200°C. In other work, Kiukkola[15] has obtained standard thermodynamic data for the mixing of uranium dioxide and oxygen gas by electromotive force measurements on galvanic cells at temperatures of 800 to 1200°C.

Production of Uranium Tetrafluoride

Uranium tetrafluoride is an important intermediate in the production of both uranium hexafluoride and uranium metal. Smiley[16] has reviewed the developments in reactor design associated with feed-materials processing for the production of uranium hexafluoride and uranium metal. The review emphasizes descriptions of process steps utilizing gas-solids reactions. Most of the discussion relates to the following chemical steps: the production of uranium trioxide from purified solutions of uranyl nitrate hexahydrate; the reduction of uranium trioxide to uranium dioxide with hydrogen; the reaction of uranium dioxide with hydrogen fluoride to produce uranium tetrafluoride; the conversion of uranium tetrafluoride to uranium hexafluoride; and the reduction of uranium hexafluoride with hydrogen to uranium tetrafluoride. In each process step, details of the reactor types developed to carry out the process are described, and new reactor designs still under study are discussed.

Stirred Fluid-Bed Reactors

In December 1961 a new uranium tetrafluoride production line went on-stream at the Paducah plant of the Union Carbide Nuclear Company.[17] The new line, which employs a series of stirred fluid-bed reactors to convert uranium dioxide to uranium tetrafluoride, replaces a system of ribbon-screw reactors. Since the fluid-bed reactors offer more efficient gas-solids contact with closer temperature control, a significant increase in both production rates and product quality has been reported with concomitant decrease in maintenance costs.

Hydrofluorination is carried out in a two-stage countercurrent system. The reactors are each 30 in. in diameter and 9.5 ft in height. Cooling air is employed to maintain the first stage at 317°C and the second stage at 535°C. Rapid heat transfer is achieved through cooling fins installed along the walls of the reactors. Mechanical agitators in each reactor prevent powder from depositing on the inner walls of the reactor and avoid sintering of uranium dioxide–uranium tetrafluoride mixtures. Anhydrous hydrogen fluoride (5 to 10% excess) enters the system at the second-stage reactor and flows countercurrent to the solids. Uranium dioxide, prepared by fluid-bed reduction of uranium trioxide, is fed continuously to the first-stage reactor. The partially reacted powder and off-gases overflow from the first stage into a hopper that serves as a separation chamber for removing solid particles from the gas stream. A single sintered Inconel filter removes the fine dust particles from the 15% hydrogen fluoride–water vapor off-gas. The solids flow from the hopper to the middle of the second-stage reactor where the conversion to uranium tetrafluoride is completed. The uranium tetrafluoride yield has consistently been 94 to 97% at processing rates as high as 21 tons of uranium per day.

Activation of Uranium Dioxide for Uranium Tetrafluoride Production

Workers at National Lead Company of Ohio[18] have demonstrated that continuous-pot denitrated uranium trioxide—a material normally exhibiting low reactivity toward reduction and hydrofluorination—can be activated by a reduction-oxidation-reduction process. This process enables a uranium trioxide of low reactivity to be converted to high-assay uranium tetrafluoride at elevated feed rates. Previous work, reported in a recent Review,[19] indicated that this proposed scheme could be adapted to existing equipment producing high-quality uranium tetrafluoride at satisfactory rates.

Recent work[18] has concerned the application of the activation process to the flow sheet shown in Fig. V-1. A test was designed to

employ a two-stage cocurrent fluid bed for the initial reduction, a screw reactor for oxidation, a screw reactor for the second reduction, and two screw reactors arranged in series for hydrofluorination. Reduction of uranium trioxide in the fluid-bed reactors was carried out at 620°C using 50% excess of dissociated ammonia as the reducing gas. Oxidation of the uranium dioxide by air to U_3O_8 was conducted at 455°C. Air flow was 30 to 50% in excess of the theoretical amount. The second reduction by ammonia was made in a screw reactor maintained at approximately 590°C. Hydrofluorination was performed in two screw reactors operating with a temperature gradient across the reactors from 260 to 550°C. The hydrogen fluoride flow rate was 20% in excess of theoretical.

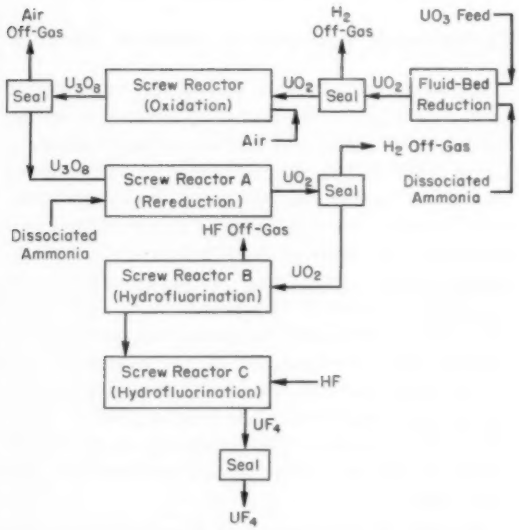

Fig. V-1 Production flow sheet for activation of continuous-pot uranium trioxide.[18]

The results of these tests indicated that, by employing this process flow sheet, green salt averaging 97.5% uranium tetrafluoride could be produced at a feed rate of approximately 9.4 tons of uranium per day. At a feed rate of 11.8 tons/day, 95% uranium tetrafluoride was produced. These results represent a substantial improvement in production capability when compared with production rates for nonactivated batch-pot or continuous-pot denitrated oxides.

Fluid-Bed Uranium Trioxide

In the fluid-bed production of uranium trioxide, a concentrated uranyl nitrate solution is injected under pressure through a nozzle into a bed of uranium trioxide at 315°C. Workers at Harwell[20] have observed that the reaction between uranium dioxide (produced by reduction of fluid-bed uranium trioxide) and hydrogen fluoride to prepare uranium tetrafluoride does not proceed readily to completion. Dell and Wheeler[20] have studied an activation procedure based on the conversion of uranium trioxide to hydrated species followed by dehydration and reduction. Experimental tests were carried out using fluidized-bed uranium trioxide of low sulfate content and having a particle size of −80 +120 mesh.

The hydration of fluid-bed uranium trioxide was shown to proceed at different rates in liquid water and in water vapor. In liquid water, $UO_3 \cdot 2H_2O$ is formed up to 70°C. At 100°C, $UO_3 \cdot H_2O$ is formed. In water vapor, hydration at 20°C leads to $UO_3 \cdot 2H_2O$, whereas a monohydrate is formed at temperatures above 40°C. Decomposition of the hydrates is complex, particularly when prepared from fluid-bed uranium trioxide which possesses a characteristic structure that influences the behavior of the hydrates formed from it. Decomposition of each hydrate leads to a mixture of gamma uranium trioxide and amorphous uranium trioxide at 400°C, the latter recrystallizing to the gamma polymorph at 520°C.

The reactivity of uranium trioxide toward reduction to uranium dioxide and subsequent hydrofluorination to uranium tetrafluoride depends on the conditions of hydration and dehydration. Crystal growth at the hydrate stage is favored by hydration at high temperatures or for prolonged periods, particularly by the use of liquid water rather than steam. This crystal growth results in decreased reactivity in the reduction reaction and leads to a form of uranium dioxide that is less reactive toward hydrofluorination. The structure of the uranium dioxide formed from hydrated uranium trioxide is greatly influenced by the structure of the hydrate crystals. The ideal structure of uranium dioxide for hydrofluorination is one in which small, highly porous aggregates of uranium dioxide microcrystallites are well separated in an expanded particle. The hydrofluorination reaction is favored by (1) hydration

under mild conditions to minimize crystal growth; (2) hydration to the dihydrate rather than the monohydrate; and (3) decomposition of the hydrate and reduction to uranium dioxide at 400°C rather than at 500°C.

Preparation of Uranium Carbides

At the present time AEC's Division of Reactor Development is supporting several programs intended to develop and evaluate bulk uranium carbides as reactor fuels. The favorable characteristics of uranium monocarbide include high uranium density, high thermal conductivity, and very low parasitic neutron capture. Dense uranium monocarbide appears to be well suited for use in sodium- and organic-cooled reactors. Promising results from preliminary evaluation of fabrication characteristics and resistance to radiation damage have initiated an expansion of research concerning uranium monocarbide both in Europe and in the United States. Battelle Memorial Institute[21] has demonstrated the technical feasibility of melting and casting uranium carbide ingots having a density that is 100% of the theoretical density and weighing up to 6 kg. The controlled carbon contents of these ingots are predictable within ±0.05 wt.% carbon. Their study has also concluded that, under suitable nonoxidizing conditions, uranium monocarbide and uranium sesquicarbide are ideal fuels for power reactors operating at temperatures at least as high as 800°C. The utility of uranium dicarbide as a fuel for nuclear reactors appears subject to reservations. As a bulk fuel it may have utility at low temperatures where the rate of graphite formation is negligible. A constitutional diagram of the uranium-carbon system appears in Fig. V-2. Incorporated in the diagram are many recent data obtained at BMI. A bibliography compiled by Bloomfield[22] covers all the data on uranium carbide which were obtained up to June 1961 and which are directly related to the use of uranium carbide as a nuclear fuel.

Reaction of Uranium Metal with Hydrocarbons

Among the most promising methods for preparing uranium monocarbide appears to be the reaction of uranium metal with hydrocarbons. Workers at United Nuclear Corporation[23] have established reaction conditions for the production of uranium monocarbide by reaction of hydrided metal with propane. By varying both the carburizing temperature and time, high-purity uranium carbide was prepared to three specific carbon contents: 4.4 ± 0.1, 4.8 ± 0.1, and 5.2 ± 0.1 wt.% carbon. Several tests were performed to evaluate sintering behavior of the various uranium monocarbide products. It was observed that uranium volatilization during sintering for 3 hr at 1500°C resulted in a slight increase in the carbon content of the sintered compacts. The specific carbon content of the uranium monocarbide appears to be critical for obtaining a high-density sintered product. Decreasing the carbon content from 4.50 to 4.31 wt.% results in an increase in density of the sintered product from 12.1 to 13.6 g/cm^3.

Carbothermic Reduction of Uranium Dioxide

High-quality uranium monocarbide has also been prepared by the direct reaction of uranium dioxide and elemental carbon at high temperatures (1600 to 1700°C). In the method developed at United Nuclear Corporation,[23] intimate contact between the reactants is achieved by compressing the blended feed materials into briquettes prior to reaction. A charge of 1000 g of uranium dioxide (−325 mesh) and 128.5 g of graphite (−200 mesh) is blended and compacted, without die lubricant, at 30 tsi pressure in a ½-in.-diameter die. The briquettes are reacted in an induction furnace for 2 hr at 1700°C under reduced pressure. The uranium monocarbide product was successfully arc melted and cast into rods.

Kinetic data on the reaction between uranium dioxide and graphite have been reported by Atomics International.[24] Studies were carried out using reactant mixtures both in the powder and pellet form. To prepare pellets from the uranium dioxide−graphite mixture, a binder was added—either acrylic plastic or stearic acid. The powder mixture was stirred with a chloroform solution of the binder, was dried at 20°C, and was pressure cast into cylindrical pellets at 50 tsi. Uranium monocarbide was prepared by heating the reaction mixture in vacuum at 1300 to 1700°C. The product obtained from powder mixtures was a sintered mass, greatly shrunken but usually retaining the shape of the

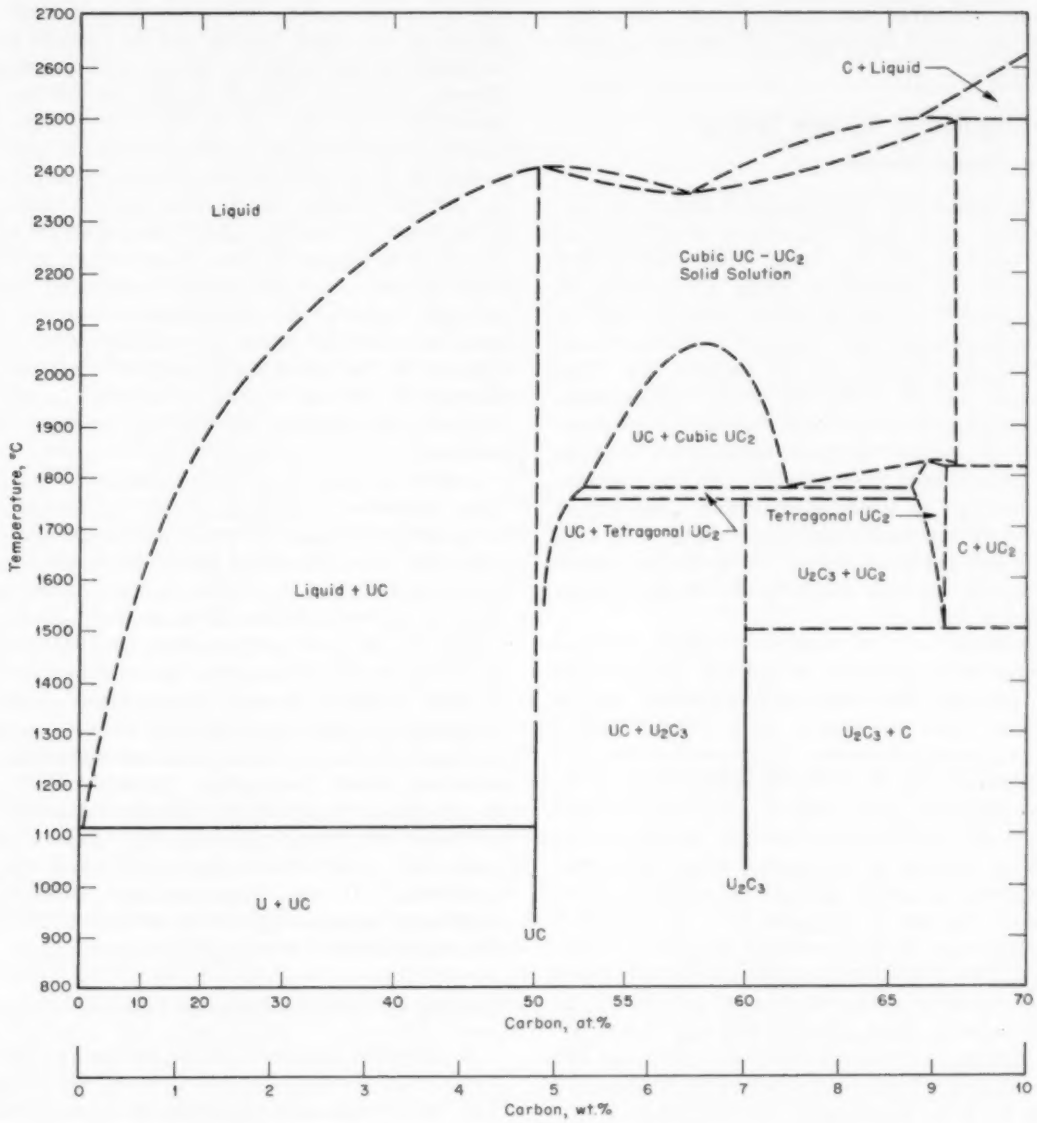

Fig. V-2 Uranium-carbon constitutional diagram.[21]

crucible. Pellets appeared cracked, with about 50% theoretical density. In the powder experiments the carbon content of the products agreed with predicted values. The carbon content of products from pellets was low by 0.25 wt.%, and this low content is believed to be an effect of the binder material. In all experiments the reaction followed a second-order rate equation, except that the rate constant often decreased abruptly when the reaction was about 90% complete. The rate data agree with the hypothesis that the activation energy is equal to the heat of the endothermic reaction. Considerable success was experienced in monitoring the reaction by measuring the evolved carbon monoxide with a gas meter. Several container materials were evaluated, and the best overall material was found to be carbide-coated graphite. Molyb-

denum appeared satisfactory only when the reactants were fabricated into pellets prior to reaction.

Precipitation of Uranium Carbide from Liquid Metals

The possibility of synthesizing uranium monocarbide and other refractory compounds of interest as reactor fuels from liquid-metal solutions is currently being investigated at Argonne.[25-27] Uranium monocarbide is prepared by precipitating with carbon the uranium dissolved in a volatile liquid-metal solvent. Fine carbon powder is stirred with a uranium-zinc-magnesium system at 800°C or with a uranium-cadmium system at 600°C until all the uranium is precipitated from solution as the carbide. Stirring is an important variable in the rate of the heterogeneous reaction between dissolved uranium and solid carbon, with stirrer speeds less than 400 rpm resulting in slow and incomplete reactions.[26]

Procedures have been established for preparing large quantities of uranium monocarbide to evaluate the ease of fabricability of the product and its utility as a reactor fuel.[26] Experimental tests were performed in tantalum crucibles, $3\frac{5}{8}$ in. in inside diameter by 8 in. high with four $\frac{3}{8}$-in. baffles. The melt was agitated with a flat tantalum paddle. Approximately 400-g batches of uranium monocarbide were prepared by adding 50% excess carbon as activated charcoal or graphite to a zinc–12 wt.% magnesium–15 wt.% uranium solution at a temperature of 800°C. The usual procedure was to stir the melt until the uranium had completely disappeared from solution and then to transfer a portion of the supernatant to remove the bulk of the solvent metals and unreacted carbon from the carbide. The carbide product was recovered in pure form by vacuum retorting to remove residual zinc and magnesium. In this system the reaction was more than 98% complete in 5 hr using agitation, provided that about 50% excess carbon was employed. Oxygen content of the products from preliminary tests was high (1.5 wt.%) and was greater for carbide made from activated charcoal than for carbide prepared from graphite.[27] Zinc and magnesium content of the carbide product was collectively less than 1 wt.%.

Considerable difficulty has been experienced[26] in achieving a separation of the carbide product and unreacted carbon. Since carbon is not well wetted by the liquid metals and the carbide is suspended in the solution, initial efforts were directed toward removing excess carbon mechanically from the top of the molten ingot. However, the material that floated on the ingot contained large amounts of uranium, presumably as the carbide. Since alkali metals appear to be effective wetting agents between carbon and zinc, a series of tests was performed to evaluate the effect of adding sodium on the uranium monocarbide precipitation reaction.[27] Both the rate and extent of reaction were increased by the presence of sodium. Also, the amount of excess carbon required was decreased substantially through the addition of sodium.

Several exploratory experiments[25,27] have been conducted to determine the reaction rate of hydrocarbon gases with uranium dissolved in cadmium. The addition of carbon in the form of hydrocarbon gases to a liquid-metal solution of uranium has the potential advantage that excess carbon is not added to the system provided that pyrolysis of the hydrocarbon does not occur as a side reaction. Several hydrocarbon gases (methane, ethane, propane, and butane) were evaluated by flowing the gas through a uranium-cadmium–1 wt.% magnesium solution at 550°C. In all cases the extent of reaction was limited to about 30%. It appears that this reaction is inherently inefficient. In tests performed with acetylene,[25] it was observed that acetylene underwent extensive pyrolysis at 600 and 800°C with the formation of elemental carbon.

Coating of Uranium Carbide Particles

A principal difficulty in the design of a nuclear reactor employing uranium carbide as the fuel material is the reactivity of the fuel with moisture to form oxide. This problem is especially complicated during fabrication operations. Engle, Goeddel, and Luby[28] have studied the rate of reaction of uranium and thorium dicarbides in moist air at 30 and 50°C. The initial reactions appear to follow a simple linear rate law with the thorium-containing carbides being about 10 times more reactive than uranium dicarbide. The reaction produces both gaseous and solid products, the latter consisting of thorium or uranium oxides and condensed hydrocarbons. The gaseous products are principally aliphatic hydrocarbons and hy-

drogen. The solid reaction products are ablative (particles flake off as the reaction proceeds), and individual particles undergo a large bulk-volume change. Lawrance and O'Connor[29] have observed the hydrolysis of thorium monocarbide in moist air and report that the reaction proceeds rapidly with the formation of hydrated thorium oxide and various hydrocarbons.

Workers at BMI[30–33] have developed a technique for coating carbide fuel particles with carbon films to protect the carbide against attack by humid air during the fabrication operation. It has been shown[30] that carbon coatings provide excellent protection for uranium dicarbide–thorium dicarbide solid solution particles against attack by moisture. Pyrolytic-carbon coatings are applied to carbide particles by the decomposition of hydrocarbons in a fluidized bed of particles at temperatures of 950 to 2000°C. The density of pyrolytic-carbon coatings decreased from 1.99 g/cm^3 at a coating temperature of 950°C to a minimum value of 1.50 g/cm^3 at 1500°C and then increased to a density of 1.94 g/cm^3 at a temperature of 1800°C.

Carbon coatings have been shown to provide good fission-product retention after neutron activation by observing the fraction of contained Xe^{133} released during a 2-hr period at temperature levels[30,32,33] from 900 to 1500°C. The total quantity of xenon released varied from approximately 1 ppm at 900°C to 20 ppm at 1500°C. Owing to these initially favorable results, studies have been initiated at ORNL[34] to evaluate pyrolytic-carbon-coated carbide fuel particles when in contact with water vapor at elevated temperatures. Tests have also been initiated for determining fission-gas release from coated particles.

Plutonium-Containing Ceramics

Interest in fast reactors has revealed a need for a breeder type fuel consisting of some form of plutonium with natural uranium. Of considerable interest for this type of application is a solid solution of plutonium monocarbide in uranium monocarbide.[35,36] Lied and White[37] at ANL have investigated the preparation of a 20 wt.% plutonium–80 wt.% uranium monocarbide solid solution. Plutonium carbide was prepared by reacting under vacuum a pelletized mixture of plutonium dioxide and carbon at 1100°C and above. The solid solution of uranium-plutonium carbide was prepared by sintering pressed pellets of the two blended carbides in vacuum at 1650°C. It was observed that prolonged treating under vacuum caused vaporization of plutonium from plutonium carbide and loss of plutonium and carbon from the 80% uranium carbide–20% plutonium carbide solid solution. A two-phase product, plutonium monocarbide and plutonium sesquicarbide, was formed when a mixture of plutonium dioxide and carbon, calculated to produce stoichiometric monocarbide, was fired under vacuum to 1300 to 1350°C.

Sheridan, Strasser, Anderson, and Taylor[38] also have observed that the reaction between plutonium dioxide and carbon at 1300 to 1650°C produces a carbide product containing at least two phases, the primary phase being plutonium sesquicarbide. Two different approaches have been tried to prepare a solid solution of uranium carbide and plutonium carbide. Carbon reduction of a 4-to-1 mixture of uranium dioxide and plutonium dioxide produced a material close to the desired 4.8 wt.% carbon when 95% of the stoichiometric amount of carbon was used in the reduction. The second method for preparing a solid solution of the carbides is represented by the equations

$$2PuO_2 + 7C \rightarrow Pu_2C_3 + 4CO$$

$$Pu_2C_3 + U + 7UC \rightarrow 10(U_{0.8}Pu_{0.2})C$$

The first step involves synthesizing plutonium sesquicarbide by reacting a stoichiometric mixture of plutonium dioxide and carbon. The resulting sesquicarbide is heated with sufficient uranium monocarbide and uranium metal powders to give a product containing 80% uranium monocarbide and 20% plutonium carbide. Moderately good grade of product has been prepared by this method; X-ray analyses have shown only faint indications of sesquicarbide in the solid solution.

Ogard, Pritchard, Douglass, and Leary[39] have prepared carbon-deficient uranium monocarbide–plutonium monocarbide solid solutions with no impurities detectable by X-ray diffraction or metallographic examination. These were produced by sintering mixtures of uranium dioxide, plutonium dioxide, and graphite at 1450 to 1850°C. Single-phase solid solutions of the compositions $U_{0.9}Pu_{0.1}C_{0.95}$, $U_{0.8}Pu_{0.2}C_{0.95}$, and $U_{0.7}Pu_{0.3}C_{0.95}$ were prepared without the need for making the monocarbide separately. Pellets

with densities up to 12.85 g/cm^3 (94.5% of theoretical density) were achieved by a second sintering of pressed pellets of the reaction product. It was not possible to prepare a single-phase plutonium monocarbide solely by sintering compacts of plutonium dioxide and graphite; the product consistently contained plutonium sesquicarbide as an impurity. However, arc melting of the product eliminated the plutonium sesquicarbide impurity and resulted in a single-phase plutonium monocarbide having 98.5% of the theoretical density.

Production of Uranium Metal

Electrolytic Reduction of Uranium Dioxide

High-quality uranium metal has been produced at Mallinckrodt Chemical Works from uranium dioxide by fused-salt electrolysis using a consumable anode that contains a uranium dioxide–carbon mixture.[40] The reduction cell consists of a cylindrical graphite crucible that serves both as the cathode of the cell and as a container for the molten electrolyte and molten metal. The electrolytic process is analogous to the Hall process for aluminum production in that the oxide reacts with carbon at the anode to form an oxide of carbon. The reactions may be represented as

$$\text{Anode reaction: } UO_2 + 2C \rightarrow U^{4+} + 2CO + 4e^-$$

$$\text{Cathode reaction: } U^{4+} + 4e^- \rightarrow U$$

Anodes are prepared by mixing uranium dioxide with coal tar pitch, pressing into shape, and carbonizing the pitch. The most satisfactory anode arrangement appears to be a configuration that provides an electrically neutral basket to contain the uranium dioxide–carbon pellets. The basket anode cell, shown in Fig. V-3, consists of a graphite crucible enclosed in a quartz tube which is heated by an induction coil outside the tube. A fused salt containing an equimolar mixture of barium fluoride and lithium fluoride provided the best production rates and current efficiencies of all salts that were evaluated. The uranium tetrafluoride content of the electrolyte was observed to have a marked effect on production rates and current efficiency. The optimum composition of electrolyte

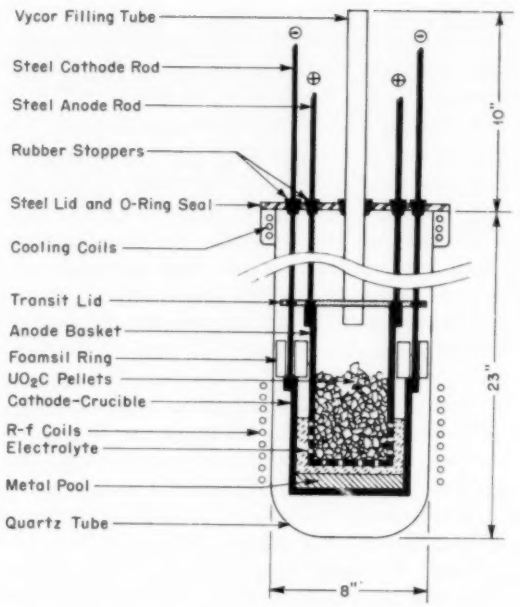

Fig. V-3 Basket anode-container cathode cell.[40]

was found to be 65 wt.% barium fluoride–10 wt.% lithium fluoride–25 wt.% uranium tetrafluoride.

In making a run the cell is heated to 700°C, and the system is evacuated to outgas the electrolyte and graphite. The system is then filled with helium and heated to 1050°C. At this temperature a preelectrolysis with reversed polarity is performed to remove oxides initally present in the electrolyte. In this step the graphite crucible serves as the anode. The preelectrolysis is continued until appreciable quantities of carbon tetrafluoride appear in the off-gases. At this point, polarity is returned to normal and the cell temperature is increased to 1150°C. Run times in demonstration tests were usually 4 to 6 hr in duration, but continued operation for as long as 39 hr has been maintained. At the end of the electrolysis, the metal and electrolyte are allowed to freeze in the cell. Sound uranium metal products up to 15 lb in weight have been produced. Impurity levels of oxygen and carbon have been surprisingly low, 10 and 320 ppm, respectively. Uranium recovery as massive metal, based on the weight of metal produced over the amount of uranium introduced as uranium dioxide and as uranium tetrafluoride, has consistently exceeded 99%.

Preparation of Aluminum-Uranium Alloys

Baird and Runnalls[41] at Chalk River have developed a method for producing highly enriched uranium-aluminum alloys by the direct reduction of uranium dioxide with aluminum in the presence of cryolite (Na_3AlF_6). The reduction operation was conducted in a graphite crucible that was 7.5 in. high, 3.8 in. in diameter, and 0.25 in. in wall thickness. The reduction procedure involved (1) placing a charge of cryolite powder around a cylinder of pure aluminum within the crucible and (2) adding a blended mixture of cryolite and uranium dioxide. The crucible was covered, placed within an induction furnace, and heated to 1120°C. The reactants were held at temperature for 7 to 10 min and then cooled to room temperature. The alloy billet was separated from adhering slag, heated to 1070°C, and poured into a casting.

The uranium yield, obtained by reduction of uranium dioxide with an excess of aluminum to form aluminum–28 wt.% uranium alloys, averaged approximately 98% during 10 runs. The small amount of uranium that was not recovered in the reduction billet was readily leached from the cryolite slag and graphite crucible with hydrochloric and nitric acids. The overall uranium yield in a series of reductions and castings was improved by recycling casting dross to a subsequent reduction.

Reduction of Uranium Trichloride in Fused Salts

Workers at Harwell have examined a fused salt–liquid metal process based on the reduction of uranium trichloride in a lithium chloride–potassium chloride eutectic by a solution of magnesium in cadmium as a means for producing enriched uranium metal.[42] The suggested process envisaged the use of enriched uranium trioxide as the primary feed material. The trioxide, suspended in a melt of lithium chloride–potassium chloride eutectic at 500°C, is reacted with chlorine in the presence of carbon to give a solution of uranium tetrachloride. The uranium tetrachloride is reduced by hydrogen to provide the feed for the liquid-metal reduction step. Experiments were carried out on the reduction of uranium trichloride to metal at 500°C. The uranium metal appears as a solution in the cadmium and is recovered by distillation of the alloy. Two alternative methods for handling the fused salt after reduction have been proposed. If the residual uranium content in the eutectic can be reduced to 50 ppm, the salt may be discarded. An alternate proposal is the recycling of the salt for electrolytic recovery of the magnesium values. The electrolytic cell is operated with a liquid-cadmium cathode, and therefore the product is a magnesium-cadmium alloy that is suitable for uranium reduction.

Because of the reactivity of the fused chlorides with oxygen and water vapor, all process development studies were carried out under an inert atmosphere. It was observed that the rate of reduction of the uranium trichloride is very rapid. The approach to equilibrium was 97% complete within 5 min of reaction time for uranium trichloride concentrations in the range of 30 wt.% to 200 ppm in the eutectic salt. Below 200 ppm the reduction appears to proceed much more slowly, and this may be a lower limit for the residual concentration of uranium trichloride obtainable practicably. The reaction between uranium trichloride and magnesium occurs in the salt phase, and the rate at which the uranium metal dissolves in the molten cadmium is the controlling step in the process.

Thorium

Recovery of Thorium from Ores

Studies are being made at ORNL on the recovery of thorium and uranium from granitic rock, since this source represents a very large potential thorium reserve for the nuclear-power industry. In preliminary sulfuric acid leaching studies[43] on 16 granite samples containing 8 to 95 ppm thorium and 1.5 to 16 ppm uranium, maximum recoveries of thorium ranged from 30 to 85% and of uranium from 15 to 65%. Sulfuric acid consumption was high—30 to 120 lb of sulfuric acid per ton of granite. A relatively high acidity ($2N$ H_2SO_4) was required to obtain rapid and efficient dissolution of the soluble thorium fraction. Thorium recoveries were not improved by grinding the granite to −200 mesh rather than −48 mesh.[44] Acid consumption also was higher for the finer ore. Preliminary estimates of costs for treating granitic rock ranged from $30 to $500 per pound of recovered thorium.

Thorium is readily recovered from the sulfuric acid leach liquor by solvent extraction with primary amines.[44] A 0.03*M* solution of 1-nonyldecylamine in a kerosene-tridecanol diluent showed an effective thorium extraction coefficient of 2000. Uranium recoveries in acid leaching of granitic rock was not improved by adding an oxidant.[45]

Reduction of Thorium Oxide

Owing to the success achieved at ANL in the reduction of uranium oxides by zinc-magnesium alloys in the presence of molten fluxes,[46] a series of tests was performed to evaluate the reduction of thorium dioxide in similar systems.[27,47] The tests showed that complete reduction of thorium dioxide to thorium metal by a zinc–5 wt.% magnesium alloy can be achieved in 2 hr at 750°C if a flux containing at least 30 mole % magnesium cations is employed. A series of tests was performed[47] to evaluate the effect of flux composition on the reduction of thorium dioxide with a zinc-magnesium alloy. These tests showed that the extent of reduction decreases progressively in the order Li > Na > K for flux systems of the type MCl-$MgCl_2$-MgF_2 where M is Li, Na, or K. Very poor reductions were observed when calcium chloride was substituted for magnesium chloride in the flux. It appears that magnesium cation is a desirable constituent in the flux, which cannot be replaced by substitution of calcium. Increasing the concentration of magnesium fluoride in the flux from 5 to 10 mole % resulted in a significant increase in the reduction yield. No advantage was gained in increasing the magnesium fluoride concentration above 10 mole %. Calcium fluoride may be satisfactorily substituted for magnesium fluoride in the flux. The optimum calcium fluoride concentration in a $CaCl_2$-$MgCl_2$-CaF_2 flux appears to be 7 mole %. Recent work[27] has shown that effective reduction of thorium dioxide by zinc-magnesium solutions occurs within a limited composition region of the $CaCl_2$-$MgCl_2$-CaF_2 flux system. This region lies above 50 mole % magnesium chloride and between 7 and 15 mole % calcium fluoride.

Reduction of Thorium Oxide by Aluminum

Raleigh at Atomics International has developed a process for the reduction of thorium oxide by aluminum as a means for preparing thorium-aluminum alloys. Details of the reduction process were covered in an earlier Review.[48] Recent work[49] on this process has shown that the primary driving force for the reduction of thorium oxide is the free energy of formation of a thorium-aluminum intermetallic, $ThAl_3$. The standard free energy of formation of $ThAl_3$ at 1050°C was estimated to be 36 kcal. Intermetallic compound formation may play a useful role in promoting metallothermic reductions in a number of systems that otherwise might be considered energetically unfavorable.

Electrorefining of Plutonium Metal

Mullins et al.,[50] at Los Alamos Scientific Laboratory, have recently developed a process for producing plutonium metal of excellent purity by an electrorefining procedure. This method has been considered for application in the preparation of high-purity metal, recycle of impure plutonium metal scrap, recycle of impure plutonium compounds after conversion to metal, and the processing of plutonium from plutonium-fueled nuclear reactors.

Figure V-4 shows the electrorefining cell assembly employed in the processing of 3.5-kg batches of plutonium metal. Operation of the cell involves the oxidation of plutonium metal at the anode to form trivalent plutonium ions in the molten-salt electrolyte, maintained at a temperature above the melting point of plutonium metal. The plutonium ions are transported through the electrolyte to the cathode, where they are reduced to metal. The molten metal drains down the cathode into a product reservoir.

The electrolyte employed in the electrorefining process was a molten salt containing 10 wt.% Pu(III) chloride, 50.4 wt.% potassium chloride, and 39.6 wt.% sodium chloride. The salt was prepared by melting potassium and sodium chloride with vacuum-distilled Pu(III) chloride in a quartz container. Plutonium(III) chloride was prepared by hydrochlorination of Pu(III) oxalate.

A massive cylinder of plutonium metal or alloy served as the anode. In most tests the impure plutonium anode was prepared by the bomb reduction of Pu(IV) fluoride. A tungsten tube immersed in the electrolyte was used as

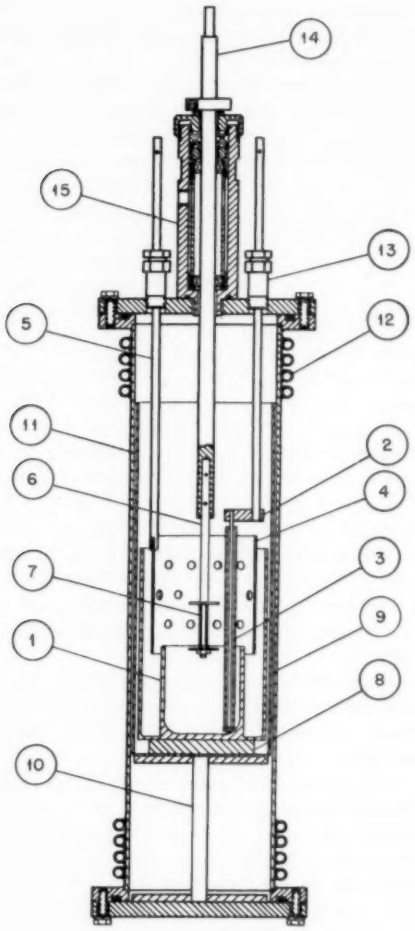

Fig. V-4 Plutonium electrorefining cell assembly, 3.5-kg scale.[50]

1. Alumina-yttria cell, $4\frac{1}{8}$ in. in outside diameter by $6\frac{1}{8}$ in. tall
2. Anode assembly
3. Tungsten anode protected by alumina sheath
4. Tungsten cathode, $3\frac{3}{8}$ in. in inside diameter by 4 in. tall by 0.030 in. thick
5. Cathode rod, $\frac{1}{4}$ in. in diameter
6. Tantalum stirrer
7. Tantalum spacer
8. Alumina spacer
9. Stainless-steel safety can
10. Stainless-steel pedestal
11. Stainless-steel furnace tube, $4\frac{3}{4}$ in. in inside diameter by 20 in. long by $\frac{1}{8}$ in. thick
12. Cooling coils
13. Teflon-lined compression seal
14. Stainless-steel shaft
15. Stirring gland

the cathode. Electrical contact was supplied to the anode metal through a tantalum rod protected by an alumina sheath. Agitation of both the electrolyte and molten anode pool was necessary throughout the entire electrorefining process. Stirring prevents the formation of insoluble intermetallic compounds on the anode surface and also prevents polarization and subsequent deposition of alkali metals at the cathode. An alumina or magnesia cell was used to contain the plutonium anode, the electrolyte, and the cathode product. The cell was contained in a stainless-steel can enclosed in a stainless-steel furnace tube provided with cooling coils. The stainless-steel tube was heated in a resistance furnace. The entire assembly was contained in a conventional glove box.

The general procedure for an experimental test consisted of loading the solid plutonium anode and the salt into the electrorefining cell and then heating the mixture to approximately 400°C under vacuum. The system was filled with helium to a pressure of 3 psig, and the cell was heated to 700°C. The stirrer and a tungsten preelectrolysis cathode ($\frac{1}{8}$-in.-diameter rod) were lowered into the molten mixture. The preelectrolysis was conducted for 1 hr at 1 amp. At the conclusion of the preelectrolysis, the current was interrupted, and the tungsten cathode rod was replaced by a cylindrical tungsten cathode. The electrolysis was resumed at a constant current of 20 to 30 amp. Operation at 30 amp corresponded to a production rate of 2.1 kg of metal per day. The cathode and anode current densities at 30 amp were 0.11 amp/cm^2 and 0.90 amp/cm^2, respectively. Product collection efficiencies were consistently greater than 93%.

The purification achieved with the 3.5-kg-scale experiments was excellent and was comparable to that achieved in previous work.[51] In tests using bomb-reduced plutonium metal as the anode, the total detectable metallic impurities were reduced from 1800 to 191 ppm. The principal impurities in the products from most electrorefining runs were elements introduced during the electrorefining process, namely, aluminum, tungsten, and iron. The source of iron is uncertain, but aluminum and tungsten obviously result from attack of the cell and cathode. Substitution of magnesia cells for alumina cells results in the reduction of aluminum contamination and does not introduce magnesium into the product. A single test was

made with a plutonium-iron alloy anode containing 2.54% iron. The iron content of the purified product was reduced to 0.018 wt.%. Therefore plutonium-rich iron alloy scrap can probably be recovered directly by electrorefining.

Several tests were performed in which plutonium trifluoride was substituted for plutonium trichloride in the molten electrolyte. In general, the yields and product purity were comparable to those obtained in the chloride electrolyte. The use of plutonium trifluoride appears very attractive since the fluoride is not hygroscopic and is much more readily available in areas were plutonium metal is produced.

Although the electrorefining process has not been optimized, preliminary estimates indicate that for the recycle of plutonium scrap the electrorefining technique is considerably cheaper than conventional aqueous methods. For a plant having a capacity of 10 kg/week, the unit cost of electrorefining was estimated to be $0.32 per gram of plutonium. Most of this cost was incurred in the recovery of recycled plutonium waste by aqueous methods.

References

1. G. M. Nesmeyanova and G. M. Alkhazashvili, The Effect of Certain Compounds on the Oxidation of Uranium in Acid Media, *Soviet J. At. Energy*, 10(6): 583–586 (March 1962); translated by Consultants Bureau from *At. Energ.*, 10(6): 587–591 (June 1961).
2. E. A. Kanevskii and V. A. Pchelkin, The Reaction Between Solid UO_2 and MnO_2 in a Sulfuric Acid Solution, *Soviet. J. At. Energy*, 10(2): 133–137 (November 1961); translated by Consultants Bureau from *At. Energ.*, 10(2): 138–142 (February 1961).
3. Columbia University, Mineral Beneficiation Laboratory, Recovery of Uranium from Chattanooga Shale, Final Report, USAEC Report RMO-4015, September 1960.
4. G. Jangg, Metallic Nuclear Fuel Obtained with Amalgam Metallurgy, *Atompraxis*, 8(3): 87–92 (March 1962) (in German).
5. *Reactor Fuel Process.*, 5(2): 45 (April 1962).
6. W. Stoll, Industrial and Economic Aspects of Obtaining Uranium with the Amalgam Process, *Atompraxis*, 8(3): 93–94 (March 1962) (in German).
7. I. H. Warren and F. A. Forward, Hydrometallurgical Production of Uranium Dioxide for Reactor Fuel Elements, *Can. Mining Met. Bull.*, 54: 743–749 (October 1961).
8. W. H. Hedley, R. J. Roehrs, and W. T. Trask, Production of Uranium Dioxide by Flame Denitration and Reduction of Uranyl Nitrate, USAEC Report MCW-1470, Mallinckrodt Chemical Works, June 22, 1962.
9. J. B. Ainscough, The Characteristics and Sintering Behaviour of Uranium Dioxide Prepared by a Homogeneous Precipitation Route, *J. Appl. Chem.*, 11(10): 365–369 (October 1961).
10. United States–Euratom Research and Development Program, Wet Preparations of UO_2 Powders, USAEC Report EURAEC-55, Comitato Nazionale per l'Energia Nucleare, Rome, Mar. 31, 1961.
11. K. J. Notz, C. W. Huntington, and W. Burkhardt, Hydrogen Reduction of Uranium Oxides. A Phase Study by Means of a Controlled-Atmosphere Diffractometer Hot Stage, *Ind. Eng. Chem., Process Design Develop.*, 1(3): 213–217 (July 1962).
12. *Reactor Fuel Process.*, 5(2): 63 (April 1962).
13. V. G. Vlasov and V. N. Shalaginov, Reduction of Uranium Trioxide with Carbon Monoxide, *J. Appl. Chem. USSR*, 34(1): 19–24 (January 1961); translated by Consultants Bureau from *Zh. Prikl. Khim.*, 34(1): 20–27 (January 1961).
14. K. Sudo and A. Kigoshi, Fundamental Studies on Uranium Oxides. II. Equilibria Among UO_2, U_4O_9, and U_3O_8, at 500–1200°C, *Sci. Repts. Res. Inst., Tohoku Univ., Ser. A*, 13(6): 448–455 (December 1961).
15. K. Kiukkola, High-Temperature Electrochemical Study of Uranium Oxides in the UO_2-U_3O_8 Region, *Acta Chem. Scand.*, 16(2): 327–345 (1962) (in English).
16. S. H. Smiley, Gas-Solids Reactors in Uranium Processing: A Critical Review, in *Progr. Nucl. Energy, Ser. IV, Technology, Engineering, and Safety*, 4: 191–278, edited by C. M. Nicholls, Pergamon Press, New York, 1961.
17. AEC Releases Details of UF_4 Process, *Chem. Eng. News*, 40(21): 50–51 (May 21, 1962).
18. W. Burkhardt, Improvement of Green Salt Quality, in Summary Technical Report for the Period January 1, 1962–March 31, 1962, USAEC Report NLCO-850, pp. 17–31, National Lead Co. of Ohio, Apr. 16, 1962. (Classified)
19. *Reactor Fuel Process.*, 5(2): 64 (April 1962).
20. R. M. Dell and V. J. Wheeler, Atomic Energy Research Establishment, Harwell, 1961. (Unpublished)
21. F. A. Rough and W. Chubb (Eds.), Progress on the Development of Uranium Carbide Type Fuels, Final Report on the AEC Fuel-Cycle Program, USAEC Report BMI-1554, Battelle Memorial Institute, Nov. 17, 1961.
22. M. Bloomfield, Uranium Carbide: A Bibliography, USAEC Report NAA-SR-Memo-6512, Atomics International, June 13, 1961.
23. United Nuclear Corp., Nuclear Fuel Research Fuel-Cycle Development Program Quarterly Progress Report, October 1–December 31, 1961, USAEC Report UNC-3001, Feb. 1, 1962.

24. W. G. Smiley, Oxidation-Reduction Reprocessing of Uranium Carbide Reactor Fuel. I. Carbothermic Reduction of UO_2, USAEC Report NAA-SR-6976, Atomics International, Mar. 15, 1962.

25. Argonne National Laboratory, Chemical Engineering Division Summary Report, July, August, September 1961, USAEC Report ANL-6413, pp. 64–65, February 1962.

26. Argonne National Laboratory, Chemical Engineering Division Summary Report, October, November, December 1961, USAEC Report ANL-6477, pp. 53–57, March 1962.

27. Argonne National Laboratory, Chemical Engineering Division Summary Report, January, February, March 1962, USAEC Report ANL-6543, June 1962.

28. G. B. Engle, W. V. Goeddel, and C. S. Luby, Reaction-Rate Studies of Thorium-Uranium Dicarbides in Moist Air, *J. Am. Ceram. Soc.*, 45(3): 136–141 (March 1962).

29. J. J. Lawrance and D. J. O'Connor, Hydrolysis of Thorium Carbides, *J. Nucl. Mater.*, 5(1): 156–157 (January 1962).

30. J. H. Oxley, M. F. Browning, N. D. Veigel, and J. M. Blocher, Jr., Microminiaturized Fuel Elements by Vapor-Deposition Techniques, *Ind. Eng. Chem., Prod. Res. Develop.*, 1(2): 102–107 (June 1962).

31. R. W. Dayton and C. R. Tipton, Jr., Progress Relating to Civilian Applications During January 1962, USAEC Report BMI-1565, Battelle Memorial Institute, Feb. 1, 1962. (Classified)

32. R. W. Dayton and R. F. Dickerson, Progress Relating to Civilian Applications During February 1962, USAEC Report BMI-1569, Battelle Memorial Institute, Mar. 1, 1962. (Classified)

33. R. W. Dayton and R. F. Dickerson, Progress Relating to Civilian Applications During March 1962, USAEC Report BMI-1574, Battelle Memorial Institute, Apr. 1, 1962. (Classified)

34. Oak Ridge National Laboratory, Gas-Cooled Reactor Program Quarterly Progress Report for Period Ending December 31, 1961, USAEC Report ORNL-3254, pp. 161–173, Apr. 6, 1962.

35. L. E. Russell, Plutonium Ceramics as Nuclear Fuels, in *Progr. Nucl. Energy, Ser. IV, Technology, Engineering, and Safety*, 4: 147–165, edited by C. M. Nicholls, Pergamon Press, New York, 1961.

36. L. E. Russell, Plutonium Ceramics as Nuclear Fuels, *J. Nucl. Energy, Pt. B, Reactor Technol.*, 2: 147–165 (February 1962).

37. R. C. Lied and G. D. White, Preliminary Studies in the System UC-PuC, *J. Am. Ceram. Soc.*, 45(4): 149–151 (April 1962).

38. W. Sheridan, A. Strasser, J. Anderson, and K. Taylor, Carbide Fuel Development. Phase III Report, September 15, 1960–September 15, 1961, USAEC Report NDA-2162-5, United Nuclear Corp. and The Carborundum Co., Sept. 30, 1961.

39. A. E. Ogard, W. C. Pritchard, R. M. Douglass, and J. A. Leary, The Preparation of Uranium Monocarbide–Plutonium Monocarbide Solid Solutions, Plutonium Sesquicarbide, and Plutonium Monocarbide, *J. Inorg. Nucl. Chem.*, 24: 29–34 (January 1962).

40. R. D. Piper and R. F. Leifield, Electrolytic Production of Uranium Metal from Uranium Oxides, *Ind. Eng. Chem., Process Design Develop.*, 1(3): 208–212 (July 1962).

41. J. Baird and O. J. C. Runnalls, The Preparation of Aluminum-Uranium Alloys by the Aluminum Reduction of Uranium Dioxide, Canadian Report CRRM-1065, December 1961.

42. B. A. Partridge and R. J. Moulton, The Reduction of UCl_3 in LiCl-KCl Eutectic by Mg in Cd, British Report AERE-R-3607, November 1961.

43. K. B. Brown, Chemical Technology Division, Chemical Development Section C, Progress Report for October–November 1960, USAEC Report CF-60-11-126, Oak Ridge National Laboratory, Mar. 3, 1961.

44. K. B. Brown, Chemical Technology Division, Chemical Development Section C, Progress Report for February–March 1961, USAEC Report CF-61-3-141, Oak Ridge National Laboratory, Aug. 15, 1961.

45. K. B. Brown, Chemical Technology Division, Chemical Development Section C, Progress Report for October–December 1961, USAEC Report ORNL-TM-107, Oak Ridge National Laboratory, Feb. 21, 1962.

46. *Reactor Fuel Process.*, 5(1): 70 (January 1962).

47. Argonne National Laboratory, Chemical Engineering Division Summary Report, October, November, December 1961, USAEC Report ANL-6477, pp. 40–43, March 1962.

48. *Reactor Fuel Process.*, 4(4): 77 (October 1961).

49. D. O. Raleigh, Equilibrium Studies in the Reduction of Thorium Oxide by Aluminum, *J. Electrochem. Soc.*, 109(6): 521–525 (June 1962).

50. L. J. Mullins, J. A. Leary, A. N. Morgan, and W. J. Maraman, Plutonium Electrorefining, USAEC Report LA-2666, Los Alamos Scientific Laboratory, Feb. 2, 1962.

51. *Reactor Fuel Process.*, 4(1): 59 (January 1961).

Index

Reactor Fuel Processing

Volume 5

Included in this issue is the index for Volume 5 of *Reactor Fuel Processing*. An index for this quarterly is prepared annually and appears in the final (Number 4) issue. A cumulative index for Volumes 4 to 6 will appear in the October 1963 issue. Here the bold numbers denote issues, and the other numbers denote pages.

A

Acetic acid, diethylene triamine penta-, cerium complexing, **2**: 56
Acetic acid, ethylene diamine tetra-, iron complexing during rare-earth extraction, **2**: 56
Acid Thorex process, **1**: 13
Actinide-element fluorides
  See also the specific actinide-element fluorides, e.g., Thorium fluoride, Uranium fluorides (UF_4), etc.
  review on preparation and properties, **2**: 27
Activation, uranium dioxide, **2**: 64–5
  uranium monocarbide by water vapor, **4**: 49
  uranium oxides before fluorination, **4**: 34
  uranium trioxide, **2**: 64–5; **4**: 76–7
Adakane-12, diluent use in solvent extraction, **4**: 15
  solvent properties, **3**: 12
Adsorption, ground disposal of waste, **2**: 55
  waste-decontamination applications using minerals, **2**: 48–9
  waste-disposal applications, **1**: 57–9; **4**: 56–8
ADU process, **2**: 62
Aging, effects on uranium monocarbide reaction rates, **2**: 36–7
Alloy 79-4, corrosion by fused salts, **4**: 31–2
  oxidation in high-temperature air, **4**: 31
Alloy Reguline Chloride Oxidation process
  See ARCO process
Alumina
  See Aluminum oxide
Aluminum, dissolution by nitric acid–mercuric nitrate solution, **4**: 11
  dissolution by sodium hydroxide, **4**: 7–8
  electrolytic dissolution, **4**: 8–9
  shavings, radioisotope removal from Hanford reactor coolant using, **4**: 56–7
  solubility, **3**: 29
  solubility in liquid bismuth, **1**: 39
  solubility in liquid cadmium, **4**: 41
Aluminum-cadmium system, distribution coefficients of various metals in, **4**: 41–2
Aluminum chloride–cesium chloride systems (liquid), hexachlorouranate-ion stability in, **2**: 37
Aluminum chloride–potassium chloride systems (liquid), hexachlorouranate-ion stability in, **2**: 37
Aluminum fluoride, complexing with uranium fluorides, **3**: 27
Aluminum-nickel alloys, corrosion, **4**: 31–2
Aluminum-nickel-plutonium alloys
  See Plutonium-aluminum-nickel alloys
Aluminum-nickel-plutonium alloys (Zircaloy-4-clad)
  See Plutonium-aluminum-nickel alloys (Zircaloy-4-clad)
Aluminum-nickel-silicon alloys, corrosion, **4**: 31–2
Aluminum-nickel-silicon systems, corrosion, **1**: 45
Aluminum nitrate–nitric acid–sodium fluoride systems
  See Nitric acid–aluminum nitrate–sodium fluoride systems
Aluminum nitrate–nitric acid systems, corrosive effects, **2**: 19
Aluminum nitrate solutions, calcination of wastes containing, **2**: 44; **4**: 58
  conversion to glasses, **4**: 63
  corrosive effects, **3**: 19
  solvent properties, **3**: 8
Aluminum nitrate–uranyl nitrate hexahydrate–nitric acid systems
  See Uranyl nitrate hexahydrate–aluminum nitrate–nitric acid systems
Aluminum oxide, **4**: 23
  coating of uranium dioxide, **2**: 63
  compatibility of Coors AD99 with molten phosphate glass, **2**: 47
  corrosion, **3**: 22
  crucibles for phosphate-glass production from wastes, **2**: 46–7
  fluidized particle bed, **4**: 32
  preparation from aluminum nitrate wastes, **2**: 44
  separation from plutonium, **4**: 33–4
  strontium removal from waste solutions using, **2**: 49–50
  transformation from amorphous to alpha structure, **2**: 46
  uranium monocarbide oxidation in air using, **2**: 36
Aluminum oxide–uranium oxides (UO_2) systems
  See Uranium oxides (UO_2)–aluminum oxide systems
Aluminum-plutonium alloys (aluminum-clad)
  See Plutonium-aluminum alloys (aluminum-clad)
Aluminum shavings
  See Aluminum
Aluminum-silicon alloys, dissolution by hydrochloric acid, **4**: 12
Aluminum-thorium alloys
  See Thorium-aluminum alloys
Aluminum-uranium alloys
  See Uranium-aluminum alloys
Alundum
  See also Aluminum oxide
  fluidized particle bed, **4**: 32
Amalgams
  See Sodium amalgam
Amberlite-200 resin, waste-disposal applications, **3**: 44–5
Amberlite IR-120 resin, radioisotope removal from Purex waste using, **4**: 48, 56
  waste-disposal applications, **3**: 46
Amberlite IRA-401 resin, Tc^{99} extraction using, **2**: 56
Americium, effect on plutonium(IV) solvent extraction, **4**: 15
  separation, **3**: 12–13; **4**: 16
Amines
  See Dipicryl amine, Triisooctyl amine, Tri-*n*-octyl amine, and Trilauryl amine
Amines, tertiary, extraction of transuranium elements using, **4**: 16
Ammonia, removal from Purex wastes by steam stripping, **2**: 48
Ammoniation, uranyl nitrate liquor, effect on later activity of uranium trioxide, **2**: 65
Ammonium bifluoride, leaching of uranium oxides (UO_2)–beryllium oxide systems, **1**: 12–13
Ammonium diuranate, uranium dioxide production using, **2**: 62
Ammonium fluoride, solvent properties, **2**: 7–8
Ammonium fluoride–ammonium nitrate–hydrogen peroxide systems, corrosive effects, **2**: 15–19
  solvent properties, **2**: 8; **3**: 7–8
Ammonium fluoride–ammonium nitrate systems, corrosion of Nionel alloy, **4**: 23
  solvent properties, **3**: 10; **4**: 10–11
Ammonium fluoride–hydrogen peroxide systems, solvent properties, **3**: 7
Ammonium fluoride–mercury nitrate [$Hg(NO_3)_2$]–nitric acid systems, solvent properties, **3**: 7
Ammonium fluoride process, **4**: 10
Ammonium nitrate–ammonium fluoride–hydrogen peroxide systems
  See Ammonium fluoride–ammonium nitrate–hydrogen peroxide systems

Ammonium nitrate–ammonium fluoride systems
See Ammonium fluoride–ammonium nitrate systems
Ammonium nitrate, tetraheptyl-, solvent properties, **3**: 12–13
Ammonium phosphomolybdate, Cs^{137} removal by, **4**: 68
Ammonium plutonyl fluorides, preparation, **4**: 35
Anthraquinone, catalytic reduction of uranyl ion using, **4**: 74
APDA Fast-Breeder Reactor
See Reactors (Enrico Fermi Fast-Breeder)
APM
See Ammonium phosphomolybdate
APPR
See Reactors (SM-1)
Aqua regia, dissolution of uranium dioxide–stainless steel alloys, **4**: 11–12
Aqueous processing, **4**: 7–28
economic evaluations, **4**: 3–4
ARCO process, **3**: 36; **4**: 3
Army Package Power Reactor
See Reactors (SM-1)
Arsenic-76, removal from Hanford reactor coolant by aluminum shavings, **4**: 57
Atmosphere, dispersal of radioactive waste, **2**: 41–2
Autoradiography, uranium distribution studies, **2**: 33

B

Barium, removal, **3**: 28
removal by electrolytic process, **2**: 36
removal by liquid alloy–eutectic system, **2**: 30–1
removal by liquid-metal system, **4**: 45
removal by melt-refining process, **4**: 36
Barium chloride (liquid), graphite-crucible impregnation by, **4**: 48–9
Barium chloride–lithium chloride–magnesium fluoride systems (liquid), solvent properties, **1**: 45
Barium fluozirconate process, economic evaluation, **4**: 3
Barium oxide–beryllium oxide–lanthanum oxide systems, melting point, **1**: 38
Barium oxide–beryllium oxide systems, melting point, **1**: 38
Baskets
See Containers
Belgium, Mol, fractional sublimation studies, **2**: 26
Benzene, diluent use in tributyl phosphate extraction processes, **4**: 15
Benzene, diethyl-, **4**: 16
Berkelium, separation, **3**: 12–13
solvent extraction, **4**: 16
Beryllia
See Beryllium oxide
Beryllium, corrosion, **3**: 33
dissolution by acids, **4**: 8
metallurgy, **3**: 30
recovery, **3**: 23
solubility, **3**: 29
Beryllium fluoride–lithium fluoride–sodium fluoride systems (liquid), corrosive effects with hydrofluoric acid sparge, **4**: 31–2
Beryllium fluoride–lithium fluoride–sodium fluoride–zirconium fluoride systems (liquid), corrosive effects, **4**: 31
Beryllium oxide, coating of uranium dioxide, **2**: 63
compatibility with liquid metal–fused salt process solutions, **2**: 33
compatibility with skull reclamation process solutions, **4**: 46
dissolution in fused-salt volatility process, **2**: 25
Beryllium oxide–barium oxide–lanthanum oxide systems
See Barium oxide–beryllium oxide–lanthanum oxide systems
Beryllium oxide–barium oxide systems
See Barium oxide–beryllium oxide systems
Beryllium oxide–calcium oxide–lanthanum oxide systems, melting point, **1**: 38
Beryllium oxide–calcium oxide–strontium oxide systems, melting point, **1**: 38
Beryllium oxide–calcium oxide systems, melting point, **1**: 38
uranium decontamination, **1**: 38
Beryllium oxide–lanthanum oxide–strontium oxide systems, melting point, **1**: 38
Beryllium oxide–lanthanum oxide systems, melting point, **1**: 38
uranium decontamination, **1**: 38
Beryllium oxide–strontium oxide systems, melting point, **1**: 38
Beryllium oxide–uranium oxides (UO_2) systems
See Uranium oxides (UO_2)–beryllium oxide systems
Bibliographies, liquid metals, **4**: 41
plutonium technology, **4**: 38–9
stress-corrosion cracking of stainless steels, **4**: 25
uranium carbides, **4**: 78
Bio-Rad HZO-1, dibutyl phosphoric acid removal from solvent-extraction aqueous phase using, **4**: 16
Biotites, strontium removal by, **2**: 49
Bismuth (liquid), corrosive effects, **3**: 33
density, **4**: 41
solubility of uranium in, **4**: 39
solvent properties, **1**: 39; **3**: 29
Bismuth-cerium-magnesium-zirconium alloys (liquid), solvent-extraction applications, **1**: 44
Bismuth-copper systems (liquid), density, **4**: 41
Bismuth fluorides, complexing with uranium fluorides, **3**: 27
Bismuth-lead alloys (liquid), corrosive effects, **4**: 46
Bismuth-magnesium-zirconium alloys (liquid), solvent properties, **3**: 31
Bismuth-uranium alloys
See Uranium-bismuth alloys
Bismuth-uranium alloys (liquid)
See Uranium-bismuth alloys (liquid)
Bismuth-uranium-zirconium alloys
See Uranium-bismuth-zirconium alloys
Boiling Nuclear Superheater Reactor
See Reactors (BONUS)
Boiling point, platinum hexafluoride, **2**: 27
review of liquid metals, **2**: 30
BONUS Reactor
See Reactors (BONUS)
Borates, flux use in waste calcination, **2**: 43
Boron nitride, corrosion by liquid magnesium-zinc systems, **2**: 33
Breeding blankets, recovery, **3**: 33
Breeding blankets (uranium-molybdenum alloy), dissolution, **1**: 9–10
Bromine fluorides (BrF), heat of formation, **4**: 35
Bromine fluorides (BrF_3), heat of formation, **4**: 35
reaction with nitrosylium hexafluorouranate, **3**: 22; **4**: 30–1
Bromine fluorides (BrF_5), flow-rate instrumentation, **4**: 18–19
heat of formation, **4**: 35
preparation, **2**: 27
reaction with nitrosylium hexafluorouranate, **3**: 22
di-*sec*-Butylphenyl phosphonate, compared with TBP as solvent for uranium-thorium separation, **4**: 14

C

Cadmium, solubility, **3**: 31
solubility in liquid aluminum, **4**: 41
Cadmium (liquid), distillation, **1**: 44
solvent properties, **1**: 39; **3**: 29
uranium-silicon reactions in, **2**: 66
Cadmium-cerium intermetallic compounds, phase studies, **4**: 40
Cadmium-lanthanum alloys, phase diagrams, **3**: 29
Cadmium-magnesium-zinc systems (liquid), corrosive effects on 405 stainless steel, **2**: 33
Cadmium-praseodymium intermetallic compounds, **4**: 40
phase studies, **2**: 29–30
Cadmium-uranium alloys
See Uranium-cadmium alloys
Cadmium-uranium intermetallic compounds
See Uranium-cadmium intermetallic compounds
Cadmium-uranium systems (liquid)
See Uranium-cadmium systems (liquid)
Calcination, aqueous wastes in molten sulfur, **4**: 58
batch processes, **2**: 42–4; **4**: 58–9
costs, **2**: 42
Demonstrational Waste Calcining Facility, **2**: 44–6; **4**: 59–62
fluid-bed process, **2**: 44–6; **4**: 59
foaming problems, **2**: 43
preconcentration, **2**: 44
spray processes, **2**: 44
stainless-steel corrosion problems, **2**: 43
thorium oxide–uranium oxide particle production, **2**: 69
waste processing, **1**: 52–7; **3**: 48–54
waste-solution corrosion studies, **4**: 25–8
zirconium fuel wastes, **2**: 46
Calcite, radioisotope removal, **4**: 57
Calcite–Florida bed phosphate–pyrite mixtures, P^{32} removal from waste by, **4**: 57
Calcite–Idaho bed phosphate–pyrite mixtures, P^{32} removal from waste by, **4**: 57
Calcium alloys (liquid), corrosive effects, **1**: 43
Calcium carbonate, strontium removal by, phosphate-ion effects, **2**: 50
Calcium-lanthanum intermetallic compounds, phase studies, **2**: 30
Calcium oxide–beryllium oxide–lanthanum oxide systems
See Beryllium oxide–calcium oxide–lanthanum oxide systems
Calcium oxide–beryllium oxide–strontium oxide systems
See Beryllium oxide–calcium oxide–strontium oxide systems
Calcium oxide–beryllium oxide systems
See Beryllium oxide–calcium oxide systems
Calcium-zinc alloys (liquid), extraction of plutonium, **1**: 42
Californium, separation, **3**: 12–13
solvent extraction, **4**: 16
CANDU Reactor
See Reactors (CANDU)
Canisters
See Containers
Carbide fuel processing, **2**: 35–7; **4**: 49–50
Carbide-oxide-carbide process, **2**: 35–6; **4**: 49
Carbon
See also Graphite
coating of uranium carbides with, **4**: 81
reaction with uranium dioxide to produce uranium monocarbide, **2**: 65–6
reaction with uranium in liquid-metal systems, **2**: 66
reaction with uranium nitrides, **1**: 46

Carbon oxides (CO), reduction processes using, 4: 75
Carbon oxides (CO_2), reaction with uranium monocarbide, 2: 37
Carbon tetrachloride, diluent use in tributyl phosphate extraction processes, 4: 15
Carbon tetrachloride–chlorine–methane systems, uranium ore chlorination, 2: 61
Carbon tetrachloride–methane systems, niobium oxide chlorination, 4: 33
uranium chlorination, 4: 33
zirconium oxide chlorination, 4: 33
Carbon tetrachloride–nitrogen systems
See also Uranium–carbon systems
corrosive effects, 2: 17
Carbothermic reduction, uranium monocarbide production from uranium dioxide, 4: 78–9
Carolinas-Virginia Reactor
See Reactors (Carolinas-Virginia)
Carpenter-20 alloy, corrosion, 4: 23
evaporation vessel use, 2: 47
Carpenter-20Cb alloy, corrosion by hydrofluoric acid–hydrogen peroxide systems, 4: 24
Casks
See Containers
Catalytic reduction process
See Reduction processes
Cathodic reduction
See Reduction processes
Centrifugation, fuel solutions prior to solvent extraction, 4: 12
suspended waste removal, 4: 57–8
Ceramic sponges, waste fixation in, 4: 63–4
Cerium, extraction by liquid alloy–eutectic system, 2: 30–1
extraction by liquid aluminum-cadmium system, 4: 41–2
extraction by liquid lead-zinc system, 1: 40; 2: 30–1
extraction by liquid metal–fused salt systems, 2: 32; 4: 43
extraction by liquid-metal system, 4: 45
extraction from Purex wastes, 2: 56
removal, 1: 41; 2: 22; 3: 28
removal by electrolytic process, 2: 36
removal by melt-refining process, 4: 36
removal from Purex wastes, 2: 48, 56
removal from wastes, 1: 57–8; 62–3
solubility, 3: 30–1
Cerium (liquid), density, 1: 41; 3: 30
Cerium-144, activity/particle-size relations for separated waste, 4: 58
separation from wastes, 3: 58
shipping, 4: 69
Cerium-bismuth-magnesium-zirconium alloys
See Bismuth-cerium-magnesium-zirconium alloys
Cerium-cadmium intermetallic compounds
See Cadmium-cerium intermetallic compounds
Cerium carbides (Ce_2C_3), preparation, 1: 47
Cerium-cobalt-plutonium alloys
See Plutonium-cerium-cobalt alloys
Cerium ions, complex formation in fused-salt systems, 4: 47
Cerium-lanthanum intermetallic compounds, phase studies, 2: 30
Cerium oxides, strontium removal from waste solutions, 2: 49
Cesium, adsorption on clinoptilolite, 2: 48
adsorption on phenolic resin, 2: 48
incorporation into glass as heat or radiation source, 2: 47–8
precipitation from Purex supernatant with ferrocyanide, 2: 58
release during oxidation of uranium dioxide, 4: 34–5
removal, 2: 22; 3: 28, 45
removal in dissolver filtrate, 1: 11
removal in uranium dioxide oxidation-reduction process, 4: 49
removal by vermiculite columns, 2: 50
removal from wastes, 1: 51, 57–8, 62–4; 2: 48, 56–7; 4: 56
separation from wastes, 3: 57–8
shipping, 2: 57–8
sorption by natural organic materials, 2: 51
volatility, 3: 52
volatilization in melt-refining process, 4: 36
Cesium-137, activity/particle-size relations for separated waste, 4: 58
incorporation into glasses as radioactive sources, 4: 69
recovery from Purex waste, 4: 68
separation from wastes, 3: 57–8
shipping containers, 4: 69
Cesium chloride (liquid), hexachlorouranate-ion stability in, 2: 37
Cesium chloride–aluminum chloride systems (liquid)
See Aluminum chloride–cesium chloride systems (liquid)
Cesium chloride–plutonium chloride ($PuCl_3$) systems
See Plutonium chloride ($PuCl_3$)–cesium chloride systems
Cesium plutonyl fluorides, preparation, 4: 35
CETR
See Reactors (Indian Point Power)
Chloride ion, effect on 304L stainless-steel corrosion in Darex dissolver solutions, 4: 20
Chlorides, removal, 2: 9–10
Chloride-volatility processes, 2: 25–6
construction materials, 4: 21
Chlorination processes, 4: 33
monazite, 2: 68
stainless steels, 1: 35–7
uranium ores, 2: 61
Chlorine, corrosive effects, 1: 36; 2: 17
solubility in molten chloride systems, 2: 34
Chlorine–carbon tetrachloride–methane systems
See Carbon tetrachloride–chlorine–methane systems
Chloroethylene, tetra-
See Ethylene, tetrachloro-
Chlorouranate ions
See Hexachlorouranate ion
Chromalizing process, 4: 31
Chromium, coatings of, for oxidation protection, 4: 31
corrosion inhibition, 3: 18
corrosive effects of dissolving, 2: 18–19
separation from uranium in skull reclamation process, 4: 43
solubility in liquid-metal systems, 4: 42
Chromium-51, removal from Hanford reactor coolant by aluminum shavings, 4: 57
Chromium-cobalt-iron-nickel alloys, corrosion, 1: 43
Chromium-cobalt-nickel-tungsten alloys
See Haynes 25 alloy
Chromium ions, effect on corrosion of stainless steels by nitric acid, 4: 21–2
Chromium-iron-manganese-molybdenum-nickel-silicon alloys
See Hastelloy B alloy
Chromium-iron-manganese-nickel alloys
See Inconel alloy
Chromium-iron-molybdenum-nickel alloys
See INOR-8 alloy
Chromium-nickel alloys
See also Corronel 230 alloy
corrosion, 1: 43
Chromium-uranium alloy
See Uranium-chromium alloy
Cladding (fuel-element), effect of type on reprocessing costs, 4: 2
electrolytic dissolution, 4: 2
Cladding removal
See Decladding
Clinoptilolite, Cs^{137} removal by, 4: 68
heat-treatment effects on selectivity for cesium adsorption, 2: 48
strontium removal by, phosphate-ion effects, 2: 49–50
waste-disposal applications, 1: 57–9; 3: 46
Coatings
See also the specific coating materials
carbon, for uranium carbides, 4: 81
chromalizing process, 4: 31
techniques for production on uranium dioxide, 2: 63
Cobalt, solubility, 3: 29
solubility in liquid bismuth, 1: 39
sorption by natural organic materials, 2: 51
Cobalt-60, activity/particle-size relations for separated waste, 4: 58
Cobalt alloys
See also Haynes 21 alloy
corrosion, 1: 43
Cobalt-cerium-plutonium alloys
See Plutonium-cerium-cobalt alloys
Cobalt-chromium-iron-nickel alloys
See Chromium-cobalt-iron-nickel alloys
Cobalt-chromium-nickel-tungsten alloys
See Haynes 25 alloy
Columbium
See Niobium
Columns (pulse)
See Pulse columns
Commercial aspects
See Economic aspects
Conasauga shale, selective sorption of strontium by, 4: 65–6
Consolidated Edison Thorium Reactor
See Reactors (Indian Point Power)
Constitutional diagrams
See Phase studies
Construction materials, compatibility with liquid metal–fused salt process solutions, 2: 32–3
corrosion problems, 4: 20–5
Consumers Public Power District Reactor
See Reactors (Hallam Power)
Containers, baskets in electrolytic dissolution process, 4: 8–9
HAPO casks, 4: 69
shipping, design for radioisotopes, 2: 57–8; 4: 69
heat-transfer calculations, 4: 66
for spent fuel elements, 1: 2; 3: 2
tanks, 2: 40–1; 4: 52–5
waste, 2: 40–1, 54–5; 4: 52–5
Contamination, environmental, by radioactive waste, 2: 41–2
Coors AD99, compatibility with molten phosphate glass, 2: 47
Copper, corrosion, 2: 23
Copper-64, removal from Hanford reactor coolant by aluminum shavings, 4: 57
Copper-bismuth systems (liquid)
See Bismuth-copper systems (liquid)
Copper-iron-manganese-nickel alloys
See Monel alloy
Corronel 230 alloy, corrosion, 4: 24
Corrosion, 2: 15–19
See also the specific materials being corroded and the specific corrodents
construction materials, 4: 20–5
crucibles by molten phosphate glasses, 4: 63
ICPP process problems, 3: 15–17
inhibition by zirconium in liquid-metal systems, 4: 46
literature survey on stainless-steel stress-corrosion cracking, 4: 25
stainless steel during calcination processes, 2: 43

Corrosion (Continued)
stainless steel by liquid bismuth–lead systems, 4: 46
stainless steel by nitric acid, chromium-ion effects, 4: 21–2
waste processing, 4: 25–8
waste-storage tanks, 4: 52–5
Costs
See Economic aspects
Criticality hazards, control during dissolution by neutron poisons, 4: 3
control in enriched-fuel processing, 4: 1
control in storage containers, 2: 15
uranium dioxide production, 2: 62
Crucibles, beryllia, compatibility with skull reclamation process solutions, 4: 46
compatibility with liquid metal–fused salt process solutions, 2: 33
corrosion by molten phosphate glasses, 4: 63
impregnation to prevent fused-salt permeation, 4: 48–9
for phosphate-glass production from waste, 2: 46–7
tungsten, compatibility with liquid uranium-magnesium-zinc solutions, 4: 45–6
Cryolite, aluminum reduction of uranium dioxide using, 4: 83
Crystal properties, plutonium dioxide, 4: 47–8
thorium dioxide, 4: 47–8
thorium-lead intermetallic compounds, 2: 30
uranium dioxide, 4: 47–8
uranium-lead intermetallic compounds, 2: 30
Curium, separation, 3: 12–13; 4: 16
Cutters (tube), 2: 5, 6

D

D2EHPA
See Phosphoric acid, di-2-ethylhexyl-
Darex process, 4: 1–2
chemical decladding of fuel elements, 1: 8
corrosion of construction materials, 4: 20–1
corrosion problems, 1: 26; 2: 18
waste disposal, 1: 52–7; 3: 51
Darex-Purex raffinate, corrosion of stainless steels, 4: 20–1
Darex wastes, calcination process, 2: 43; 4: 58–9
Darex-Zirflex process, corrosion problems, 2: 18
Davison Chemical Co., agreement with AEC, 3: 1
Decalso, Cs^{137} removal by, 4: 68
radioisotope shipping uses, 2: 57–8; 4: 69
Decladding, aluminum dissolution by sodium hydroxide, 4: 7–8
ammonium fluoride process, 4: 10
beryllium dissolution by acids: 4: 8
chemical means, 1: 8; 2: 35; 3: 5–6; 4: 7–10, 23
electrolytic-dissolution process, 2: 36
mechanical means, 1: 7–8; 2: 5–7; 3: 5; 4: 7
oxidative method, 2: 35
uranium carbide fuel by steam, 4: 49
Decomposition
See Thermal decomposition
Decontamination, hot cells, 1: 24–5
Decontamination factors, effects of solvent quality, 4: 15
fission products in electrolytic process, 2: 36
Demonstrational Waste Calcining Facility, 2: 44–6; 4: 59–62
Densimeters, 1: 17–18; 4: 49
Density, bismuth liquid systems, 4: 41
lanthanum liquid, 2: 30
measurement in fused-salt systems, 4: 49
Depleted uranium, base charges for, as uranium hexafluoride, 4: 4
Detroit Edison Reactor
See Reactors (Enrico Fermi Fast-Breeder)
Dibutylbutyl phosphonate, uranium extraction from nitrate eluates, 2: 61
Dibutyl phosphoric acid
See Phosphoric acid, dibutyl-
Diethyl benzene
See Benzene, diethyl-
Diethylene triamine pentaacetic acid
See Acetic acid, diethylene triamine penta-
Difluorotetrachloroethane
See Ethane, difluorotetrachloro-
Diluents
See also the specific diluent compounds
evaluation of, for solvent-extraction processes, 4: 14–15
Dipicryl amine, cesium removal by, 4: 68
Dipicryl amine–nitrobenzene systems, cesium removal by, 4: 68–9
Direct fluorination processes, 2: 26–7; 3: 25–7; 4: 33–5
Dissolution, 2: 7–11, 22
See also as subheading under specific materials
cladding materials, 4: 8–10
dissolver vessel corrosion, 3: 17
electrolytic, 2: 8–11; 3: 8–9; 4: 2, 8–9, 21–3
corrosion problems, 2: 18
fuel cores, 4: 10–12
Nitrofluor process, 4: 30–1
stainless-steel-matrix fuels, 4: 20–1
temperature effects on rate, 4: 10–11
Distribution coefficients, metals in liquid metal–fused salt systems, 2: 32; 4: 41, 43
metals in liquid-metal systems, 2: 30–1; 4: 41–2
Dodecanes, diluent use in solvent extraction, 4: 15
solvent properties, 3: 12
Dowex 1 resin, neptunium adsorption, 1: 17
plutonium adsorption, 3: 69
Dowex 1-X10 resin, fission-product removal, 2: 56
Dowex 50W resin, plutonium adsorption, 3: 64–5
waste-disposal applications, 3: 58
Dowex 50W-X8 resin, Np^{237} adsorption, 2: 55–6
Dowex 50W-X12 resin, strontium adsorption, 2: 49
DPA
See Dipicryl amine
Dresden Power Reactor
See Reactors (Dresden Power)
Drums, waste, evaluation for ocean disposal, 2: 54–5
Dry halogenation processes, 2: 25–6; 3: 24–5; 4: 32–3
Drying
See Spray drying
DTPA
See Acetic acid, diethylene triamine penta-
Duolite C-3 resin, cesium recovery using, 2: 56–7
Cs^{137} removal by, 4: 68
strontium removal by, 2: 49
waste-disposal applications, 3: 45–6
Duolite CS-100 resin, waste-disposal applications, 3: 44
Dysprosium, removal, 3: 28
solubility, 3: 31

E

EBR
See Reactors (Experimental Breeder)
EBR-II fuel pins
See Fuel elements (pins) and *see also* Uranium-fissium alloys
Economic aspects, 1: 1–6; 2: 1–4; 3: 1–3; 4: 1–6
aqueous processes, 4: 3–4
duplicating processing equipment, 4: 19
fuel cycles, 4: 4–6
fuel shipping, 4: 6
fuel storage, 4: 6
granitic rock leaching for uranium and thorium recovery, 4: 83–4
nonaqueous processes, 4: 3
plutonium electrorefining, 4: 86
pot calcination of wastes, 2: 42
uranium price reduction effects on reactor fuel-cycle costs, 4: 5
waste storage, 4: 55
EDTA
See Acetic acid, ethylene diamine tetra-
Einsteinium, separation, 3: 12–13
solvent extraction, 4: 16
Electrical heating
See Heating
Electrodes, consumable uranium dioxide–carbon systems, 4: 82
plutonium, use in plutonium electrorefining, 4: 84–5
uranium dioxide–carbon consumable anode, 2: 66
Electrolytic dissolution
See Dissolution
Electrolytic processes, 3: 8–9, 35–6
fission-product removal, 2: 36
plutonium refining, 4: 84–6
reduction, 2: 67–8; 4: 46–8, 67–8, 82
salt-cycle process, 2: 34–5
uranium carbide reduction, 4: 49
uranium carbide reduction in fused salts, 2: 36
uranium dioxide–plutonium dioxide systems, 4: 46–7
uranium dioxide production, 3: 62
uranium dioxide reduction, 2: 66; 4: 82
uranium purification in aqueous solutions, 2: 13
uranium tritaoctoxide reduction, 4: 48
uranyl chloride reduction in fused salts, 2: 34–5
waste-disposal applications, 3: 46
Electrorefining, 2: 13; 3: 32–3
Enriched fuels, processing costs, 4: 1–2
Enriched uranium, base charges for, as uranium hexafluoride, 4: 4
price reduction effects on reactor fuel-cycle cost, 4: 5
Enrico Fermi Fast-Breeder Reactor
See Reactors (Enrico Fermi Fast-Breeder)
Entropy, iodine pentafluoride, 4: 35
EOCR
See Reactors (Experimental Organic-Cooled) (EOCR)
Epidote, radioisotope adsorption, 4: 57
Erbium, removal, 3: 28
solubility, 3: 31
Erosion, nozzles in fluid-bed calcination process, 2: 44
Ethane, difluorotetrachloro-, diluent use in tributyl phosphate extraction processes, 4: 15
Ethylene diamine tetraacetic acid
See Acetic acid, ethylene diamine tetra-
Ethylene polymers, 4: 23
Ethylene, tetrachloro-, solvent properties, 3: 11

2-Ethylhexylphenyl phosphoric acid
See Phosphoric acid, 2-ethylhexylphenyl-
EUREX Plant, **3**: 2
Eurochemic plant, **3**: 2
Europium, removal, **3**: 28
solubility, **3**: 31
Europium compounds, reduction, **3**: 32
Evaporation, liquid wastes, **3**: 47–8
Evaporators, corrosion, **4**: 24–5
Experimental Breeder Reactor
See Reactors (Experimental Breeder)
Experimental Organic-Cooled Reactor
See Reactors (Experimental Organic-Cooled) (EOCR)

F

Fermi Fast-Breeder Reactor
See Reactors (Enrico Fermi Fast-Breeder)
Fermium, separation, **3**: 12–13
solvent extraction, **4**: 16
Fernald Plant, waste disposal, **3**: 43
Fiberglas, **4**: 23
Final disposal
See Waste processing and disposal
Fission products, activity/particle-size relations for separated waste, **4**: 58
fixation in ceramic sponges, **4**: 63–4
ion exchange, **1**: 16–17
recovery from Purex wastes, **2**: 56
recovery from wastes, **4**: 67–8
release during melt refining of uranium-fissium alloys, **2**: 28; **4**: 36–8
release during oxidation of uranium dioxide, **4**: 34–5
removal, **3**: 28
removal in acid Thorex process, **1**: 13
removal by Dowex 1-X10 resin, **2**: 56
removal by electrolytic process, **2**: 36
removal by liquid-metal processes, **4**: 41
removal in melt-refining process, **2**: 29
removal from plutonium, **4**: 33–4
removal in salt-cycle process, **2**: 35
removal from uranium-bismuth liquid alloys, **4**: 45
removal from uranium by chlorination, **4**: 33
removal during oxidation-reduction process for uranium dioxide, **4**: 49
shipping-container design, **2**: 57–8
volatilization in melt-refining process, **2**: 28; **4**: 36–8
Fissium alloys
See Uranium-fissium alloys
Fixation, waste in ceramic sponges, **4**: 63–4
Flame denitration process, pilot plant, **2**: 44–5
uranium dioxide production, **4**: 74–5
Florida bed phosphate–calcite–pyrite mixtures
See Calcite–Florida bed phosphate–pyrite mixtures
Flow rate, effect on 304L stainless-steel corrosion in Darex dissolver solutions, **4**: 20
instrumentation, **4**: 17–19
Flow sheets, actinide-lanthanide separation, **3**: 13
EBR-II blanket processing, **4**: 44
Enrico Fermi Fast-Breeder Reactor blanket dissolution, **1**: 9
flame denitration pilot plant, **2**: 45
fused-salt volatility processes, **1**: 31
Hallam Power Reactor fuel-element dissolution, **1**: 10
isotope separation from wastes, **1**: 61–4
liquid-metal extraction processes, **3**: 32
Molten-Salt Reactor fuel processing, **3**: 24
neptunium recovery in Redox process, **4**: 14
pot calcination, **3**: 54
Purex phosphate-glass pilot plant, **2**: 47
Purex process, **1**: 14
Purex process waste backcycle, **4**: 14
reclamation process for melt-refining skulls, **4**: 44
Redox process waste backcycle, **4**: 13
sodium formate precipitation of sodium fluozirconate, **4**: 16–17
strontium recovery from Purex 1WW, **4**: 67–9
transuranium-element separation, **4**: 16
TRIGA Reactor fuel processing, **3**: 8
uranium dioxide production, **1**: 68
uranium-molybdenum alloy dissolution, **3**: 6–7
uranium trioxide activation process, **4**: 76–7
uranium-zirconium alloy dissolution, **2**: 8
waste disposal, **1**: 52
Fluid beds, calcination, **2**: 44–6; **4**: 59–62
uranium tetrafluoride production in, **4**: 76, 77
Fluidized beds, alumina, in fluorination processes, **4**: 34
heat removal, use in Zircex process, **2**: 25–6
heat transfer, **4**: 33
hydrochlorination in, **4**: 32
Fluoboric acid–hydrofluoric acid systems, leaching of uranium dioxide–beryllium oxide systems, **1**: 13
solvent properties, **3**: 10
Fluoboric acid–nitric acid systems, corrosive effects, **3**: 18
Fluophosphoric acid, mono-, dissolution of uranium dioxide–thorium oxide systems, **1**: 29–30
Fluoride compounds
See also specific fluoride compounds
preparation, **2**: 27
properties, **4**: 35
removal, **2**: 8
Fluoride-volatility processes
See Fused-salt volatility processes
Fluorination processes
See Direct fluorination processes
Fluorine, corrosive effects, **3**: 27
flow-rate instrumentation, **4**: 18–19
reaction with uranium dioxide, **1**: 37; **3**: 26
Fluorite, radioisotope adsorption, **4**: 57
Fluorocarbon plastics, corrosion, **2**: 19
Fluxes, use in waste calcination, **2**: 43
Foam separations, liquid-waste processing, **3**: 43–4
Foaming, effects on calcination processes, **2**: 43
Food chains, contamination by radioactive waste, **2**: 41
Fractional crystallization processes, **4**: 45
technetium hexafluoride purification by, **2**: 27
Fractional sublimation processes, **2**: 26; **4**: 32–3
Free energy, bromine fluorides, **4**: 35
iodine pentafluoride, **4**: 35
Fuel cycles, **2**: 1–2; **3**: 2–3
BONUS Reactor estimated costs, **4**: 5
Carolinas-Virginia Reactor estimated costs, **4**: 5
costs, **1**: 2–5; **2**: 2–3
Dresden Reactor estimated costs, **4**: 5
economics, **4**: 4–6
Hallam Power Reactor estimated costs, **4**: 5
Indian Point Reactor estimated costs, **4**: 5
Peach Bottom Reactor estimated costs, **4**: 5
Piqua Reactor estimated costs, **4**: 5
uranium price reduction effects on costs, **4**: 5
Yankee Power Reactor, **4**: 5
Fuel elements
See also the specific fuel-element materials, e.g., Uranium carbides, Uranium oxides, Uranium oxides (UO_2)–thorium oxide systems, etc.
irradiated, **1**: 1–2
mechanical decladding, **2**: 5–7
Fuel elements (ceramic), fluorination, **1**: 37
Fuel elements (Hastelloy-X-clad), dissolution, **3**: 10
Fuel elements (impregnated graphite), disintegration, **3**: 9–10
dissolution, **2**: 10–11
leaching, **1**: 12
Fuel elements (Nichrome-clad), chemical decladding, **1**: 27
electrolytic dissolution, **3**: 9
Fuel elements (pellets), chemical decladding, **3**: 5
processing, **3**: 25–6
Fuel elements (pins), melt-refining process, **4**: 36–8
nitridation, **4**: 36
processing, **3**: 27–9
Fuel elements (stainless-steel-clad), processing, **3**: 25–6, 27–9, 36–7
Fuel elements (uranium), cutting, **2**: 5
dissolution, **1**: 8–9, 29–30; **2**: 7
Fuel elements (uranium carbides), leaching, **1**: 12
processing, **1**: 46
Fuel elements [uranium carbides (UC)], processing, **3**: 34–7
Fuel elements (uranium-molybdenum alloy), dissolution, **1**: 9–10; **2**: 7
Fuel elements [uranium oxides (UO_2)], fluorination, **1**: 37
processing, **2**: 34; **3**: 25–6, 34–7; **4**: 46–9
Fuel elements [uranium oxides (UO_2)(stainless-steel-clad)], chemical decladding, **1**: 35–6
Fuel elements [uranium oxides (UO_2)–Nichrome systems (Nichrome-V-clad)], dissolution, **2**: 8–10
Fuel elements [uranium oxides (UO_2)–stainless steel systems], dissolution, **1**: 11–12
Fuel elements [uranium oxides (UO_2)–thorium oxide systems], chemical decladding, **1**: 8
dissolution, **1**: 29–30
Fuel elements (uranium-zirconium alloy), cutting, **2**: 5
dissolution, **1**: 30–5
Fuel elements (uranium-zirconium alloy) (Zircaloy-clad), dissolution, **2**: 7–8
Fuel elements (Zircaloy-clad), processing, **3**: 25–6
Fuel elements (zirconium-clad), dissolution, **3**: 23
processing, **3**: 36
Fuel pins
See Fuel elements (pins) and *see also* Uranium-fissium alloys
Fuel solutions
See also specific solutions by name of constituents
treatment at AEC facilities before solvent extraction, **4**: 12
Fuels
See also the specific fuel materials by name
enriched, processing costs, **4**: 1–2
shipping economics, **4**: 6
storage economics, **4**: 6
Fused-salt extraction processes
See Liquid metal–fused salt extraction processes
Fused salt–hydrofluoric acid systems
See Hydrofluoric acid–fused salt systems

Fused-salt volatility processes, 1: 30–5; 2: 23–5; 3: 22–4; 4: 3
alloy corrosion studies, 4: 31–2
corrosion problems, 1: 29–30
Fused salts
See also specific fused-salt systems by name of constituent salts
a-c resistance heating, 4: 49
atomization, 3: 23
electrolysis in, 4: 46–9
electrolytic production of uranium in, 4: 83
electrolytic use in plutonium electrorefining process, 4: 84–6
electrolytic use in uranium metal production, 2: 66–8
flux use in thorium dioxide reduction process, 4: 84
frozen-wall containment, 1: 34–5
Fusion point
See Melting point

G

G-7 laminate, 4: 23
Gadolinium, removal, 3: 28
solubility, 3: 31
Gallium (liquid), solubility of uranium in, 4: 39
Gamma-ray emitters, activity/particle-size relations for separated waste, 4: 58
release during oxidation of uranium dioxide, 4: 34
Gas-Cooled Reactor Experiment
See Reactors (Gas-Cooled, Experiment)(GCRE)
GCRE
See Reactors (Gas-Cooled, Experiment)(GCRE)
General Electric Test Reactor
See Reactors (General Electric Test)(GETR)
GETR
See Reactors (General Electric Test)(GETR)
Glasses, compatibility with crucible materials, 2: 47
conversion of wastes to, 2: 46–8
corrosive effects, 4: 63
Cs^{137}-containing, use as radioactive sources, 4: 69
radioisotope incorporation for heat and radiation sources, 2: 47–8
waste conversion to, 4: 62–3
Goethite, radioisotope adsorption, 4: 57
Gold, corrosion, 2: 23
Gold-platinum alloys, compatibility with molten phosphate glass, 2: 47
Grace (W. R.) and Co., 4: 1–2
Granite, leaching for uranium and thorium recovery, 4: 83–4
Graphite
See also Carbon
electrolytic dissolution, 4: 8–9
hydrofluorinator use, 2: 24–5
impregnation to prevent fused-salt permeation, 4: 48–9
reaction with uranium dioxide, 1: 46
Graphite (impregnated), disintegration, 3: 9–10
leaching, 1: 12
Graphite (tungsten-coated), thermal cycling, 2: 33
Ground disposal
See Waste processing and disposal

H

Hafnium, solubility in liquid bismuth, 1: 39
Hafnium alloys, corrosion by plutonium alloys, 2: 33
Hallam Power Reactor
See Reactors (Hallam Power)
HAPO casks, 4: 69
Hastelloy alloy, evaluation as crucible material, 4: 63
Hastelloy B alloy, corrosion, 2: 23, 24
Hastelloy C alloy, corrosion, 1: 36; 3: 19
Hastelloy F alloy, corrosion, 1: 26, 44; 3: 15–17; 4: 23, 27–8
corrosion in Zirflex process, 1: 25–6
Hastelloy X alloy, dissolution, 3: 10
Haynes 6B alloy, corrosion, 2: 16
Haynes 21 alloy, corrosion, 2: 15–16, 18; 3: 19
corrosion by Darex dissolver solutions, 4: 21
Haynes 25 alloy, corrosion, 1: 43–4; 2: 17, 18; 3: 19
corrosion by Darex dissolver solutions, 4: 21
Haynes EB4358 alloy, corrosion, 1: 26
Haynes EB5459 alloy, corrosion, 1: 26
Haynes Multimet alloy, corrosion, 1: 43–4
Hazards
See Criticality hazards
Head-end treatments, 1: 8–13; 3: 6–10
fission-product removal from fuel solutions, 4: 12
Heat capacity, iodine pentafluoride, 4: 35
Heat exchangers, corrosion, 3: 17; 4: 24–5
Heat of formation, bromine fluorides, 4: 35
Heat sources, radioisotope-containing glasses, 2: 47–8
Heat transfer, calculations, for high-level wastes, 4: 66–7
for Purex-waste shipping containers, 4: 66
for radioisotope shipping containers, 2: 57–8
direct fluorination processes, 3: 25
titanium corrosion effects, 4: 20
Heat-Transfer Reactor Experiments
See Reactors (Heat-Transfer, Experiments)(HTRE)
Heat-treatment, effect on cesium-adsorption selectivity of clinoptilolite, 2: 48
effect on corrosion of Haynes 21 alloy, 4: 21
effect on corrosion of Haynes 25 alloy, 4: 21
Heating, a-c resistance, for fused salts, 4: 49
ohmic, for liquid metals, 2: 30
Hexachlorouranate ion, stability in fused-salt solvents, 2: 37
Hexane–tributyl phosphate solutions, uranium extraction, sulfate-ion effects, 2: 61–2
HFIR
See Reactors (High-Flux Isotope)(HFIR)
High-Flux Isotope Reactor
See Reactors (High-Flux Isotope)(HFIR)
HNPF
See Reactors (Hallam Power)
Holmium, removal, 3: 28
solubility, 3: 31
Hot cells, decontamination, 1: 24–5
HTRE
See Reactors (Heat-Transfer, Experiments)(HTRE)
Huey test, 3: 19
Hydridation, tantalum, 4: 20
Hydrochloric acid, beryllium dissolution, 4: 8
corrosive effects, 3: 19
dissolution of aluminum-clad oxide target elements, 4: 12
dissolution of aluminum-silicon alloys, 4: 12
reaction with uranium-zirconium alloys, 4: 32
solvent properties, 3: 6, 9
Hydrochloric acid–nitric acid systems, corrosion of construction materials, 4: 21
corrosive effects, 2: 18
dissolution of stainless-steel-matrix fuels, 4: 20
dissolution of uranium dioxide–stainless steel fuels, 4: 11–12
leaching of uranium dioxide–beryllium oxide systems, 1: 12–13
solvent properties, 2: 9–10; 3: 9–10
stainless-steel dissolution, 1: 8
Hydrofluoric acid, beryllium dissolution, 4: 8
flow-rate instrumentation, 4: 18–19
fuel-element dissolution, 1: 10–11
reaction with uranium hexachloride, 4: 33
scandium recovery by, 2: 62
solvent properties, 2: 7–8; 3: 8
Hydrofluoric acid–fluoboric acid systems
See Fluoboric acid–hydrofluoric acid systems
Hydrofluoric acid–fused salt systems, corrosive effects, 4: 31–2
Hydrofluoric acid–hydrogen peroxide systems, corrosive properties, 4: 23–4
solvent properties, 3: 6
Hydrofluoric acid–nitric acid–mercury nitrate [$Hg(NO_3)_2$] systems
See Nitric acid–mercury nitrate [$Hg(NO_3)_2$]–hydrofluoric acid systems
Hydrofluoric acid–nitric acid systems, corrosive effects, 2: 8, 22–3; 4: 24
dissolution of Zircaloy-clad uranium-Zircaloy alloys, 4: 11–12
solvent properties, 1: 10–11; 2: 22; 3: 6; 4: 11–12
Hydrofluoric acid–nitrogen oxide (N_2O_3) systems, solvent properties, 4: 30
Hydrofluoric acid–nitrogen oxide (N_2O_4) systems, corrosive effects, 2: 22; 3: 22; 4: 30
reactions with uranium dioxide–thorium oxide systems, 1: 29–30
solvent properties, 3: 22; 4: 30
Hydrofluoric acid–nitrosyl fluoride systems, solvent properties, 4: 30–1
Hydrofluorinators, corrosion by fused-salt volatility process solutions, 2: 23–5
Hydrogen, reduction processes using, 1: 45–6; 2: 62–3; 4: 75
Hydrogen chloride
See also Hydrochloric acid
corrosive effects, 2: 17
reaction with uranium-zirconium alloys, 3: 24
solubility in molten chloride systems, 2: 34
Hydrogen fluoride
See also Hydrofluoric acid
fluorination of stainless-steel chlorides, 1: 36–7
fluorination of uranium oxides (UO_2), 1: 36–7
reduction of uranium dioxide, 2: 63–4; 4: 76–7
Hydrogen peroxide–ammonium fluoride–ammonium nitrate systems
See Ammonium fluoride–ammonium nitrate–hydrogen peroxide systems
Hydrogen peroxide–hydrofluoric acid systems
See Hydrofluoric acid–hydrogen peroxide systems
Hydrolysis, of halides, for oxide coating of uranium dioxide, 2: 63
of plutonium compounds during nitric acid dissolution of irradiated uranium, 4: 10
thorium nitrate in steam for thorium oxide production, 2: 68–9
Hymu 80 alloy
See Alloy 79-4

I

ICPP process, corrosion problems, 3: 15–17
  fuel dissolution, 3: 8
  head-end processes, 1: 12
  plant design, 2: 13–15
  plutonium separation, 1: 15–16
  pulse columns, 3: 15
  safety, 1: 75–6
  waste disposal, 1: 52–7; 3: 51, 53
Idaho bed phosphate–calcite–pyrite mixtures
  See Calcite–Idaho bed phosphate–pyrite mixtures
Idaho Chemical Processing Plant
  See ICPP process
Impregnated graphite
  See Graphite (impregnated)
Incoloy 804 alloy, corrosion, 1: 43
Inconel alloy, corrosion, 1: 36; 2: 18, 23–4
Inconel 600 alloy, evaluation as crucible material, 4: 63
Indian Point Reactor
  See Reactors (Indian Point)
Indium (liquid), solvent properties, 3: 29
Indium-uranium alloys
  See Uranium-indium alloys
Inert gases, removal during oxidation-reduction process for uranium dioxide, 4: 49
INOR-1 alloy, corrosion, 2: 23, 24
INOR-8 alloy, corrosion, 1: 26, 32, 33; 2: 17, 23–4; 3: 23; 4: 31–2
  corrosion by fused salts, 4: 31
Instrumentation, 4: 17–19
  densimeters, 1: 17–18; 4: 49
  flowmeters, 4: 18–19
  interfacial velocity meters, 3: 13–14
  mass-transfer determinations, 3: 13–14
  pressure gauges, 1: 18
  Purex process, 2: 13
  salt-cycle process, 4: 49
Insulation, nitric acid effects, 4: 23
  radiation effects, 4: 23
Intermetallic compounds
  See also specific intermetallics by name of constituent metals
  thermodynamic properties, 2: 29–30; 4: 39–40
Iodine, release during oxidation of uranium dioxide, 4: 34–5
  removal, 2: 7
  removal from Purex wastes by steam stripping, 2: 48
  removal during oxidation-reduction process for uranium dioxide, 4: 49
  volatilization in melt-refining process, 4: 36
Iodine fluorides (IF_5), properties, 4: 35
Ion exchange, 1: 16–17; 4: 16
  cesium recovery, 2: 56–7
  dibutyl phosphoric acid removal, 4: 15–16
  fission-product removal, 2: 56
  mixed columns of natural organic materials, 2: 51
  Np^{237} recovery, 2: 55
  plutonium, 3: 69–70
  plutonium metal production, 3: 64–5
  strontium recovery from Purex waste, 2: 55
  strontium-removal capacity of various materials, 2: 49
  Tc^{99} extraction, 2: 56
  uranium recovery from acid sulfate leach solutions, 2: 61
  waste-disposal applications, 1: 51, 52; 2: 55
  waste-processing applications, 2: 48–51; 3: 44–6; 4: 56–8
Iridium, solubility in liquid bismuth, 1: 39
Iridium-platinum alloys, compatibility with molten phosphate glass, 2: 47
Iron, dissolution, 2: 10
  solubility, 3: 29
Iron alloys
  See also Hastelloy B alloy, INOR-8 alloy, and Monel alloy
  corrosion, 1: 43
Iron-chromium-cobalt-nickel alloys
  See Chromium-cobalt-iron-nickel alloys
Iron fluorides, complexing with uranium fluorides, 3: 27
Iron ions, effect on uranium oxide oxidation, 2: 61
Iron-molybdenum-nickel alloys, corrosion, 4: 31–2
Iron-molybdenum-nickel-vanadium alloys, corrosion, 4: 31–2
Iron-nickel-vanadium alloys, corrosion, 4: 31–2
Iron oxides, strontium removal from waste solutions using, 2: 49
Iron-platinum alloys (liquid), corrosive effects, 3: 33
Isooctyl amine, tri-, solvent properties, 3: 12
Isopropyl alcohol, solvent use in thorium oxide production, 2: 69
Isotopes, separation from wastes, 1: 61–4

K

Kaolinite, strontium removal by, 2: 49
Kel-F plastic, 3: 17
  radiation effects, 3: 17
Kerosene, diluent use in tributyl phosphate extraction processes, 4: 15
Krypton, release during melt-refining process, 2: 29; 4: 36–8
  solubility, 3: 29
Krypton-85, release from irradiated uranium during thermal cycling, 4: 37, 40
Krypton-xenon systems, release during oxidation of uranium dioxide, 4: 34–5
Kynar plastic, 4: 23
  corrosion, 3: 17
  radiation effects, 3: 17

L

L-nickel alloy, corrosion, 3: 23
  corrosion by fused salts, 4: 31
LAMPRE
  See Reactors (Los Alamos Molten Plutonium, Experiment)(LAMPRE)
Lanthanide elements
  See Rare earths and the specific elements by name
Lanthanum, extraction using liquid aluminum–cadmium system, 4: 41–2
  removal, 3: 28
  solubility, 3: 31
Lanthanum (liquid), density, 2: 30; 3: 30
  viscosity, 1: 41
Lanthanum-cadmium alloys
  See Cadmium-lanthanum alloys
Lanthanum-calcium intermetallic compounds
  See Calcium-lanthanum intermetallic compounds
Lanthanum-cerium intermetallic compounds
  See Cerium-lanthanum intermetallic compounds
Lanthanum oxide–barium oxide–beryllium oxide systems
  See Barium oxide–beryllium oxide–lanthanum oxide systems
Lanthanum oxide–beryllium oxide–calcium oxide systems
  See Beryllium oxide–calcium oxide–lanthanum oxide systems
Lanthanum oxide–beryllium oxide–strontium oxide systems
  See Beryllium oxide–lanthanum oxide–strontium oxide systems
Lanthanum oxide–beryllium oxide systems
  See Beryllium oxide–lanthanum oxide systems
Lauryl amine, tri-, solvent properties, 2: 12; 3: 12
LCNA alloy, corrosion, 1: 25–6; 2: 16–17; 4: 27–8
Leaching
  See also as subheading under specific materials
  calcined wastes, 4: 58
  ceramic sponges containing radioisotopes, 4: 64
  granitic rock for thorium recovery, 4: 83–4
  uranium from ores, 4: 72
Lead-bismuth alloys (liquid)
  See Bismuth-lead alloys (liquid)
Lead chloride (liquid), solvent properties, 1: 43–4; 2: 7
Lead chloride–lead systems (liquid)
  See Lead–lead chloride systems (liquid)
Lead chloride–potassium chloride systems (liquid), solvent-extraction applications, 1: 44–5
  solvent properties, 2: 34
Lead–lead chloride systems (liquid), corrosive effects, 1: 43–4
Lead oxides, flux use in waste calcination, 2: 43
  strontium removal from waste solutions using, 2: 49
Lead-thorium intermetallic compounds
  See Thorium-lead intermetallic compounds
Lead-uranium alloys
  See Uranium-lead alloys
Lead-uranium intermetallic compounds
  See Uranium-lead intermetallic compounds
Lead-zinc alloys, phase diagrams, 3: 29
Lead-zinc alloys (liquid), distribution coefficients of various metals in, 2: 30–1
  solvent-extraction applications, 1: 40
Lectures, solvent-extraction processes, 3: 12
Legislation, fuel-element shipping, 1: 1–2
Lignite, radioisotope sorption by, 2: 51
Lignite-peat mixtures
  See Peat-lignite mixtures
Lignite-vermiculite mixtures, sorption column use, 2: 51
Lime-soda softening process, waste-disposal use, 1: 51
Liquid-metal extraction processes, 3: 32–3; 4: 41–2
  See also Liquid metal–fused salt extraction processes
  alloy-eutectic system, 2: 30–1
  lead-zinc system, 2: 30–1
  magnesium-zinc system, 2: 32
  melt-refining skull reclamation, 4: 43
  uranium-plutonium separation, 4: 43
Liquid-Metal Fuel Reactor
  See Reactors (Liquid-Metal Fuel)
Liquid metal–fused salt extraction processes, 3: 34
  alloy–fused salt eutectic system, 2: 32; 4: 41, 43
Liquid metal–fused salt systems, uranium trichloride reduction in, 4: 83
Liquid-metal systems
  See also specific liquid-metal systems by name of constituent metals
  publications, 4: 41
  reduction reactions in, 4: 42
Liquid wastes, conversion to solids, 3: 47–54
  disposal, 3: 43–7
Literature surveys
  See Bibliographies
Lithium-7, recovery, 3: 23
Lithium chloride, corrosive effects of solutions, 3: 19

Lithium chloride–barium chloride–magnesium fluoride systems
See Barium chloride–lithium chloride–magnesium fluoride systems
Lithium chloride–magnesium chloride–magnesium fluoride systems (liquid), solvent properties, **1**: 45
Lithium chloride–magnesium chloride–potassium chloride systems (liquid), solvent properties, **3**: 30–1
Lithium chloride–potassium chloride systems (liquid), electrolytic reduction bath, **2**: 36, 67–8
solvent properties, **4**: 48
uranium dioxide dissolution in, **2**: 34
Lithium chloride–potassium chloride–zinc chloride systems (liquid), reactions with uranium carbides (UC), **1**: 47
Lithium fluoride–beryllium fluoride–sodium fluoride systems (liquid)
See Beryllium fluoride–lithium fluoride–sodium fluoride systems (liquid)
Lithium fluoride–beryllium fluoride–sodium fluoride–zirconium fluoride systems (liquid)
See Beryllium fluoride–lithium fluoride–sodium fluoride–zirconium fluoride systems (liquid)
Lithium fluoride–potassium fluoride–sodium fluoride–uranium fluorides (UF_4)–zirconium fluoride systems
See Uranium fluorides (UF_4)–lithium fluoride–potassium fluoride–sodium fluoride–zirconium fluoride systems
Lithium fluoride–potassium fluoride–uranium fluorides (UF_4) systems (liquid)
See Uranium fluorides (UF_4)–lithium fluoride–potassium fluoride systems (liquid)
Lithium fluoride–sodium fluoride–uranium fluorides (UF_4)–zirconium fluoride systems
See Uranium fluorides (UF_4)–lithium fluoride–sodium fluoride–zirconium fluoride systems
Lithium fluoride–sodium fluoride–zirconium fluoride systems (liquid), corrosive effects, **3**: 23; **4**: 31
dissolution of uranium-zirconium alloys, **1**: 30–5
review of properties, **2**: 30
solvent properties, **3**: 23
Los Alamos Molten Plutonium Reactor Experiment
See Reactors (Los Alamos Molten Plutonium, Experiment)(LAMPRE)
Low-decontamination oxidation-reduction process, **2**: 35
Lutetium, removal, **3**: 28
solubility, **3**: 31
in liquid bismuth, **1**: 39

M

Magnesium, evaluation of various types for reduction processes, **2**: 67
reduction of uranium tetrafluoride to uranium, **2**: 66–7
solubility in liquid-metal systems, **1**: 39; **4**: 42
Magnesium (liquid), solvent properties, **1**: 42; **4**: 43
Magnesium alloys (liquid), corrosive effects, **1**: 43
Magnesium-bismuth-cerium-zirconium alloys (liquid)
See Bismuth-cerium-magnesium-zirconium alloys (liquid)
Magnesium-cadmium-zinc systems (liquid)
See Cadmium-magnesium-zinc systems (liquid)
Magnesium chloride (liquid), solvent properties, **3**: 31
Magnesium chloride–lithium chloride–potassium chloride systems (liquid)
See Lithium chloride–magnesium chloride–potassium chloride systems (liquid)
Magnesium chloride–magnesium fluoride–lithium chloride systems (liquid)
See Lithium chloride–magnesium chloride–magnesium fluoride systems (liquid)
Magnesium chloride–potassium chloride–sodium chloride systems (liquid), solvent-extraction applications, **1**: 44
solvent properties, **3**: 31
Magnesium chloride–potassium chloride systems (liquid), solvent-extraction applications, **1**: 44
solvent properties, **2**: 34
uranium dioxide dissolution in, **2**: 34
Magnesium fluoride–barium chloride–lithium chloride systems (liquid)
See Barium chloride–lithium chloride–magnesium fluoride systems (liquid)
Magnesium fluoride–magnesium chloride–lithium chloride systems (liquid)
See Lithium chloride–magnesium chloride–magnesium fluoride systems (liquid)
Magnesium oxide, coating of uranium dioxide with, **2**: 63
Magnesium-silver systems (liquid), metal extraction using, **4**: 41, 45
Magnesium-thorium alloys
See Thorium-magnesium alloys
Magnesium-uranium-zinc alloys (liquid)
See Uranium-magnesium-zinc alloys (liquid)
Magnesium-zinc systems (liquid), corrosive effects on boron nitride, **2**: 33
reduction of thorium oxide, **1**: 41; **4**: 84
reduction of uranium tritaoctoxide, **1**: 40–7
solvent properties, **2**: 29–30; **3**: 30–1
uranium-carbon reactions in, **2**: 66
uranium-silicon reactions in, **2**: 66
Maintenance, direct and remote, **4**: 19–20
effect of number of failures on remedial course, **4**: 20
Manganese-56, removal from Hanford reactor coolant by aluminum shavings, **4**: 57
Manganese alloys
See Hastelloy B alloy and Monel alloy
Manganese oxide (MnO_2), fission-product removal from fuel solutions using, **4**: 12
Manuals, **1**: 73
Maritime Gas-Cooled Reactor
See Reactors (Maritime Gas-Cooled) (MGCR)
Marlex polyethylene, **4**: 23
corrosion, **3**: 17
radiation effects, **3**: 17
Mass transfer, instrumentation, **3**: 13–14
Materials of construction
See Construction materials and specific materials by name
Melamine plastics, corrosion, **2**: 19
Melt-refining processes, **1**: 38–9; **2**: 28–9; **3**: 27–9; **4**: 36–9
skull reclamation, **4**: 43–4
Melting point, beryllium oxide fluxes, **1**: 38
platinum hexafluoride, **2**: 27
review of liquid metals, **2**: 30
technetium hexafluoride, **2**: 27
Mercury, corrosive effects, **3**: 33
solvent properties, **3**: 29
Mercury (gaseous), corrosive effects, **3**: 33
Mercury chloride ($HgCl_2$) solutions, solvent properties, **3**: 6
Mercury nitrate [$Hg(NO_3)_2$]–ammonium fluoride–nitric acid systems
See Ammonium fluoride–mercury nitrate [$Hg(NO_3)_2$]–nitric acid systems
Mercury nitrate [$Hg(NO_3)_2$]–nitric acid–hydrofluoric acid systems
See Nitric acid–mercury nitrate [$Hg(NO_3)_2$]–hydrofluoric acid systems
Mercury nitrate [$Hg(NO_3)_2$]–nitric acid systems
See Nitric acid–mercury nitrate [$Hg(NO_3)_2$] systems
Metals (liquid)
See Liquid metals
Metasomatic replacement
See Replacement reactions
Methane, reaction with uranium hydride to produce uranium carbide, **2**: 64
Methane–carbon tetrachloride–chlorine systems
See Carbon tetrachloride–chlorine–methane systems
Methane–carbon tetrachloride systems
See Carbon tetrachloride–methane systems
Methanol–hydrogen chloride systems
See Hydrogen chloride–methanol systems
Methyl isobutyl ketone processes
See Redox process
MGCR
See Reactors (Maritime Gas-Cooled) (MGCR)
Minerals, P^{32} removal from waste by, **4**: 57
Sr^{90} sorption by, **2**: 49; **4**: 66
waste-decontamination processes using, **2**: 48–9
Mines, waste disposal in, **2**: 51–2; **3**: 55–6; **4**: 65–6
Mixer-settlers, centrifugal, **4**: 2–3
design, **2**: 14–15; **3**: 12
Mol, Belgium, fractional sublimation work, **2**: 26
Molybdenum, corrosion, **2**: 23; **3**: 33
removal, **1**: 31, 41; **2**: 22; **3**: 28
removal difficulties using melt-refining process, **2**: 29
solubility in liquid zinc, **2**: 29
Molybdenum (tungsten-coated), thermal cycling, **2**: 33
Molybdenum alloys
See Hastelloy B alloy and INOR-8 alloy
Molybdenum chlorides, volatility, **1**: 45
Molybdenum-iron-nickel alloys
See Iron-molybdenum-nickel alloys
Molybdenum-iron-nickel-vanadium alloys
See Iron-molybdenum-nickel-vanadium alloys
Molybdenum-nickel alloys
See also INOR-1 alloy
corrosion, **4**: 31–2
Molybdenum oxide (MoO_3), radiation effects on sublimation rate, **2**: 38
Molybdenum-tungsten alloys, compatibility with liquid metals and alloys, **2**: 33
Molybdenum-uranium alloys
See Uranium-molybdenum alloys
Molybdenum-uranium alloys (aluminum-clad)
See Uranium-molybdenum alloys (aluminum-clad)
Monazite, chlorination, **2**: 68
Monel alloy, corrosion, **2**: 22–3, 24; **3**: 15–17, 22; **4**: 30
corrosion by hydrofluoric acid–hydrogen peroxide systems, **4**: 23–4
Montmorillonite, strontium removal by, **2**: 49
Mullite (tungsten-coated), thermal cycling, **2**: 33

N

NaK, corrosive effects, **1**: 17
National Reactor Testing Station, waste disposal, **3**: 43

Neodymium, extraction by liquid metal–fused salt systems, **4**: 43
recovery in Redox process, **4**: 13–14
removal, **2**: 22; **3**: 28
solubility, **3**: 30–1
Neptunium, separation, **1**: 17; **3**: 12–13
Neptunium-237, recovery by ion exchange, **2**: 55
Nevada Test Site, waste disposal, **3**: 43
Nichrome alloy, electrolytic dissolution, **3**: 9
Nichrome–uranium oxides (UO_2) systems
See Uranium oxides (UO_2)–Nichrome systems
Nichrome-V alloy, corrosion, **2**: 17
dissolution, **1**: 27; **2**: 8–10
Nickel, corrosion, **1**: 36; **2**: 17, 23; **3**: 27; **4**: 30
dissolution, **2**: 10
gauze, catalytic use in uranyl-ion reduction, **4**: 73–4
Nickel alloys
See also Hastelloy B alloy, INOR-1 alloy, INOR-8 alloy, L-nickel alloy, Monel alloy, and Nionel alloy
corrosion, **1**: 43
Nickel-aluminum alloys
See Aluminum-nickel alloys
Nickel-aluminum-plutonium alloys
See Plutonium-aluminum-nickel alloys
Nickel-aluminum-plutonium alloys (Zircaloy-4-clad)
See Plutonium-aluminum-nickel alloys (Zircaloy-4-clad)
Nickel-aluminum-silicon alloys
See Aluminum-nickel-silicon alloys
Nickel-aluminum-silicon systems
See Aluminum-nickel-silicon systems
Nickel-chromium alloys
See Chromium-nickel alloys and Corronel 230 alloy
Nickel-chromium-cobalt-iron alloys
See Chromium-cobalt-iron-nickel alloys
Nickel-chromium-cobalt-tungsten alloys
See Haynes 25 alloy
Nickel-copper-iron-manganese alloys
See Monel
Nickel ferrocyanide, cesium precipitation from Purex supernatant using, **2**: 58
Nickel-iron-molybdenum alloys
See Iron-molybdenum-nickel alloys
Nickel-iron-molybdenum-vanadium alloys
See Iron-molybdenum-nickel-vanadium alloys
Nickel-iron-vanadium alloys
See Iron-nickel-vanadium alloys
Nickel-molybdenum alloys
See INOR-1 alloy and Molybdenum-nickel alloys
Nickel-molybdenum-iron alloys
See Alloy 79-4
Niflex process, corrosion problems, **1**: 26
Niobium, basket use in electrolytic dissolution process, **4**: 8–9
corrosion, **3**: 16
dissolution, **3**: 6
removal, **1**: 16–17; **2**: 11, 22; **3**: 12
in dissolver filtrate, **1**: 11
from fuel solution by manganese dioxide, **4**: 12
from Purex wastes by ion exchange, **2**: 48
from wastes, **1**: 57–8
solubility in liquid zinc, **2**: 29
Niobium oxides (Nb_2O_5), chlorination, **4**: 33
Niobium oxides (Nb_2O_5)–uranium oxides (UO_2) systems
See Uranium oxides (UO_2)–niobium oxides (Nb_2O_5) systems
Niobium-zirconium alloys, corrosion, **3**: 33
Niobium-95–zirconium-95 mixtures, activity/particle-size relations for separated waste, **4**: 58
Nionel alloy, corrosion, **1**: 26; **2**: 18; **3**: 17
by ammonium fluoride–ammonium nitrate solutions, **4**: 23
evaporation vessel use, **2**: 47
Nionel alloy (low-carbon)
See LCNA alloy
Nitric acid, corrosion inhibition, **3**: 17–18
corrosion of insulating materials, **4**: 23
corrosion of stainless steels, **4**: 21–3
corrosive effects, **2**: 17–19; **3**: 19; **4**: 24
leaching of impregnated graphite, **1**: 12
leaching of uranium oxides (UO_2)–beryllium oxide systems, **1**: 12–13
solvent properties, **1**: 8–10; **2**: 7–9; **3**: 8–10; **4**: 10
Nitric acid–aluminum nitrate–sodium fluoride systems, corrosive properties, **4**: 24
Nitric acid–aluminum nitrate systems
See Aluminum nitrate–nitric acid systems
Nitric acid–ammonium fluoride–mercury nitrate [$Hg(NO_3)_2$] systems
See Ammonium fluoride–mercury nitrate [$Hg(NO_3)_2$]–nitric acid systems
Nitric acid–hydrochloric acid systems
See Hydrochloric acid–nitric acid systems
Nitric acid–hydrofluoric acid systems
See Hydrofluoric acid–nitric acid systems
Nitric acid–mercury nitrate [$Hg(NO_3)_2$] systems, dissolution of aluminum, **4**: 11
dissolution of Zircaloy-4, **4**: 11
Nitric acid–mercury nitrate [$Hg(NO_3)_2$]–hydrofluoric acid systems, dissolution of aluminum-clad aluminum-plutonium alloys, **4**: 11
Nitric acid–sulfuric acid systems, corrosive effects, **3**: 18–19
fuel-element dissolution, **1**: 11–12
leaching of uranium oxides (UO_2)–beryllium oxide systems, **1**: 12–13
Nitric acid–uranyl nitrate hexahydrate–aluminum nitrate systems
See Uranyl nitrate hexahydrate–aluminum nitrate–nitric acid systems
Nitridation, EBR-II declad fuel pins, **4**: 36
uranium carbides, **1**: 46; **2**: 36–7; **4**: 49–50
Nitrobenzene–dipicryl amine systems
See Dipicryl amine–nitrobenzene systems
Nitrofluor process, **2**: 22–3; **3**: 22; **4**: 30–1
Nitrogen–carbon tetrachloride systems
See Carbon tetrachloride–nitrogen systems
Nitrogen oxide (N_2O_3)–hydrofluoric acid systems
See Hydrofluoric acid–nitrogen oxide (N_2O_3) systems
Nitrogen oxide (N_2O_4)–hydrofluoric acid systems
See Hydrofluoric acid–nitrogen oxide (N_2O_4) systems
Nitrogen oxides (N_2O_4)–nitrosyl chloride systems, dissolution of uranium, **1**: 29–30
Nitrosyl chloride–nitrogen oxides (N_2O_4) systems
See Nitrogen oxides (N_2O_4)–nitrosyl chloride systems
Nitrosyl fluoride–hydrofluoric acid systems
See Hydrofluoric acid–nitrosyl fluoride systems
Nitrosylium hexafluorouranate, conversion to uranium hexafluoride, **3**: 22; **4**: 30–1
Nonaqueous processes, **4**: 30–50
economic evaluations, **4**: 3
Nontronite, strontium removal by, **2**: 49
Nozzles, erosion in fluid-bed calcination process, **2**: 44
fused-salt atomization by, **3**: 23–4
N.S. *Savannah* Reactor
See Reactors (N.S. *Savannah*)
Nuclear Fuel Services, Inc., **3**: 1; **4**: 1–2

O

Ocean disposal
See Waste disposal and processing
Octylamine, tri-*n*-, solvent properties, **3**: 12
Ohmic heating
See Heating
OMRE
See Reactors (Organic-Moderated, Experiment) (OMRE)
Optical emission spectroscopy
See Spectroscopy (optical emission)
Organic compounds
See also specific compounds by name
alkane reactions with uranium, **2**: 65–6
removal from Purex wastes by steam stripping, **2**: 48
Organic-Moderated Reactor Experiment
See Reactors (Organic-Moderated, Experiment) (OMRE)
Osmium, solubility, **3**: 29
solubility in liquid bismuth, **1**: 39
Oxidation, Alloy 79-4, **4**: 31
beryllium chloride for deposition of beryllium oxide coatings, **2**: 63
fission products, for removal from liquid-metal fuels, **4**: 45
uranium dioxide, **1**: 45–6
uranium dioxide fission-product release during, **4**: 34–5
uranium monocarbide, **1**: 46–7
Oxidation-reduction processes, **2**: 34–36; **3**: 37
activation of uranium oxides, **2**: 64–5; **4**: 34, 76–7
equilibria in uranium dioxide–uranium tritaoctoxide systems, **4**: 76
for uranium carbides, **4**: 49
for uranium dioxide, **4**: 49
Oxide fuel processing, **2**: 34; **4**: 46–9
Oxide target elements (aluminum-clad), dissolution by hydrochloric acid, **4**: 12
Oxygen, corrosive effects, **2**: 17

P

Palladium, extraction using liquid aluminum-cadmium system, **4**: 41–2
extraction by liquid metal–fused salt systems, **4**: 43
removal, **1**: 41
solubility in liquid zinc, **2**: 29
Particles
See Thorium oxide spheres and Thorium oxide–uranium oxide spheres
Peach Bottom Reactor
See Reactors (Peach Bottom)
Peat, radioisotope sorption by, **2**: 51
Peat-lignite mixtures, sorption-column use, **2**: 51
Peat-soil mixtures, sorption-column use, **2**: 51
Peat-vermiculite mixtures, sorption-column use, **2**: 51
Pebble-Bed Reactor
See Reactors (Pebble-Bed)
Pentaacetic acid, diethylene triamine-, cerium complexing, **2**: 56
Perflex process, **1**: 11
Permutit SK resin, **4**: 16
plutonium adsorption, **3**: 69
Phase studies, alloys, **4**: 40
cadmium-praseodymium intermetallic compounds, **2**: 29–30
calcium-lanthanum intermetallic compounds, **2**: 30
cerium-lanthanum intermetallic compounds, **2**: 30
intermetallic compounds, **4**: 40

Phase studies (Continued)
platinum hexafluoride solid-solid transition point, 2: 27
technetium hexafluoride solid-solid transition point, 2: 27
uranium-carbon constitutional diagram, 4: 79
uranium-fissium alloys, 2: 29
Phenol formaldehyde plastics, corrosion, 2: 19
Phenolic resins, radioisotope removal from Purex waste, 2: 48
Phosphate ion, effect on strontium removal by various materials, 2: 49–50
Phosphates, use as flux in waste calcination, 2: 43
Phosphine oxide, trioctyl-, solvent properties, 3: 12–13
Phosphonate, diamylamyl-, solvent properties, 3: 12–13
Phosphonate, dibutylbutyl-, uranium extraction from nitrate eluates, 2: 61
Phosphonate, di-*n*-butylphenyl-, solvent properties, 3: 12–13
Phosphonate, di-*sec*-butylphenyl-, solvent properties, 3: 12–13
Phosphoric acid, dibutyl-, removal from solvent-extraction aqueous phase by ion exchange, 4: 15–16
solvent properties, 3: 12
Phosphoric acid, di-2-ethylhexyl-, rare-earth extraction, 2: 56
solvent properties, 3: 12–13
Phosphoric acid, 2-ethylhexylphenyl-, solvent use in transuranium-element extraction, 4: 16
Phosphoric acid, monofluo-, dissolution of uranium dioxide–thorium oxide systems, 1: 29–30
Phosphorus-32, removal from Hanford reactor coolant, 4: 57
Photometers, probe type filter, for fused-salt systems, 4: 49
Picryl amine, di-
See Dipicryl amine
Piqua Reactor
See Reactors (Piqua)
Pits, open, waste disposal in, 4: 64–5
Plant design, 2: 4; 4: 19–20
Plant operation, 4: 19–20
Plastics
See also specific plastics by chemical and trade names
corrosion, 2: 19
Platinum, corrosion, 2: 23
by molten phosphate glasses, 4: 63
crucible liner use in phosphate-glass production from waste, 2: 46–7
solubility in liquid bismuth, 1: 39
Platinum alloys, corrosion by molten phosphate glasses, 4: 63
Platinum fluoride (PtF_6), boiling point, 2: 27
melting point, 2: 27
preparation, 2: 27
reagent use in preparation of other fluorides, 2: 27
solid-solid transition point, 2: 27
Platinum-gold alloys
See Gold-platinum alloys
Platinum-iridium alloys
See Iridium-platinum alloys
Platinum-iron alloys
See Iron-platinum alloys
Platinum-rhodium alloys, compatibility with molten phosphate glass, 2: 47
Plutonium, adsorption on Florida pebble phosphate, 2: 48–9
bibliography, 4: 38–9
complex formation in fused-salt systems, 4: 47
dissolution, 1: 45
electrorefining, 4: 84–6
extraction, 4: 12–14, 15
by liquid alloy–eutectic system, 2: 30–1
by liquid calcium-zinc alloys, 1: 42
by liquid lead-zinc system, 2: 30–1
by liquid-metal system, 4: 41, 45
hydrolysis during nitric acid dissolution of irradiated uranium, 4: 10
ion-exchange recovery, 1: 16–17; 4: 16
loss minimization by waste backcycling in Purex process, 4: 13
losses in recycle, 3: 2–3
metallurgy, 3: 30
precipitation as hydride from magnesium-zinc solution, 2: 32
production, 2: 61–9; 3: 64–7
recovery, from EBR-II blanket by liquid-metal extraction, 2: 32
in salt-cycle process, 2: 35
from scrap, 3: 67–9
separation, 1: 13–14, 15–16; 2: 11–12; 3: 11, 25–6, 34–6
separation by fluorination, 4: 33–4
solubility in magnesium alloys, 4: 43
technology, 3: 69–70
Plutonium (liquid), density, 3: 30
Plutonium alloys (liquid), corrosive effect, 1: 43; 2: 33
Plutonium-aluminum alloys (aluminum-clad), dissolution, 4: 11
Plutonium-aluminum-nickel alloys, dissolution, 3: 7
Plutonium-aluminum-nickel alloys (Zircaloy-4-clad), dissolution, 4: 11
Plutonium carbides (PuC)–uranium carbides (UC) systems
See Uranium carbides (UC)–plutonium carbides (PuC) systems
Plutonium carbides (Pu_2C_3), preparation, 1: 47; 2: 66
Plutonium-cerium-cobalt alloys (liquid), corrosive effects, 3: 33
Plutonium chloride ($PuCl_3$)–cesium chloride systems, cooling-curve analysis, 2: 37
Plutonium chloride ($PuCl_3$)–rubidium chloride systems, cooling-curve analysis, 2: 37
Plutonium fluorides, review on preparation and properties, 2: 27
Plutonium fluorides (PuF_3), precipitation, 3: 66
reduction to metal, 3: 66–7
Plutonium fluorides (PuF_4), conversion from PuO_2, 3: 70
reduction to metal, 3: 65–6
volatility, 1: 34
Plutonium fluorides (PuF_6), preparation from plutonium tetrafluoride using platinum hexafluoride, 2: 27
thermal decomposition, 2: 27; 3: 26; 4: 34
Plutonium oxides, direct fluorination processing, 2: 26
reduction, 4: 45
separation from plutonium, 4: 33–4
Plutonium oxides (peroxides), hydrofluorination, 3: 65–6
precipitation, 3: 65
Plutonium oxides (PuO_2), conversion from PuF_4, 3: 70
fluorination, 3: 26
precipitation from plutonium trichloride–fused salt solutions, 4: 48
Plutonium oxides–thorium oxide systems, precipitation from fused-salt solutions, 4: 48
Plutonium oxides–uranium oxides systems, crystal properties, 4: 47–8
electrolytic processing, 2: 34
Plutonium oxides (PuO_2)–uranium oxides (UO_2) systems, electrolytic codeposition from fused salts, 4: 47
precipitation from fused-salt solutions, 4: 48
pyrochemical processing, 4: 46
Plutonium peroxides
See Plutonium oxides (peroxides)
Plutonium Recycle Program, 4: 46–9
See also Reactors (Plutonium Recycle Test)
Plutonium-thorium alloys, plutonium recovery, 3: 69
Plutonium-uranium alloys
See Uranium-plutonium alloys
Plutonium-zinc alloys, thermodynamic properties, 1: 39
Plutonyl fluorides, 4: 35
Poisons (neutron), applications in storage containers, 2: 15
criticality hazards control using, 4: 3
Polarographs, applications in Purex process 2: 13
Polymers, ethylene, corrosion, 2: 19
propylene, 4: 23
styrene, 4: 23
Potassium chloride (liquid), hexachlorouranate-ion stability in, 2: 37
Potassium chloride–aluminum chloride systems (liquid)
See Aluminum chloride–potassium chloride systems (liquid)
Potassium chloride–lead chloride systems
See Lead chloride–potassium chloride systems
Potassium chloride–lead chloride systems (liquid)
See Lead chloride–potassium chloride systems (liquid)
Potassium chloride–lithium chloride–magnesium chloride systems
See Lithium chloride–magnesium chloride–potassium chloride systems
Potassium chloride–lithium chloride systems (liquid)
See Lithium chloride–potassium chloride systems (liquid)
Potassium chloride–magnesium chloride–sodium chloride systems
See Magnesium chloride–potassium chloride–sodium chloride systems
Potassium chloride–magnesium chloride systems
See Magnesium chloride–potassium chloride systems
Potassium chloride–magnesium chloride systems (liquid)
See Magnesium chloride–potassium chloride systems (liquid)
Potassium chloride–sodium chloride systems (fused), solvent properties, 1: 45
Potassium chloride–sodium chloride systems (liquid), solvent properties, 2: 34
Potassium chloride–sodium chloride–zinc chloride systems (liquid), solvent properties, 1: 45
Potassium chloride–zinc chloride systems (liquid), solvent properties, 3: 31
Potassium fluoride–lithium fluoride–sodium fluoride–uranium fluorides (UF_4)–zirconium fluoride systems
See Uranium fluorides (UF_4)–lithium fluoride–potassium fluoride–sodium fluoride–zirconium fluoride systems
Potassium fluoride–lithium fluoride–uranium fluorides (UF_4) systems (liquid)
See Uranium fluorides (UF_4)–potassium fluoride–lithium fluoride systems
Potassium plutonyl fluorides, preparation, 4: 35
Potassium-sodium alloys (liquid), corrosive effects, 3: 17

Praseodymium, extraction using liquid aluminum-cadmium system, 4: 41–2
removal, 3: 28
solubility, 3: 29, 31
solubility in liquid zinc, 2: 29
Praseodymium (liquid), density, 3: 30
viscosity, 1: 41
Praseodymium-cadmium intermetallic compounds
See Cadmium-praseodymium intermetallic compounds
PRDC Reactor
See Reactors (Enrico Fermi Fast-Breeder)
Precipitation processes, 4: 16–17
fission-product recovery, 2: 56
Pressure gauges, 1: 18
Primene JM-T solvent, solvent properties, 3: 12–13
Promethium, recovery from Purex wastes, 2: 56
removal, 3: 28
solubility, 3: 31
Promethium-147, separation from wastes, 3: 58
Propane, uranium carbide production using, 2: 36, 64; 4: 78
uranium dioxide production by flame denitration using, 4: 74
Propylene polymers, 4: 23
Protactinium, separation, 1: 42–3; 2: 11, 32; 3: 11–12
Pulse columns, design, 3: 14–15
pulse amplitude determination, 4: 17–18
Purex-Darex raffinate
See Darex-Purex raffinate
Purex phosphate-glass pilot plant, flow diagram, 2: 47
Purex process, 2: 12–13; 4: 10
cost, 4: 1–2
improvements, 4: 12–16
plant design, 1: 18–25
plutonium separation, 1: 13–14
solvent technology, 3: 12
uranium loss minimization by waste backcycling, 4: 13
Purex wastes, backcycling, 4: 12–14
calcination, 2: 43; 4: 58–9
composition, 4: 25–6
conversion to glasses, 2: 46–7; 4: 63
corrosive properties, 4: 25–7, 63
costs of pot calcination, 2: 42
disposal, 1: 52–7, 58–9, 63; 3: 51
disposal in salt mines, 4: 66
fission-product recovery, 2: 56
mine-area requirement for storage, 2: 51
radioisotope removal, 2: 48, 55; 4: 56, 67–9
steam stripping, 2: 48
storage costs, 1: 50–1
strontium recovery, 2: 55; 4: 67–9
Pyrite, radioisotope adsorption, 4: 57
Pyrite–calcite–Florida bed phosphate mixtures, radioisotope adsorption, 4: 57
Pyrite–calcite–Idaho bed phosphate mixtures, radioisotope adsorption, 4: 57
Pyroceram, corrosion, 2: 17
Pyroceram (tungsten-coated), thermal cycling, 2: 33
Pyrochemical processes, 4: 46–50
Pyrolytic carbon, coating of uranium carbides with, 4: 81
Pyrometallurgical processes, 1: 38–44; 2: 27–33; 3: 27–34; 4: 36–46
Pyrophoricity, uranium monocarbide, 2: 37
Pyrrhotite, radioisotope adsorption, 4: 57

R

Radiation effects, insulating materials, 4: 23
molybdenum trioxide sublimation rate, 2: 38
plastics, 3: 17
Radiation sources, radioisotope-containing glasses, 2: 47–8
Radioactive wastes
See Purex wastes, Darex wastes, TBP-25 wastes, Thorex wastes, and Waste disposal and processing
Radioisotopes
See also specific isotopes by name
removal, from Hanford reactor coolant by aluminum shavings, 4: 56–7
from Purex wastes, 4: 56
from wastes, 3: 57–9
Radium, separation from thorium, 4: 39
Rare earths, lanthanide separation from transuranium actinides, 4: 16
oxides, reduction, 4: 45
separation, 2: 11; 3: 28
by electrolytic process, 2: 36
in salt-cycle process, 2: 35
from thorium in monazite chlorination, 2: 68
from wastes, 1: 61–4; 2: 56; 3: 57–9
solubility, 3: 31
RBOF (Receiving Basin for Off-Site Fuels), 4: 6
Reactors (BONUS), fuel-cycle estimated cost, 4: 5
Reactors (CANDU), fuel-cycle costs, 2: 2–3
Reactors (Carolinas-Virginia), fuel-cycle estimated cost, 4: 5
Reactors (Consolidated Edison Thorium)
See Reactors (Indian Point Power)
Reactors (Dresden Power), fuel-cycle estimated cost, 4: 5
fuel-processing plant design, 1: 18–25
Reactors (Enrico Fermi Fast-Breeder), breeding blanket dissolution, 1: 9–10
fuel-element dissolution, 1: 8–9
Reactors (Experimental Breeder I) (EBR-I), fuel processing, 1: 33–4, 35
Reactors (Experimental Breeder II) (EBR-II), blanket processing, 2: 32; 3: 32–3; 4: 43–4
fuel processing, 1: 38–9; 2: 28–9, 32; 3: 27–9; 4: 36–8
Reactors (Experimental Organic-Cooled) (EOCR), fuel dissolution, 1: 11–12
Reactors (Gas-Cooled, Experiment) (GCRE), fuel dissolution, 1: 12–13
Reactors (General Electric Test) (GETR), fuel dissolution, 1: 11–12
Reactors (Hallam Power), fuel-cycle estimated cost, 4: 5
fuel dissolution, 1: 9–10
Reactors (Heat-Transfer, Experiments) (HTRE), fuel dissolution, 3: 9
fuel processing, 1: 8–10
Reactors (High-Flux Isotope) (HFIR), 4: 16
aluminum-clad oxide target elements, dissolution of, 4: 12
fuel processing, 3: 12–13
Reactors (Indian Point Power), chemical decladding of fuel elements, 1: 8
fuel-cycle estimated cost, 4: 5
fuel processing, 4: 14
Reactors (Liquid-Metal Fuel), fission-product removal from fuel, 4: 45
Reactors (Los Alamos Molten-Plutonium, Experiment) (LAMPRE), plutonium fuel alloy corrosive effects, 2: 33
Reactors (Maritime Gas-Cooled) (MGCR), fuel dissolution, 1: 12–13
Reactors (N.S. *Savannah*), fuel dissolution, 4: 12
uranium monocarbide fuel, 4: 78
Reactors (Organic-Moderated, Experiment) (OMRE), fuel dissolution, 1: 11–12
Reactors (Peach Bottom), fuel-cycle estimated cost, 4: 5
Reactors (pebble bed), fuel processing, 2: 10–11
Reactors (Piqua), fuel-cycle estimated cost, 4: 5
Reactors (Plutonium Recycle Test), fuel dissolution, 3: 7; 4: 11
Reactors (S1G), fuel dissolution, 1: 11–12
Reactors (Shippingport Pressurized-Water) (PWR), fuel processing, 3: 36
Reactors (SM-1), fuel dissolution, 1: 11–12; 3: 9; 4: 12, 20
Reactors (sodium-cooled), uranium monocarbide fuel, 4: 78
Reactors (Sodium, Experiment) (SRE), fuel-element decladding, 1: 7–8
Reactors (TRIGA), fuel dissolution, 1: 25–6
fuel processing, 2: 25; 3: 7
Reactors (Yankee Power), fuel-cycle estimated cost, 4: 5
fuel dissolution, 4: 12, 20
Receiving Basin for Off-Site Fuels, 4: 6
Redox process, head-end processes, 3: 6–7
improvements, 4: 12–16
neptunium accumulation flow pattern, 4: 14
Redox wastes, backcycling, 4: 12–13
conversion to glasses, corrosion problems, 4: 63
Reduction processes, 2: 31–2
See also Oxidation-reduction processes
aluminum-thorium alloy production, 4: 84
aluminum-uranium alloy production, 4: 83
carbon monoxide, of uranium trioxide, 4: 75
carbothermic, of uranium dioxide, 4: 49, 78–9
catalytic, for uranium dioxide production, 4: 73–4
electrolytic, for codeposition of oxides, 4: 47
uranium dioxide to metal, 2: 66
uranium production from uranium dioxide, 4: 82
uranium trichloride to uranium, 2: 67–8
of uranium tritaoctoxide, 4: 48
of uranyl(VI) ion, 2: 34–5; 4: 46–7
flame denitration, for uranium dioxide production, 4: 74–5
hydrogen, for uranium dioxide production, 2: 62–3; 4: 75–7
uranium trichloride to uranium, 4: 83
liquid metal–fused salt systems, 4: 42
magnesium-zinc, for thorium dioxide, 4: 84
plutonium oxides, 4: 45
rare-earth oxides, 4: 45
sodium amalgam, for uranium production, 4: 73
uranium carbide to uranium, 2: 36
uranium dioxide to uranium tetrafluoride, 2: 63–4
uranium tetrafluoride to uranium using magnesium, 2: 66–7
uranium trichloride to uranium, 4: 42
Refining, plutonium, electrolytically, 4: 84–6
uranium, electrolytically, 2: 13
Regeneration processes, 3: 37–9
Remote control, 4: 19
Replacement reactions, strontium removal in metasomatic, 2: 49–50
Rhenium, solubility, 1: 39; 3: 29
Rhenium-uranium alloys
See Uranium-rhenium alloys
Rhodium, removal, 1: 41
Rhodium alloys
See Platinum-rhodium alloys
Rhodium fluorides (RhF_5), properties, 1: 37–8
Richfield sand, strontium selective sorption by, 4: 65–6
Rock phosphates, radioisotope removal from wastes by, 4: 57
Rubidium chloride–plutonium chloride ($PuCl_3$) systems
See Plutonium chloride ($PuCl_3$)–rubidium chloride systems

Rubidium plutonyl fluorides, preparation, 4: 35
Russia
See Union of Soviet Socialist Republics
Ruthenium, processing of waste containing, 2: 43
release during oxidation of uranium dioxide, 4: 34–5
removal, 1: 41, 46; 2: 11, 22; 3: 12
difficulties using melt-refining process, 2: 29
by electrolytic process, 2: 36
from fuel solution by manganese dioxide, 4: 12
by liquid lead-zinc system, 2: 30–1
by natural organic materials, 2: 51
from Purex waste by ion exchange, 4: 56
from Purex wastes by steam stripping, 2: 48
in Thorex process, 4: 14
during uranium dioxide oxidation-reduction process, 4: 49
from wastes, 1: 57–8
volatility, 3: 52–3
Ruthenium-106, activity/particle-size relations for separated waste, 4: 58
hazards of disposal in open pits, 4: 64
volatilization from ceramic sponges, 4: 63–4
Ruthenium chloride, volatility, 1: 45

S

S1G Reactor
See Reactors (S1G)
Safety, ICPP process, 1: 75–6
Salt cavities, waste disposal in, 1: 59–61; 2: 51–2; 3: 55–6; 4: 66
Salt-cycle process, 2: 34–5; 3: 34–6; 4: 48–9
Salts (atomized), particle size, 3: 23–4
Salts (fused)
See Fused salts
Samarium, extraction by liquid metal–fused salt systems, 4: 43
removal, 3: 28
solubility, 3: 30–1
in liquid bismuth, 1: 39
Sand, selective sorption of strontium by Richfield, 4: 65–6
Saran plastic, corrosion, 3: 17
radiation effects, 3: 17
Sawdust-soil mixtures
See Soil-sawdust mixtures
Saws, mechanical decladding of fuel elements, 1: 7–8
Scandium, recovery from poisoned solvent extractants, 2: 62
solubility in liquid cadmium, 1: 39
Sea disposal
See Waste disposal and processing
Seepage pits, waste disposal, 3: 54–5; 4: 64–5
Shale, chlorination for uranium recovery, 4: 72–3
selective sorption of strontium by Conasauga, 4: 66
waste disposal in, 2: 52–4
Shearing, 3: 5
Shears, design, 2: 5–7
mechanical decladding of fuel elements, 1: 7–8
Shell E2342, diluent use in solvent extraction, 4: 15
Shipping, fuel elements, laws, 1: 1–2
fuels, economics, 4: 6
wastes, heat-transfer problems, 4: 66
Shipping containers
See Containers
Silica, removal from enriched-uranium solutions, 4: 12
Silicon alloys
See Hastelloy B alloy
Silicon-aluminum-nickel systems
See Aluminum-nickel-silicon systems
Silver, corrosion, 2: 23
solubility in liquid-metal systems, 4: 42
Silver-magnesium systems (liquid)
See Magnesium-silver systems (liquid)
SIR
See Reactors (S1G)
Skulls
See also Slag
reclamation from melt-refining process, 4: 43–4
Slag, uranium recovery, 1: 41, 72; 3: 32
SM-1 Reactor
See Reactors (SM-1)
Soda-lime softening process, waste-disposal use, 1: 51
Sodalite, radioisotope adsorption, 4: 57
Sodium (gaseous), corrosive effects, 3: 33
Sodium (liquid), corrosive effects, 3: 33
Sodium amalgam, reduction of uranium chloride to uranium by, 4: 73
Sodium chloride, hexachlorouranate-ion stability in, 2: 37
Sodium chloride–magnesium chloride–potassium chloride systems (liquid)
See Magnesium chloride–potassium chloride–sodium chloride systems (liquid)
Sodium chloride–potassium chloride systems (liquid)
See Potassium chloride–sodium chloride systems (liquid)
Sodium chloride–potassium chloride–zinc chloride systems (liquid)
See Potassium chloride–sodium chloride–zinc chloride systems (liquid)
Sodium fluoride, pellet bed, uranium hexafluoride sorption on, 4: 31–2
Sodium fluoride–beryllium fluoride–lithium fluoride systems (liquid)
See Beryllium fluoride–lithium fluoride–sodium fluoride systems (liquid)
Sodium fluoride–beryllium fluoride–lithium fluoride–zirconium fluoride systems (liquid)
See Beryllium fluoride–lithium fluoride–sodium fluoride–zirconium fluoride systems (liquid)
Sodium fluoride–lithium fluoride–potassium fluoride–uranium fluorides (UF_4)–zirconium fluoride systems (liquid)
See Uranium fluorides (UF_4)–lithium fluoride–potassium fluoride–sodium fluoride–zirconium fluoride systems (liquid)
Sodium fluoride–lithium fluoride–uranium tetrafluoride–zirconium fluoride systems
See Uranium fluorides (UF_4)–lithium fluoride–sodium fluoride–zirconium fluoride systems
Sodium fluoride–lithium fluoride–zirconium fluoride systems (liquid)
See Lithium fluoride–sodium fluoride–zirconium fluoride systems (liquid)
Sodium fluoride–nitric acid–aluminum nitrate systems
See Nitric acid–aluminum nitrate–sodium fluoride systems
Sodium fluoride–zirconium fluoride systems (liquid), corrosive effects, 3: 23
solvent properties, 3: 23
Sodium fluozirconate, precipitation, 4: 16–17
Sodium formate process, economic evaluation, 4: 3
sodium fluozirconate precipitation using, 4: 16–17
Sodium hydroxide, dissolution of aluminum, 4: 7–8
uranium recovery from impure uranium tetrafluoride using, 2: 68
Sodium hypophosphite, ruthenium volatility control during waste calcination using, 2: 43
Sodium nitrate, effects on Sr^{90} removal by minerals, 4: 57
solvent properties, 3: 8
Sodium plutonyl fluorides, preparation, 4: 35
Sodium-potassium alloys (liquid)
See Potassium-sodium alloys (liquid)
Sodium Reactor Experiment
See Reactors (Sodium, Experiment)(SRE)
Soil-peat mixtures, sorption column use, 2: 51
Soil-sawdust mixtures, sorption column use, 2: 51
Soltrol-170, diluent use in solvent extraction, 4: 15
Solvent-extraction processes, 1: 13–16; 2: 5–21; 3: 1–2, 10–21; 4: 12–16
See also Liquid-metal extraction processes and Liquid metal–fused salt extraction processes
cesium recovery from waste solutions, 4: 68
cost, 4: 1–2
decontamination factors, solvent quality effects, 4: 15
diluents, 4: 14–15
fission-product recovery, 2: 56
fuel solution pretreatment by centrifuging, 4: 12
lectures, 3: 12
plant design, 1: 18–25
solvent stability, 4: 15–16
uranium recovery from nitrate eluates, 2: 61
Sparging, hot gas, waste-disposal applications, 3: 47–8
Spectroscopy (optical emission), analysis of uranium-fissium alloys using, 2: 29
Spheres
See Thorium oxide spheres and Thorium oxide–uranium oxide spheres
Sponges (ceramic), waste fixation in, 4: 63–4
Spray drying, uranium-zirconium alloy processing, 2: 26–7
SRE
See Reactors (Sodium, Experiment)(SRE)
Stainless steel
See also Carpenter-20 alloy
corrosion, 1: 26, 43, 44; 2: 15–16, 18–19; 3: 15–17, 18–19; 4: 25, 46
by nitric acid, 4: 21–3
in Zirflex Process, 1: 25–6
dissolution, 1: 8; 2: 10, 22; 3: 5
in fused-salt volatility process, 2: 25
electrolytic dissolution, 3: 9; 4: 8–9
removal from uranium carbide fuel in electrolytic-dissolution process, 2: 36
stress-corrosion cracking, literature survey, 4: 25
Stainless steel (304L), corrosion, 4: 24–5
during calcination processes, 2: 43
in Darex dissolver solutions, 4: 20–1
by Darex-Purex raffinate, 4: 21
by waste solutions, 4: 25–6
Stainless steel (308L), corrosion by Darex-Purex raffinate, 4: 21
Stainless steel (316L), corrosion, 4: 23
Stainless steel (347), corrosion, 4: 27–8
by Darex-Purex raffinate, 4: 20–1
by waste solutions, 4: 25–6
Stainless steel (348), corrosion, 4: 24–5
Stainless steel (405), corrosion by liquid cadmium-magnesium-zinc systems, 2: 33
Stainless steel (tungsten-coated), thermal cycling, 2: 33
Stainless steel–matrix fuels, dissolution by hydrochloric acid–nitric acid mixtures, 4: 20

Stainless steel–nitrate solutions, calcination of wastes containing, 4: 58
Stainless steel–uranium alloys
See Uranium–stainless steel alloys
Stainless steel–uranium oxides (UO_2) systems
See Uranium oxides (UO_2)–stainless steel systems
Stainless steel–uranium-zirconium alloys
See Uranium-zirconium–stainless steel alloys
Steam, uranium carbide removal from cladding using, 4: 49
Steam stripping, Purex wastes, 2: 48
Steels, corrosion, 1: 43; 3: 33
Stills, cadmium distillation, 1: 44
Storage, criticality control, 2: 15
fuels, economics, 4: 6
Storage of radioactive wastes
See Waste disposal and processing
STR process, economic evaluation, 4: 3–4
Stress corrosion, stainless steels, literature survey, 4: 25
waste-storage tanks, 4: 52–5
Strontium, extraction, using liquid alloy–eutectic system, 2: 30–1
with liquid lead-zinc alloys, 1: 40
by liquid-metal system, 4: 45
incorporation into glass as heat or radiation source, 2: 47–8
removal, 2: 22; 3: 28, 44–5
by electrolytic process, 2: 36
by ion-exchange materials, 2: 49–50
in melt-refining process, 4: 36
from Purex wastes, 2: 48, 55; 4: 56
from wastes, 1: 51, 58
separation from wastes, 1: 61–2, 63
sorption, by Conasauga shale, 4: 66
by natural organic materials, 2: 51
by Richfield sand, 4: 65–6
Strontium-90, activity/particle-size relations for separated waste, 4: 58
reactions with minerals, 2: 49
separation from wastes, 2: 56; 3: 57–8; 4: 57, 67–9
shipping, 2: 57–8
shipping containers, 4: 69
Strontium oxide–beryllium oxide–calcium oxide systems
See Beryllium oxide–calcium oxide–strontium oxide systems
Strontium oxide–beryllium oxide–lanthanum oxide systems
See Beryllium oxide–lanthanum oxide–strontium oxide systems
Strontium oxide–beryllium oxide systems
See Beryllium oxide–strontium oxide systems
Styrene polymers, 4: 23
Sublimation
See also Fractional sublimation processes
molybdenum trioxide rate, radiation effects, 2: 38
Submarine Intermediate Reactor
See Reactors (S1G)
Submarine Thermal Reactor process, economic evaluation, 4: 3–4
Sulfate ion, effects on strontium recovery from Purex wastes, 2: 55
effects on uranium extraction from nitric acid solutions, 2: 61–2
Sulfex process, chemical decladding of fuel elements, 1: 8
corrosion problems, 1: 26; 3: 17
Sulfex-Zirflex process, corrosion problems, 2: 18
Sulfoxide, dibenzyl-, solvent properties, 3: 12
Sulfoxide, di-*n*-octyl-, solvent properties, 3: 12
Sulfoxide, ethyl dodecyl-, solvent properties, 3: 12
Sulfur (liquid), waste calcination in, 4: 58
Sulfuric acid, beryllium dissolution, 4: 8
corrosive effects, 3: 17–18
fuel-element dissolution, 1: 11–12
granitic rock leaching, 4: 83–4
solvent properties, 1: 8, 11–12; 3: 5–6, 10; 4: 8
stainless-steel dissolution, 1: 8
Sulfuric acid–nitric acid systems
See Nitric acid–sulfuric acid systems

T

Tanks
See Containers
Tantalum, basket use in electrolytic dissolution process, 4: 8–9
corrosion, 1: 43; 3: 33
in Darex dissolver solutions, 4: 20
by plutonium alloys, 2: 33
hydrogen embrittlement, 4: 20
Tantalum (tungsten-coated), thermal cycling, 2: 33
Tantalum alloys, corrosion, 1: 43
Tantalum-thorium alloys
See Thorium-tantalum alloys
TBP
See Tributyl phosphate
TBP processes
See also Purex process and Thorex process
waste disposal, 1: 52–7
TBP-25 waste, calcination process, 2: 43; 4: 58–9
composition, 4: 25–6
conversion to glasses, 4: 63
corrosive properties, 4: 25–7
TCE
See Ethylene, tetrachloro-
Technetium-99, recovery from Purex wastes, 2: 56
Technetium fluoride (TcF_6), melting point, 2: 27
preparation by direct fluorination of metal, 2: 27
purification by fractional sublimation, 2: 27
solid-solid transition point, 2: 27
Television, remote maintenance use, 4: 19
Tellurium, release during oxidation of uranium dioxide, 4: 34–5
removal, 2: 22; 3: 28
during oxidation-reduction process for uranium dioxide, 4: 49
Temperature effects, dissolution rate of uranium dioxide, 4: 10–11
304L stainless-steel corrosion in Darex dissolver solutions, 4: 20
Terbium, removal, 3: 29
solubility, 3: 31
Tetrachloroethylene, solvent properties, 3: 11
Tetraphenyl boron, cesium removal by, 4: 68
Thallium-uranium alloys
See Uranium-thallium alloys
Thermal cycling, of irradiated uranium, Kr^{85} release during, 4: 37, 40
tungsten-coated construction materials, 2: 33
Thermal decomposition, plutonium hexafluoride, 2: 27; 4: 34
Thermal flowmeters
See Flow rate
Thermodynamic properties, alloys, 4: 39–40
bromine fluorides, 4: 35
intermetallic compounds, 2: 29–30; 4: 39–40
iodine pentafluoride, 4: 35
liquid metals, review, 2: 30
Thorex process, 4: 14
waste calcination, costs, 2: 42
waste disposal, 1: 52–7; 3: 55–6
waste storage, 1: 50–1; 2: 51
Thorium, electrorefining, 1: 73; 3: 32–3
leaching from impregnated graphite, 1: 12
losses in recycle, 3: 2–3, 7
melting, 3: 29
production, 2: 61–2
by thorium oxide reduction, 4: 84
recovery, 1: 42–3; 3: 11–12, 32–3; 4: 16
from granite ores, 4: 83–4
separation from radium, 4: 39
solubility in liquid zinc, 1: 43; 2: 29
solvent extraction, 4: 14–15
solvent extraction by liquid metal–fused salt system, 4: 43
Thorium-232, recovery, 1: 13
Thorium alloys, corrosion by liquid plutonium alloys, 2: 33
Thorium-aluminum alloys, production by aluminum reduction of thorium oxide, 4: 84
Thorium carbide, oxidation, 1: 47
reaction with zinc chloride, 4: 42
Thorium chloride, condensation product of monazite chlorination, 2: 68
Thorium compounds, reduction, 3: 31–2
Thorium fluoride, complexing with uranium fluorides, 3: 27
reduction, 4: 42
review on preparation and properties, 2: 27
Thorium hydroxide, firing for thorium oxide particle production, 2: 69
Thorium-lead intermetallic compounds, crystal structure, 2: 30
Thorium-magnesium alloys, production by magnesium reduction of thorium tetrafluoride, 4: 42
Thorium nitrate, thorium oxide production using, 2: 68–9
Thorium ores, chlorination, 2: 68
leaching, 4: 83–4
Thorium oxide, crystal properties, 4: 47–8
dissolution, 2: 10–11
in fused-salt volatility process, 2: 25
processing, 2: 11
reduction, by aluminum for thorium-aluminum alloy production, 4: 84
in fused-salt systems, 2: 32
by liquid magnesium-zinc alloys, 1: 41
in liquid-metal systems, 2: 32
to thorium by magnesium-zinc alloy, 4: 84
Thorium oxide–plutonium oxide systems
See Plutonium oxides–thorium oxide systems
Thorium oxide spheres, preparation, 2: 68–9
Thorium oxide–uranium oxides spheres, preparation, 2: 68–9
Thorium oxide–uranium oxides (UO_2) systems, dissolution, 1: 29–30
precipitation from fused-salt solutions, 4: 48
solubility in hydrochloric acid–nitric acid systems, 1: 8
Thorex processing, 4: 14
Thorium-plutonium alloys
See Plutonium-thorium alloys
Thorium-tantalum alloys, phase studies, 4: 40
thermodynamic properties, 4: 40
Thorium-uranium systems, separation by solvent extraction, 4: 14
solubility in liquid magnesium, 1: 42
Thorium-zinc alloys, disposal in salt mines, 4: 66
phase studies, 4: 40
thermodynamic properties, 1: 39; 4: 40
Thulium, removal, 3: 28
solubility, 3: 31
Tin fluorides, complexing with uranium fluorides, 3: 27

Tin-zirconium alloys
See also Zircaloy-2 alloy and Zircaloy-4 alloy
corrosion, 1: 26–7; 2: 8, 18; 3: 16, 18–19; 4: 24
in chloride-volatility process, 4: 21
in Darex dissolver solutions, 4: 20
Titanium 45A, corrosion, 4: 24, 27–8
Titanium fluorides, complexing with uranium fluorides, 3: 27
Toluene, diluent use in tributyl phosphate extraction processes, 4: 15
Transuranium elements, separation, 3: 12–13
solvent extraction, 4: 16
Transuranium processing facility
See TRU facility
Tributyl phosphate, compared with di-*sec*-butylphenyl phosphonate as solvent for uranium-thorium separation, 4: 14
degradation, 2: 12–13
in ICPP process, 1: 15–16
in Purex process, 1: 14–15
rare-earth extraction, 2: 56
Russian solvent-extraction data, 4: 14–15
solvent properties, 2: 11–12; 3: 10–11, 12–13
Tributyl phosphate–hexane solutions
See Hexane–tributyl phosphate systems
Tributyl phosphate processes
See also Purex process, TBP-25 waste, and Thorex process
waste disposal, 1: 52–7
TRIGA Reactors
See Reactors (TRIGA)
Triiodide, cesium removal by, 4: 68
Triisooctyl amine, solvent properties, 3: 12–13
Trilauryl amine, solvent properties, 2: 12; 3: 12
Tri-*n*-octyl amine, solvent properties, 3: 12
TRU facility, 3: 12–13; 4: 16
corrosion problems, 3: 19
Tube cutters, 2: 5, 6
Tungsten, compatibility, with liquid uranium-magnesium-zinc solutions, 4: 45–6
with magnesium-zinc fused-salt systems, 2: 33
corrosion, 1: 43; 3: 33
Tungsten alloys, corrosion by liquid plutonium alloys, 2: 33
Tungsten-chromium-cobalt-nickel alloys
See Haynes 25 alloy
Tungsten coatings, use on materials in liquid metal–molten salt solutions, 2: 33
Tungsten-molybdenum alloys
See Molybdenum-tungsten alloys

U

Ultrasene, diluent use in solvent extraction, 4: 15
UNH
See Uranyl nitrate
Union of Soviet Socialist Republics, solvent-extraction work with tributyl phosphate, 4: 14–15
Uranate ions
See Hexachlorouranate ion
Uranium, autoradiographic distribution determination, 2: 33
chlorination, 4: 33
cutting, 2: 5
density of liquid, 3: 30
diffusivity in liquid zinc, 4: 39
dissolution, 1: 8–9, 29–30; 2: 7, 10–11
by nitric acid, 4: 10
extraction, 4: 12–16
using liquid aluminum-cadmium system, 4: 41–2
using liquid lead-zinc system, 2: 30–1
from ore concentrates, 2: 61–2
Kr^{85} release during thermal cycling of irradiated, 4: 37, 40
leaching from impregnated graphite, 1: 12
loss minimization by waste backcycling in Purex process, 4: 13
losses in recycle, 3: 2–3, 7
melting, 3: 29
production, 1: 70–2; 2: 61–9; 4: 72–86
by electrolytic reduction of uranium dioxide, 2: 66; 4: 82
by magnesium reduction of uranium tetrafluoride, 2: 66–7
by reduction of uranium chloride, 4: 73
by uranium trichloride reduction in liquid metal–fused salt system, 4: 83
reaction, with carbon in liquid-metal systems, 2: 66
with propane to produce uranium dicarbide, 2: 64
reclamation by liquid-metal extraction from melt-refining-process residues, 2: 32
recovery, 1: 42–3; 2: 12; 3: 10–11, 22, 25–6, 34–6
from granite ores, 4: 83–4
from impure uranium tetrafluoride, 2: 68
from ores, 2: 61–2
from slag, 1: 72
reducing-agent use, 4: 45
separation, from chromium in skull reclamation process, 4: 43
from fission products by chlorination, 4: 33
solubility, 3: 29
in liquid bismuth, 4: 39
in liquid cadmium, 1: 39
in liquid gallium, 4: 39
in liquid magnesium-zinc systems, 2: 29–30
in liquid-metal systems, 4: 42
in liquid zinc, 1: 43
Uranium (depleted), base charges for, as uranium hexafluoride, 4: 4
Uranium (enriched), base charges for, as uranium hexafluoride, 4: 4
price reduction effects on reactor fuel-cycle cost, 4: 5
Uranium (liquid), density, 3: 30
Uranium-233, separation, 1: 13; 3: 11–12, 32–3
Uranium-aluminum alloys, production by aluminum reduction of uranium dioxide, 4: 42, 83
Uranium-bismuth alloys, thermodynamic properties, 1: 39–40
Uranium-bismuth alloys (liquid), fission-product removal, 4: 45
Uranium-bismuth-zirconium alloys, phase diagrams, 3: 29
Uranium borides (UB_2), preparation, 1: 47
Uranium-cadmium alloys, phase diagrams, 3: 29–30
thermodynamic properties, 1: 39
Uranium-cadmium intermetallic compounds, thermodynamic properties, 4: 39
Uranium-cadmium systems (liquid), thermodynamic properties, 4: 39
Uranium carbides, bibliography, 4: 78
carbon coating of, 4: 81
decladding by steam, 4: 49
electrolytic processing in fused-salt bath, 4: 49
fractional sublimation processing following chloridation, 2: 26
leaching, 1: 12
nitridation processing, 4: 49
oxidation-reduction processing, 4: 49
production, 4: 78–82
from metallic uranium and propane, 2: 36
Uranium carbides (UC), activation by water vapor, 4: 49
age effects on reaction rates, 2: 36–7; 3: 38
carbide-oxide-carbide process, 1: 46; 2: 35–6; 4: 49
hydrofluorination processing, 2: 26
nitridation, 1: 46; 2: 36–7; 4: 50
oxidation, 1: 46–7
precipitation with carbon from liquid-metal solutions, 4: 80
preparation, 1: 47, 69–70; 2: 65–6
by carbothermic reduction of uranium dioxide, 4: 78–9
by reaction of uranium with hydrocarbons, 4: 78
processing, 1: 46; 2: 35–7; 3: 37–9; 4: 49–50
by chlorination, 4: 33
pyrophoricity, 2: 37
reactions, with fused lithium chloride–potassium chloride–zinc chloride systems, 1: 47
with liquid zinc, 1: 47
Uranium carbides (UC)–plutonium carbide (PuC) systems, preparation, 4: 81–2
Uranium carbides (UC_2), oxidation, 1: 47
preparation, 1: 69–70; 2: 65–6
Uranium carbides (U_2C_3), reaction with zinc chloride, 4: 42
Uranium-carbon systems, constitutional diagram, 4: 79
Uranium chlorides (UCl_3), conversion to uranium hexafluoride, 4: 34
reduction, in alumina–fused salt system, 2: 31
in fused salts, 2: 67–8
to uranium, 4: 42
to uranium in fused salt–liquid metal system, 4: 83
Uranium chlorides (UCl_4), fractional sublimation separation process, 4: 33
Uranium chlorides (UCl_5), preparation from uranium monocarbide, 4: 33
reduction to uranium by sodium amalgam, 4: 73
Uranium chlorides (UCl_6), preparation from uranium monocarbide, 4: 33
reaction with hydrofluoric acid, 4: 33
Uranium-chromium alloy, extraction using magnesium-silver alloy, 4: 41, 45
Uranium-fissium alloys, phase studies, 2: 29
swelling during melt refining, 2: 28–9
Uranium fluorides, review on preparation and properties, 2: 27
Uranium fluorides (UF_4), chemical properties, 3: 27
electrolytic reduction to metal, 1: 71–2
fluorination, 4: 34
magnesium reduction to uranium metal, 2: 67
production, 2: 63–5; 3: 63–4; 4: 76–8
uranium recovery from impure, 2: 68
Uranium fluorides (UF_4)–lithium fluoride–potassium fluoride systems (liquid), electrolytic-dissolution bath, 2: 36
Uranium fluorides (UF_4)–lithium fluoride–potassium fluoride–sodium fluoride–zirconium fluoride systems (liquid), corrosive effects, 2: 23
Uranium fluorides (UF_4)–lithium fluoride–sodium fluoride–zirconium fluoride systems, fluorination, 1: 33–4
Uranium fluorides (UF_6), chemical properties, 3: 27
conversion, to uranium carbides, 1: 69–70
to uranium dioxide, 1: 67–8
flow-rate instrumentation, 4: 18–19
production, by fluorination of uranium tetrafluoride, 4: 34

Uranium fluorides (UF_6), production (Continued)
by fluorination of uranium trichloride, 4: 32
by nitrosylium hexafluorouranate reaction with bromine trifluoride, 4: 30–1
reduction to UF_4, 3: 63–4
separation from plutonium hexafluoride, 4: 34
sorption on sodium fluoride pellet bed, 4: 31–2
Uranium hydrides, reaction with alkanes to produce uranium monocarbide, 2: 64; 4: 78
Uranium-indium alloys, thermodynamic properties, 1: 39
Uranium-lead alloys, thermodynamic properties, 1: 39
Uranium-lead intermetallic compounds, crystal structure, 2: 30
Uranium-magnesium-zinc alloys (liquid), compatibility with tungsten, 4: 45–6
corrosive effects, 1: 43
Uranium-molybdenum alloys, dissolution, 1: 9–10; 2: 7; 3: 6–7
Uranium-molybdenum alloys (aluminum-clad), separation by Zircex process, 2: 25
Uranium nitrates [$U(NO_3)_4$], preparation, 3: 63
Uranium nitrides, carbidation, 1: 46
Uranium ores, chlorination, 2: 61; 4: 72–3
leaching, 2: 61–2; 4: 72–3
Uranium oxides, direct fluorination processing, 2: 26
hydrofluorination, 4: 34
oxidation, iron-ion effects, 2: 61
wet preparation process, 4: 75
Uranium oxides–plutonium oxides systems
See Plutonium oxides–uranium oxides systems
Uranium oxides–thorium oxides spheres
See Thorium oxide–uranium oxides systems
Uranium oxides (UO_2), activation for uranium tetrafluoride production, 2: 64–5
carbidation, 1: 46–7; 2: 64
carbothermic reduction, 4: 49, 78–9
chlorination, 4: 46
coating techniques for particles, 2: 63
conversion to uranium carbides, 1: 69–70
criticality hazards in production, 2: 62
crystal-growth characteristics, 2: 35
crystal properties, 4: 47–8
decontamination, during fluorination, 4: 34–5
during oxidation, 4: 34–5
direct fluorination processing, 4: 33
dissolution, 2: 11, 22; 3: 7
in fused-salt volatility process, 2: 25
in molten chloride systems, 2: 34
by nitric acid, ~. 10
dissolution rate, temperature effects, 4: 10–11
electrolytic reduction to uranium metal, 2: 66; 4: 82
fluorination, 1: 36–7; 2: 63–4; 3: 25–6; 4: 33, 76–7
fractional sublimation processing following chloridation, 2: 26
hydrofluorination, 4: 76–7
hydrofluorination kinetics, 2: 63–4
leaching from graphite, 2: 11
oxidation, 1: 45–6, 68–9
oxidation-reduction process, 4: 49
oxidative decanning, 2: 35
processing, 3: 34–7
production, 1: 66–9; 2: 62–3; 3: 61–3
by catalytic reduction process, 4: 73–5
by cathodic reduction of uranyl chloride, 2: 34–5
by electrolysis of uranyl chloride, 4: 47
by electrolytic reduction of uranium tritaoctoxide, 4: 48
by flame denitration process, 4: 74–5
by hydrogen reduction, 4: 75
reduction, 2: 66; 4: 42, 82
with aluminum for aluminum-uranium alloy production, 4: 83
to metal, 1: 70–2
separation from plutonium, 4: 33–4
solubility, 1: 45
Uranium oxides (UO_2) (stainless-steel-clad), decladding with chlorine, 2: 26
direct fluorination processing, 4: 33
Uranium oxides (UO_2) (Zircaloy-clad), direct fluorination processing, 4: 33
Uranium oxides (UO_2)–aluminum oxide systems, dissolution, 3: 10
Uranium oxides (UO_2)–beryllium oxide systems, dissolution, 3: 10
leaching, 1: 12–13
Uranium oxides (UO_2)–carbon mixtures, consumable electrode use in uranium metal production, 2: 66
Uranium oxides (UO_2)–Nichrome systems, dissolution, 2: 8–10
Uranium oxides (UO_2)–niobium oxides (Nb_2O_5) systems, separation by chlorination, 4: 33
Uranium oxides (UO_2)–plutonium oxides (PuO_2) systems
See Plutonium oxides (PuO_2)–uranium oxides (UO_2) systems
Uranium oxides (UO_2)–stainless steel alloys, dissolution by aqua regia, 4: 11–12
Uranium oxides (UO_2)–stainless steel systems, dissolution, 1: 11–12
Uranium oxides (UO_2)–thorium oxide systems
See Thorium oxide–uranium oxides (UO_2) systems
Uranium oxides (UO_2)–uranium oxide (U_3O_8) systems, oxidation-reduction equilibria, 4: 76
Uranium oxides (UO_2)–zirconium oxide systems, dissolution in fused-salt volatility process, 2: 25
separation process development, 4: 33
Uranium oxides (UO_3), activation, 2: 64–5; 4: 76–7
production, 1: 68–9
reduction, 2: 62–3; 3: 61; 4: 73–8
Uranium oxides (U_3O_8), dissolution, 1: 45
in liquid lithium chloride–potassium chloride systems, 4: 48
production, 1: 68–9
reduction, 1: 54–6, 70–2; 4: 48
in liquid magnesium-zinc alloys, 1: 40–1
in liquid metal–fused salt system, 2: 31–2
Uranium oxides (U_4O_9), production, 1: 68–9
Uranium-plutonium alloys, plutonium recovery, 3: 69
Uranium-rhenium alloys, phase studies, 4: 40
thermodynamic properties, 4: 40
Uranium silicides (U_3Si_2), preparation, 1: 47; 2: 66
production, 1: 70
Uranium silicides (USi_3), preparation, 1: 47; 2: 66
Uranium–stainless steel alloys, dissolution, 3: 9
Uranium-thallium alloys, thermodynamic properties, 1: 39
Uranium-thorium systems
See Thorium-uranium systems
Uranium-zinc alloys, thermodynamic properties, 1: 39
Uranium-zinc intermetallic compounds, crystallization, 4: 45
Uranium-Zircaloy alloys (Zircaloy-clad), dissolution by hydrofluoric acid–nitric acid solutions, 4: 11
Uranium-zirconium alloys, cutting, 2: 5
direct fluorination, 2: 26–7
dissolution, 1: 10–11, 30–5, 43–4; 3: 7, 8
hydrochlorination, 4: 32
processing, 2: 25–7; 3: 24–5; 4: 16–17, 30, 32
Uranium-zirconium hydride systems, dissolution, 3: 7
Uranium-zirconium–stainless steel alloys, dissolution, 1: 33–4
Uranyl carbonate, catalytic reduction to uranium dioxide, 4: 73–4
Uranyl chloride, reduction, 1: 66–7; 2: 34–5; 3: 61–2; 4: 47
Uranyl(VI) ion, complex formation, concentration effects, 4: 46
electrolytic reduction, 4: 46–7
Uranyl nitrate, ammoniation effects on later activity of uranium trioxide, 2: 65
corrosive effects, 3: 19
flame reduction to uranium dioxide, 4: 74–5
Uranyl nitrate hexahydrate–aluminum nitrate–nitric acid systems, corrosive properties, 4: 25
Urea plastics, corrosion, 2: 19

V

Vanadium, solubility, 3: 29
in liquid zinc, 2: 29
Vanadium-iron-molybdenum-nickel alloys
See Iron-molybdenum-nickel-vanadium alloys
Vanadium-iron-nickel alloys
See Iron-nickel-vanadium alloys
Vermiculite, cesium removal by, 2: 50
strontium removal by, 2: 49
phosphate-ion effects, 2: 50
waste-disposal applications, 1: 51–2; 3: 55
Vermiculite-lignite mixtures
See Lignite-vermiculite mixtures
Vermiculite-peat mixtures
See Peat-vermiculite mixtures
Viscosity, review of liquid metals, 2: 30
Volatility processes, 1: 29–38; 2: 22–7; 3: 22–7; 4: 30–5

W

Waste disposal and processing, 1: 50–65; 2: 40–58; 3: 41–59; 4: 19, 52–69
adsorption processes, 4: 56–8
backcycling, in Purex process, 4: 12–14
in Redox process, 4: 12–13
calcination, 2: 46; 4: 58–62
of aluminum nitrate wastes, 2: 44
processes, 2: 42–6
centrifugation, 4: 57–8
container evaluation for ocean disposal, 2: 54–5; 3: 41–2
cooling of stored wastes, 2: 40–1
corrosion problems, 3: 19; 4: 25–8
costs of pot calcination, 2: 42
deep permeable formation disposal, 4: 65–6
deep well disposal, 2: 54
economic aspects, 4: 55
final disposal methods, 2: 51–5; 3: 54–6; 4: 64–7
fixation in ceramic sponges, 4: 63–4
ground disposal, 2: 55; 3: 42–3, 56, 57; 4: 65
high-level-waste heating problems, 4: 66–7
hydraulic fracturing, 2: 52–4
incorporation into glasses, 4: 62–3
ion-exchange processes, 2: 48–51; 4: 56–8

Waste disposal and processing (Continued)
isotope separation, 2: 55–8
mine disposal, 1: 59–61; 2: 51–2; 3: 55–6; 4: 66
ocean disposal, 2: 54–5; 3: 41–2
porous-strata disposal, 2: 54
salt-cavity disposal, 1: 59–61; 2: 51–2; 3: 55–6; 4: 66
seepage-pit disposal, 4: 64–5
shale-formation disposal, 2: 52–4
solution compositions, 4: 25–7
steam stripping, 2: 48
storage hazards, 2: 40–1; 4: 56
storage-tank management, 4: 52–6
tank design, for nonheating wastes, 4: 52, 54
for self-heating wastes, 4: 52–4
tank failures, 2: 40–1
tank performance data, 4: 55
temperature rise around line source of waste, 2: 52
water contamination, 2: 41
Water, contamination by radioactive waste, 2: 41
Water vapor, reaction with uranium monocarbide, 2: 37
uranium monocarbide activation using, 4: 49
Wells, waste disposal in, 4: 65–6
waste disposal in porous strata of, 2: 54
Winlo process, 2: 66–7
Wolfram
See Tungsten

X

Xenon, release during melt-refining process, 2: 29; 4: 36–7
Xenon-krypton systems
See Krypton-xenon systems

Y

Yankee Power Reactor
See Reactors (Yankee Power)
Ytterbium, removal, 3: 28
Yttrium, corrosion, 1: 43
extraction, by liquid metal–fused salt systems, 2: 32; 4: 43
by liquid-metal system, 4: 45
by liquid alloy–eutectic system, 2: 30–1
solubility, 3: 30–1
Yttrium alloys, corrosion by liquid plutonium alloys, 2: 33
Yttrium compounds, reduction, 3: 32
Yttrium-zinc alloys, phase studies, 4: 40
thermodynamic properties, 4: 40

Z

Zinc (liquid), reactions with uranium monocarbide, 1: 47
solubilities of metals in, 2: 29
solvent properties, 1: 43; 3: 29
uranium diffusivity in, 4: 39
Zinc-65, removal from Hanford reactor coolant by aluminum shavings, 4: 57
Zinc-cadmium-magnesium systems (liquid)
See Cadmium-magnesium-zinc systems (liquid)
Zinc-calcium alloys
See Calcium-zinc alloys
Zinc chloride, hexachlorouranate-ion stability in, 2: 37
reaction, with thorium carbide, 4: 42
with uranium carbide, 4: 42
Zinc chloride–potassium chloride–sodium chloride systems (liquid)
See Potassium chloride–sodium chloride–zinc chloride systems (liquid)
Zinc chloride–potassium chloride systems (liquid)
See Potassium chloride–zinc chloride systems (liquid)
Zinc ferrocyanide, cesium precipitation from Purex supernatant, 2: 58
Zinc-lead alloys
See Lead-zinc alloys
Zinc-magnesium systems (liquid)
See Magnesium-zinc systems (liquid)
Zinc-magnesium-uranium alloys (liquid)
See Uranium-magnesium-zinc alloys (liquid)
Zinc-plutonium alloys
See Plutonium-zinc alloys
Zinc-thorium alloys
See Thorium-zinc alloys
Zinc-uranium alloys
See Uranium-zinc alloys
Zinc-uranium intermetallic compounds
See Uranium-zinc intermetallic compounds
Zinc-yttrium alloys
See Yttrium-zinc alloys
Zircaloy alloy, dissolution, 3: 7–8
in ammonium fluoride process, 4: 10
by hydrofluoric acid–nitric acid systems, 4: 11–12
Zircaloy-uranium alloys (Zircaloy-clad)
See Uranium-Zircaloy alloys (Zircaloy-clad)
Zircaloy-2 alloy, corrosion, 3: 19
dissolution, 2: 8
electrolytic dissolution, 3: 8; 4: 9
Zircaloy-4 alloy, dissolution, 4: 11
Zircex process, 2: 25–6
corrosion problems, 2: 18
Zirconium, corrosion, 2: 8; 3: 19
corrosion inhibition by, 4: 46
dissolution, 2: 22; 3: 9, 4: 8–9
dissolution rate in fused salts following hydrofluorination, 2: 25
extraction, using liquid alloy–eutectic system, 2: 30–1
by liquid-metal system, 4: 45
hydrochlorination in Zircex process, heat removal during, 2: 25–6
ion exchange, 1: 16–17
removal, 1: 16–17, 41, 57–8; 2: 8, 11, 22, 30–1; 3: 12, 28; 4: 45
by electrolytic process, 2: 36
from fuel solutions by manganese dioxide, 4: 12
by melt-refining process, 2: 29
by precipitation, 4: 16
from Purex waste by ion exchange, 2: 48; 4: 56
by Thorex process, 4: 14
solubility in liquid zinc, 2: 29
Zirconium-95–niobium-95 mixtures
See Niobium-95–Zirconium-95 mixtures
Zirconium alloys, dissolution, 3: 22
Zirconium-bismuth-cerium-magnesium alloys
See Bismuth-cerium-magnesium-zirconium alloys
Zirconium-bismuth-uranium alloys
See Uranium-bismuth-zirconium alloys
Zirconium chloride, conversion to uranium dioxide, 3: 24–5
volatility, 1: 45
Zirconium fluoride–beryllium fluoride–lithium fluoride–sodium fluoride systems (liquid)
See Beryllium fluoride–lithium fluoride–sodium fluoride–zirconium fluoride systems (liquid)
Zirconium fluoride–lithium fluoride–potassium fluoride–sodium fluoride–uranium fluorides (UF_4) systems
See Uranium fluorides (UF_4)–lithium fluoride–potassium fluoride–sodium fluoride–zirconium fluoride systems
Zirconium fluoride–lithium fluoride–sodium fluoride systems
See Lithium fluoride–sodium fluoride–zirconium fluoride systems
Zirconium fluoride–lithium fluoride–sodium fluoride systems (liquid)
See Lithium fluoride–sodium fluoride–zirconium fluoride systems (liquid)
Zirconium fluoride–lithium fluoride–sodium fluoride–uranium fluorides (UF_4) systems
See Uranium fluorides (UF_4)–lithium fluoride–sodium fluoride–zirconium fluoride systems
Zirconium hydride–uranium systems
See Uranium–zirconium hydride systems
Zirconium-matrix fuels, 4: 23–4
Zirconium oxide, ion-exchange material use, 4: 16
Zirconium oxide–uranium oxides (UO_2) systems
See Uranium oxides (UO_2)–zirconium oxide systems
Zirconium–stainless steel–uranium alloys
See Uranium-zirconium–stainless steel alloys
Zirconium-tin alloys
See Zircaloy-2 alloy and Zircaloy-4 alloy
Zirconium-uranium alloys
See Uranium-zirconium alloys
Zirconium wastes, processing by fluid-bed calcination, 2: 46
Zirflex-Darex process
See Darex-Zirflex process
Zirflex process, 4: 23
corrosion problems, 1: 25–6; 2: 15–19
economic evaluation, 4: 1, 3
modifications, 4: 1
waste disposal, 1: 55–7
Zirflex-Sulfex process
See Sulfex-Zirflex process

LEGAL NOTICE

This document was prepared under the sponsorship of the U. S. Atomic Energy Commission. Neither the United States, nor the Commission, nor any person acting on behalf of the Commission:

A. Makes any warranty or representation, expressed or implied, with respect to the accuracy, completeness, or usefulness of the information contained in this report, or that the use of any information, apparatus, method, or process disclosed in this report may not infringe privately owned rights; or

B. Assumes any liabilities with respect to the use of, or for damages resulting from the use of any information, apparatus, method, or process disclosed in this report.

As used in the above, "person acting on behalf of the Commission" includes any employee or contractor of the Commission, or employee of such contractor, to the extent that such employee or contractor of the Commission, or employee of such contractor prepares, disseminates, or provides access to, any information pursuant to his employment or contract with the Commission, or his employment with such contractor.

NUCLEAR SCIENCE ABSTRACTS

The U. S. Atomic Energy Commission, Division of Technical Information, publishes *Nuclear Science Abstracts (NSA)*, a semimonthly journal containing abstracts of the literature of nuclear science and engineering.

NSA covers (1) research reports of the U. S. Atomic Energy Commission and its contractors; (2) research reports of government agencies, universities, and industrial research organizations on a world-wide basis; and (3) translations, patents, books, and articles appearing in technical and scientific journals.

Complete indexes covering subject, author, source, and report number are included in each issue. These are cumulated quarterly, semiannually, and annually providing a detailed and convenient key to the literature.

Availability of *NSA*

SALE *NSA* is available on subscription from the Superintendent of Documents, U. S. Government Printing Office, Washington 25, D. C., at $22.00 per year for the semimonthly abstract issues and $15.00 per year for the four cumulated-index issues. Subscriptions are postpaid within the United States, Canada, Mexico, and all Central and South American countries, except Argentina, Brazil, British and French Guiana, Surinam, and British Honduras. Subscribers in these Central and South American countries, and in all other countries throughout the world, should remit $27.50 per year for subscriptions to semimonthly abstract issues and $17.50 per year for the four cumulated-index issues.

EXCHANGE *NSA* is also available on an exchange basis to universities, research institutions, industrial firms, and publishers of scientific information. Inquiries should be directed to the Division of Technical Information Extension, U. S. Atomic Energy Commission, P. O. Box 62, Oak Ridge, Tennessee.

TECHNICAL PROGRESS REVIEWS may be purchased from Superintendent of Documents, U. S. Government Printing Office, Washington 25, D. C. for $2.00 per year for each subscription or for $0.55 per issue. The use of the coupon below will facilitate the handling of your order.

POSTAGE AND REMITTANCE: Postpaid within the United States, Canada, Mexico, and all Central and South American countries except as hereinafter noted. Add $0.50 per year, or $0.15 per single issue, for postage to all other countries, including Argentina, Brazil, British and French Guiana, Surinam, and British Honduras. Payment should be by check, money order, or document coupons, and MUST accompany order. Remittances from foreign countries should be made by international money order, or draft on an American bank, payable to the Superintendent of Documents, or by UNESCO book coupons.

order form

SUPERINTENDENT OF DOCUMENTS
U. S. GOVERNMENT PRINTING OFFICE
WASHINGTON 25, D. C.

Enclosed:
document coupons ☐ check ☐ money order ☐

Charge to Superintendent of Documents No._____

Please send a one-year subscription to

☐ REACTOR MATERIALS
☐ POWER REACTOR TECHNOLOGY
☐ NUCLEAR SAFETY
☐ REACTOR FUEL PROCESSING

(Each subscription $2.00 a year; $0.55 per issue.)

SUPERINTENDENT OF DOCUMENTS
U. S. GOVERNMENT PRINTING OFFICE
WASHINGTON 25, D. C.

(Print clearly)

Name_____

Street_____

City_____ Zone____ State_____